ACTA PHARMACEUTICA SCIENCIA

International Journal in Pharmaceutical Sciences, Published Quarterly

ISSN: 2636-8552
e-ISSN: 1307-2080,
Volume: 62, No: 2, 2024
Formerly: Eczacılık Bülteni / Acta Pharmaceutica Turcica
Founded in 1953 by Kasım Cemal GÜVEN

ACTA PHARMACEUTICA SCIENCIA

International Journal in Pharmaceutical Sciences
is Published Quarterly
ISSN: 2636-8552
e-ISSN: 1307-2080,
Volume: 62, No: 2, 2024
Formerly: Eczacılık Bülteni/Acta Pharmaceutica Turcica
Founded in 1953 by Kasım Cemal Güven

Address
İstanbul Medipol Üniversitesi
Kavacık Güney Kampüsü
Göztepe Mah. Atatürk Cad.
No: 40 34810 Beykoz/İSTANBUL
Tel: 0216 681 51 00

E-mail
editor@actapharmsci.com
secretary@actapharmsci.com

Web site
http://www.actapharmsci.com

Contents

Aims and Scope of Acta Pharmaceutica Sciencia
Gülden Zehra OMURTAG V

Instructions for Authors VI

EDITORIAL XXIV

Herb-drug interaction
Sevim ROLLAS 241

REVIEW ARTICLE 243

Vehicle noise pollution awareness for human health and environmental impacts: A comprehensive review
Akif YAVUZ, Ayşe Nur HAZAR-YAVUZ, Enes HACIBEKTAŞOĞLU 244

ORIGINAL ARTICLES 267

The potential impact of vascular endothelial growth factor rs699947 polymorphisms on breast tumors susceptibility in a sample of Iraqi females
Hiba A. ABDULHUSSEIN, Estabraq AR. ALWASITI, Nawfal K. KHIRO
Anees K. NILE 268

Efficacy of statin therapy on achieving target goal of LDL among Iraqi patients
Ahmed AL-SHAMMARI, Qusay SHANDOO 278

Study of formulation effects on the charge variant profile of antibody-maytansine conjugates by icIEF method
Ayat ABBOOD 288

Effects of tadalafil on vancomycin-induced nephrotoxicity in rats
Hassanen A. ABDULAMEER, Adeeb A. AL-ZUBAIDY 301

Development and validation of a stability indicating LC method for the analysis of chlordiazepoxide and trifluoperazine hydrochloride in the presence of their degradation products
Payal CHAUHAN, Rakesh PARMAR, Anuja TRIPATHI 312

Natural polymers for targeted drug delivery to the colon: A comparative study of tamarind gum and karaya gum
Jaymin PATEL, Kaushika PATEL, Shreeraj SHAH 333

The applicability of bioluminescent bacteria for preliminary screening of antibacterial activity: Comparative analysis of aqueous and ethanol extracts from plant raw material
Yuliia Yu HAVRYCHENKO, Andrei M. KATSEV, Sergei L. SAFRONYUK,
Dhruv VASHISHT 355

HPLC investigation of hidden danger deoxynivalenol (vomitoxin) in baby foods from grain sources in Türkiye
Ozan Emre EYUPOGLU, Duygu YAZICIOGLU, Gizem Sena ELAGÖZ,
Mücteba Eşref TATLIPINAR, Gülden Zehra OMURTAG 373

Chemical composition and biological activities of seed butter extracted from *Garcinia gummi-gutta* (L.) Roxb.
Neenthamadathil Mohandas KRISHNAKUMAR, George SHINEY 384

Neuroprotective application of *Hemidesmus indicus* root extract and its silver nanoparticles implication against monosodium glutamate induced neurotoxicity in albino rats
Mahesh CHINTALA, Syed Sagheer AHMED, Ajay BANKAD VENKATESH, Pooja RANGENAHALLI CHIDANANDA MURTHY, Ramesh BEVINHALLI, Bharathi DODDLA RAGHUNATHANAIDU 403

Evaluation of fluconazole-loaded nanocellulose-reinforced xanthan gum film for drug delivery applications
Vipin JAIN, Rimpy PAHWA, Rashmi SHARMA, Munish AHUJA 423

Anti-anemic potential of *Moringa oleifera* flower extract against phenylhydrazine-induced anemia in rats
Nikitha MANJEGOWDA, Mani Rupesh KUMAR, Bharathi DODDLA RAGHUNATHANAIDU, Anjali BABU, Karthik SRIDHARA, Ramesh BEVINHALLI, Syed Sagheer AHMED 448

Sprayable microemulsion of diphenhydramine hydrochloride for dermal delivery
Muhammet Davut ARPA, Tuğba ARSLAN, Huriye ERASLAN, Neslihan ÜSTÜNDAĞ OKUR 462

Study of different factors affecting spreadability and release of Ibuprofen from carbopol gels using screening design methodology
Lama AL HAUSHEY 480

Aims and Scope of Acta Pharmaceutica Sciencia

Acta Pharmaceutica Sciencia is a continuation of the former "Eczacılık Bülteni" which was first published in 1953 by Prof. Dr. Kasım Cemal GÜVEN's editorship. At that time, "Eczacılık Bülteni" hosted scientific papers from the School of Medicine-Pharmacy at İstanbul University, Türkiye.

In 1984, the name of the journal was changed to "Acta Pharmaceutica Turcica" and it became a journal for national and international manuscripts, in all fields of pharmaceutical sciences in both English and Turkish. (1984-1995, edited by Prof. Dr. Kasım Cemal GÜVEN, 1995-2001, edited by Prof. Dr. Erden GÜLER, 2002-2011, edited by Prof. Dr. Kasım Cemal GÜVEN)

Since 2006, the journal has been published only in English with the name, "Acta Pharmaceutica Sciencia" which represents internationally accepted high-level scientific standards. The journal has been published quarterly except for an interval from 2002 to 2009 in which its issues were released at intervals of four months. The publication was also temporarily discontinued at the end of 2011 but since 2016, Acta Pharmaceutica Sciencia has continued publication with the reestablished Editorial Board and also with the support of you as precious scientists.

Yours Faithfully

Prof. Dr. Gülden Zehra OMURTAG
Editor

INSTRUCTIONS FOR AUTHORS

Manuscripts must be prepared using the manuscript template.

Manuscripts should contain the following elements in the following order:

Title Page

Abstract

Keywords

Introduction (without author names and affiliations)

Methodology

Results and Discussion

Statement of Ethics

Conflict of Interest Statement

Author Contributions

Funding Sources (optional)

Acknowledgments (optional)

References

It is best to use the Times New Roman font, 11 font size, and all kinds of articles must be 1.5 spaced including text, references, tables, and legends.

The title should be concise and informative. Avoid abbreviations and formulae, where possible. The title page should include full title, author names and affiliations, present addresses, corresponding author, and ORCID numbers for every author. Also, the full manuscript should include a full title page.

Abstracts should not be separated into categories; it should be written in a paragraph format.

Keywords: Max. 5

Graphics may be included with both in the text and uploaded as separate files.

Sections: (Capital letters should be used in) Introduction, Methodology, Results and Discussion, Statement of Ethics, Conflict of Interest Statement, Author Contributions, Funding Sources (optional), Acknowledgments (optional).

Table and figure titles should not be abbreviated exp. fig. is not acceptable. It should be written as; Table 1. .... Figure 1. .....

Figure captions: A caption should comprise a brief title (not on the figure itself) and a description of the illustration. Keep text in the illustrations themselves to a minimum but explain all symbols and abbreviations used. Figure captions should be written on the bottom.

Titles: Number tables consecutively by their appearance in the text and place any table notes below the table body. Table captions should be written on the top.

References in the text should be identified using Arabic numerals. Years of the references should not be written boldly. More than one reference from the same author(s) in the same year must be identified by the letters “a”, “b”, “c”, etc., placed after the year of publication. References should conform to Vancouver style and be numbered consecutively in the order in which they are cited in the text.

*Obligatory files are manuscript main document, title page and copyright form for submission. If exist, supplementary files should also be added.

1. Scope and Editorial Policy

1.1 Scope of the Journal

Acta Pharmaceutica Sciencia (Acta Pharm. Sci.), formerly known as Bulletin of Pharmacy and Acta Pharmaceutica Turcica is a peer-reviewed scientific journal publishing current research and reviews covering all fields of pharmaceutical sciences since 1953.

The original studies accepted for publication must be unpublished work and should contain data that have not been published elsewhere as a whole or a part. The reviews must provide critical evaluation of the state of knowledge related with the subject.

All manuscripts have to be written in clear and concise English.

Including the October 2023 issue, the journal has started to be published online only. It will also publish special issues for national or international scientific meetings and activities in the interested field.

1.2 Manuscript Categories

Manuscripts can be submitted as Research Articles.

Research Articles are definitive accounts of significant, original studies. They are expected to present important new data or provide a fresh approach to an established subject.

1.3 Prior Publication

Authors should submit only original work that has not been previously published and is not under consideration for publication elsewhere. Academic theses, including those on the Web or at a college Web site, are not considered to be prior publication.

1.4 Patents and Intellectual Property

Authors need to resolve all patent and intellectual property issues. Acceptance and publication will not be delayed for pending or unresolved issues of this type. Note that Accepted manuscripts and online manuscripts are considered published documents.

1.5 Professional Ethics

Editors, reviewers, and authors are expected to adhere to internationally accepted criteria for scientific publishing. Helsinki declaration is applied and accepted for the ethical standards of the journal.

World Medical Association. (2001). World Medical Association Declaration of Helsinki. Ethical principles for medical research involving human subjects. Bulletin of the World Health Organization, 79(4),373-374.

1.5.1 Author Consent

Submitting authors are reminded that consent of all coauthors must be obtained prior to submission of manuscripts. If an author is removed after submission, the submitting author must have the removed author consent to the change by e-mail or faxed letter to the assigned editor.

1.5.2 Plagiarism

Manuscripts must be original with respect to concept, content, and writing. It is not appropriate for an author to reuse wording from other publications, including one's own previous publications, whether or not that publication is cited. Suspected plagiarism should be reported immediately to the editorial office. Report should specifically indicate the plagiarized material within the manuscripts. Acta Pharmaceutica Sciencia uses iThenticate or Turnitin software to screen submitted manuscripts for similarity to published material. Note that your manuscript may be screened during the submission process.

1.5.3 Use of Human or Animal Subjects

For research involving biological samples obtained from animals or human subjects, editors reserve the right to request additional information from au-

thors. Studies submitted for publication approval must present evidence that the described experimental activities have undergone local institutional review assessing safety and humane usage of study subject animals. In the case of human subjects, authors must also provide a statement that study samples were obtained through the informed consent of the donors, or in lieu of that evidence, by the authority of the institutional board that licensed the use of such material. Authors are requested to declare the identification or case number of institution approval as well as the name of the licensing committee in a statement placed in the section describing the Material and Methods utilized in the studies.

World Medical Association. (2001). World Medical Association Declaration of Helsinki. Ethical principles for medical research involving human subjects. Bulletin of the World Health Organization, 79(4),373-374.

1.6 Issue Frequency

The Journal publishes 4 issues per year.

2. Preparing the Manuscript

2.1 General Considerations

Manuscripts should be kept to a minimum length. Authors should write in clear, concise English, employing an editing service if necessary. For professional assistance with improving English and/or the figures, or formatting in the manuscript before submission please contact to editorial office by e-mail for suggestions.

The responsibility for all aspects of manuscript preparation rests with the authors. Applying extensive changes or rewriting of the manuscript will not be undertaken by the editors. A standard list of Abbreviations, Acronyms, and Symbols is in section 5.

It is best to use the font “Times New Roman”. Other fonts, particularly those that do not come bundled with the system software, may not translate properly. Ensure that all special characters (e.g., Greek characters, math symbols) are present in the body of the text as characters and not as graphic representations. Be sure that all characters are correctly represented throughout the manuscript—e.g., 1 (one) and l (letter l), 0 (zero) and O (letter o).

All text (including the title page, abstract, all sections of the body of the paper, figure captions, scheme or chart titles, and footnotes and references) and tables should be in one file. Graphics may be included with the text or uploaded as separate files. Manuscripts that do not adhere to the guidelines may be returned to authors for correction.

2.1.1 Articles of All Kind

Use page size A4. Vertically orient all pages. Articles of all kind must be double-spaced including text, references, tables, and legends. This applies to figures, schemes, and tables as well as text. They do not have page limitations but should be kept to a minimum length. The experimental procedures for all experimental steps must be clearly and fully included in the experimental section of the manuscripts.

2.1.2 Nomenclature

It is the responsibility of the authors to provide correct nomenclature. It is acceptable to use semisynthetic or generic names for certain specialized classes of compounds, such as steroids, peptides, carbohydrates, etc. In such a case, the name should conform to the generally accepted nomenclature conventions for the compound class. Chemical names for drugs are preferred. If these are not practical, generic names, or names approved by the World Health Organization, may be used.

Authors may find the following sources useful for recommended nomenclature:

- The ACS Style Guide; Coghill, A. M., Garson, L. R., Eds.; American Chemical Society: Washington DC, 2006.
- Enzyme Nomenclature; Webb, E. C., Ed.; Academic Press: Orlando, 1992.
- IUPHAR database of receptors and ion channels (http://www.guidetopharmacology.org/).

2.1.3 Compound Code Numbers

Code numbers (including peptides) assigned to a compound may be used as follows:

- Once in the manuscript title, when placed in parentheses AFTER the chemical or descriptive name.
- Once in the abstract.
- Once in the text (includes legends) and once to label a structure. Code numbers in the text must correspond to structures or, if used only once, the chemical name must be provided before the parenthesized code number, e.g., “chemical name (JEM-398).” If appearing a second time in the text, a bold Arabic number must be assigned on first usage, followed by the parenthesized code number, e.g., “1 (JEM-398).” Subsequently, only the bold Ara-

bic number may be used. All code numbers in the text must have a citation to a publication or a patent on first appearance.

Compounds widely employed as research tools and recognized primarily by code numbers may be designated in the manuscript by code numbers without the above restrictions. Their chemical name or structure should be provided as above. Editors have the discretion of determining which code numbers are considered widely employed.

2.1.4 Trademark Names

Trademark names for reagents or drugs must be used only in the experimental section. Do not use trademark or service mark symbols.

2.1.5 Interference Compounds

Active compounds from any source must be examined for known classes of assay interference compounds and this analysis must be provided in the General Experimental section. Many of these compounds have been classified as Pan Assay Interference Compounds (PAINS; see Baell & Holloway, J. Med. Chem. 2010, 53, 2719-2740). These compounds shown to display misleading assay readouts by a variety of mechanisms by forming reactive compounds. Provide firm experimental evidence in at least two different assays that reported compounds with potential PAINS liability are specifically active and their apparent activity is not an artifact.

2.2 Manuscript Organization

2.2.1 Title Page

The title of the manuscript should reflect the purposes and findings of the work in order to provide maximum information in a computerized title search. Minimal use of nonfunctional words is encouraged. Only commonly employed abbreviations (e.g., DNA, RNA, ATP) are acceptable. Code numbers for compounds may be used in a manuscript title when placed in parentheses AFTER the chemical or descriptive name.

Authors' Names and Affiliations: The authors' full first names, middle initials, last names (with capital letters for only last names), and affiliations with addresses at time of work completion should be listed below the title. The name of the corresponding author should be marked with an asterisk (*).

2.2.2 Abstract and Keywords

Articles of all types must have an abstract following the title page. The maximum length of the Abstract should be 200 words, organized in a findings-oriented format in which the most important results and conclusions are sum-

marized. Code numbers may be used once in the abstract. After the abstract, a section of Keywords not more than five has to be given. Be aware that the keywords, chosen according to the general concept, are very significant during searching and indexing of the manuscripts.

Keywords: instructions for authors, template, journal

2.2.3 Introduction

The Introduction should argue the case for the study, outlining only essential background, and should not include the findings or the conclusions. It should not be a review of the subject area but should finish with a clear statement of the question being addressed. Authors should use this template when preparing a manuscript for submission to the ACTA Pharmaceutica Sciencia.

2.2.4 Methodology

Materials, synthetic, biological, demographic, statistical or experimental methods of the research should be given detailed in this section. The authors are free to subdivide this section in the logical flow of the study. For the experimental sections, authors should be as concise as possible in experimental descriptions. General reaction, isolation, preparation conditions should be given only once. The title of an experiment should include the chemical name and a bold Arabic identifier number; subsequently, only the bold Arabic number should be used. Experiments should be listed in numerical order. Molar equivalents of all reactants and percentage yields of products should be included. A general introductory section should include general procedures, standard techniques, and instruments employed (e.g., determination of purity, chromatography, NMR spectra, mass spectra, names of equipment) in the synthesis and characterization of compounds, isolates and preparations described subsequently in this section. Special attention should be called to hazardous reactions or toxic compounds. Provide analysis for known classes of assay interference compounds.

The preferred forms for some of the more commonly used abbrevations are mp, bp, ^{o}C, K, min, h, mL, μL, g, mg, μg, cm, mm, nm, mol, mmol, μmol, ppm, TLC, GC, NMR, UV, and IR. Units are abbreviated in table column heads and when used with numbers, not otherwise. (See section 4 for more abbreviations)

2.2.5 Results and Discussion

This section could include preparation, isolation, synthetic schemes and tables of biological and statistical data. The discussions should be descriptive. Authors should discuss the analysis of the data together with the significance of results and conclusions. An optional conclusions section is not required.

2.2.6 Ancillary Information

Include pertinent information in the order listed immediately before the references.

PDB ID Codes: Include the PDB ID codes with assigned compound Arabic number. Include the statement "Authors will release the atomic coordinates and experimental data upon article publication."

Homology Models: Include the PDB ID codes with assigned compound Arabic number. Include the statement "Authors will release the atomic coordinates upon article publication."

Corresponding Author Information: Provide telephone numbers and email addresses for each of the designated corresponding authors.

Present/Current Author Addresses: Provide information for authors whose affiliations or addresses have changed.

Author Contributions: Include statement such as "These authors contributed equally."

Acknowledgments: Authors may acknowledge people, organizations, and financial supporters in this section.

Abbreviations Used: Provide a list of nonstandard abbreviations and acronyms used in the paper, e.g., YFP, yellow fluorescent protein. Do not include compound code numbers in this list. It is not necessary to include abbreviations and acronyms from the Standard Abbreviations and Acronyms listed in section 4.

2.2.7 References and Notes

Vancouver style is used in the reference list and citations. List manuscripts as "in press" only accepted for publication. Manuscripts available on Web with a DOI number are considered published. For manuscripts not accepted, use "unpublished work" after the names of authors. Incorporate notes in the correct numerical sequence with the references. Footnotes are not used. List submitted manuscripts as "in press" only if formally accepted for publication. Manuscripts available on the Web with a DOI number are considered published. For manuscripts not accepted, use "unpublished results" after the names of authors. Incorporate notes in the correct numerical sequence with the references. Footnotes are not used. In-text citations should be given superscript numbers (see examples) according to order in the manuscript.

References

Please check with your faculty for any specific referencing or formatting requirements.

- References are listed in numerical order, and in the same order in which they are cited in text. The reference list appears at the end of the paper.
- Begin your reference list on a new page and title it 'References'.
- The reference list should include all and only those references you have cited in the text. (However, do not include unpublished items such as correspondence.)
- Use Arabic numerals (1, 2, 3, 4, 5, 6, 7, 8, 9) as a superscripts.
- Abbreviate journal titles in the style used in the NLM Catalog.
- Check the reference details against the actual source – you are indicating that you have read a source when you cite it.
- Use of DOI URL at the end of reference is strongly advised.

Examples

For printed articles

• Article with 1-6 authors:

Author AA, Author BB, Author CC, Author DD. Title of article. Abbreviated title of journal, Date of publication YYYY;volume number(issue number):page numbers.

Sahin Z, Ertas M, Berk B, Biltekin SN, Yurttas L, Demirayak S. Studies on non-steroidal inhibitors of aromatase enzyme; 4-(aryl/heteroaryl)-2-(pyrimidin-2-yl)thiazole derivatives. Bioorg Med Chem, 2018; 26(8): 1986–1995. https://doi.org/10.1016/j.bmc.2018.02.048.

• Article with more than 6 authors:

Author AA, Author BB, Author CC, Author DD, Author EE, Author FF, et al. Title of article. Abbreviated title of journal, Date of publication YYYY Mon DD;volume number(issue number):page numbers.

For electronic journal articles

Author AA, Author BB, Author CC, Author DD, Author EE, Author FF. Title of article. Abbreviated title of Journal [Internet], Year of publication [cited YYYY Mon DD];volume number(issue number):page numbers. Available from: URL DOI

For books and book chapters

Book: a.) Print book OR b.) Electronic book

a.) Author AA. Title of book. # edition [if not first]. Place of Publication: Publisher; Year of publication. Pagination.

b.) Author AA. Title of web page [Internet]. Place of Publication: Sponsor of Website/Publisher; Year published [cited YYYY Mon DD]. Number of pages. Available from: URL DOI: (if available)

2.2.8 Tables

Tabulation of experimental results is encouraged when this leads to more effective presentation or to more economical use of space. Tables should be numbered consecutively in order of citation in the text with Arabic numerals. Footnotes in tables should be given italic lowercase letter designations and cited in the tables as superscripts. The sequence of letters should proceed by row rather than by column. If a reference is cited in both table and text, insert a lettered footnote in the table to refer to the numbered reference in the text. Each table must be provided with a descriptive title that, together with column headings, should make the table self-explanatory. Titles and footnotes should be on the same page as the table. Tables may be created using a word processor's text mode or table format feature. The table format feature is preferred. Ensure each data entry is in its own table cell. If the text mode is used, separate columns with a single tab and use a return at the end of each row. Tables may be inserted in the text where first mentioned or may be grouped after the references.

2.2.9 Figures, Schemes/Structures, and Charts

The use of illustrations to convey or clarify information is encouraged. Structures should be produced with the use of a drawing program such as ChemDraw. Authors using other drawing packages should, in as far as possible, modify their program's parameters so that they conform to ChemDraw preferences. Remove all color from illustrations, except for those you would like published in color. Illustrations may be inserted into the text where mentioned or may be consolidated at the end of the manuscript. If consolidated, legends should be grouped on a separate page(s). Include as part of the manuscript file.

To facilitate the publication process, please submit manuscript graphics using the following guidelines:

1. The preferred submission procedure is to embed graphic files in a Word document. It may help to print the manuscript on a laser printer to ensure all artwork is clear and legible.

2. Additional acceptable file formats are: TIFF, PDF, EPS (vector artwork) or CDX (ChemDraw file). If submitting individual graphic files in addition to them being embedded in a Word document, ensure the files are named based on graphic function (i.e., Scheme 1, Figure 2, Chart 3), not the scientific name. Labeling of all figure parts should be present and the parts should be assembled into a single graphic.

EPS files: Ensure that all fonts are converted to outlines or embedded in the graphic file. The document settings should be in RGB mode. NOTE: While EPS files are accepted, the vector-based graphics will be rasterized for production. Please see below for TIFF file production resolutions.

3. TIFF files (either embedded in a Word doc or submitted as individual files) should have the following resolution requirements:

- Black & White line art: 1200 dpi
- Grayscale art (a monochromatic image containing shades of gray): 600 dpi
- Color art (RGB color mode): 300 dpi
- The RGB and resolution requirements are essential for producing high-quality graphics within the published manuscript. Graphics submitted in CMYK or at lower resolutions may be used; however, the colors may not be consistent and graphics of poor quality may not be able to be improved.
- Most graphic programs provide an option for changing the resolution when you are saving the image. Best practice is to save the graphic file at the final resolution and size using the program used to create the graphic.

4. Graphics should be sized at the final production size when possible. Single column graphics are preferred and can be sized up to 240 points wide (8.38 cm.). Double column graphics must be sized between 300 and 504 points (10.584 and 17.78 cm's). All graphics have a maximum depth of 660 points (23.28 cm.) including the caption (please allow 12 points for each line of caption text).

Consistently sizing letters and labels in graphics throughout your manuscript will help ensure consistent graphic presentation for publication.

2.2.10 Image Manipulation

Images should be free from misleading manipulation. Images included in an account of research performed or in the data collection as part of the research require an accurate description of how the images were generated and produced. Apply digital processing uniformly to images, with both samples and

controls. Cropping must be reported in the figure legend. For gels and blots, use of positive and negative controls is highly recommended. Avoid high contrast settings to avoid overexposure of gels and blots. For microscopy, apply color adjustment to entire image and note in the legend. When necessary, authors should include a section on equipment and settings to describe all image acquisition tools, techniques and settings, and software used. All final images must have resolutions of 300 dpi or higher. Authors should retain unprocessed data in the event that the editors request them.

2.3 Specialized Data

2.3.1 Biological Data

Quantitative biological data are required for all tested compounds. Biological test methods must be referenced or described in sufficient detail to permit the experiments to be repeated by others. Detailed descriptions of biological methods should be placed in the experimental section. Standard compounds or established drugs should be tested in the same system for comparison. Data may be presented as numerical expressions or in graphical form; biological data for extensive series of compounds should be presented in tabular form.

Active compounds obtained from combinatorial syntheses should be resynthesized and retested to verify that the biology conforms to the initial observation. Statistical limits (statistical significance) for the biological data are usually required. If statistical limits cannot be provided, the number of determinations and some indication of the variability and reliability of the results should be given. References to statistical methods of calculation should be included.

Doses and concentrations should be expressed as molar quantities (e.g., mol/kg, μmol/kg, M, mM). The routes of administration of test compounds and vehicles used should be indicated, and any salt forms used (hydrochlorides, sulfates, etc.) should be noted. The physical state of the compound dosed (crystalline, amorphous; solution, suspension) and the formulation for dosing (micronized, jet-milled, nanoparticles) should be indicated. For those compounds found to be inactive, the highest concentration (*in vitro*) or dose level (in vivo) tested should be indicated.

If human cell lines are used, authors are strongly encouraged to include the following information in their manuscript:

· the cell line source, including when and from where it was obtained;

· whether the cell line has recently been authenticated and by what method;

· whether the cell line has recently been tested for mycoplasma contamination.

2.3.2 Purity of Tested Compounds

Methods: All scientifically established methods of establishing purity are acceptable. If the target compounds are solvated, the quantity of solvent should be included in the compound formulas. No documentation is required unless asked by the editors.

Purity Percentage: All tested compounds, whether synthesized or purchased, should possess a purity of at least 95%. Target compounds must have a purity of at least 95%. In exceptional cases, authors can request a waiver when compounds are less than 95% pure. For solids, the melting point or melting point range should be reported as an indicator of purity.

Elemental Analysis: Found values for carbon, hydrogen, and nitrogen (if present) should be within 0.4% of the calculated values for the proposed formula.

2.3.3 Confirmation of Structure

Adequate evidence to establish structural identity must accompany all new compounds that appear in the experimental section. Sufficient spectral data should be presented in the experimental section to allow for the identification of the same compound by comparison. Generally, a listing of 1H or 13C NMR peaks is sufficient. However, when the NMR data are used as a basis of structural identification, the peaks must be assigned.

List only infrared absorptions that are diagnostic for key functional groups. If a series contains very closely related compounds, it may be appropriate merely to list the spectral data for a single representative member when they share a common major structural component that has identical or very similar spectral features.

3. Submitting the Manuscript

3.1 Communication and Log in to Author's Module

All submissions to Acta Pharmaceutica Sciencia should be made by using e-Collittera (Online Article Acceptance and Evaluation) system on the journal main page (www. actapharmsci.com).

3.2 Registration to System

It is required to register into the e-Collittera system for the first time while entering by clicking "Create Account" button on the registration screen and the fill the opening form with real information. Some of the information required in form is absolutely necessary and the registration will not work if these fields are not completely filled.

After the registration, a “Welcome” mail is sent to the user by the system automatically reminding user name and password. Authors are expected to return to the entry screen and log on with their user name and password for the submission. Please use only English characters while determining your username and password.

If you already registered into the e-Collittera system and forget your password, you should click on “Forgot My Password” button and your user name and password will be mailed to your e-mail in a short while.

3.3 Submitting a New Article

The main page of author module consists of various parts showing the situation of manuscripts in process. By clicking the New Manuscript button, authors create the beginning of new submission, a process with a total of 9 consecutive levels. In first 7 levels, information such as the article’s kind, institutions, authors, title, summary, keywords etc. are asked respectively as entered. Authors can move back and forth while the information is saved automatically. If the is transaction is discontinued, the system move the new submission to “Partially Submitted Manuscripts” part and the transaction can be continued from here.

3.1.1 Sort of Article Authors should first select the type of article from the drop-down menu.

Warning. If “Return to Main Page” button is clicked after this level, the article automatically assigned as “Partially Submitted Manuscripts”.

3.2.2 Institutions Authors should give their institutional information during submission.

3.2.3 Authors The authors’ surnames, names, institutional information appear as entered order in the previous page. Filling all e-mail addresses are required. Institutional information is available in Manuscript Details table at the top of the screen. After filling all required fields, you may click the Continue button.

3.2.4 Title should be English, explaining the significance of the study. If the title includes some special characters such as alpha, beta, pi or gamma, they can easily be added by using the Title window. You may add the character by clicking the relevant button and the system will automatically add the required character to the text.

Warning. No additions to cornered parenthesis are allowed. Otherwise, the system will not be able to show the special characters.

3.2.5 Abstract The summary of the article should be entered to Abstract window at this level. There must be an English summary for all articles and the quantity of words must be not more than 200. If special characters such as alpha, beta, pi or gamma are used in summary, they can be added by Abstract window. You may add the character by clicking the relevant button and the system will automatically add the required character to the text. The abstract of the articles is accessible for arbitrators; so, you should not add any information related to the institutions and authors in this summary part. Otherwise, the article will be returned without evaluation. Authors will be required to comply with the rules.

Warning. No additions to cornered parenthesis are allowed. Otherwise, the system will not be able to show the special characters.

3.2.6 Keywords There must be five words to define the article at the keywords window, which will be diverged with commas. Authors should pay attention to use words, which are appropriate for "Medical Subjects Headings" list by National Library of Medicine (NLM).

3.2.7 Cover Letter If the submitting article was published as thesis and/or presented in a congress or elsewhere, all information of thesis, presented congress or elsewhere should be delivered to the editor and must be mentioned by the "Cover Letter" field.

3.3.1 Adding Article This process consists of four different steps beginning with the loading of the article in to system. Browse button is used to reach the article file, under the Choose a file to upload tab. After finding the article you may click to Choose File and file will be attached.

Second step is to select the file category. Options are: Main Document, Black and White Figure, Color Figure and Video.

The explanation of the files (e.g., Figure 1, Full Text Word File, supplements etc.) should be added on third step and the last step is submitting the prepared article into the system. Therefore, Download button under the Send your file by clicking on download button tab is clicked.

Reminder. If the prepared article includes more than one file (such as main document, black and white figure, video), the transaction will be continued by starting from the first step. The image files must be in previously defined format. After all required files were added, Continue button should be clicked. All details and features of the article might be reached from the Article Information page.

This page is the last step of the transaction which ensures that entered information is controlled.

3.3.2 Your Files After adding the article you may find all information related to article under Your Files window.

File Information This window includes file names, sizes, forming dates, categories, order numbers and explanations of files. The details about the files can be reached by clicking on Information button.

If you click on Name of File, the file download window will be opened to reach the copy of the file in system.

File Download This window submits two alternatives, one of them is to ensure the file to be opened in valid site and the second one is to ensure to download submitted file into the computer.

Opening the Category part on fourth column can change the category of the file.

Opening the Order column on fifth column can change the order of file.

The file can be deleted by clicking on Delete button on the last column. Before deleting, system will ask the user again if it is appropriate or not.

3.3.3 Sending Article Last level is submitting the article and the files into the system. Before continuing the transaction, Article Information window must be controlled where it is possible to return back; by using Previous button and required corrections can be made. If not, clicking the Send the Article button completes transaction.

3.3.4 Page to Follow the Article The Main Page of Author ensures possibility to follow the article. This page consists of three different parts; some information and bridges related to the sent articles, revision required articles and the articles that are not completed to be sent.

3.3.4.1 Articles Not Completed to be Sent After the sending transaction was started, if article is not able to continue until the ninth step or could not be sent due to technical problems shown at this part. Here you can find the information such as the article's number which is assigned by system, title and formation date. You may delete the articles by using Delete button on the right column, if the article is not considered to send into the system.

3.3.4.2 Articles that Require Revision Articles, which were evaluated by the referee and accepted by the editor with revision, continues to Waiting for Revision table.

The required revisions can be seen in "Notes" part by clicking the articles title.

In order to send any revision, Submit Revision button on the last column should be clicked. This connection will take the author to the first level of Adding Article and the author can complete the revision transaction by carrying out the steps one by one. All changes must be made in the registered file, and this changed file must be resent. Author's most efficacious replies relating to the changes must be typed in "Cover Letter" part.

If the is transaction is discontinued, the system move the revised article to Submitted Manuscripts part and the transaction can be continued from here.

After the transaction was completed, the system moves the revised article to "Submitted Manuscripts" part.

3.3.5 Submitted Manuscripts Information related to articles can be followed through the Submitted Manuscripts line. Here you can find the information such as the article's number assigned by system, title, sending date and transaction situation. The Manuscript Details and summary files can be reached by clicking the title of the article and the Processing Status part makes it possible to follow the evaluation process of the article.

Article Review Process

Articles uploaded to the Manuscript submission system are checked by the journal administration for format consistency and similarity rate which is required to be less than 20%. Then sent to the chief editor if found appropriate.

Articles that are not suitable are sent back to the author for correction and resubmit (sent back to the author). Studies that have not been prepared using the draft for submitting to Acta Pharmaceutica Sciencia "acta_msc_tmp" and that have not been adapted in terms of format, will be directed to the editor-in-chief, after the 3rd time, by giving the information that "the consistency requirements have not been met".

The manuscripts sent to the chief editor will be evaluated and sent to the "language and statistics editor" if deemed appropriate.

Studies found appropriate after language-statistics editor will be sent to field editors. If the field editor does not deem it appropriate after evaluating the article scientifically, he/she will inform the editor-in-chief of its negative comments, otherwise, at least two independent referee comments will be asked.

Authors should consider that this time may take time because of the reviewer assignments and acceptance for review may take time for some cases.

Our review system is double-blind. The editor, who evaluates according to

the comments of the referees, submits his/her comment and suggestion to the editor-in-chief. In this way, the article takes one of the acceptance, rejection, or revision decisions. In the case of revision, after the author revises, the editor submits his/her final opinion to the editor-in-chief. The editor-in-chief conveys his or her final decision to the author. After the accepted articles are subjected to the final control by the journal and the corresponding author, the article starts to be included in the "accepted papers" section by giving the inactive DOI number. When the article is placed in one of the following issues, the DOI number will be activated and displayed in the "current issue" section on the journal homepage.

EDITORIAL

Herb-drug interaction

Editorial Article

Sevim ROLLAS*

Marmara University, Faculty of Pharmacy, Department of Pharmaceutical Chemistry, Istanbul, Türkiye. Retired Professor.

Recent epidemiological reports indicate that nearly 80% of the global population incorporates complementary and alternative medicine into their healthcare practices. Herbs are frequently self-administered concurrently with therapeutic drugs. Consequently, clinicians are advised to proactively gather information regarding herb-drug combination in their patients and establish monitoring protocols, particularly for individuals with habitual and concurrent herbal consumption. Herbal products can competitively inhibit cytochrome P450 (CYP) isoenzymes, potentially elevating blood levels of prescription medications and exposing patients to the risk of adverse effects. Studies by Bailey et al. (1991,1998) revealed the modification of felodipine biotransformation in the presence of grapefruit juice. Recent investigations further suggest that herbal products may induce both pharmacodynamic and pharmacokinetics interactions of pharmaceuticals.

The majority of drugs, herbal products and food constituent undergo are metabolism mediated by CYP enzymes. Interactions between herbal product and prescription drugs, manifested as co-medication, encompass the inhibition or induction of metabolizing enzymes and drug efflux proteins, such as P-glicoprotein (P-gp) and multiple resistance proteins (MRPs). The chemical structure of active herbal ingredient significantly modulates drug efflux and metabolism. Adverse effects may arise from the concominant use of herbal products with therapeutic drugs, owing to the alteration of drug metabolism and efflux pathways. Numerous herbal products demonstrate the capacity to induce or inhibit CYP isoenzyme, thereby influencing the metabolism of a broad spectrum of drugs. Predominant among the isoenzymes responsible for the biotransformation of herbal products are CYP3A4/5 and CYP2D6. CYP3A4 metabolizes more than 50% of presently administered therapeutic drugs.

* Corresponding author: Sevim ROLLAS
E-mail: sevimrollas@gmail.com
ORCID: 0000-0002-4144-6952

In the recent years, extencive investigation into herb-drug interaction have primarily concentrated on elucidating the pharmacokinetic and pharmacodynamic effects associated with anticancer, anti-HIV, cardiovascular, antidiabetic, antihypertensive, antibiotic, and neuropsychiatric medications. However, there remains a substantial need for augmented data derived from comprehensive case reports, in vitro and in vivo studies as well as clinical trials, focusing on the coadministration of naturel products alongside conventional drugs. Moreover, the establishment of a phytovigilance database stands as a prospective initiative for systematically cataloging herb-drug interactions. Notably, the FDA Adverse Event Reporting System (FAERS) and the Center Adverse Event Reporting System (CAERS) emerge as pivotal conduits for sourcing critical information pertaining to herb-drug interactions.

REVIEW ARTICLE

Acta Pharm. Sci. Vol 62:(2), 2024
Review article
DOI: 10.23893/1307-2080.APS6216

Vehicle noise pollution awareness for human health and environmental impacts: A comprehensive review

Akif YAVUZ[1], Ayşe Nur HAZAR-YAVUZ[2*], Süleyman Enes HACIBEKTAŞOĞLU[3]

1 Faculty of Mechanical Engineering, Istanbul Technical University, Istanbul, Türkiye
2 Department of Pharmacology, Faculty of Pharmacy, Marmara University, Istanbul, Türkiye
3 Occupational Health and Safety, Faculty of Health Sciences, Sinop University, Sinop, Türkiye

ABSTRACT

This comprehensive review explores the extensive and intricate effects of vehicle noise on human health and provides insights into experimental studies using animal models, primarily rats, to understand the impact of low-frequency vehicle noise. Furthermore, the effects of factors such as engine type and size, vehicle speed, air conditions and traffic density on vehicle noise levels are reviewed. The adverse health consequences of vehicle noise include disruptions in sleep patterns, anxiety, mood disorders, cardiovascular risks, noise-induced hearing loss, and gastrointestinal problems. To mitigate these risks, various recommendations and regulations (WHO Environmental Noise Guidelines for the European Region) are put in place, emphasizing the need for noise reduction in transportation and the responsible use of sound-emitting devices. This study serves as a comprehensive resource for understanding the intricate relationships between vehicle noise and human and animal health, emphasizing the importance of addressing vehicle noise pollution for overall well-being and public health.

Keywords: vehicle noise, human health, animal models, low frequency noise

* Corresponding author: Ayşe Nur HAZAR-YAVUZ
E-mail: ayse.hazar@marmara.edu.tr
ORCIDs:
Akif YAVUZ: 0000-0002-9447-7306
Ayşe Nur HAZAR YAVUZ: 0000-0003-0784-8779
Süleyman Enes HACIBEKTAŞOĞLU: 0000-0002-8997-8480
(Received 2 Nov 2023, Accepted 21 Nov 2023)

INTRODUCTION

Vehicle noise from cars, trucks, motorcycles and other transportation and agriculture vehicles has both direct and indirect effects on health. The specific impact on organ health varies depending on factors such as the type and intensity of noise, duration of noise exposure, individual sensitivity and general health status[1]. Vehicle noise can disrupt sleep cycles, especially at night. Poor sleep quality can affect the functioning of various organs and systems, including the brain, immune system and metabolism. Chronic exposure to vehicle noise, especially in densely populated urban areas, has been associated with an increased risk of hypertension. High noise levels can trigger stress responses leading to higher blood pressure levels, which, together with sleep disturbances, can strain the heart and increase the risk of cardiovascular disease[2]. Prolonged exposure to high levels of vehicle noise is associated with an increased risk of heart disease and stroke. Noise, which activates stress response of body and causes the release of stress hormones such as cortisol, can negatively affect various systems, including immune systems. Especially for individuals living near busy roads, prolonged exposure to vehicle noise can cause anxiety and mood disorders[3].

Chronic noise-related stress affects mental health and well-being. High-decibel vehicle noise, such as that produced by motorcycles, modified car engines or loud exhaust systems, can cause noise-induced hearing loss over time[4]. Chronic stress from continuous exposure to vehicle noise can potentially exacerbate gastrointestinal conditions such as irritable bowel syndrome or worsen symptoms of existing conditions. Although vehicle noise can have indirect effects on health through stress responses and sleep disturbance, it is important to note that the primary health risks are usually associated with prolonged exposure to high-decibel noise and the chronic stress it causes[5]. Reducing exposure to vehicle noise, using noise-canceling technologies, and implementing noise mitigation measures in urban planning and transportation infrastructure can help reduce these health risks. Furthermore, maintaining a healthy lifestyle, managing stress and getting medical care, when necessary, can also contribute to the health of people in noisy environments.

Numerous recommendations and legal frameworks have been established, both in Türkiye and globally, with the objective of mitigating the impact of noise exposure on human health. The WHO Environmental Noise Guidelines for the European Region established in 2018 offer recommendations aimed at safeguarding human health against environmental noise exposure stemming from diverse sources, including transportation-related sources such as road

traffic, railway, and aircraft noise, as well as noise generated by wind turbines and leisure activities[6]. Recommendations related to road traffic are given below:

- The Guideline Development Group (GDG) strongly advocates diminishing average noise exposure levels caused by road traffic to levels below 53 dB L_{den}. Noise levels exceeding this threshold are linked with detrimental health outcomes, emphasizing the imperative for noise reduction measures in the context of road traffic.
- GDG strongly proposes decreasing nocturnal noise exposure levels resulting from road traffic to levels below 45 dB L_{night}. Noise levels surpassing this threshold during nighttime hours have been correlated with detrimental effects on sleep, underscoring the imperative need for noise reduction measures specific to night-time road traffic.
- To mitigate health-related consequences, GDG highly recommends for policymakers to enact appropriate measures aimed at diminishing noise exposure emanating from aircraft, particularly within populations exposed to noise levels surpassing the stipulated guideline values for both average and nocturnal noise exposure. The GDG further suggests the implementation of specific interventions involving modifications to infrastructure.

The Regulation on Environmental Noise Control, which was enacted in 2022, aims to prevent the negative effects of environmental noise on the environment and human health, to prepare noise maps and noise action plans, to implement noise control measures to reduce environmental noise and to inform the public about environmental noise management works in Türkiye[7].

In this regulation, environmental noise criteria for transportation sources are determined as follows:

- The level of environmental noise emitted from transportation sources shall not exceed 65 dB(A) $LA_{eq.5min}$ during the day, 60 dB(A) $LA_{eq.5min}$ in the evening and 55 dB(A) $LA_{eq.5min}$ at night.
- Transportation vehicles are required to utilize state-of-the-art technologies to minimize environmental noise emissions.
- The noise reduction apparatus installed in the horns and exhaust systems of motor vehicles must not be altered or rendered non-functional.
- Horns or sound-emitting devices on or within motor vehicles should not be operated in a manner that creates noise disturbances, except in cases of mandatory necessity.

METHODOLOGY

Vehicle noise levels and affecting parameters

Today, vehicles, especially transportation vehicles, are an important part of human daily lives. However, the noise emitted by vehicles poses a significant problem for both the environment and human health. The main parameters that cause vehicle noise can be defined as the contact of the vehicle wheels with the ground, engine operation and air resistance. In addition to these basic parameters, vehicle noise is generated and propagated into the environment as a result of the combination of many factors[8,9]. The parameters affecting the levels of vehicle noise are given in Table 1.

Table 1. The effects of different parameters on vehicle noise level

Parameters Affecting Vehicle Noise Level	Comments
Engine Power and Type	Engine power and type of the vehicle is one of the main factors affecting noise levels. Generally, engines with larger cylinder displacement and engines that can produce more power emit more noise to the environment. The noise emitted by a diesel internal combustion engine is considerably higher than the noise emitted by a gasoline engine. The amount of this excess varies depending on vehicle models and engine displacement, but on average diesel engines generate 6 to 10 dB(A) more noise[10,11].
Vehicle Speed	Regardless of the type of vehicle, increasing vehicle speeds have a significant impact on noise levels from vehicles. As the vehicle speed increases, the airflow creates more friction on the vehicle surface, which can lead to an increase in aerodynamic noise. High-speed trains and airplanes in particular can generate high noise levels at high speeds. The influence and importance of vehicle design parameters on aerodynamic noise levels is high. Vehicle designs play an important role in reducing noise level. In addition, wheel noise occurs when the vehicle's wheels come into contact with the road surface. Therefore, as the speed of the vehicle increases, the wheels have the potential to generate more noise[12,13].
Wheel and Road Interaction	The contact of the wheels with the road surface is one of the main sources of noise emission. The roughness of the road surface, type of road surface material, and road maintenance all impact on vehicle noise[14,15].
Tire types	The tires of a vehicle produce noise when they come into physical contact with the road. Factors such as tire patterns, material, pressure, and types have effects on tire-induced vehicle noise[16,17].
Vehicle Technology	Unlike gasoline and diesel engines, recently developed new generation electric vehicle models have engines (electric motors) that operate at lower noise levels and have features such as better noise insulation. This means that new generation vehicles cause less noise pollution[18-20].

Air Temperature	The temperature of the air has an impact on the speed and path of sound spread. Sound waves propagate faster in cold weather, which can lead to an increase in noise levels from vehicles. Hot weather, on the other hand, can cause sound to propagate more slowly[21,22].
Air Humidity	Air density and speed of sound are affected by air humidity. High humidity levels can cause sound to propagate faster and increase noise levels[23,24].
Echoes and Reflections	This issue is related to the reflection and reverberation of sound waves by environmental factors emitted from vehicle noise sources. The echoes and reflections are very significant in terms of noise dispersion. Reflection means that sound waves emitted from a noise source are reflected back when they encounter an obstacle. This reflection can cause the sound to be reflected more than once, resulting in a more complex noise pattern. Environmental echoes and reflections can cause noise levels to increase by reflecting sound waves from nearby environmental features (e.g. buildings, walls and vehicles). These echoes can contribute to the transmission of noise over greater distances. High building density and heavy traffic, especially in urban areas, can cause more of these echoes and increase noise pollution. Therefore, the environmental characteristics of the area through which a vehicle passes influence our level of noise detection[25,26].
Horn Use and Exhaust System	Today, the excessive use of horns by vehicle drivers where they are not needed and the characteristics of vehicle exhaust systems can lead to an increase in vehicle noise levels[27,28].

Traffic density: The presence of too many vehicles on the road causes high levels of noise. Urban traffic density is one of the most important parameters that increase noise from vehicles[29,30]. In road vehicles, each type of vehicle has specific level of noise (dBA). Although the sound pressure levels of all vehicle types vary depending on different parameters, the average vehicle noise levels emitted by different vehicle types was determined in the literature[31]. In addition, sound pressure levels are modeled as a function of vehicle speed for different vehicle types and equations are given in the Table 2 below.

Table 2. Noise level calculations for different vehicle types[31]

Vehicle Class	Equation
Heavy Trucks	12.59logV+60.64
Long Trucks	10.88logV+63.98
Medium Trucks	24.06logV+34.90
Short Trucks	14.60logV+44.69
Cars	30.41logV+13.59
V = Speed of vehicle (km/h)	

The increase of the dB unit, which expresses the level of noise, has a logarithmic character. Therefore, the addition of noise levels cannot be done arithmetically. The summation of sound levels obtained from different noise sources is performed logarithmically. The total sound pressure level emitted by vehicles can be estimated using the following equation:

$$SPL_{total}=10\log_{10}\left[10^{SPL1/10}+10^{SPL2/10}+10^{SPL3/10}+10^{SPLn/10}\right]dB$$

SPL_1: First vehicle sound source

SPL_2: Second vehicle sound source

SPL_3: Third vehicle sound source

SPL_n: nth vehicle sound source

In the above equation, is the total sound pressure level and n is the number of noise sources. The effect of vehicle types and speeds on noise pollution is made more understandable with 7 different models. The effects of various types of vehicles (Heavy Trucks, Long Trucks, Medium Trucks, Short Trucks, and Cars) in traffic on sound pressure levels are compared in terms of different vehicle speeds (10 km/h, 20 km/h, and 100 km/h). In some models, the density of trucks in traffic is low levels (Model 1-5), while in some models this density is quite high levels (Model 6-7). The aim here is to mathematically analyze the effects of various types of vehicles and vehicle speeds on noise levels. In this way, detailed information about the sound pressure levels from trucks and cars can be obtained. Using the equations given in Table 2, the noise levels generated by each vehicle are calculated as a function of vehicle speed. Then, by defining certain ratios for each vehicle type, its density in traffic is simulated. As a result, calculations are performed and the sound pressure levels in different models are determined. Details about the models and results are available in the Table 3.

Table 3. Vehicle noise simulation

Model Number	Distribution of Vehicle Types					Noise Emission Level (dBA)		
	Heavy Trucks	Long Trucks	Medium Trucks	Short Trucks	Cars			
Model 1	%0	%0	%0	%0	%100	54	63	84
Model 2	%0.3	%1.6	%2.5	%3.4	%92.2	88	92	106
Model 3	%1	%3.2	%4.6	%6.3	%84.9	91	95	107
Model 4	%3.5	%4.9	%7.1	%9.6	%74.9	94	97	108
Model 5	%7.2	%6.7	%9.8	%13.9	%62.4	96	99	110
Model 6	%13.2	%16.7	%20.1	%27.8	%22.2	99	103	112
Model 7	%50.3	%29.4	%16.7	%3.6	%0	103	106	115

With only cars in traffic (Heavy Trucks= Long Trucks= Medium Trucks= Short Trucks=0%, Cars=100%), the sound pressure levels emitted for average vehicle speeds of 10 km/h, 20 km/h, and 100 km/h are 54 dBA, 63 dBA, and 84 dBA, respectively. However, as the proportion of trucks in traffic increase, sound pressure levels at all vehicle speeds increase. Especially heavy trucks have a significant impact on vehicle-borne noise generation. In Model 1, the SPL level when there are no heavy trucks is 54dB (10 km/h), while in Model 2, the SPL level increases to 88dB when there are 0.3% heavy trucks in the traffic. In Model 7, where the proportion of heavy trucks is the highest, the SPL levels are quite high for all vehicle speeds (10 km/h, 20 km/h, and 100 km/h). In this model, there are no cars in traffic. Therefore, the emitted noise levels are 103 dBA, 106 dBA, and 115dBA at 10 km/h, 20 km/h, and 100 km/h.

Vehicle noise, commonly referred to as transportation noise, encompasses the sound waves generated during the operation of motorized vehicles, including automobiles, trains, airplanes, ships, and the others. This noise is typically quantified in decibels (dB). While standard conversation registers at approximately 60 dB, the noise level during an aircraft's takeoff can reach 120 dB or even higher. These levels are subject to fluctuations influenced by the factors elucidated above. Trucks and commercial vehicles, due to their larger engine capacities and passenger/cargo-carrying capabilities, generally induce higher noise levels. Noise levels during truck operation frequently range from 85 to 90 dB or beyond. These elevated noise levels contribute to environmental noise pollution, particularly in densely populated urban traffic zones, thereby posing considerable risks to human health. Given its utilization in both freight and passenger transportation, rail transportation raises a distinct and pertinent concern regarding noise levels. High-speed trains may produce less noise

compared to traditional locomotives, but even high-speed trains can generate noise levels exceeding 100 dB. Locomotives and freight trains can produce noise levels as high as 110 dB. Aviation noise primarily occurs during aircraft takeoffs, landings, and in-flight operations. The intensity of this noise can exhibit substantial variations contingent upon the aircraft type, engine characteristics, and flight altitude. A commercial passenger aircraft, during takeoff and landing, can generate noise levels ranging from 130 to 140 dB. This can result in serious noise-related health issues for individuals residing in proximity to airports. Maritime transportation noise levels are contingent on factors such as ship type, engine power, and sea conditions. Ships can produce noise levels in the range of 90-100 dB during their engine operations[32-34].

Effects of noise levels on human health

Noise is an important environmental pollution that has been proven to have a significant adverse impact on human health and to which we are highly exposed in our lives. Noise emissions can cause various physical and psychological problems on human health[35,36]. Noise pollution is a growing concern in our increasingly urbanized and modernized world. Noise pollution refers to the situation where environmental sound levels are excessively high and disturbing. While most noise sources did not exist years ago, new noise sources are entering our lives every day. Vehicle noise is one of the main noise sources that have entered our lives in the last century of human history and affect public health. Although vehicle noise seems to be an inevitable part of modern life, its harmful effects on human health cannot be ignored. Table 4 below shows the effects of different noise levels on human health[37]. In addition, Table 5 shows the sound pressure levels that can be legally exposed to in a day in Türkiye[38].

Table 4. Effects of noise levels on human health

Noise Magnitude (dB)	Effects on Human Health
<65 dB	It is not directly harmful to human health.
65 dB – 90 dB	Tension and stress increases in people.
	Respiratory acceleration is observed.
	Tachycardia is observed.
	Blood pressure rises.
90 dB – 120 dB	Damage occurs to cells related to hearing.
<120 dB	Fatal effects may occur.

Table 5. Noise levels that can be legally exposed to in Türkiye in a day

Duration of exposure to noise (h)	Maximum noise level (dBA)
7.5	80
4	90
2	95
1	100
0.5	105
0.25	110
1/8	115

Effects on ear and hearing

Hearing is a vital sense that allows us to connect with the world around us. The hearing system is a complex structure of organs, tissues and sensory receptors that work in harmony to convert sound waves into meaningful information. But this remarkable system is vulnerable to a variety of external influences, including vehicle noise, one of the modern world's forms of pollution. Vehicle noise is a type of noise that can have significant and long-term effects on the hearing system and overall hearing health. Drawing on scientific studies and literature, the multifaceted effects of noise on the hearing system have been examined. Some of the effects of noise on the hearing system are given Table 6[39-43].

Table 6. Effects of vehicle noise on the hearing system

Effects	Comments
Hearing Loss	Noise-Induced Hearing Loss (NIHL) is one of the most direct and alarming effects of noise exposure. The hearing system can be severely damaged by prolonged or intense exposure to loud noise. In particular, it damages the hair cells in the cochlea, leading to permanent hearing loss. NIHL is usually irreversible and hearing loss can range from mild to severe
Hyperacusis	Hyperacusis refers to a condition of increased sensitivity to sounds, especially high-pitched noises. It often occurs after noise trauma and can make every day sounds painfully loud.
Hidden Hearing Loss	Hidden hearing loss is a recently discovered type of hearing loss. This type of hearing loss refers to a condition where traditional hearing tests fail to detect damage to the hearing system, but individuals may have difficulty hearing in noisy environments.
Tinnitus	Tinnitus is defined as a continuous ringing, buzzing or hissing sound in the ears. Noise exposure is associated with damage to the hair cells, especially in the cochlea, and can cause tinnitus to occur. Tinnitus is a distressing condition and can negatively affect a person's quality of life.
Altered Auditory Processing	Chronic exposure to noise can affect how the brain processes sound. This can lead to difficulties in understanding speech and processing complex auditory information.

Tympanic Membrane Damage	Exposure to extremely loud noises, especially aircrafts, can tear the eardrum, causing pain and sometimes permanent damage.
Difficulty understanding speech	Vehicle noise can cause speech comprehension difficulties. With high levels of vehicle noise, speech sounds are masked by the noise. This makes it difficult to understand speech.
Temporary Threshold Shift (TTS)	After exposure to loud noise, individuals may experience a temporary decrease in their hearing sensitivity, known as TTS. This is typically reversible and can recover within a few hours or days, but repeated TTS can contribute to permanent hearing damage over time.

Effects on heart

Vehicle noise directly or indirectly affects our physical health and especially heart health. Detailed ways in which vehicle noise affects the heart are given Table 7[44-46].

Table 7. Effects of vehicle noise on heart

Effects	Comments
High Blood Pressure	Chronic noise exposure is associated with hypertension (high blood pressure). Increased blood pressure, if left uncontrolled, can lead to heart disease, stroke, and other cardiovascular problems.
Disruption of Sleep Patterns	Noise can interfere with quality sleep time, leading to sleep deprivation and poor sleep quality. Inadequate sleep is associated with an increased risk of heart disease and other cardiac problems.
Increased Stress Response	Exposure to high levels of continuous noise can trigger a reaction in the body, causing the release of stress hormones such as cortisol and adrenaline. These hormones can increase blood pressure and heart rate, putting more strain on the heart.
Inflammatory Response	Prolonged exposure to noise can trigger an inflammatory response in the body. Inflammation can lead to the development of atherosclerosis and other heart-related problems.
Endothelial Dysfunction	The inner lining of blood vessels, known as the endothelium, plays a critical role in regulating blood flow. Stress from vehicle noise can lead to endothelial dysfunction, impairing blood vessel function and potentially causing heart problems.
Heart Rhythm Irregularities	Some studies suggest that noise pollution may increase the risk of cardiac arrhythmias (irregular heartbeats), which can be harmful to heart health[47].

Effects on the brain and neural system

The brain is not an organ resistant to the effects of noise pollution. The effects of vehicle noise on the brain and nervous system are given Table 8[48-50].

Table 8. Effects of vehicle noise on the brain and neural system

Effects	Comments
Stress Response	Vehicle noise is a very important stress factor. Prolonged or intense noise exposure can trigger the release of stress hormones such as cortisol and adrenaline. Noise pollution can lead to a range of psychological problems, including chronic stress, anxiety, and depression.
Cognitive Impairments	Chronic exposure to vehicle noise can impair cognitive functions. Some studies have shown that noise can interfere with attention, memory, problem-solving and decision-making abilities[51].
Sleep Disorders	Noise emissions from vehicles can disrupt sleep patterns, leading to sleep deprivation and poor sleep quality. Adequate sleep is vital for cognitive functioning and sleep disturbances can affect memory, learning and general mental state.
Reduced Brain Plasticity	Noise-induced stress can reduce the brain's plasticity, its ability to adapt and reorganize. This can have implications for learning and recovery from brain injuries.
Changes in Brain Structure	Some studies show that chronic noise exposure can lead to structural changes in the brain, including changes in the size of certain brain regions. These structural changes may be linked to cognitive and emotional problems[51].

Effects on the endocrine system

The endocrine system is known as a network of glands and organs in the body. The hormones within this system help the body functions, like metabolism, growth and development, emotions, mood, sexual function, and even sleep quality. The effects of noise pollution on the endocrine system are multifaceted and complex. These effects are listed Table 9[52-54].

Table 9. Effects of vehicle noise on the endocrine system

Effects	Comments
Long-Term Stress	Chronic stress, often triggered by noise pollution, disrupts the balance of hormones in the endocrine system. This can lead to imbalances in various hormones, including insulin, thyroid hormones and reproductive hormones.
Adrenal Gland Function	The adrenal glands, part of the endocrine system, are responsible for the production of stress hormones. Continuous exposure to vehicle noise can lead to overactivity or dysregulation of these glands, affecting hormone balance.
Metabolic Impact	Stress from vehicle noise can interfere with metabolic processes, potentially causing problems such as weight gain and metabolic syndrome.
Thyroid Hormones	Noise-induced stress can affect the function of the thyroid gland, affecting the production of thyroid hormones. This can lead to metabolic problems, fatigue, and psychological problems.
Reproductive Hormones	Noise emissions have been linked in some studies to disruptions in the menstrual cycle and changes in reproductive hormone levels. These changes can affect fertility and reproductive health[55].

Effects on the gastrointestinal system

The gastrointestinal system, also known as the digestive system, includes various organs such as the mouth, esophagus, stomach, liver, gall bladder, pancreas and intestines, and works in harmony to maintain the body's balance of energy and nutrients. Noise pollution can have complex effects on the gastrointestinal system. These effects are listed Table 10[56,57].

Table 10. Effects of vehicle noise on the gastrointestinal system

Effects	Comments
Stress-Induced Digestive Problems	Especially prolonged or intense noise can trigger the stress response of body. This stress can lead to overproduction of stress hormones such as cortisol, which can disrupt normal digestive processes. Chronic stress is associated with problems such as irritable bowel syndrome (IBS), indigestion and changes in bowel habits.
Increased Acidity Level	Stress caused by noise can lead to an increase in stomach acid production. This can exacerbate conditions such as gastritis or gastroesophageal reflux disease (GERD) and cause stomach disorders.
Inflammatory Response	Prolonged exposure to noise can trigger an inflammatory response in the body. Chronic inflammation can lead to the development of IBD, Crohn's disease and ulcerative colitis.
Gut Microbiota	Stress caused by noise pollution can affect the composition and diversity of the gut microbiota. This can affect nutrient absorption, digestion and overall gut health.

Noise studies in experimental animals

The known effects of vehicle noise on human health above were mostly obtained using studies on people known to be exposed to noise. Since the negative effects of continuous or repeated exposure to this type of noise on human health are known, modeling in humans and investigating the unknown effects of noise cannot be widely used. For this reason, vehicle-related noise can be modelled using experimental animals and the effects and mechanism of noise can be investigated.

Noise problems caused by vehicles are generally not observed in high-frequency bands (≥2000 Hz). High-frequency sounds are sounds in which sound waves vibrate faster and create shorter waves. Such sounds are often called "thin" or "treble"[58]. For example, the ringing of a bell or bird calls are high-frequency. These tones are not observed in noise originating from vehicles, instead low-frequency noises are observed. For this reason, low-frequency sounds are used when creating vehicle-related noise models in experimental animals.

Some experimental animal studies that may reflect vehicle noise types and the results obtained from these studies are summarized below.

Vasilyeva et al. investigated the effects of low-frequency noise (LFN) exposure on rats. Rats were exposed to single or multiple LFN sessions with varying sound pressure levels. The results showed a significant increase in chromosomal aberrations in bone marrow cells, along with the appearance of dicentric chromosomes, indicative of DNA double-strand breaks. Additionally, there were significantly elevated levels of low-molecular-weight DNA (lmwDNA) in the blood plasma after LFN exposure, and this effect persisted in the week following exposure. The findings suggest that LFN exposure may have mutagenic effects and cause extensive cell death, possibly through enhancing cellular apoptosis[59].

Venet et al. investigated the alone and combined effects of LFN and carbon disulfide (CS_2) exposure on rat hearing. The study involved exposure to LFN at 106 dB sound pressure level (SPL) and increasing concentrations of CS_2 during four weeks. Exposure to noise alone resulted in auditory deficits in a specific frequency range, indicating the potential to affect cochlear regions detecting mid-range frequencies. When rats were co-exposed to CS_2 at higher concentrations and noise, the damaged frequency range expanded, with significant deficits observed at 9.6 kHz. However, histological examination revealed that neither hair cells nor ganglion cells were damaged by CS_2. This discrepancy between functional and histological data highlights the need to consider CS_2 as a significant factor in hearing conservation regulations[60].

Mancera et al. examined the effects of mining vehicle noise on the behavior and physiological responses of wild mice. The noise was categorized into high-frequency (>2 kHz) and low-frequency (≤2 kHz) ranges. The results showed that exposure to high-frequency noise led to increased stress-related behaviors, such as reduced time spent in nests and increased circling, especially in females. These effects were associated with elevated levels of fecal corticosterone, indicating stress. In contrast, exposure to low-frequency noise reduced grooming and circling, suggesting a milder stress response. Low-frequency noise also increased fecal corticosterone levels in males, potentially due to gender-based differences in frequency sensitivity. The findings highlight the potential impact of different frequency spectra of mining noise on animal welfare and survival[61].

This study investigated the health effects of exposure to inaudible LFN on the inner ear of mice, simulating the levels to which people might be exposed in daily life. The research focused on stress-reactive molecules in the inner ear. Exposure to LFN led to a significant increase (more than 5-fold) in the transcript level of heat shock protein 70 (Hsp70) in the whole inner ear. However,

the levels of other stress-reactive molecules were largely unchanged. Specifically, the transcript level of Cebpb, a transcriptional activator for Hsp70, was more than threefold increased by LFN exposure. While Hsp70 levels increased in the vestibule, they remained comparable in the cochleae of LFN-exposed and unexposed mice. These findings suggest that the inner ear may be negatively affected by stress from inaudible LFN exposure, and Hsp70 and Cebpb levels could serve as potential biomarkers for response to LFN exposure[62].

Chalansonnet et al. examined the impact of LFN combined with CS_2 exposure on balance in rats. It found that this combination significantly decreased saccade number and duration, indicating vestibular impairment. However, the effects were reversible and did not result in histopathological changes or behavioral differences. The study suggests that post-rotatory nystagmus, a specific eye movement, could serve as an early, non-invasive indicator of CS_2 intoxication in occupational health monitoring programs[63].

This study investigated the impact of acute LFN exposure on mice. Exposure to LFN at 100 Hz and 95 dB for just 1 hour caused irreversible balance issues in the mice. It also resulted in decreased vestibular function and damage to the otoconial membrane in the vestibule. However, overexpression of the stress-reactive molecular chaperone, heat shock protein 70 (Hsp70), which is induced by prolonged LFN exposure, rescued the LFN-induced imbalance and structural damage to the otoconial membrane[64].

Maes et al. investigated those two experiments examined the impact of irregular, moderate-intensity auditory noise on rats' performance in an operant discrimination task. The first experiment revealed that noise impaired discrimination performance. The second experiment showed that discrimination performance was best when the noise condition at test matched the noise condition at training. The results highlight the importance of considering noise conditions in research, suggesting the need for a 2x2 factorial design with noise presence/absence during training and testing as factors in studies on noise effects in humans and animals[65].

Stewart et al. used a rat model to investigate the effects of noise exposure on the vestibular system. Noise exposure led to hearing loss and caused substantial damage to sensory stereocilia bundles in various parts of the inner ear. Vestibular afferent activity was moderately reduced, and changes were observed in the response to head rotation. However, immediate clinically measurable vestibular signs were not evident. The study suggests that noise exposure can damage the peripheral vestibular system, potentially leading to vestibular disorders over time[66].

McCarthy et al. investigated the impact of noise stress on the biological function of leukocytes involved in wound healing in rats. Rats exposed to 80 dB sound pressure level for 24 hours showed reduced secretion of superoxide radical and interleukin-1 by neutrophils and macrophages compared to control animals. Lymphocyte function remained unaffected. The findings suggest that short-term noise stress can alter the biological functions of specific leukocyte subpopulations[67].

Escabi et al. investigated that rats serve as valuable models for studying noise-induced hearing loss due to their similarities with human auditory physiology. This paper reviews the use of the rat model in researching the effects of noise exposure on the mammalian auditory system, including both hearing loss and central nervous system alterations. It also highlights the rat model's relevance in studying cochlear synaptopathy. The rat model offers insights into the structural, anatomical, physiological, and perceptual aspects of hearing affected by noise[68].

Baldwin et al. exposed rats to daily noise and investigated its effects on microvascular leakiness in the mesenteric microcirculation and mast cell degranulation. Rats exposed to noise had increased microvascular leaks, but those given dietary supplements of vitamin E with α-lipoic acid or Traumeel showed reduced leakiness and mast cell degranulation. This suggests that dietary supplements can mitigate the structural damage caused by excessive noise in rats[69].

RESULTS and DISCUSSION

Noise pollution constitutes a significant component of environmental degradation in both developed and developing nations. It can be regarded as a form of technological residue that extensively contributes to environmental pollution by disturbing the inherent features of the environment. Additionally, noise pollution poses a notable detriment to human health and well-being. In the realm of environmental issues, noise pollution is gaining increasing significance, necessitating urgent efforts for mitigation. Prolonged exposure to noisy environments is observed to lead to severe health issues among individuals[70,75].

This study highlights key parameters influencing vehicle noise, such as engine power and type, vehicle speed, wheel and road interaction, tire types, vehicle technology, air temperature, air humidity, echoes and reflections, horn use, exhaust systems, and traffic density. These factors can lead to considerable variations in noise levels emitted by different types of vehicles, from cars to trucks, helicopters, and jets. The study presents detailed models that simulate noise levels based on the proportion of vehicle types in traffic and vehicle

speeds, emphasizing the significant impact of trucks, especially heavy trucks, on overall noise pollution. Moreover, the study underscores the substantial noise levels generated by different modes of transportation, including road vehicles, trains, airplanes, and ships. These noise levels can reach potentially harmful levels, particularly for individuals living near transportation routes and urban centers.

The hearing system is among the most vulnerable, with Noise-Induced Hearing Loss (NIHL) being a primary concern. Prolonged exposure to loud noise can lead to permanent hearing damage, often ranging from mild to severe. This article underscores the urgency of addressing noise pollution to safeguard individuals from hearing-related issues, including hyperacusis, hidden hearing loss, tinnitus, and difficulties in auditory processing. Furthermore, the article delves into the significant repercussions on heart health. Chronic noise exposure is associated with high blood pressure, sleep disturbances, increased stress responses, inflammatory reactions, endothelial dysfunction, and potential heart rhythm irregularities. These findings underscore the importance of noise reduction measures to protect cardiovascular health. The impact on the brain and neural system is equally extensive. Noise pollution serves as a significant stressor, contributing to a range of psychological problems, cognitive impairments, sleep disorders, reduced brain plasticity, and structural changes in the brain. These effects emphasize the necessity of addressing noise pollution for the overall well-being of the nervous system. The article also uncovers the intricate effects on the endocrine system, wherein chronic stress disrupts hormone balance, adrenal gland function, metabolic processes, thyroid function, and reproductive hormones. These disruptions have profound implications for overall health and require urgent attention. Finally, the article addresses the complex consequences of noise pollution on the gastrointestinal system, revealing the potential for stress-induced digestive problems, increased acidity, inflammatory responses, and disruptions in gut microbiota. These issues may lead to conditions such as irritable bowel syndrome and inflammatory bowel diseases, necessitating a comprehensive approach to mitigate noise-induced gastrointestinal complications.

In conclusion, this article provides a comprehensive overview of various experiments conducted on experimental animals, primarily rats, to understand the effects of LFN and noise pollution. These studies shed light on the potential health impacts of noise exposure, covering a range of aspects from genetic and physiological responses to behavioral and auditory changes in these animals. Some key findings include the potential mutagenic effects of LFN exposure,

its impact on hearing deficits, the role of different frequency spectra in stress-related behaviors, and the involvement of stress-reactive molecules in the inner ear's response to noise. Furthermore, the article explores the combined effects of LFN with other factors such as carbon disulfide (CS2), shedding light on their influence on balance and vestibular functions in rats. Additionally, it touches upon the potential for dietary supplements to mitigate structural damage caused by noise exposure in experimental animals. Overall, these studies emphasize the intricate interplay between noise and various biological systems in animals, offering insights into potential biomarkers and responses to noise exposure. These animal experiments not only provide valuable insights into the biological and physiological effects of noise but also underscore the importance of considering noise conditions in research design, which has implications for both animal studies and human health research. Moreover, the use of animal models, particularly rats, proves to be a valuable tool for investigating noise-induced hearing loss and other health-related consequences.

To mitigate the health risks posed by vehicle noise, various recommendations and legal frameworks have been established, both globally and in Türkiye. The WHO Environmental Noise Guidelines for the European Region offer specific guidelines to safeguard human health against environmental noise exposure from various sources, with a focus on road traffic, aircraft noise, and more. Türkiye has enacted the Regulation on Environmental Noise Control to prevent the negative effects of environmental noise, including noise maps, noise action plans, and the implementation of noise control measures. These measures and guidelines are crucial for reducing the harmful impact of vehicle noise on public health. They emphasize the need for noise reduction in transportation sources, the use of state-of-the-art noise-reduction technologies, and the responsible operation of sound-emitting devices in motor vehicles. By implementing these recommendations and regulations and by adopting a healthy lifestyle, managing stress, and seeking medical care when necessary, individuals and communities can work together to mitigate the health risks associated with vehicle noise in noisy environments. Official reassessment of road noise occurs under the following circumstances: when a new road is constructed, when new residential properties are built, when alterations are made to an existing road, and when there is an increase in traffic volume on a road. Strategies to mitigate the environmental repercussions of road traffic noise include the adoption of quieter vehicles, installation of noise-absorbing tires, advancement in noise-reducing road surfaces, enforcement of traffic measures such as speed reduction, installation of noise barriers, and enhancement of home insulation.

A significant portion of the populace remains uninformed about the issue of noise pollution, despite its substantial impact on many individuals. The lack of awareness among the general population contributes to the escalation of noise pollution. Therefore, there is a pressing need to raise awareness about the detrimental effects of noise pollution.

STATEMENTS OF ETHICS

This article does not contain any studies with human participants or animals performed by any of the authors.

CONFLICT OF INTEREST STATEMENT

The authors declare there is no conflict of interest associated with this study.

AUTHOR CONTRIBUTIONS

All authors contribute the work equally throughout.

REFERENCES

1. Moudon AV. Real noise from the urban environment: how ambient community noise affects health and what can be done about it. Am J Prev Med, 2009;37(2):167-171. Doi: 10.1016/j.amepre.2009.03.019

2. Gloag D. Noise and health: public and private responsibility. BMJ, 1980;281(6252):1404.

3. Welch D. Shepherd D, Dirks KN, McBride D, Marsh S. Road traffic noise and health-related quality of life: a cross-sectional study. Noise health, 2013;15(65), 224-230. Doi: 10.4103/1463-1741.113513

4. Clark C, Stansfeld, SA. The effect of transportation noise on health and cognitive development: a review of recent evidence. Int J Comp Psychol, 2007;20(2):145-158. Doi:10.46867/IJCP.2007.20.02.10

5. Jalali M, Saki G, Sarkaki AR, Karami K, Nasri S. Effect of noise stress on count, progressive and non-progressive sperm motility, body and genital organ weights of adult male rats. J Hum Reprod Sci, 2012;5(1):48-51. Doi: 10.4103/0974-1208.97801

6. World Health Organization. Environmental noise guidelines for the European region. Regional Office for Europe: World Health Organization; 2018. 160.

7. Environmental Noise Control Regulation. T.R. Ministry of Environment, Urbanization and Climate Change. Official Gazette dated 30 November 2022 and numbered 32029.

8. Wang X. Vehicle noise and vibration refinement. Elsevier: Woodhead Publishing; 2010. 448.

9. Close WH, Wesler JE. Vehicle noise sources and noise-suppression potential. Transp Res Rec Special Report, 1975;152:14-33.

10. Lu MH, Jen MU. Source identification and reduction of engine noise. Noise Control Eng J, 2010;58(3):251-258. Doi:10.3397/1.3427147

11. Liu Y, Jia YB, Zhang XJ, Liu ZC, Ren YC, Yang B. Noise test and analysis of automobile engine. Appl Mech Mater, 2013;307:196-199. Doi:10.4028/www.scientific.net/AMM.307.196

12. Freitas E, Mendonça C, Santos JA, Murteira C, Ferreira JP. Traffic noise abatement: how different pavements, vehicle speeds and traffic densities affect annoyance levels. Transp Res D Transp Environ, 2012;17(4):321-326. Doi:10.1016/j.trd.2012.02.001

13. Behzad M, Hodaei M, Alimohammadi I. Experimental and numerical investigation of the effect of a speed bump on car noise emission level. Appl Acoust, 2007;68(11-12):1346-1356. Doi:10.1016/j.apacoust.2006.07.003

14. O'Boy DJ, Dowling AP. Tyre/road interaction noise-numerical noise prediction of a patterned tyre on a rough road surface. J Sound Vib, 2009;323(1-2):270-291. Doi:10.1016/j.jsv.2008.12.024

15. Sakhaeifar M, Banihashemrad A, Liao G, Waller B. Tyre-pavement interaction noise levels related to pavement surface characteristics. Road Mater Pavement Des, 2018;19(5):1044-1056. Doi:10.1080/14680629.2017.1287770

16. Ponniah J, Tabib S, Lane B, Raymond C. Evaluation of the effectiveness of different mix types to reduce noise level at the tire/pavement interface [Internet]. (2010, September). Halifax: Transportation Association of Canada; 2010 [2023 October 30].

17. Veres RE. A tire noise investigation and test method. SAE Trans, 1976;85:651-670.

18. Dupont JB, Aydoun R, Bouvet P. Simulation of the noise radiated by an automotive electric motor: influence of the motor defects. SAE Int J Altern Powertrains, 2014;3(2):310-320. Doi:10.4271/2014-01-2070

19. Campello-Vicente H, Peral-Orts R, Campillo-Davo N, Velasco-Sanchez E. The effect of electric vehicles on urban noise maps. Appl Acoust, 2017;116:59-64. Doi:10.1016/j.apacoust.2016.09.018

20. Cesbron J, Bianchetti S, Pallas MA, Le Bellec A, Gary V, Klein P. Road surface influence on electric vehicle noise emission at urban speed. Noise Mapp, 2021;8(1):217-227. Doi:10.1515/noise-2021-0017

21. Bühlmann E, Ziegler T. Temperature effects on tyre/road noise measurements. In Proc. of Internoise. Institute of Noise Control Engineering/Japan & Acoustical Society of Japan. 2011.

22. Santer BD, Mears C, Doutriaux C, Caldwell P, Gleckler PJ, Wigley TML, et al. Separating signal and noise in atmospheric temperature changes: The importance of timescale. J Geophys Res Atmos, 2011;116:D22105. Doi:10.1029/2011JD016263

23. Cramer O. The variation of the specific heat ratio and the speed of sound in air with temperature, pressure, humidity, and CO_2 concentration. J Acoust Soc Am, 1993;93(5):2510-2516. Doi:10.1121/1.405827

24. Harris CM. Effects of humidity on the velocity of sound in air. J Acoust Soc Am, 1971;49(3B):890-893.

25. Hothersall DC, Simpson S. The reflection of road traffic noise. J Sound Vib, 1983;90(3):399-405. Doi:10.1016/0022-460X(83)90721-6

26. Garg N, Maji S. A critical review of principal traffic noise models: strategies and implications. Environ Impact Assess Rev, 2014;46:68-81. Doi:10.1016/j.eiar.2014.02.001

27. Wang B, Duhamel D. Horn effect of tyre/road noise: modelling and experiments of acoustic network resonators in horn-like structures. Int J Veh Noise Vib, 2018;14(2):191-217. Doi:10.1504/IJVNV.2018.10016439

28. Elnady T, Abom M, Yang Y. Systematic optimization of an exhaust system to meet noise radiation criteria at idle. SAE Int J Passeng Cars-Mech, 2014;7(2014-01-0006):915-926. Doi: 10.4271/2014-01-0006

29. Salomons EM, Pont MB. Urban traffic noise and the relation to urban density, form, and traffic elasticity. Landsc Urban Plan, 2012;108(1):2-16. Doi:10.1016/j.landurbplan.2012.06.017

30. Maghrour Zefreh M, Torok A. Theoretical comparison of the effects of different traffic conditions on urban road traffic noise. J Adv Transp, 2018;2018:7949574. Doi:10.1155/2018/7949574

31. Jung FW, Blaney CT, Kazakov AL. Noise emission levels for vehicles in Ontario. Transp Res Rec, 1986;1058:32-39.

32. Close WH, Wesler JE. Vehicle noise sources and noise-suppression potential. Transp Res Rec Special Report, 1975;152:14-33.

33. Ortega JC, Kryter KD. Comparison of aircraft and ground vehicle noise levels in front and backyards of residences. J Acoust Soc Am, 1982;71(1):216-217. Doi:10.1121/1.387352

34. Björkman M, Rylander R. Maximum noise levels in city traffic. J Sound Vib, 1997;205(4):513-516. Doi:10.1006/JSVI.1997.1019

35. Stansfeld S, Haines M, Brown B. Noise and health in the urban environment. Rev Environ Health, 2000;15(1-2):43-82. Doi:10.1515/REVEH.2000.15.1-2.43

36. Zaharna M, Guilleminault C. Sleep, noise and health. Noise Health, 2010;12(47):64-69. Doi:10.4103/1463-1741.63205

37. Li Q, Qiao F, Yu L. Impacts of pavement types on in-vehicle noise and human health. J Air Waste Manag Assoc, 2016;66(1):87-96. Doi:10.1080/10962247.2015.1119217

38. Darbyshire JL, Young JD. An investigation of sound levels on intensive care units with reference to the WHO guidelines. Crit Care, 2013;17:1-8. Doi:10.1186/cc12870

39. Daniel E. Noise and hearing loss: a review. J Sch Health, 2007;77(5):225-231. Doi:10.1111/j.1746-1561.2007.00197.x

40. Clark WW, Bohne BA. Effects of noise on hearing. Jama, 1999;281(17):1658-1659. Doi:10.1001/jama.281.17.1658

41. Clark WW. Hearing: the effects of noise. Otolaryngol Head Neck Surg, 1992;106(6):669-676. Doi: 10.1177/019459989210600610

42. Glorig A. The effects of noise on hearing. J Laryngol Otol, 1961;75(5):447-478. Doi: 10.1017/s0022215100057960

43. Pickles J. An Introduction to the Physiology of Hearing. 3rd edition. London-New York: Academic Press; 1982. 400.

44. Babisch W. Cardiovascular effects of noise. Noise Health, 2011;13(52):201-204. Doi: 10.4103/1463-1741.80148

45. Hahad O, Kröller-Schön S, Daiber A, Münzel T. The cardiovascular effects of noise. Dtsch Arztebl Int, 2019;116(14):245-250. Doi:10.3238/arztebl.2019.0245

46. Lusk SL, Gillespie B, Hagerty BM, Ziemba RA. Acute effects of noise on blood pressure and heart rate. Arch Environ Health, 2004;59(8):392-399. Doi:10.3200/AEOH.59.8.392-399

47. Kraus U, Schneider A, Breitner S, Hampel R, Rückerl R, Pitz M, et al. Individual daytime noise exposure during routine activities and heart rate variability in adults: a repeated measures study. Environ Health Perspect, 2013;121(5):607-612. Doi:10.1289/ehp.1205606

48. Jafari MJ, Khosrowabadi R, Khodakarim S, Mohammadian F. The effect of noise exposure on cognitive performance and brain activity patterns. Open Access Maced J Med Sci, 2019;7(17):2924-2931. Doi:10.3889/oamjms.2019.742

49. Arjunan A, Rajan R. Noise and brain. Physiol Behav, 2020;227:113136. Doi:10.1016/j.physbeh.2020.113136

50. Frank TD, Daffertshofer A, Beek PJ, Haken H. Impacts of noise on a field theoretical model of the human brain. Physica D, 1999;127(3-4):233-249. Doi:10.1016/S0167-2789(98)00294-2

51. Thompson R, Smith RB, Karim YB, Shen C, Drummond K, Teng C, et al. Noise pollution and human cognition: an updated systematic review and meta-analysis of recent evidence. Environ Int, 2022;158:106905. Doi: 10.1016/j.envint.2021.106905

52. Ising H, Braun C. Acute and chronic endocrine effects of noise: review of the research conducted at the Institute for Water, Soil and Air Hygiene. Noise health, 2000;2(7):7-24.

53. Chamkori A, Shariati M, Moshtaghi D, Farzadinia P. Effect of noise pollution on the hormonal and semen analysis parameters in industrial workers of Bushehr, Iran. Crescent J Med Bio Sci, 2016;3(2):45-50.

54. Ising H, Babisch W, Kruppa B. Noise-induced endocrine effects and cardiovascular risk. Noise health, 1999;1(4):37-48.

55. Farzadinia P, Bigdeli M, Akbarzadeh S, Mohammadi M, Daneshi A, Bargahi A. Effect of noise pollution on testicular tissue and hormonal assessment in rat. Andrologia, 2016;48(9):957-961. Doi: 10.1111/and.12524

56. Gue M, Fioramonti J, Frexinos J, Alvinerie M, Bueno L. Influence of acoustic stress by noise on gastrointestinal motility in dogs. Dig Dis Sci, 1987;32:1411-1417. Doi: 10.1007/BF01296668

57. Mu ZB, Huang YX, Zhao BM, Liu ZX, Zhang BH, Wang QL. Effect of explosive noise on gastrointestinal transit and plasma levels of polypeptide hormones. World J Gastroenterol, 2006;12(14):2284-2287. Doi: 10.3748/wjg.v12.i14.2284

58. Curthoys IS, Grant JW. How does high-frequency sound or vibration activate vestibular receptors?. Exp brain res, 2015;233:691-699. Doi: 10.1007/s00221-014-4192-6

59. Vasilyeva IN, Bespalov VG, Semenov AL, Baranenko DA, Zinkin VN. The effects of low-frequency noise on rats: evidence of chromosomal aberrations in the bone marrow cells and the release of low-molecular-weight DNA in the blood plasma. Noise Health, 2017;19(87):79-83. Doi: 10.4103/nah.NAH_39_16

60. Venet T, Carreres-Pons M, Chalansonnet M, Thomas A, Merlen L, Nunge H, et al. Continuous exposure to low-frequency noise and carbon disulfide: combined effects on hearing. Neurotoxicology, 2017;62:151-161. Doi: 10.1016/j.neuro.2017.06.013

61. Mancera KF, Lisle A, Allavena R, Phillips CJ. The effects of mining machinery noise of different frequencies on the behaviour, faecal corticosterone and tissue morphology of wild mice (Mus musculus). Appl Anim Behav Sci, 2017;197:81-89. Doi:10.1016/j.applanim.2017.08.008

62. Ninomiya H, Ohgami N, Oshino R, Kato M, Ohgami K, Li X, et al. Increased expression level of Hsp70 in the inner ears of mice by exposure to low frequency noise. Hear Res, 2018;363:49-54. Doi: 10.1016/j.heares.2018.02.006

63. Chalansonnet M, Carreres-Pons M, Venet T, Thomas A, Merlen L, Seidel C, et al. Combined exposure to carbon disulfide and low-frequency noise reversibly affects vestibular function. Neurotoxicology, 2018;67:270-278. Doi: 10.1016/j.neuro.2018.06.010

64. Negishi-Oshino R, Ohgami N, He T, Li X, Kato M, Kobayashi M, et al. Heat shock protein 70 is a key molecule to rescue imbalance caused by low-frequency noise. Arch Toxicol, 2019;93:3219-3228. Doi: 10.1007/s00204-019-02587-3

65. Maes JHR, De Groot G. Effects of noise on the performance of rats in an operant discrimination task. Behav Processes, 2003;61(1-2):57-68. Doi: 10.1016/s0376-6357(02)00163-8

66. Stewart C, Yu Y, Huang J, Maklad A, Tang X, Allison J, et al. Effects of high intensity noise on the vestibular system in rats. Hear Res, 2016;335:118-127. Doi: 10.1016/j.heares.2016.03.002

67. McCarthy DO, Ouimet ME, Daun JM. The effects of noise stress on leukocyte function in rats. Res Nurs Health, 1992;15(2):131-137. Doi: 10.1002/nur.4770150207

68. Escabi CD, Frye MD, Trevino M, Lobarinas E. The rat animal model for noise-induced hearing loss. J Acoust Soc Am, 2019;146(5):3692-3709. Doi: 10.1121/1.5132553

69. Baldwin AL, Bell IR. Effect of noise on microvascular integrity in laboratory rats. JAALAS, 2007;46(1):58-65.

70. Basner M, Babisch W, Davis A, Brink M, Clark C, Janssen S, et al. Auditory and non-auditory effects of noise on health. Lancet, 2014;12;383(9925):1325-1332. Doi: 10.1016/S0140-6736(13)61613-X

71. Liu J, Zhu B, Xia Q, Ji X, Pan L, Bao Y, et al. The effects of occupational noise exposure on the cardiovascular system: a review. J Public Health Emerg, 2020;4:12. Doi:10.21037/jphe.2020.03.07

72. Szalma J, Hancock P. Noise effects on human performance: a meta-snalytic synthesis. Psychol Bull, 2011;137:682-707. Doi: 10.1037/a0023987

73. Islam MT, Nahar N, Islam MJ, Islam MA, Hossen MAM. Traffic induced noise pollution and its impact on human health in Chittagong city corporation. J Environ Sci Nat Resour, 2015;8(2):37-40. Doi:10.3329/jesnr.v8i2.26862

74. Patel DB, Solanki HKA. Noise pollution, effect of noise on behaviour of animals and human health. Effects of Noise Pollution on Human Health, 2021;3(1):1-5. Doi:10.46505/IJBI.2021.3105

75. Yin X, Li Z, Zhao T, Yang L. Effects of genes, lifestyles, and noise kurtosis on noise-induced hearing loss. Noise Health, 2023;25(118):143-157. Doi: 10.4103/nah.nah_65_22

ORIGINAL ARTICLES

Acta Pharm. Sci. Vol 62:(2), 2024
Research article
DOI: 10.23893/1307-2080.APS6217

The potential impact of vascular endothelial growth factor *rs699947* polymorphisms on breast tumors susceptibility in a sample of Iraqi females

Hiba A. ABDULHUSSEIN[1*], Estabraq AR. ALWASITI[2], Nawfal K. KHIRO[3], Anees K. NILE[3]

1 Department of Pharmacy, Al-Hilla University College, Babylon, Iraq
2 Department of Chemistry and Biochemistry, College of Medicine, Al-Nahrain University, Baghdad, Iraq
3 Department of General Surgery, College of Medicine, Al-Nahrain University, Baghdad, Iraq

ABSTRACT

The angiogenic factor vascular endothelial growth factor (VEGF) plays a pivotal role in tumor initiation, progression, and metastasis. Polymorphisms in VEGF gene can alter the activity of the gene's promoter, leading to increased or decreased VEGF secretion. This study aimed to investigate the association of VEGF *rs699947* polymorphisms with breast cancer risk in female from Baghdad-Iraq in a case control study which was done on 60 female patients with breast cancer and 60 female patients with benign breast tumor which compared with 75 age, BMI and sex-matched healthy subjects. Blood samples were collected from fasting patients and controls and put into EDTA tube for DNA extraction for subsequent screening of VEGF rs699947 gene polymorphisms by PCR-RFLP method. Results revealed that the incidence of malignant tumor were associated with the genotypic distribution and allelic frequency of VEGF rs699947 gene polymorphisms in that the AA genotype and A allele showed a strong correlation with the risk of malignant breast tumor in comparison with controls. The findings of this study proposed that VEGF rs699947 variant (AA) significantly increased the risk of breast cancer. It was also concluded that A allele is associated with the increased risk of breast cancer.

Keywords: breast cancer, rs699947, VEGF

* Corresponding author: Hiba A. ABDULHUSSEIN
E-mail: hibaabdulhussein@yahoo.com
ORCIDs:
Hiba A ABDULHUSSEIN: 0009-0002-8617-0387
Estabraq AR ALWASITI: 0000-0002-1291-0656
Nawfal K KHIRO: 0000-0003-3833-3305
Anees K. NILE: 0000-0002-4769-7306
(Received 1 Apr 2023, Accepted 31 May 2024)

INTRODUCTION

The angiogenic factor vascular endothelial growth factor (VEGF) plays a pivotal role in tumor initiation, progression, and metastasis. In addition to aiding tumor migration and invasion, VEGF signaling helps cancer cells avoid death by apoptosis[1]. Many types of solid cancer, including breast cancer, have VEGF as an upregulated biomarker. Higher levels of VEGF were found in malignant breast lesions than in benign breast tissues. Multiple studies have found that micro vessel density and poor prognosis are strongly correlated with VEGF expression in tumor tissue[2].

The VEGF gene, which encodes a family of proteins, is found on the short arm of chromosome 6 (6p12-p21) and is made up of eight exons and seven introns that undergo alternative splicing. During embryogenesis, skeletal growth, and reproductive processes, VEGF (also known as VEGFA) plays a crucial role as a regulator of physiological angiogenesis. It also plays a role in tumor-related pathological angiogenesis. Cancer cannot develop without angiogenesis, which is required for primary tumor growth, invasiveness, and metastasis. 8 Multiple tumor tissues had an increased level of VEGF expression[3]. Lymphangiogenesis, the process by which new blood and lymphatic vessels are formed to supply a growing tumor, is a hallmark of several types of cancer, including the most common type of female cancer, breast cancer. Increased expression of VEGF is linked to tumor growth and metastasis, as shown by *in vitro* and *in vivo* studies. Tumor-induced angiogenesis and tumor growth are both restrained by blocking VEGF signaling[4,5].

There is evidence that SNPs in the promoter, intron, exon, or untranslated regions (3′- and 5′-UTR) can have an effect on protein expression and function. Differential VEGF expression has been linked to several single-nucleotide polymorphisms (SNPs) in the VEGF gene. Two of these SNPs (2578 and 1154) are found in the VEGF promoter, one is in exon 1 of the VEGF gene16, and the other is in exon 8, which corresponds to the 3′UTR region of the gene[6]. Furthermore, other SNPs have been defined, but no correlation between them and VEGF expression has been found. VEGF genetic polymorphisms in BC have been the subject of a number of studies, with conflicting results[7].

This study aimed to investigate the association of VEGF *rs699947* polymorphisms with breast cancer risk in female population in Baghdad.

METHODOLOGY

Study protocol

Sixty female patients with breast cancer and sixty female patients with benign breast tumors were enrolled in a case control study between May 2022 and December 2022 at Al-Imamain Al-Kadhemain Medical City in Baghdad, Iraq. The age range of the malignant group was 29–48 years old, while that of the benign group was 29–46 years old; both groups were compared to a group of 75 age-, BMI-, and sex-matched healthy females. The research was carried out in Al-Nahrain University's Department of Chemistry and Biochemistry in the College of Medicine in Baghdad, Iraq. Women who had a suspicious breast lesion confirmed by histopathology following a clinical breast examination and/or imaging study were considered for inclusion in the current study.

Exclusion criteria

1. Subjects that had a history of any acute or chronic diseases (eg. Acute and chronic hepatitis).

2. Subjects that had a history of any type of cancer (eg. Colorectal and endometrium cancer).

3. Patients received hormonal treatment or chemotherapy.

4. Pregnant women.

5. Age above 65 years' old

The study was approved by the Institutional Review Board (IRB) of the College of Medicine, University of Al-Nahrain, Baghdad, Iraq. In addition, an informed written consent for participation in the study was signed by investigated subjects according to the Helsinki principles.

All eligible control subjects and studied patients were subjected to the following:

- Thorough clinical examinations in addition to full medical history
- Genetic screening for VEGF rs699947 gene polymorphisms in malignant breast tumor, benign breast tumor and control groups using polymerase chain reaction-restriction fragment length polymorphism (PCR-RFLP) method.

Sample collection and preparation

Blood samples were collected from fasting for 6 hours patients and controls. These samples were put into EDTA tube for DNA extraction for subsequent screening of VEGF rs699947 gene polymorphisms.

DNA extraction[8]

Blood Genomic DNA Extraction Kit (Geneaid, Taiwan) is designed for rapid extraction and purification of pure genomic DNA from whole blood using the glass fiber matrix of the spin columns.

Genotyping

Single nucleotide polymorphisms (SNPs) of VEGF/rs699947 were detected by PCR-RFLP method. Amplification was performed in programmable thermal cycler gradient PCR system The primers used for detection of polymorphisms are listed in Table 1. PCR primers were obtained from previous studies with melting temperature of 68°C, primer length is 19 nucleotides, and PCR amplicon length 455 base pair[7].

Table 1. The primers used in the study

Primer Name	Seq.	Annealing Temp. (°C)	Product size	SNPs
VEGF-F	5`-GGCCTTAGGACACCATACC -3`	61	455 bp	rs699947
VEGF-R	5`-CACAGCTTCTCCCCTATCC -3`			

PCR was done using GoTaq® Green Master Mix from Promega, containing Taq DNA polymerase (5 U/µl), dNTP (400µM), MgCl2 (3mM) and reaction buffer (2X,PH=8.5) at optimal concentration for efficient amplification of DNA templates by PCR. The PCR reaction mixtures were brought together according to the manufacturer procedure of the master mix (Promega). When necessary, the appending was done on frozen cooling blocks and ice inside a laminar flow cabinet. Twenty microliter volumes were used for the PCR amplifications, with ten microliters of GoTaq Green Master Mix (2X), one microliter for each primer (10 pmol), six microliters of nuclease-free water, and two microliters of template DNA. The following temperature program was used for PCR cycling on a PCR Express (Thermal Cycler, BioRad, USA): denatured at 95°C for 5 minutes, followed by 30 cycles of denaturation at 95°C for 30 seconds, annealing at 61°C for 30 seconds, and extension at 72°C for 30 seconds. The reactions were halted after a 10-minute incubation at 10 degrees Celsius and a 5-minute extension incubation at 72 °C.

The PCR product for amplified gene was digested with the restriction enzyme BstYI. The PCR products were electrophoresed on agarose gel containing 0.5 μg/mL ethidium bromide and visualized on a UV transilluminator.

After the complete digestion with the restriction enzyme BstYI at 37°C for 30 min, the resulting DNA fragments were analyzed by electrophoresis on a 2% agarose gels. DNA step ladders (100 b.p) were used to determine the length of the DNA fragments. The result of the digestion showed that the DNA fragment with a homozygote C allele of VEGF / rs699947 was not digested with the restriction enzyme and appear as a single band of 455bp whereas samples with a homozygote A allele should produce two fragments of 209 and 246 bp but actually only one fragment appeared at a region of about 240bp as it digested by the enzyme while a heterozygote A and C allele samples showed two bands of 455 and 240 bp

Statistical analysis

The data of the study were analyzed using the SPSS software 20. Categorical variables were expressed as numbers and analyzed by cross tabulation to assess the frequency and percentage of each variable among studied groups. The correlation was done between all parameters using Chi square to test the relationships between categorical variables with the measurement of Phi that is considered as a chi-square-based measure of association to indicate the strength of the association (given that values ranged from 0-0.5 considered as weak association while values above 0.5 considered as strong association) in addition to *p* values which is considered as significant at ≤0.05. Logistic regression was used to calculate odd ratio (ORs) and 95% confidence interval (CI) for breast cancer risk associated with the genetic polymorphisms of VEGF gene[9].

RESULTS and DISCUSSION

Results postulated in Table 2 and Figure 1 showed that the genotypic distribution of the rs699947 polymorphism showed a nearly similar distribution between controls and benign patients in that CC, CA and AA genotypes represent 46.7, 34.7, 18.7%; respectively of controls and 45, 28.3, 26.7%; respectively in benign group. Patients with malignant tumor showed a different pattern of genotypic distribution in comparison with control and benign groups in which the CC, CA and AA genotypes represent 20, 45, 35%. These apparent differences in the genotypic distribution confirmed by Chi^2 results which showed non-significant differences in the genotypic distribution between controls and benign groups (p=0.479, Phi=0.102) while significant differences were obtained between controls and cancerous patients (p=0.004; Phi=0.287), benign and malignant groups (p=0.013; Phi=0.270), and among all studied groups (p=0.011; Phi=0.26).

Table 2. Genotypic distribution of rs699947 polymorphism among all studied groups

			rs699947 polymorphism			Total
			CC	CA	AA	
GROUP	CONTROL	Count	35	26	14	75
		% within GROUP	46.7%	34.7%	18.7%	100.0%
	BENIGN	Count	27	17	16	60
		% within GROUP	45.0%	28.3%	26.7%	100.0%
	CANCER	Count	12	27	21	60
		% within GROUP	20.0%	45.0%	35.0%	100.0%
Chi^2	Control vs benign	p-value	0.479			
		Phi	0.102			
	Control vs cancer	p-value	0.004			
		Phi	0.287			
	Benign vs cancer	p-value	0.013			
		Phi	0.27			
	Among all groups	p-value	0.011			
		Phi	0.26			

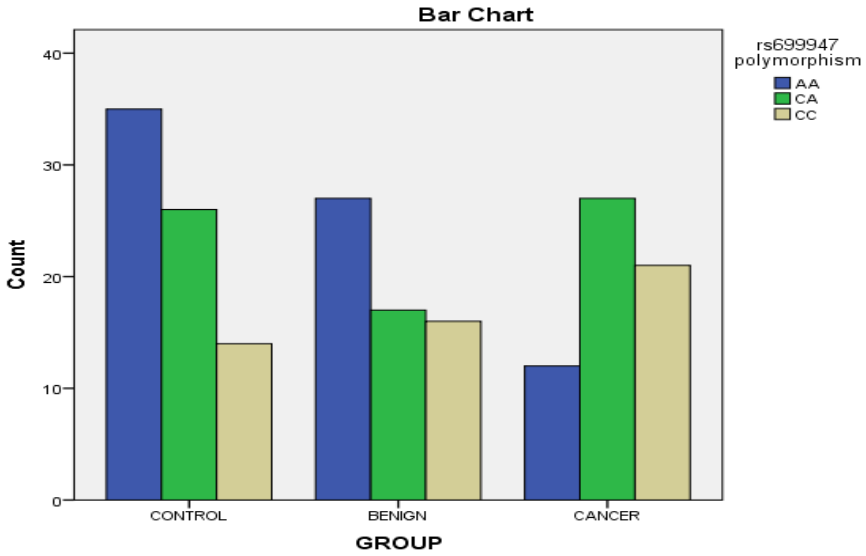

Figure 1. Distribution of VEGF rs699947 genotypes in all studied groups

Results illustrated in Table 3 revealed that the incidence of malignant tumor were associated with the allelic frequency in that the A allele showed a strong correlation with the malignant tumor in comparison with controls as indicated by the Odds ratio results which showed a significant association between A allele frequency and the prevalence of cancer (p= 0.005) and the results also showed that the risk of malignancy showed to be higher by about 2.41 times in patients with A allele than those with C allele. Additionally, A allele also showed to be associated with the incidence of malignant tumor in comparison with benign tumor as it represented by the Odds ratio results which revealed a significant association between the allelic frequency and the incidence of malignancy (p= 0.01) and the results also demonstrated that patients with A allele have a higher risk to get malignant tumor by about twice with that have C allele in benign. On the other hand, allelic frequency showed non-significant effect on the incidence of benign tumor in comparison with controls (p= 0.42, OR=1.123 and 95% CI=0.75-2.01).

Table 3. Allelic distribution of rs699947 polymorphism among all studied groups

			rs699947 polymorphism		Total
			C Allele	A Allele	
GROUP	CONTROL	Count	96	54	150
		% within GROUP	64%	36%	100.0%
	BENIGN	Count	71	49	120
		% within GROUP	59.2%	40.8%	100.0%
	CANCER	Count	51	69	120
		% within GROUP	42.5%	57.5%	100.0%
Odds ratio	Control vs benign	P-value	0.42		
		OR (95% CI)	1.23 (0.75-2.01)		
	Control vs cancer	P-value	0.005		
		OR (95% CI)	2.41 (1.47-3.93)		
	Benign vs cancer	P-value	0.01		
		OR (95% CI)	1.96 (1.17-3.28)		

Several studies reported that the polymorphism of VEGF rs699947 C/A gene showed to be correlated with an overall increased risk of breast cancer as it links to the rate of the expression of VEGF that influenced by the polymorphism of this SNP that located in the promoter region of the VEGF gene[7,10] studies also stated that this SNP responsible for differentiated VEGF gene expression as it showed a reduction in the serum concentration of VEGF in patients homozy-

gous for −2578 A alleles. In the present study, the prevalence of rs699947 in CC, CA and AA genotypes represent 20, 45, 35%; respectively in patients with malignant tumor which showed to be identified as significantly differ from that in the healthy individuals (46.7, 34.7 and 18.7%; respectively) as indicated by the significant Chi^2 results (p=0.004; Phi=0.287). The genotypic distribution of cancerous patients also showed to be significantly (p=0.013; Phi=0.270) differ from that of benign tumor which in turn showed a pattern of distribution similar to that of controls as illustrated in Table 2. Results demonstrated in the current study were consistent with the study conducted by al Balawi et al. who demonstrated that the prevalence of CC, CA, AA in the patient samples were 37%, 45% and 18% that differ significantly from that of healthy controls which provide a prevalence of 54%,37%, and 09% respectively[10] and also showed an agreement with the study conducted by Rezaei et al. who demonstrated that the prevalence of CC, CA, AA in the samples of cancerous were 30.4%, 55.2% and 14.4% which is showed to be significantly differ from the prevalence in the controls in which CC, CA, AA genotypes represented 43.7%, 46.5% and 9.8%; respectively[7].

The A allele of rs699947 was shown to be more frequent in malignant group than that of healthy subjects (57.5 vs 36 respectively) and the Odds ratio results revealed that the risk of breast cancer in patients with A allele were 2.4 time more than the patients with C allele which is comparable to the results conducted in Saudi Arabia which demonstrated that A allele increased the risk of breast cancer when compared with C allele by about 1.8 times[10]. Multiple mechanisms implicate VEGF as a critical factor in angiogenesis, including increased endothelial cell proliferation and survival, increased endothelial cell migration and invasion, increased permeability of existing vessels forming a lattice network for endothelial cell migration, and increased chemotaxis and homing of bone marrow-derived vascular precursor cells[11,12]. Independent of vascular processes, VEGF has several critical roles, including proangiogenic effects, autocrine effects on tumor cell function (survival, migration, invasion), immune suppression, and homing of bone marrow progenitors to “prepare” an organ for subsequent metastasis[13,14]. Several functional polymorphisms of the VEGF gene, including the VEGF 2578C/A polymorphism, have been identified in some studies and may influence serum VEGF expression level. Several prior studies reported that functional genetic polymorphisms could alter mRNA or protein expression, thus generating significant influence on disease development across a wide spectrum of diseases, including cancer[10,15]. Numerous studies have been conducted recently on the links between VEGF gene variations and the risk of breast cancer, but the reported results have been contradictory. Our results suggested that a variant of VEGF called rs699947 (AA)

significantly raised the risk of breast cancer which is consistent with previous literatures[7,10,16].

The findings of the current study proposed that VEGF rs699947 variant (AA) significantly increased the risk of breast cancer. It was also concluded that A allele is associated with the increased risk of breast cancer.

STATEMENT OF ETHICS

The study was conducted in compliance with the ethical guidelines derived from the Declaration of Helsinki. The procedure was conducted after obtaining verbal and analytical consent from the patients before to collecting the sample. The Institutional Review Board (IRB) of the College of Medicine, University of Al-Nahrain, Baghdad, Iraq, examined and approved the study protocol, subject information, and permission form. This approval was granted by a local ethics commission, as indicated by document number 154 dated 07/12/2021.

CONFLICT OF INTEREST STATEMENT

The authors declared no conflict of interest.

AUTHOR CONTRIBUTIONS

Concept – E.A.; Design – H.A., E.A.; Supervision – E.A., N.F., A.N.; Resources – N.F., H.A.; Materials – H.A.; Data Collection and/or Processing – H.A.; Analysis and/or Interpretation – H.A.; Literature Search – H.A.; Writing – H.A.; Critical Reviews – H.A., E.A., N.K., A.N.

FUNDING SOURCES

The work was not supported or funded by any drug company.

ACKNOWLEDGMENTS

No part of this article was presented in any conference or published before.

REFERENCES

1. Lugano R, Ramachandran M, Dimberg A. Tumor angiogenesis: causes, consequences, challenges and opportunities. Cell Mol Life Sci, 2020;77:1745-1770. Doi: 10.1007/s00018-019-03351-7

2 Al-Mohaya MA, Alfadhel AK, Mustafa M, Alquwayz TS, Al-Anazi MA. Vascular endothelial growth factor (VEGF-2578 C > A) gene polymorphism as a genetic biomarker for breast cancer: a case control study. Gene Rep, 2021;22. Doi:10.1016/j.genrep.2020.101007

3. Maiborodin I, Mansurova A, Chernyavskiy A, Romanov A, Voitcitctkii V, Kedrova A, et al. Cancer angiogenesis and opportunity of influence on tumor by changing vascularization. J Pers Med, 2022;12(3):327. Doi: 10.3390/jpm12030327

4. Oliveira-Ferrer L, Milde-Langosch K, Eylmann K, Rossberg M, Müller V, Schmalfeldt B, et al. Mechanisms of tumor-lymphatic interactions in invasive breast and prostate carcinoma. Int J Mol Sci, 2020;21(2):602. Doi: 10.3390/ijms21020602

5. Brogowska KK, Zajkowska M, Mroczko B. Vascular endothelial growth factor ligands and receptors in breast cancer. J Clin Med, 2023;12(6):2412. Doi: 10.3390/jcm12062412

6. Saetan N, Honsawek S, Tanavalee A, Ngarmukos S, Yuktanandana P, Poovorawan Y. Association between common variants in VEGFA gene and the susceptibility of primary knee osteoarthritis. Cartilage, 2022;13(4):66-76. Doi: 10.1177/19476035221132260

7. Rezaei M, Hashemi M, Sanaei S, Mashhadi MA, Taheri M. Association between vascular endothelial growth factor gene polymorphisms with breast cancer risk in an Iranian population. Breast Cancer (Auckl), 2016;10. Doi: 10.4137/BCBCR.S39649

8. Vogelstein B, Gillespie D. Preparative and analytical purification of DNA from agarose. Proc Natl Acad Sci USA, 1979;76(2):615-619. Doi: 10.1073/pnas.76.2.615

9. Szumilas M. Explaining odds ratios. J Can Acad Child Adolesc. Psychiatry, 2010;19(3):227.

10. Al Balawi IA, Mir R, Abu-Duhier F. Potential impact of vascular endothelial growth factor gene variation (-2578C> A) on breast cancer susceptibility in Saudi Arabia: a case-control study. Asian Pac J Cancer Prev, 2018;19(4):1135-1143. Doi: 10.22034/APJCP.2018.19.4.1135

11. Ghalehbandi S, Yuzugulen J, Pranjol MZI, Pourgholami MH. The role of VEGF in cancer-induced angiogenesis and research progress of drugs targeting VEGF. Eur J Pharmacol, 2023;949. Doi: 10.1016/j.ejphar.2023.175586

12. Ansari MJ, Bokov D, Markov A, Jalil AT, Shalaby MN, Suksatan W, et al. Cancer combination therapies by angiogenesis inhibitors; a comprehensive review. Cell Commun Signal, 2022;20(1):49. Doi: 10.1186/s12964-022-00838-y

13. Niu G, Chen X. Vascular endothelial growth factor as an anti-angiogenic target for cancer therapy. Curr Drug Targets, 2010;11(8):1000-1017. Doi: 10.2174/138945010791591395

14. Ahmad A, Nawaz MI. Molecular mechanism of VEGF and its role in pathological angiogenesis. J Cell Biochem, 2022;123(12):1938-1965. Doi: 10.1002/jcb.30344

15. Flego V, Ristić S, Pavlić SD, Lender DM, Bulat-Kardum L, Kapović M, et al. Tumor necrosis factor-alpha gene promoter-308 and-238 polymorphisms in patients with lung cancer as a second primary tumor. Med Sci Monit, 2013;19:846-851. Doi: 10.12659/MSM.889554

16. Sambyal V, Guleria K, Kapahi R, Manjari M, Sudan M, Uppal MS, et al. Association of VEGF haplotypes with breast cancer risk in North-West Indians. BMC Med Genomics, 2021;14(1):209. Doi: 10.1186/s12920-021-01060-4

Acta Pharm. Sci. Vol 62:(2), 2024
Research article
DOI: 10.23893/1307-2080.APS6218

Efficacy of statin therapy on achieving target goal of LDL among Iraqi patients

Ahmed Hamza AL-SHAMMARI[1*], Qusay Jassam SHANDOOKH[2]

1 Kut University College, School of Pharmacy, Department of Clinical Pharmacy, Alkut, Wasit, Iraq
2 Al-Yarmouk University College, School of Pharmacy, Department of Clinical Pharmacy Baqubah/Diyala, Iraq

ABSTRACT

Dietary and statin treatment planning are central to the management of dyslipidemia. The treatment's efficacy is determined by how well it achieves the level of low-density lipoprotein (LDL)- target goal established by European guidelines for that reason the target (LDL) in patients receiving different types and doses of statin therapy were evaluated in this prospective, cross-sectional study was conducted on patients recruited from Al Karama Teaching Hospital, Kut, Iraq to assess the levels of serum LDL in addition to data collected directly from the patients included demographic characteristics, BMI, and types, doses, and duration of statins used which showed that target goal (optimal) was achieved in 82.4% in patients taking statin. The LDL-target goal was achieved in 85.4% of patients taking statin with moderate risk, in 82.6% with high risk, and 80.6 % with very high risk which indicate that the targeted LDL levels were achieved in good proportion in patients with high and moderate risk of dyslipidemia with a less extent proportion in patients with very high-risk of dyslipidemia. It was also demonstrated that the LDL target levels were achieved more efficiently with a higher dose of statins.

Keywords: cardiovascular diseases, dyslipidemia, statin target goal

* Corresponding author: Ahmed Hamza AL-SHAMMARI
E-mail: ahmedhamzamezaal@gmail.com
ORCIDs:
Ahmed Hamza AL-SHAMMARI: 0000-0001-6215-6551
Qusay Jassam SHANDOOKH: 0009-0001-7122-9625
(Received 6 Jul 2023, Accepted 21 Jul 2023)

INTRODUCTION

Expert guidelines and recommendations are often the basis for a physician's implementation of a particular course of action in a therapeutic setting. Since the advent of evidence-based medicine (EBM), doctors have been more open to making "evidence-based" judgments. In the field of lipid-lowering

medicine, this is also true. Coronary heart disease (CHD) and other metabolic and chronic health problems may be avoided if hypercholesterolemia is treated[1]. Statin usage is on the rise throughout Europe, with a 31% yearly increase in prevalence, according to earlier research[2].

For every 1.0 mmol/l decrease in LDL-cholesterol, statin medication has been shown to lower the risk of major coronary events, coronary revascularization, and stroke over a five-year period by 21%. Statins have been found to decrease mortality and the requirement for coronary artery bypass grafting or angioplasty in patients with coronary artery disease. Higher dosages of statins have been shown in previous trials to halt the advancement of atherosclerosis and even produce regression, so lowering the risk of cardiovascular disease and even dementia[3]. Other statins including rosuvastatin, have anti-platelet action in addition to their lipid-lowering effects[4].

For the corresponding targets, different "target goals" are defined in most guidelines according to the levels of risk, to guide the lipid management in different groups and to minimize the risk of cardiovascular events on a scientific basis. The achieved statin target goal in present study as all selected patients had complicated with cardiovascular diseases or other diseases (HT, DM, HF, CKD) was low density Lipoprotein-C <100 mg/dl for patients with moderate and high risk and low-density Lipoprotein-C <70 mg/dl for patients with very high risk according European guideline[5].

The aim of the current study is to evaluate the target level of LDL in patients receiving different types and doses of statin therapy.

METHODOLOGY

A prospective, cross-sectional study was conducted in Al Karama Teaching Hospital- Kut, Iraq. This study included 250 patients taking statin with mean age of 54.3±6.8 years was selected after eligibility to inclusion criteria which include patients of age ranged between 40-69 years, patients taking statin therapy for treatment or prevention of cardiovascular diseases for a duration of statin intake of ≥3 months and exclusion criteria that include patients taking other lipid lowering agent alone or in combination with statin and patient suffered from cancer.

Sampling and data collection

A convenient sample of patients taking statin presented to outpatient's clinics in Al Karama Teaching Hospital- Kut, Iraq**.** The data was collected from the patients directly and filled in a prepared questionnaire that included the followings:

1. Demographic characteristics of patients taking statin: Age and gender.
2. BMI of patients taking statin.
3. Serum LDL levels.
4. Statins characteristics: Types of statins used, statin doses and duration of statin use.

The investigations of the patients taking statin were implemented in the Laboratory of Al Karama Teaching Hospital. The statin taken by the selected patients was within different doses.

The approval was taken from Research Ethical Committee in Kut University College-Iraq. An oral informed consent was taken from all participants that enrolled in the current study.

RESULTS and DISCUSSION

Distribution of BMI according to statin targeting were illustrated in table 1 which revealed that there were non-significant differences were observed between patients taking statin with achieved target and patients not achieved target regarding BMI (p=0.3). The demographic characteristic of all patients subjected to the present research were illustrated in table 1 that showed the age and gender distribution. Non-significant differences were observed between patients taking statin with achieved target and patients not achieved target regarding their age (p=0.1). A significant association was observed between female patients taking statin and not achieving statin target (p=0.01). Results illustrated in Table 2 showed that the mean± SD of LDL was 74.7±22.9 mg/dl; 7.6 % of them had high LDL and the rest showed normal LDL levels.

Table 1. Distribution of BMI and demographic characteristics according to statin targeting

Variable	No.	%	Statin targeting				P
			Achieved		Not achieved		
			No.	%	No.	%	
BMI							
Normal	61	24.4	52	85.2	9	14.8	0.3*
Overweight	99	39.6	84	84.8	15	15.2	
Obese	90	36.0	70	77.8	20	22.2	
Age groups							
40-49 years	41	14.1	30	73.2	11	26.8	0.1*
50-59 years	99	33.2	81	81.8	18	18.2	
60-69 years	110	44.5	95	86.4	15	13.6	
Gender							
Male	168	67.2	147	87.5	21	12.5	0.01**
Female	82	32.8	59	72	23	28	

*Fishers exact test, **Chi-square test.

Table 2. Levels of LDL in patients subjected to the study

Variable	No.	%
LDL mean±SD (74.7±22.9 mg/dl)		
Normal	231	92.4
High	19	7.6
Total	250	100.0

Table 3 showed that the statin target goal (optimal LDL-C) was achieved in 82.4% of patients taking statin and not achieved in 17.6% of them and it was achieved in 85.4% of patients taking statin with moderate risk and in 82.6% of patients with high risk, while 80.6% of patients with very high risk was achieved the target goal of statin.

Table 3. Statin target of patients taking statin

Variable	No.	%
Statin target goal (optimal LDL-C)		
Achieved	206	82.4
Not achieved	44	17.6
Total	250	100.0
Statin target goal (moderate risk)		
Achieved	41	85.4
Not achieved	7	14.6
Total	48	100.0
Statin target goal (high risk)		
Achieved	90	82.6
Not achieved	19	17.4
Total	109	100.0
Statin target goal (very high risk)		
Achieved	75	80.6
Not achieved	18	19.4
Total	93	100.0

Table 4 showed the statin used among patients and the distribution of their characteristics which revealed that Atrovastatin used in 58.4% and Rosuvastatin in 41.6 % of patients subjected to the current study. The statin doses were 20 mg (53.2%) and 40 mg (46.8%). Durations of taking statins were 3- 6 months (29.6 %), 7-12 months (12 %) and more than 12 months (58.4%). The results revealed that there were non-significant differences between patients taking statin with achieved target and patients not achieved target regarding types of statin ($p=0.4$) and duration of statin use ($p=0.07$). A significant association was observed between low dose statin and not achieving statin target ($p<0.01$).

Table 4. Distribution of statin characteristics according to statin targeting

Variable	No.	%	Statin targeting				P
			Achieved		Not achieved		
			No.	%	No.	%	
Types of statins							
Atrovastatin	146	58.4	123	83.1	23	16.9	0.4*
Rosuvastatin	104	41.6	83	81.9	21	18.1	
Statin doses							
20 mg	133	53.2	105	78.9	28	21.1	<0.01**
40 mg	117	46.8	101	86.3	16	13.7	
Duration of statin use							
3-6 months	74	29.6	55	74.3	19	25.7	0.07**
7- 12 months	30	12	26	86.7	4	13.3	
More than 12 months	146	58.4	123	84.2	23	15.8	

* Fishers exact test, **Chi-square test.

When it comes to the secondary prevention of cardiovascular illnesses, the primary objective of most doctors is to either bring low density lipoproteins-C under control or reduce their levels. In order to accomplish this objective, an intensive regimen of statin medication is used, and in certain cases, a combined therapy is required[6,7]. Statin treatment, on the other hand, could not accomplish this objective without the cooperation of patients, who needed to adopt a healthier way of life by making adjustments to their diet and level of physical activity[8,9].

In the present study, the majority of patients on statins with moderate and high risk attained the ideal LDL-C 100 objective, but a smaller percentage of patients with extremely high risk did not. Our patients did not achieve the very low (70m /dl) target goal recommended for the very high-risk population, which may be attributable to the fact that this goal requires a high dose and potency of statin, a healthy lifestyle, and good therapy adherence. These outcomes exceed those seen in research conducted by Jimmy et al., who reported that only 83 out of 183 individuals with dyslipidemia reached their statin target objective[10].

Current results exceed those obtained from research conducted by Arca et al., on adults with dyslipidemia who were given statins[11]. Our study's outcomes may have been better than previous studies' not because of better patient or statin management of dyslipidemia, but because of the intensive course of statin medication employed, the kind and amount of statins used, patient adherence, and physicians' prescribing habits. We found that patients at very high risk achieved the statin target goal (LDL-C 70 mg/dl), while patients at moderate and high risk achieved the statin target goal (LDL-C 100 mg/dl) in a cross-sectional retrospective study conducted in the United States by Jones et al[12]. Despite these works, the proportion of patients with extremely high-risk dyslipidemia who achieved statin target goal (70 mg/dl LDL-C) in a Greek trial by Xanthopoulou et al. was lower than in our research[13]. The proportion of extremely high-risk patients that achieved statin optimum target (70 mg/dl LDL-C) in the current investigation is lower than that in the Vintila et al. study in Romania[14].

Farhan et al. did research on 200 obese and overweight individuals with dyslipidemia in Iraq and found that rigorous treatment with statin significantly reduced blood LDL-C, HDL-C, and cholesterol[15]. For individuals with dyslipidemia, our research is the first to address the statin aim objective. The lack of a unified understanding of what constitutes dyslipidemia is a significant challenge to researchers in the Middle East who are trying to determine the optimal statin target aim. Furthermore, there are no specific lipid recommendations for treating dyslipidemia. The majority of nations in the Middle East follow lipid recommendations derived from sources outside the region[16].

Our findings were better than those observed in the Dyslipidemia International Study, which included patients with dyslipidemia from Europe and China who were treated with statins according to EAS/ESC criteria for very-high CV risk[17]. Prescription of statins as secondary therapy without focusing on target goal, combined with a lack of subsequent monitoring of lipid levels in patients, the possibility of side effects (muscle side effects), poor education about the safety of statins, and low adherence, may explain why our study's goal of achieving LDL-C levels of 100 mg/dl was not met. The risk of ischemic heart disease attacks is reduced by 60% and the risk of stroke is reduced by 17%, according to a meta-analysis research conducted by Law et al in the UK[18].

Results obtained in the current work revealed that female patients on statins were more likely to fail in reach their statin goal ($p=0.001$), which may be attributable to factors such as non-adherence to therapy, poor dietary habits, and the presence of several comorbid conditions. This conclusion is in line with the findings of the Chinese trial conducted by Li et al., which found that

extremely high risk patients were reaching the objective aim of treatment with statins (LDL-C 70 mg/dl)[19]. Women are more prone to acquire dyslipidemia than males, and they also have worse compliance and adherence to statin medication, according to research conducted in Saudi Arabia and published in 1966 by Alnouri et al.[20].

A higher statin dosage was associated with meeting the objective in the current investigation ($p<0.01$). This discovery is in agreement with the findings of other literatures, such as the research by Martin et al.[21] in the United States and the study by Bittencourt[22] in Brazil, which both discovered that a high dosage of statin administered in accordance with the appropriate guidelines is beneficial in the prevention and treatment of dyslipidemia. Patients with dyslipidemia who take large doses of statins are at increased risk of diabetes mellitus of about 30% and other side effects, according to research by Wang et al. in China[23]. Other studies also demonstrated that statin therapy is effective in lowering LDL-C levels, particularly among individuals at extremely high risk, as proven by a series of studies conducted in the United States and published by Kapur et al[24].

It was concluded that the targeted LDL levels were achieved in good proportion in patients with high and moderate risk of dyslipidemia with a less extent proportion in patients with very high-risk of dyslipidemia. It was also demonstrated that the LDL target levels were achieved more efficiently with a higher dose of statins.

STATEMENT OF ETHICS

The research was carried out adhering to the Declaration of Helsinki's ethical guidelines. The procedure was conducted after obtaining verbal and analytical consent from the patients before to collecting the sample. The Research Ethical Committee in Kut University College, Wasit, Iraq, examined and approved the study protocol, subject information, and permission form. This approval was granted by a local ethics commission, as indicated by document number 454 dated 12/11/2022.

CONFLICT OF INTEREST STATEMENT

The authors declared no conflict of interest.

AUTHOR CONTRUBITIONS

Design: AL-SHAMMARI AH, SHANDOOKH QJ; Aquisition of data: AL-SHAMMARI AH, Analysis of data: AL-SHAMMARI AH, Manuscript preparation: AL-SHAMMARI AH, Revision of the manuscript: SHANDOOKH QJ, Statistical analysis: AL-SHAMMARI AH, Technical and financial support: AL-SHAMMARI AH, SHANDOOKH QJ, Supervision: SHANDOOKH QJ.

REFERENCES

1. Wu N-Q, Li J-J. Clinical considerations of lipid target and goal in dyslipidemia control. Chronic Dis Transl Med, 2016;2(1):3-6. Doi: 10.1016/j.cdtm.2016.05.002

2. Tomasik T, Windak A, Seifert B, Kersnik J, Kijowska V, Dubas K. Lipid-lowering pharmacotherapy in Central and Eastern European countries in cardiovascular prevention: self-reported prescription patterns of primary care physicians. J Cardiovasc Pharmacol Ther, 2013;18(3):234-242. Doi: 10.1177/1074248412471196

3. Ghodke RM, Tour N, Devi K. Effects of statins and cholesterol on memory functions in mice. Metab Brain Dis, 2012;27:443-451. Doi: 10.1007/s11011-012-9343-5

4. Pignatelli P, Carnevale R, Di Santo S, Bartimoccia S, Nocella C, Vicario T, et al. Rosuvastatin reduces platelet recruitment by inhibiting NADPH oxidase activation. Biochem Pharmacol, 2012;84(12):1635-1642. Doi: 10.1016/j.bcp.2012.09.011

5. Jellinger PS, Handelsman Y, Rosenblit PD, Bloomgarden ZT, Fonseca VA, Garber AJ, et al. American Association of Clinical Endocrinologists and American College of Endocrinology guidelines for management of dyslipidemia and prevention of cardiovascular disease. Endocr Pract, 2017;23:1-87. Doi: 10.4158/EP171764.APPGL

6. Jarari AM, Al-Attar HA, Abdel-Moneim MM, Pathak RM, Sheriff DS. Evaluation of body iron and oxidative stress status in smoker/hypertensive/diabetic patients suffering acute myocardial infarction episode. Jordan J Biol Sci, 2011;4(1); 43-50.

7. Wang Q, Liang C. Role of lipid-lowering therapy in low-density lipoprotein cholesterol goal attainment: focus on patients with acute coronary syndrome. J Cardiovasc Pharmacol, 2020;76(6):658-670. Doi: 10.1097/FJC.0000000000000914

8. Members TF, Piepoli MF, Hoes AW, Agewall S, Albus C, Brotons C, et al. 2016 European guidelines on cardiovascular disease prevention in clinical practice: the sixth joint task force of the European Society of Cardiology and other societies on cardiovascular disease prevention in clinical practice. Eur J Prev Cardiol, 2016;*37*(29),2315-2381. Doi: 10.1093/eurheartj/ehw106

9. Catapano AL, Graham I, De Backer G, Wiklund O, Chapman MJ, Drexel H, et al. 2016 ESC/EAS guidelines for the management of dyslipidaemias. Atherosclerosis, 2016;253:281-344. Doi: 10.1016/j.atherosclerosis.2016.08.018

10. Jose J, Al-Tamimi FAA, Helal MM, Jimmy B, Al Riyami Q, Al Busaidi I. Targeted study to evaluate the cardiovascular risk factor status among patients and efficacy of statins in attaining goal lipid levels in a regional hospital in Sultanate of Oman. Saudi Pharm J, 2015;23(4):371-376. Doi: 10.1016/j.jsps.2014.11.006

11. Arca M, Ansell D, Averna M, Fanelli F, Gorcyca K, Iorga ŞR, et al. Statin utilization and lipid goal attainment in high or very-high cardiovascular risk patients: insights from Italian general practice. Atherosclerosis, 2018;271:120-127. Doi: 10.1016/j.atherosclerosis.2018.02.024

12. Jones PH, Nair R, Thakker KM. Prevalence of dyslipidemia and lipid goal attainment in statin-treated subjects from 3 data sources: a retrospective analysis. J Am Heart Assoc, 2012;1(6):e001800. Doi: 10.1161/JAHA.112.001800

13. Xanthopoulou I, Davlouros P, Siahos S, Perperis A, Zaharioglou E, Alexopoulos D. First-line treatment patterns and lipid target levels attainment in very high cardiovascular risk outpatients. Lipids Health Dis, 2013;12(1):1-9. Doi: 10.1186/1476-511X-12-170

14. Vintila A-M, Iordachescu I, Horumba M. LDL-cholesterol goal attainment in light of the 2019 dyslipidemia guidelines. Rom J Cardiol, 2019;29(4):558-562.

15. Farhan HA, Khazaal FA, Mahmoud IJ, Haji GF, Alrubaie A, Abdulraheem Y, et al. Efficacy of atorvastatin in treatment of Iraqi obese patients with hypercholesterolemia. Al-Kindy Col Med J, 2014;10(2):62-69.

16. Al Rasadi K, Almahmeed W, AlHabib KF, Abifadel M, Farhan HA, AlSifri S, et al. Dyslipidaemia in the Middle East: current status and a call for action. Atherosclerosis, 2016;252:182-187. Doi: 10.1016/j.atherosclerosis.2016.07.925

17. Gitt AK, Ambegaonkar B, Brudi P, Horack M, Lautsch D. Low LDL-cholesterol target achievement in statin-treated patients in clinical practice in China and Europe: results of the Dyslipidemia International Study (DYSIS). J Am Coll Cardiol, 2015;65(10S):A1482. Doi: 10.1016/S0735-1097(15)61482-6

18. Law MR, Wald NJ, Rudnicka A. Quantifying effect of statins on low density lipoprotein cholesterol, ischaemic heart disease, and stroke: systematic review and meta-analysis. Br Med J, 2003;326(7404):1423. Doi: 10.1136/bmj.326.7404.1423

19. Li X, Xu Y, Li J, Hu D. The gender differences in baseline characteristics and statin intervention among outpatients with coronary heart disease in China: the China Cholesterol Education Program. Clin Cardiol, 2009;32(6):308-314. Doi: 10.1002/clc.20514

20. Alnouri F, Wood D, Kotseva K, Ibrahim ME. Which statin worked best to achieve lipid level targets in a European registry? A post-hoc analysis of the EUROASPIRE III for coronary heart disease patients. J Saudi Heart Assoc, 2014;26(4):183-191. Doi: 10.1016/j.jsha.2014.04.005

21. Martin SS, Gosch K, Kulkarni KR, Spertus JA, Mathews R, Ho PM, et al. Modifiable factors associated with failure to attain low-density lipoprotein cholesterol goal at 6 months after acute myocardial infarction. Am Heart J, 2013;165(1):26-33. e3. Doi: 10.1016/j.ahj.2012.10.005

22. Bittencourt MS, Cesena FHY. Statin dose in primary prevention: aim for the target! Heart, 2019 Jul;105(13):969-971. Doi: 10.1136/heartjnl-2019-314723

23. Wang S, Cai R, Yuan Y, Varghese Z, Moorhead J, Ruan XZ. Association between reductions in low-density lipoprotein cholesterol with statin therapy and the risk of new-onset diabetes: a meta-analysis. Sci Rep, 2017 Jan 10;7:39982. Doi: 10.1038/srep39982

24. Kapur NK, Musunuru K. Clinical efficacy and safety of statins in managing cardiovascular risk. Vasc Health Risk Manag, 2008;4(2):341-353. Doi: 10.2147/vhrm.s1653

Acta Pharm. Sci. Vol 62:(2), 2024
Research article
DOI: 10.23893/1307-2080.APS6219

Study of formulation effects on the charge variant profile of antibody-maytansine conjugates by icIEF method

Ayat ABBOOD*

Department of Medicinal Chemistry and Quality Control, Faculty of Pharmacy, Tishreen University, Lattakia, Syria

ABSTRACT

A whole-column imaging-detection capillary isoelectric focusing method (icIEF) was used to study the effects of formulation and thermal stability on the charge variant profile of maytansinoid antibody conjugates. The unconjugated monoclonal antibody showed a narrow pI range (8.9-9.0), while its conjugates to maytansine derivative had more acidic charge variants)pI values: 7.6 to 9.0(. Four formulation prototypes at acidic pH (5.5) were studied. The presence of acetate and citrate in the formulation of maytansine antibody conjugate led to more heterogeneous charge variant profiles and to a shift to acidic isoforms as a result of amidation of amine groups of N-terminus of the light and heavy chains of the antibody. After forced thermal stress conditions (one month at 40°C), slight modifications in the charge variant profiles of maytansinoid antibody conjugates were observed in the four formulation prototypes compared to the control sample (-80°C), indicating no protein degradation by deamidation.

Keywords: antibody, conjugate, charge variant, p*I*, icIEF

INTRODUCTION

Monoclonal antibodies (mAbs) are a very important therapeutic class for the treatment of various diseases[1]. Unconjugated antibodies were used as antitumor due to their specificity to targeted cancer cells and there less side effects.

* Corresponding author: Ayat ABBOOD
E-mail: ayatabboud@tishreen.edu.sy
ORCID: 0000-0001-8387-3875
(Received 25 Jun 2023, Accepted 24 Jul 2023)

To improve their efficiency in the treatment of cancer, conjugating antibodies with chemotherapeutic drugs via linkers have been extensively investigated[2-4]. After selectively binding to targeted cancer cells, antibody-drug conjugates (ADCs) release the cytotoxic agents to these cells. The release of actives agents from ASCs is achieved by the cleavage of the ADC linkers due to pH changes, redox reaction or enzymatic activity.

The physicochemical characteristics of ADCs greatly affect their therapeutic performance. Therefore, it is very important to assess the homogeneity and stability of ADCs. Homogeneous conjugation with drugs is very important to generate effective antitumor ADCs[5-6]. mAbs are generally conjugated with cytotoxic molecules through cleavable or non-cleavable linkers through amino acid residues, primarily lysine and cysteine residues[6]. An antibody usually may contain up to 80 lysine residues[7]. Lysine-based ADCs are heterogeneous with a wide drug-to-antibody ratio (DAR) distribution. DAR is the average number of drugs conjugated to the antibody[8].

During ADC development, formulation should be studied to find the best conditions to minimize heterogeneity and increase the stability of the formulated products. mAb and ADC formulations are composed of several excipients to maintain pH and to increase the stability of protein. Sugars (e.g., sucrose), surfactants (e.g., polysorbate 20 [PS20] and PS80), and amino acids (e.g., histidine, arginine, and glycine) are usually used as excipients for mAb and ADC formulations[9-12]. Formulation excipients may lead to chemical modifications of mAbs and their drug conjugates. Therefore, assessing the behaviour of the ADCs in formulation is essential to ensure their safety and efficacy.

Instability is a serious problem in all stages of therapeutic ADC development, from discovery to production and utilization[13-15]. Stability is affected by ADC formulation. Therefore, it is very important to study the impact of the formulation composition on ADC stability. ADC stability studies are usually performed under stress conditions (40°C) to accelerate the aggregation and chemical modifications of ADCs, and therefore to choose the best formulation[16,17].

Chemical modifications, resulting of the formulation excipients or during the storage, may lead to change the charge variant profiles of ADCs (i.e., a decrease or an increase of p*I* values)[18-24]. The characterization of the charge variant profile of ADCs is an important tool to assess their quality[25-27]. Monitoring the charge variants of mAb or ADC provides information on protein stability, product purity from batch to batch, the pathways of degradation, etc[28-30]. Different analytical methods have been used to assess the charge heterogeneity of ADC, such as chromatographic methods[31-32], electrophoretic methods[33-36].

Whole-column imaging-detection capillary isoelectric focusing methods (icIEF) permit the separation of proteins based on their isoelectric point (p*I*), offering simultaneous detection along the entire length of the column, higher resolution, speed, and quantitative analysis[37-38]. In a previous study[39], an icIEF method was developped for the analytical characterization of the charge heterogeneity of a novel humanized anti-EphA2 antibody conjugated to a maytansine derivative. In this work, the impact of the purification method, formulation excipients and thermal stability on the charge variant profile of the novel humanized anti-EphA2 antibody conjugated to a cytotoxic maytansine derivative were studied using the previously published developed icIEF method[39].

METHODOLOGY

Materials

Formulation excipients, inclding sucrose and mannitol (used to prevent mAb and ADC aggregation), polysorbate 80 (a surfactans for increasing the solubility of mAbs and ADCs) and buffering agents for controlling pH and stabilizing mAbs and ADCs (e.g., glycine, histidine, citric acid and acetic acid) were purchased from Sigma. Urea, which was used to increase protein sample solubility and stability was from Sigma. Kit ICE280 chemical test, Kit iCE280 electrolytic solution, methyl cellulose 1% and p*I* Markers (6.61 and 9.5) were obtained from Convergent Bioscience. Pharmalyte solutions (3-10 and 8-10.5) were obtained from GE Healthcare. A monoclonal naked antibody and its maytansinoid conjugates were analyzed. The composition of their formulation was mentioned in the result and discussion section.

Sample preparation

The protein sample solution was composed of 0.35% methyl cellulose, 4% pharmalytes (3–10) and pharmalytes (8–10.5) (1:1 ratio), 2M urea and p*I* markers (6.61 and 9.5). After centrifugation, the sample was transferred to a glass autosampler vial and centrifuged to remove bubbles before being placed in the autosampler carousel for analysis.

icIEF apparatus

An iCE280 instrument with PrinCE autosampler and capillary cartridge from Convergent Bioscience were used. The separation capillary column was transparent and had a fluorocarbon-coated inner surface (50mm, 100µm ID, 200µm OD). The column was installed in into a glass cartridge. The cathodic solution contained 100mM NaOH and 0.1% methyl cellulose, while the anodic solution contained 80mM H_3PO_4 and 0.1% methyl cellulose. Protein focusing time was set at 10 or 12min at 3000V. Detection at 280nm was achieved with a CCD camera.

RESULTS and DISCUSSION

The EphA2 receptor is one of 16 related receptor tyrosine kinases (RTKs) that are activated by membrane-associated ligands known as ephrins. EphA2 protein levels have been reported to be elevated in many types of cancer[40]. The studied mAb is anti-EphA2 of molecular weight of 145478 g/mol. Figure 1 presented the icIEF profile of the unconjugated anti-EphA mAb, which was characterized by two major peaks corresponding to p*I* values of 8.9 and 9.0.

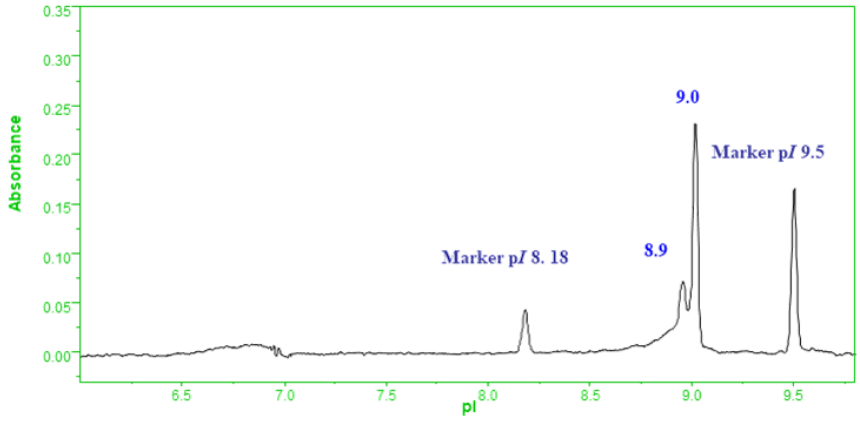

Figure 1. icIEF profile of unconjugated antibody. Final concentration of unconjugated antibody in sample matrix is 0.2mg/ml diluted in 0.35% methyl cellulose,4% 3–10 pharmalytes/ 8–10.5 pharmalytes (1:1 ratio), 2M urea. pI markers: 8. 18, 9.50. Focusing time: 10min at 3000V.

Small-molecule drugs are covalently attached to antibodies through chemical linkers to improve their antitumor efficiency. The side chain of lysine residues is commonly used for conjugation. As mentioned before, mAbs often contain up to 80 lysine residues and chemical conjugation results in a heterogeneous mixture of unconjugated mAbs and conjugated mAbs with a variable number of cytotoxins bonded to different sites on the antibody.

Anti-EphA2 mAbs were conjugated to a maytansinoid derivative through non-cleavable linker with the free amine groups of lysine residues. The antitumor action of resulted ADC is based on the release of the maytansinoid derivative linker, which kills cancer cells by interfering with their division upon antibody/antigen binding.

The conjugation processes take place by linking the cytotoxic-linker with the free amine group of lysine of the anti-EphA2 mAb in a single step, resulting in maytansinoid drug conjugates with 1 to 10 maytansinoid molecules of about 160 kDa. The ratio of maytansinoid molecules to mAb is around 6.2 moles of drug per mole of mAb.

This work aimed to study the effects of purification methods, different formulation excipients and thermal stress stability on the icIEF charge variant profile of maytansinoid antibody conjugates.

Charge heterogeneity profile of maytansinoid antibody conjugates

After conjugation, it is also necessary to purify the crude product to limit the amount of free drug in the sample, and other impurities.

Two strategies were used to purify the resulting ADCs after conjugation, of the anti-EphA2 mAb using the tangential flow filtration method (TFF). TFF was performed immediately after conjugation (immediate TFF) or after an overnight holding time after conjugation to allow hydrolysis and removal of weakly bound linkers (improved process; 24 H). The two batches of maytansinoid antibody conjugate were formulated in HGS buffer consisted of histidine 10mM, glycine 130mM and sucrose 5% (w/v). The icIEF profiles of maytansinoid antibody conjugates are presented in Figure 2.

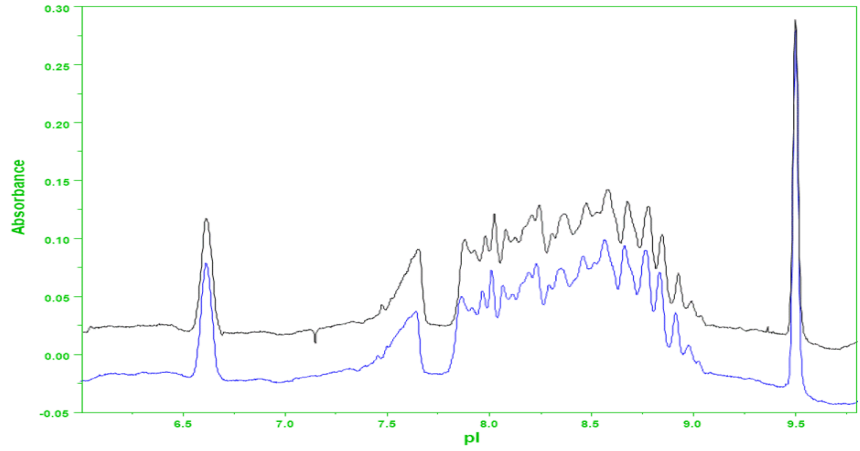

Figure 2. icIEF profile of two batches of maytansinoid antibody conjugates: immediate TFF (black), improved process: 24h (blue). Experimental conditions: Final concentration 1mg/mL in 0.35% methyl cellulose, 4% 3–10 pharmalytes/8–10.5 pharmalytes in 1:1 ratio and 2M urea. pI markers: 6.61, 9.50. Focusing time was 12min at 3000V.

Maytansinoid antibody conjugates were more heterogeneous and acidic than unconjugated mAb (p*I* values of 7.6 to 9.0). This heterogeneity of conjugated mAb is related to the covalently linking of the cytotoxic drug to the free amine groups of lysine of mAbs.These charge variants differed by the number of amine groups of lysine conjugated to the linker molecule, leading to a decrease in their p*I* with an increase in the number of modified amino groups (more acidic). There was no significant difference in charge variant profiles between the two batches: immediate TFF and improved process 24h (Figure 3).

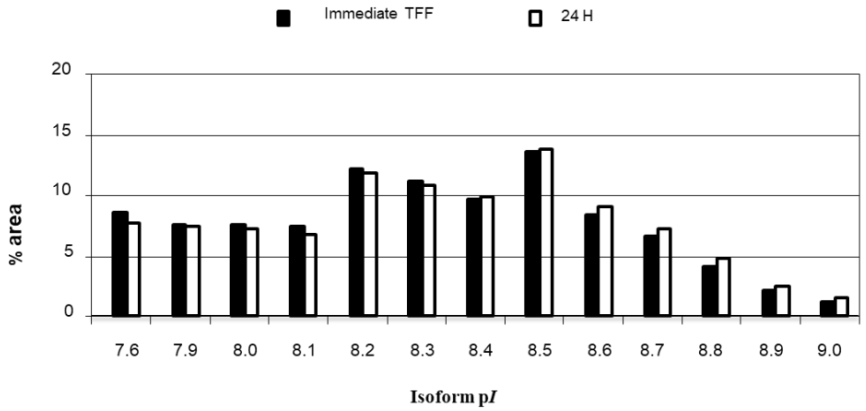

Figure 3. Comparison of % specie area by icIEF of two batches of maytansinoid antibody conjugate: immediate TFF, improved process: 24h. Experimental conditions as mentioned in Figure 1.

icIEF profiles of formulation prototypes of maytansinoid antibody conjugates: (immediate TFF)

To bring ADC to the market, ADC formulation should be developed to ensure the quality, efficacy, and safety of the product. The excipients of the formulation may generate chemical modifications to ADCs, leading to a change in the charge variant profile of ADCs. For instance, deamidation and amidation of amine lysine groups lead to an increase in acidic variants (decreasing p*I* values) while oxidation or succinimide formation lead to an increase in basic variants (increasing p*I* value)[41]. Modifications of p*I* (one unit or more) may alter the pharmacokinetics of ADCs and therefore their biological effects[42].

Maytansinoid antibody conjugates were formulated in four prototypes detailed in Table 1, including formulation buffer composition and ADC concentration. The pH of the four formulation prototypes was maintained at acidic value of 5.5.

Table 1. Formulation buffer composition, concentration and DAR of immediate TFF ADC

Sample	Formulation buffer	Concentration
Control	His 10mM, Gly 130mM, Sucrose 5% (w/v) pH 5.5	2 mg/mL
Prototype-1	His 10mM, Gly 130mM, Sucrose 5% (w/v), PS80 0.01% pH 5.5	2 mg/mL
Prototype-2	Acetate 10mM, Sucrose 5%, mannitol 2.5%, PS80 0.01% pH 5.5	2 mg/mL
Prototype-3	Citrate 1 mM, Sucrose 5%, mannitol 2.5%, PS80 0.01% pH 5.5	2 mg/mL

The prototype-1 formulation only differed from the control formulation by the addition of polysorbate80. Prototype-2 and -3 formulations were composed of acetate and citrate in addition to sucrose, mannitol and PS80.

The icIEF profiles of the four formulation prototypes of maytansinoid antibody conjugate were presented in the Figure 4. Maytansinoid antibody conjugate in control formulation (HGS buffer) and prototype-1 (HGS + PS80) had similar charge profiles but different from those obtained for the prototypes-2 (acetate) and the prototype-3 (citrate).

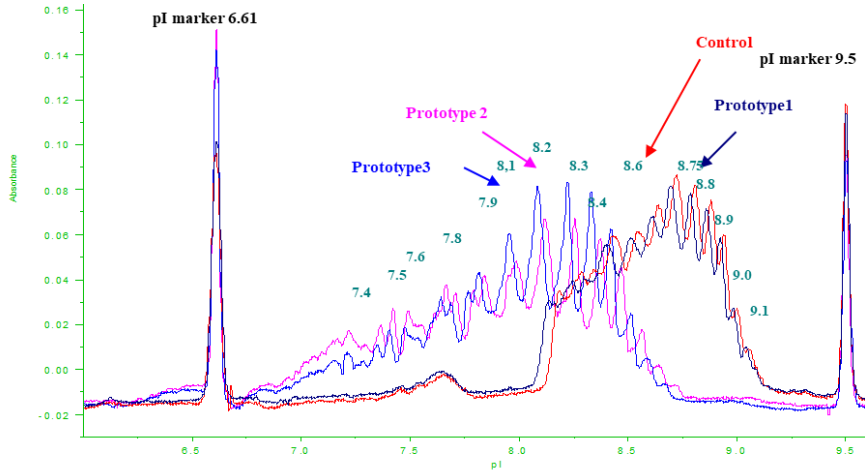

Figure 4. icIEF profiles of formulation prototypes of maytansinoid antibody conjugates. Experimental conditions: Final concentration 0.7 mg/mL in 0.35% methyl cellulose, 2% 3–10 pharmalyte, 2% 8–10.5 pharmalyte (1:1 ratio) and 2M urea. p*I* markers: 6.61, 9.50. Focusing time was 12min at 3000V.

The comparison of p*I* ranges of these prototypes, presented in the Table 2, demonstrated a shift to acidic isoforms in prototype-2 and prototype-3. Furthermore, maytansinoid antibody conjugate displayed a more heterogeneous charge profile than control and prototype-1. Different studied have reported covalent modification of a recombinant monoclonal antibody by citric acid in a citrate buffered formulation leading to the formation of acidic species as a result of the amidation of the N-terminus of the light and the heavy chain of the antibody[16, 23]. As mentioned before, the charge heterogeneity profile of maytansinoid antibody conjugate in acetate buffer was similar to that obtained in the citrate buffer. A chemical modification (formation of amide and imide) in the acetate buffer may be suggested to explain the formation of acidic species in a similar manner to the citrate buffer.

Table 2. p*I* range and difference of four prototypes of maytansinoid antibody conjugates

	Control	Prototype-1	Prototype-2	Prototype-3
pI range	8.1-9.1	8.1-9.1	7.4-8.6	7.4—8.6
Δ pI	1	1	1.2	1.2

Stability study of maytansinoid antibody conjugates formulation prototypes

Stability studies at higher temperatures allow for prediction of stability at the intended storage temperature. To determine which formulation impacts the thermal stability of maytansinoid antibody conjugate, it was incubated one month at 40°C in the four formulation prototypes. Stability studies are performed at 40°C in order to speed up changes in the quality characteristics of the ADCs. The exposure of ADCs to 40°C may accelerate aggregation and chemical modifications, such as deamidation and oxidation of ADCs[43].

The icIEF profiles of stressed samples of maytansinoid antibody conjugate prototypes showed that the total peak area of the 40°C stressed samples were lower than that of the control sample (-80°C). These decreases in total area were 18%, 12%, 20%, and 21% for the control maytansinoid antibody conjugate, prortotype-1, prortotype-2, and prortotype-3 respectively. Maytansinoid antibody conjugate in formulation prortotype-1 showed less protein precipitation at 40°C compared to other formulations. The percentages of charge species obtained for the 40°C stressed samples were roughly similar to the control sample (-80°C) for all formulation prototypes (Figure 5). The slight modification of charge profiles of maytansinoid antibody conjugate under stressed conditions in the four formulation prototypes indicated no protein degradation by deamidation.

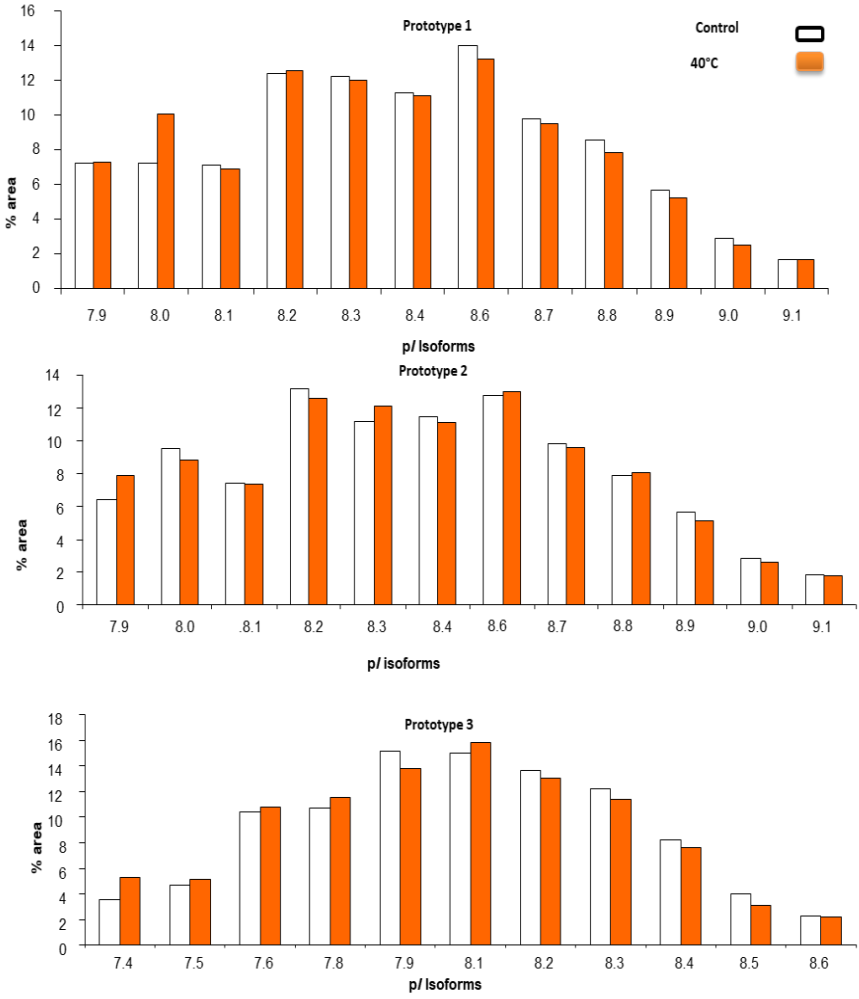

Figure 5. Percent area of pI isoforms 40°C stressed samples (red) of four formulation prototypes of maytansinoid antibody conjugates compared with a control (-80°C) (white)

The icIEF profile of anti-EphA2 monoclonal antibodies demonstrated two major peaks with p*I* values of 8.9 and 9.0. Maytansinoid conjugates of this antibody were more heterogeneous and acidic than unconjugated mAb (p*I* values between 7.6 and 9.0). No significant difference in the charge variant profiles was observed between the two batches: immediate purification by angential flow filtration or after holding one night before purification. The citrate and acetate-buffered formulations had similar charge variant profiles while HGS formulation without or with polysorbate80 had the same charge variant profiles. The presence of citrate and acetate led to the formation of acidic spe-

cies as compared to HGS formulation. Aggregation of maytansinoid antibody conjugate and slight modification of charge variant profile in the studied four formulation prototypes were observed after thermal forced conditions.

STATEMENT OF ETHICS

Ethical approval was not required to perform this study.

CONFLICT OF INTEREST STATEMENT

The author declares that there is no conflict of interest.

AUTHOR CONTRIBUTIONS

Ayat Abbood carried out the analysis and wrote the article.

FUNDING SOURCES

No funding or other financial support was received for this study.

ACKNOWLEDGMENTS

Not Applicable.

REFERENCES

1. Kaplon H, Reichert JM. Antibodies to watch in 2021. Mabs, 2021;13(1):1860476. Doi: 10.1080/19420862.2020.1860476

2. Khongorzul P, Ling CJ, Khan FU, Ihsan AU, Zhang J. Antibody-drug conjugates: a comprehensive review. Mole Cancer Res, 2020;18(10):3-19. Doi: 10.1158/1541-7786.MCR-19-0582

3. Dean AQ, Luo S, Twomey JD, Zhang B. Targeting cancer with antibody-drug conjugates: promises and challenges. Mabs, 2021;13(1):1951427. Doi: 10.1080/19420862.2021.1951427

4. Fu Z, Li S, Han S. Antibody drug conjugate: the "biological missile" for targeted cancer therapy. Signal Transduct Targeted Ther, 2022;7(1):93. Doi: 10.1038/s41392-022-00947-7

5. Anami Y, Otani Y, Xiong W, Ha SYY, Yamaguchi A, Rivera-Caraballo KA, et. al. Homogeneity of antibody-drug conjugates critically impacts the therapeutic efficacy in brain tumors. Cell Rep, 2022;39(8):10839. Doi: 10.1016/j.celrep.2022.110839

6. Tsuchikama K, An Z. Antibody-drug conjugates: recent advances in conjugation and linker chemistries. Protein cell, 2018;9(1):33-46. Doi: 10.1007/s13238-016-0323-0

7. Alves NJ. Antibody conjugation and formulation. Antib Ther, 2019;15;2(1):33-39. Doi: 10.1093/abt/tbz002

8. Fukunaga A, Maeta S, Reema B, Nakakido M, Tsumoto K. Improvement of antibody affinity by introduction of basic amino acid residues into the framework. Biochem Biophy Rep, 2018;15:81-85. Doi: 10.1016/j.bbrep.2018.07.005

9. Rayaprolu BM, Strawser JJ, Anyarambhatla G. Excipients in parenteral formulations: selection considerations and effective utilization with small molecules and biologics. Drug Dev Ind Pharm, 2018;44(10):1565-1571. Doi: 10.1080/03639045.2018.1483392

10. Carpenter JF, Pikal MJ, Chang BS, Randolph TW. Rational design of stable lyophilized protein formulations: some practical advice. Pharm. Res, 1997;14(8):969-975. Doi: 10.1023/a:1012180707283

11. Kamerzell TJ, Esfandiary R, Joshi SB, Middaugh CR, Volkin D. Protein-excipient interactions: mechanisms and biophysical characterization applied to protein formulation development. Adv Drug Deliv Rev, 2011;63(13):1118-1159. Doi: 10.1016/j.addr.2011.07.006

12. Wang SS, Yan YS, Ho K. US FDA-approved therapeutic antibodies with high-concentration formulation: summaries and perspectives. Antib Ther, 2021;4(4):262-272. Doi: 10.1093/abt/tbab027

13. Ma H, Ó'Fágáin C, O'Kennedy R. Antibody stability: a key to performance – analysis, influences and improvement. Biochimie, 2020;177:213-215. Doi: 10.1016/j.biochi.2020.08.019

14. Wang W, Singh S, Zeng DL, King K, Nema S. Antibody structure, instability, and formulation. J Pharm Sci, 2007;96(1):1-26. Doi: 10.1002/jps.20727

15. Zhang Y, Williams Iii R, Tucker H O. Formulation strategies in immunotherapeutic pharmaceutical products. World J Clin Oncol, 2007;11(5):275-282. Doi: 10.5306/wjco.v11.i5.275

16. He F, Woods CE, Becker GW, Narhi LO, Razinkov VI. High-throughput assessment of thermal and colloidal stability parameters for monoclonal antibody formulations. J Pharm Sci, 2011;100(12):5126-5141. Doi: 10.1002/jps.22712

17. Niedziela-Majka A, Kan E, Weissburg P, Mehra U, Sellers S, Sakowicz R. High-throughput screening of formulations to optimize the thermal stability of a therapeutic monoclonal antibody. J Biomol Screen, 2015;20(4):552-259. Doi: 10.1177/1087057114557781

18. Narayanan H, Dingfelder F, Morales IC, Patel B, Heding KE, Bjelke JR, et al. Design of biopharmaceutical formulations accelerated by machine learning. Mol Pharm, 2021;18(10):3843-3853. Doi: 10.1021/acs.molpharmaceut.1c00469

19. Valliere-Douglass JF, Connell-Crowley L, Jensen R, Schnier PD, Trilisky E, Leith M. et al. Photochemical degradation of citrate buffers leads to covalent acetonation of recombinant protein therapeutics. Protein Sci, 2010;19(1):2152-2163. Doi: 10.1002/pro.495

20. Xu Y, Wang D, Mason B, Rossomando T, Li N, Liu D, et al. Structure, heterogeneity and developability assessment of therapeutic antibodies. mAbs, 2019;11(2):239-264. Doi: 10.1080/19420862.2018.1553476

21. Grassi L, Cabrele C. Susceptibility of protein therapeutics to spontaneous chemical modifications by oxidation, cyclization, and elimination reactions. Amino Acids, 2019;51(10-12):1409-1431. Doi: 10.1007/s00726-019-02787-2

22. Shukla AA, Wolfe LS, Mostafa SS, Norman C. Evolving trends in mAb production processes. Bioeng Transl Med, 2017;2(1):58-69. Doi: 10.1002/btm2.10061

23. Chumsae C, Zhou LL, Shen Y, Wohlgemuth J, Fung E, Burton R, et al. Discovery of a chemical modification by citric acid in a recombinant monoclonal antibody. Anal Chem, 2014;86(18):8932-8936. Doi: 10.1021/ac502179m

24. Wakankar A, Chen Y, Gokarn Y, Jacobson FS. Analytical methods for physicochemical characterization of antibody drug conjugates. mAbs, 2011;3(2):161-172. Doi: 10.4161/mabs.3.2.14960

25. Wagh A, Song H, Zeng M, Tao L, Das TK. Challenges and new frontiers in analytical characterization of antibody-drug conjugates. mAbs, 2018;1(2):222-243. Doi: 10.4161/mabs.3.2.14960

26. Cauchon NS, Oghamian S, Hassanpour S, Abernathy M. Innovation in chemistry, manufacturing, and controls – a regulatory perspective from industry. J Pharm Sci, 2019;108(7):2207-2237. Doi: 10.1016/j.xphs.2019.02.007

27. Torkashvand F, Vaziri B. Main quality attributes of monoclonal antibodies and effect of cell culture components. Iran Biomed J, 2017;21(3):131-141. Doi: 10.18869/acadpub.ibj.21.3.131

28. Hintersteiner B, Lingg N, Zhang P, Woen S, Hoi KM, Stranner S, et al. Charge heterogeneity: basic antibody charge variants with increased binding to Fc receptors. mAbs, 2016;8(8):1548-1560. Doi: 10.1080/19420862.2016.1225642

29. Sule SV, Fernandez JE, Mecozzi VJ, Kravets Y, Yang WC, Feng P, et al. Assessing the impact of charge variants on stability and viscosity of a high concentration antibody formulation. J Pharm Sci, 2017;106(12):3507-3514. Doi: 10.1016/j.xphs.2017.08.016

30. Yüce M, Sert F, Torabfam M, Parlar A, Gürel B, Çakır N, et al. Fractionated charge variants of biosimilars: a review of separation methods, structural and functional analysis. Anal Chim Acta, 2021;1152:238189. Doi: 10.1016/j.aca.2020.12.064

31. Zhu X, Huo S, Xue C, An B, Qu J. Current LC-MS-based strategies for characterization and quantification of antibody-drug conjugates. J Pharm Sci, 2020;10(3):209-220. Doi: 10.1016/j.jpha.2020.05.008

32. N Thallaj, A Abbood. Comparison between chromatofocusing and icIEF charge variant profiles of unconjugated monoclonal antibodies and their drug conjugates. Tishreen University Journal-Medical Sciences Series, 2023:45(2):47-57.

33. Kaur H, Beckman J, Zhang Y, Li ZJ, Szigeti M, Guttman A. Capillary electrophoresis and the biopharmaceutical industry: therapeutic protein analysis and characterization. TrAC

Trends Anal Chem, 2021;144:116407. Doi: 10.1016/j.trac.2021.116407

34. Chen T, Chen Y, Stella C, Medley CD, Gruenhagen JA, Zhang K. Antibody-drug conjugate characterization by chromatographic and electrophoretic techniques. J Chromatogr B, 2016;1032:39-50. Doi: 10.1016/j.jchromb.2016.07.023

35. Lin J, Lazar AC. Determination of charge heterogeneity and level of unconjugated antibody by imaged cIEF. Methods Mol Biol (Clifton, N.J.), 2013;1045:295-302. Doi: 10.1007/978-1-62703-541-5_19

36. Wu J, McElroy W, Pawliszyn J, Heger CD. Imaged capillary isoelectric focusing: applications in the pharmaceutical industry and recent innovations of the technology. TrAC Trends Anal Chem. 2022;150:116567. Doi: 10.1016/j.trac.2022.116567

37. Salas-Solano O, Kennel B, Park SS, Roby K, Sosic Z, Boumajny B, et al. Robustness of iCIEF methodology for the analysis of monoclonal antibodies: an interlaboratory study. J Sep Sci, 2012;35(22):3124-3129. Doi: 10.1002/jssc.201200633

38. Mack S, Cruzado-Park I, Chapman J, Ratnayake C, Vigh G. A systematic study in CIEF: defining and optimizing experimental parameters critical to method reproducibility and robustness. Electrophor, 2009;30(23):4049-4058. Doi: 10.1002/elps.200800690

39. Abbood A. Optimization of the imaged cIEF method for monitoring the charge heterogeneity of antibody-maytansine conjugate. J Anal Methods Chem, 2023;8150143. Doi: 10.1155/2023/8150143

40. Xiao T, Xiao Y, Wang W, Tang YY, Xiao Z, Su M. Targeting EphA2 in cancer. J Hematol Oncol, 2020;13(1):114. Doi: 10.1186/s13045-020-00944-9

41. Le Basle Y, Chennell P, Tokhadze N, Astier A, Sautou V. Physicochemical stability of monoclonal antibodies: a review. J Pharma Sci, 2020;109(1):169-190. Doi: 10.1016/j.xphs.2019.08.009

42. Liu H, Gaza-Bulseco G, Sun J. Characterization of the stability of a fully human monoclonal IgG after prolonged incubation at elevated temperature. J Chromatogr B, 2006;837(1-2):35-45. Doi: 10.1016/j.jchromb.2006.03.053

43. Khawli LA, Goswami S, Hutchinson R, Kwong ZW, Yang J, Wang X, et al. Charge variants in IgG1: isolation, characterization, in vitro binding properties and pharmacokinetics in rats. mAbs, 2010;2(6):613-624. Doi: 10.4161/mabs.2.6.13333

Acta Pharm. Sci. Vol 62:(2), 2024
Research article
DOI: 10.23893/1307-2080.APS6220

Effects of tadalafil on vancomycin-induced nephrotoxicity in rats

Hassanen A. ABDULAMEER[1*], Adeeb A. AL-ZUBAIDY[2]

1 Medico-legal Directorate, MOH, Laboratories Department, Baghdad, Iraq
2 Department of Pharmacology, College of Medicine, University of Warith Al-Anbiyaa, Karbala, Iraq

ABSTRACT

Tadalafil (TAD) is a member of the Phosphodiesterase 5 (PDE 5) inhibitors used to treat erectile dysfunction. However, recent evidence suggests that it has beneficial nephroprotective effects via a variety of mechanisms. The aim of the present study was to investigate the protective effect of TAD against vancomycin (VAN) - induced nephrotoxicity in rats (n=24), which divided into three groups; model control group that received intraperitoneal VAN, TAD group that received oral TAD and intraperitoneal VAN and normal healthy group. TAD group demonstrated a significant decrease in serum levels of renal function biomarkers and a significant increase in creatinine clearance level compared to the model control group. Furthermore, it showed a significant reduction in the renal levels of malondialdehyde (MDA), neutrophil gelatinase-associated lipocalin (NGAL), and TNF-α with a significant elevation in the renal level of glutathione (GSH) compared to the model control group. Histologically, TAD group showed a significant reduction in renal tissue injury that prove its nephroprotective effect due to its antioxidant and anti-inflammatory properties.

Keywords: oxidative stress, nephrotoxicity, tadalafil, vancomycin

INTRODUCTION

The kidney performs many vital functions, including eliminating medications in their initial state or metabolites. Many drugs undergo filtration, secretion,

* Corresponding author: Hassanen A. ABDULAMEER
E-mail: toxo849@gmail.com
ORCIDs:
Hassanen A. ABDULAMEER: 0009-0008-3068-3486
Adeeb A. AL-ZUBAIDY: 0000-0002-5207-383X
(Received 4 Sep 2023, Accepted 2 Nov 2023)

reabsorption, and elimination by the kidney, making it a common site of toxicity[1]. As well as, the kidneys take about 25% of the cardiac output, which expose them to more circulating drug than other organs[2]. Several medications like amphotericin B, vancomycin, aminoglycosides, and platin-containing chemotherapeutics are highly nephrotoxic[3]. Vancomycin (VAN) is a glycopeptide used as a first-line antibacterial drug for treating infections caused by methicillin-resistant *Staphylococcus aureus* (MRSA)[4]. Subsequently, numerous randomized clinical trials demonstrated that VAN poses a higher risk of nephrotoxicity than most other antibiotics[5]. The reported incidence of VAN-induced nephrotoxicity was 14.3%[6]. The recommended criteria for VAN-induced nephrotoxicity were a rise in serum creatinine level of at least 0.5 mg/dL or a 50% increase over baseline in consecutive daily tests[7]. The accurate pathophysiological mechanisms of VAN-induced nephrotoxicity are not yet completely known. However, the existing consensus states that vancomycin's nephrotoxic effect is primarily due to its intracellular accumulation in the proximal convoluted tubules[5].

Tadalafil (TAD) is a member of phosphodiesterase enzyme type-5 inhibitors approved in the management of erectile dysfunction, lower urinary tract symptoms (LUTS) secondary to benign prostatic hypertrophy (BPH)[8], and pulmonary arterial hypertension[9]. TAD inhibits the PDE5 enzyme with a greater selectivity (in comparison with sildenafil and vardenafil), thus improving intracellular levels of cGMP[10]. Experimental studies have confirmed that PDE-5 inhibitors improve endothelial function[11,12] and reduce infarct size in animal models of myocardial infarction[13]. PDE-5 inhibitors exert beneficial renal effects in the I/R rat model[14,15]. Several previous studies have shown that tadalafil can significantly improve renal injury due to several nephrotoxic agents[16–18], but the effect of TAD on VAN-induced nephrotoxicity has not been investigated. Therefore, the present study was conducted to determine the in vivo influence of orally administered TAD on VAN-induced renal injury in rats.

METHODOLOGY

Drugs

Vancomycin (vial) was obtained from Gulf pharmaceutical industries, United Arab Emirates and dissolved in distilled water according to the manufacturer's instructions. TAD powder was obtained from Hangzhou hyper chemical market, China and suspended in 0.5% carboxymethyl cellulose (CMC)[19,20].

Animals

Adult male Wistar albino rats weighing 175–285g were housed for two weeks for acclimatization under controlled conditions, including 12 h light/dark cy-

cles and controlled temperature (25 ºC), with free access to standard food and water.

Experimental design

Twenty-four male Wistar albino rats (*Rattus norvegicus*) were randomly assigned to three groups of 8 rats each as follows: (1) Normal control group: Maintained on standard food and water for 14 days. (2) Model control (VAN) group: Treated with intraperitoneal VAN (200mg/kg/ twice daily) for 14 days. (3) TAD group: Treated with oral TAD (5mg/kg/ once daily) and intraperitoneal VAN (200mg/kg/twice daily) for 14 days.

The induction of significant nephrotoxicity in the rat model depended on a pilot study and a previous study by Uhuo and his colleagues[21]. The dose of TAD was selected according to previous studies[18,22].

Samples collection

On the 15th day, the rats were anaesthetized by a mixture of ketamine 90mg/kg (Alfasan, Holland) and xylazine 10mg/kg (Bimeda, Canada) given intramuscularly. After that, Rats were sacrificed by decapitation. The blood samples were taken from the trunk and allowed to clot at room temperature. Thereafter centrifuged for 15-20 minutes at 3000 rpm. The isolated serum was kept at -80 ºC to be available afterwards for biochemical examination. Both kidneys of each rat were excised and washed with phosphate buffer saline (pH 7.4). One of the kidneys was rapidly frozen with dry ice and stored at -80 ºC to be available afterwards for homogenization. At the same time, the other kidney was kept in a neutral buffered formalin of 10% for histopathological analysis.

Renal tissue homogenization

Kidney tissues were homogenized in phosphate buffer saline in a proportion of 10% (w/v), using tissue homogenizer (IKA, Germany) for 1 minute at 4 ºC. After that, centrifuged at 3000 rpm for 20 minutes.

Biochemical analyses

Urea and creatinine serum levels were measured according to the urease-modified Berthelot method[23] and Jaffe method[24] respectively, using reagent kits (Linear Chemicals, Spain) with UV/Visible spectrophotometer (Cecil, England). Creatinine clearance was calculated using a neural network-based calculator of rat creatinine clearance from serum creatinine and body weight[25]. Renal levels of glutathione (GSH), malondialdehyde (MDA), neutrophil gelatinase-associated lipocalin (NGAL), and tumor necrosis factor- alpha (TNF-α) as well as serum cystatin C level, were measured according to the sandwich

ELISA technique[26], using rat ELISA kits (MyBioSource, USA) with ELISA plate reader (HUMAN Diagnostic Worldwide, Germany).

Histopathological analysis

Kidney tissue processing was done using the paraffin section technique[27]. The slides were examined under a light microscope (Olympus, Japan) at 20X magnification. Kidney tissue damage was graded according to the affected area in the tubulointerstitial area of the cortex, including tubular epithelial cell swelling, cast deposition, necrosis, desquamation, and interstitial inflammation as follows: 0 for normal tissues, 1 (mild) for < 25%, 2 (moderate) for > 25% but < 50%, 3 (severe) for ≥ 50% but < 75%, 4 (very severe) for ≥ 75%.

Statistical analysis

SPSS software version 26 was applied for data analysis. Numerical data are expressed as Mean ± SEM and one-way ANOVA with least significant differences (LSD) post hoc test for comparison among groups. For histopathological scores, Kruskal-Wallis and Mann-Whitney U tests were used. The difference was considered significant when p value was < 0.05.

RESULTS and DISCUSSION

Effects of tadalafil on renal function biomarkers

Serum levels of cystatin C, urea, and creatinine were significantly higher ($p < 0.05$) in the VAN group as compared to their corresponding levels in the normal healthy group. Furthermore, the level of creatinine clearance (Cr Cl) was significantly lower ($p < 0.05$) in the VAN group compared to that of the normal group. On the other hand, the TAD group showed significantly lower ($p < 0.05$) serum levels of renal function biomarkers and a significant ($p < 0.05$) higher level of Cr Cl as compared with their corresponding levels in the VAN group (Table 1).

Table 1. Effects of tadalafil on renal function biomarkers (mean + SEM)

Groups	Serum cystatin C (ng/ml)	Serum urea (mg/dl)	Serum Cr (mg/dl)	Cr Cl (ml/min)
Normal	269.62±10.43	28.68±1.29	0.49±0.03	0.79±0.07
VAN	553.15±27.82[a]	42.28±1.69[a]	1.30±0.21[a]	0.35±0.08[a]
TAD	324.11±11.03[ab]	34.39±2.08[ab]	0.55±0.03[b]	0.74±0.05[b]

Cr: creatinine; Cr Cl: creatinine clearance; a: $p < 0.05$ compared to normal group; b: $p < 0.05$ compared to VAN group.

Effects of tadalafil on oxidative stress biomarkers

The VAN group showed a significant increment ($p < 0.05$) in the level of renal tissue malondialdehyde (MDA) and a significant decline ($p < 0.05$) in the level of renal tissue glutathione (GSH) as compared to their corresponding levels in the normal group. On the other hand, the TAD group showed significantly lower ($p < 0.05$) level of renal tissue MDA and significantly higher ($p < 0.05$) level of GSH in renal tissue as compared to the VAN group (Table 2).

Table 2. Effects of tadalafil on renal tissue oxidative stress biomarkers (mean + SEM)

Groups	MDA (nmol/ml)	GSH (µg/ml)
Normal	1.17±0.04	38.14±1.08
VAN	4.04±0.10 [a]	10.83±0.23 [a]
TAD	1.83±0.03 [ab]	28.69±0.40 [ab]

MDA: malondialdehyde; GSH; glutathione; a: $p < 0.05$ compared to normal group; b: significant difference $p < 0.05$ compared to VAN group.

Effects of tadalafil on inflammatory biomarkers

Table 3 showed that the levels of neutrophil gelatinase-associated lipocalin (NGAL) and tumor necrosis factor-alpha (TNF-α) in renal tissue were significantly higher ($p < 0.05$) in the VAN group than in the normal group. More interestingly, the TAD group showed significantly lower ($p < 0.05$) renal tissue levels of NGAL and TNF-α compared with the VAN group.

Table 3. Effects of tadalafil on renal tissue inflammatory biomarkers (mean + SEM)

Groups	NGAL (pg/ml)	TNF-α (pg/ml)
Normal	254.02±12.41	870.43 ± 50.93
VAN	1269.73±62.24 [a]	1761.96±46.4 [a]
TAD	351.30±11.37 [ab]	872.2±84.7 [b]

NGAL: neutrophil gelatinase-associated lipocalin; TNF-α: tumor necrosis factor- alpha; a: $p < 0.05$ compared to normal group; b: $p < 0.05$ compared to VAN group.

Histopathological examination

VAN group showed significant kidney tissue damage ($p < 0.05$) as compared to the normal group, with the development of tubular epithelial cell swelling, desquamation, necrosis, cast deposition and interstitial inflammation (Figure 1-B). VAN group had 87.5% highly severe (score 4) and 12.5% severe (score 3) histopathological changes compared to healthy kidney tissue. More interestingly, The TAD group showed a significant decline ($p < 0.05$) in kidney tissue injury compared to the VAN group (Figure 1-C). In comparison to those of normal kidney tissue, the TAD group showed 12.5% mild (score 1), 75% moderate (score 2), and 12.5% severe (score 3) histopathological changes.

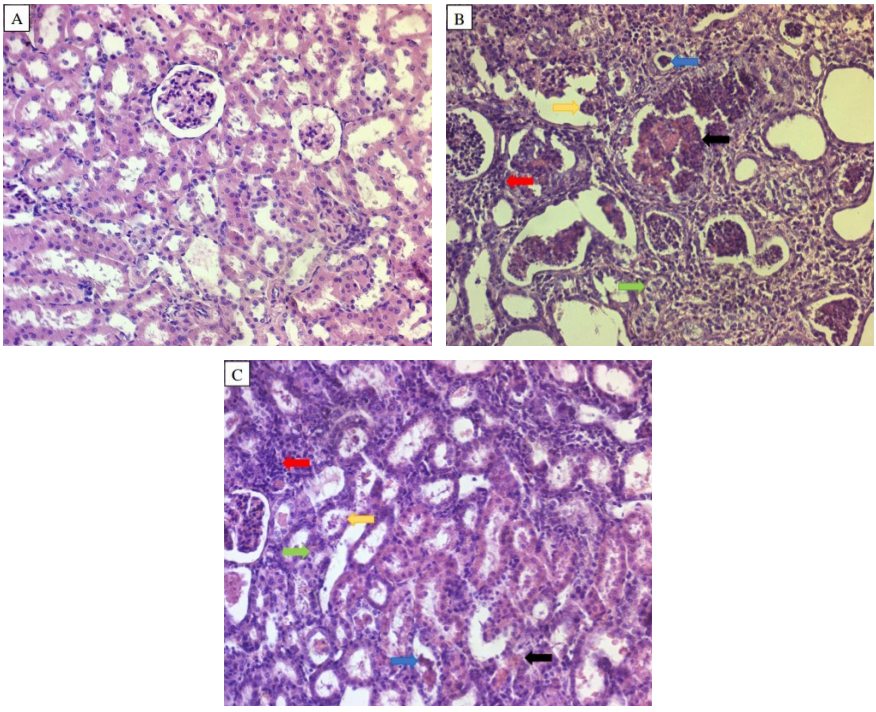

Figure 1. Kidney tissue sections of the experimental groups

(A): Normal healthy group, (B): VAN group, (C): TAD group, green arrow: tubular epithelial cell swelling, yellow arrow: desquamation, black arrow: necrosis, blue arrow: cast deposition, red arrow: interstitial inflammation [H&E, 20X]

Oxidative stress is one of the primary mechanisms of intracellular renal damage induced by VAN, which may result in acute tubular necrosis (ATN). VAN increases oxygen consumption by inducing mitochondrial oxidative phosphorylation. High oxygen consumption promotes reactive oxygen species (ROS)

generation. ROS cause depolarization of the mitochondrial membrane and liberation of cytochrome C, which activates the apoptotic caspases chain. Subsequently, necrosis will develop after ATP depletion[28].

The current study demonstrated that intraperitoneal VAN administration in a total dose of 400mg/kg for fourteen days deteriorates renal function in accordance with a previous study[21] and could be related to oxidative stress, which could enhance the formation of a set of vasoactive mediators that can deteriorate renal functions directly by causing renal vasoconstriction and thus reduce GFR[29]. Likewise, oxidative stress can enhance the action of adenosine[30]. In the VAN group, the renal tissue level of MDA was significantly increased, while the renal tissue level of GSH was significantly reduced, in agreement with previous studies[21,31,32]. The highly sensitive compound to ROS is lipid. MDA is produced as a byproduct of lipid peroxidation by ROS[31]. GSH is a significant tissue antioxidant that directly overcomes reactive hydroxyl free radicals and other oxygen free radicals. It functions as a substrate of glutathione peroxidase, permitting the reduction of peroxides. So, the exhaustion of GSH is considered an indicator of oxidative stress[33]. NGAL and TNF-α renal tissue levels were significantly increased in the VAN group in agreement with previous studies[34,35], which could be attributed to NF-κB pathway activation by high ROS, resulting in the release of many cytokines that cause inflammation and necrosis[36]. Histologically, VAN causes significant kidney tissue damage with the development of tubular epithelial cell swelling, desquamation, necrosis, cast deposition and interstitial inflammation in line with previous study[32]. ROS subsequently cause cellular energetics depletion[5]. Cell necrosis is historically regarded as a passive process due to the loss of cellular energetics. ATP depletion results in a loss of a cytoskeletal element, cell polarity, and membrane integrity with increased back leak of tubular filtrate. As well as ATP depletion causes a high increase in intracellular ca^{+2} level which can participate in cell death[30].

On the other hand, oral daily TAD during parenteral VAN administration improved renal function in consistency with a recent study done by Mohammed et al. showing that the antioxidant, anti-inflammatory, and anti-apoptotic effects of TAD reduce gentamicin-induced renal injury in rats[17]. Moreover, TAD group showed significantly lower renal MDA and higher renal GSH levels. This finding is in accordance with a previous study[18], which can be attributed to the activation of the Nrf2/HO-1 mediated antioxidant pathway[37]. The TAD group showed significantly lower renal levels of inflammatory biomarkers NGAL and TNF-α in agreement with previous studies[16,22]. This anti-inflammatory effect of tadalafil can probably be attributed to inhibiting NF-κB activation through

increased intracellular levels of cGMP and cGMP-dependent protein kinase (PKG)[38]. Histologically, TAD group showed a significant reduction in renal tissue injury as compared to the VAN group. TAD treatment markedly reduced the development of tubular cell swelling, desquamation, cast, necrosis, and interstitial inflammation. These outcomes appear in accordance with a previous study done by Gasanove et al. showed tadalafil administration before renal ischemia/reperfusion injury attenuated necrosis, leukocyte infiltration, brush border abnormality, and glomerular sclerosis in rat kidney compared to that of the induced group[39]. In conclusion, according to this research's findings, the protective effect of TAD against VAN-induced nephrotoxicity could be attributed to the antioxidant and anti-inflammatory properties of TAD.

STATEMENT OF ETHICS

The protocol of the current study was approved by the Institutional Review Board (IRB) of the College of Medicine / Al-Nahrain University, with an ethical clearance number of 178 on August 23, 2022.

CONFLICT OF INTEREST STATEMENT

The authors declare to have no conflict of interest.

AUTHOR CONTRIBUTIONS

Hassanen A. ABDULAMEER conducted experiments, interpreted the results, wrote the draft of the manuscript and formatted the manuscript to Journal specifications. Adeeb A. AL-ZUBAIDY designed the research concept, supervised the conduct of all experiments, and reviewed the manuscript. All authors read and approved the final manuscript.

REFERENCES

1. Sri Laasya TP, Thakur S, Poduri R, Joshi G. Current insights toward kidney injury: decrypting the dual role and mechanism involved of herbal drugs in inducing kidney injury and its treatment. Curr Res -Biotechnol, 2020;2:161-175. Doi: 10.1016/j.crbiot.2020.11.002

2. Griffin BR, Faubel S, Edelstein CL. Biomarkers of drug-induced kidney toxicity. Ther Drug Monit, 2019;41(2):213-226. Doi: 10.1097%2FFTD.0000000000000589

3. Gray MP, Barreto EF, Schreier DJ, Kellum JA, Suh K, Kashani KB, et al. Consensus obtained for the nephrotoxic potential of 167 drugs in adult critically ill patients using a modified Delphi method. Drug Saf, 2022;45(4):389-398. Doi: 10.1007/s40264-022-01173-4

4. Brown NM, Goodman AL, Horner C, Jenkins A, Brown EM. Treatment of methicillin-resistant Staphylococcus aureus (MRSA): updated guidelines from the UK. JAC Antimicrob Resist, 2021;3(1). Doi: 10.1093/jacamr/dlaa114

5. Kan W-C, Chen Y-C, Wu V-C, Shiao C-C. Vancomycin-associated acute kidney injury: a narrative review from pathophysiology to clinical application. Int J Mol Sci, 2022;23(4):2052. Doi: 10.3390/ijms23042052

6. Kunming P, Can C, Zhangzhang C, Wei W, Qing X, Xiaoqiang D, et al. Vancomycin associated acute kidney injury: a longitudinal study in China. Front Pharmacol, 2021;12:632107. Doi: 10.3389/fphar.2021.632107

7. Rybak M, Lomaestro B, Rotschafer JC, Moellering Jr. R, Craig W, Billeter M, et al. Therapeutic monitoring of vancomycin in adult patients: a consensus review of the American Society of Health-System Pharmacists, the Infectious Diseases Society of America, and the Society of Infectious Diseases Pharmacists. AJHP, 2009;1;66(1):82-98. Doi: 10.2146/ajhp080434

8. Carson CC, Rosenberg M, Kissel J, Wong DG. Tadalafil – a therapeutic option in the management of BPH-LUTS. Int J Clin Pract, 2014;68(1):94-103. Doi: 10.1111/ijcp.12305

9. Henrie AM, Nawarskas JJ, Anderson JR. Clinical utility of tadalafil in the treatment of pulmonary arterial hypertension: an evidence-based review. Core Evid, 2015;10:99-109. Doi: 10.2147/ce.s58457

10. Mónica FZ, De Nucci G. Tadalafil for the treatment of benign prostatic hyperplasia. Expert Opin Pharmacother, 2019;20(8):929-937. Doi: 10.1080/14656566.2019.1589452

11. Radovits T, Arif R, Bömicke T, Korkmaz S, Barnucz E, Karck M, et al. Vascular dysfunction induced by hypochlorite is improved by the selective phosphodiesterase-5-inhibitor vardenafil. Eur J Pharmacol, 2013;710(1-3):110-119. Doi: 10.1016/j.ejphar.2013.04.012

12. Yaguas K, Bautista R, Quiroz Y, Ferrebuz A, Pons H, Franco M, et al. Chronic sildenafil treatment corrects endothelial dysfunction and improves hypertension. Am J Nephrol, 2010;31(4):283-291. Doi: 10.1159/000279307

13. Hutchings DC, Anderson SG, Caldwell JL, Trafford AW. Phosphodiesterase-5 inhibitors and the heart: compound cardioprotection?. Heart, 2018;104(15):1244-1250. Doi: 10.1136/heartjnl-2017-312865

14. Lahoud Y, Hussein O, Shalabi A, Nativ O, Awad H, Khamaisi M, et al. Effects of phosphodiesterase-5 inhibitor on ischemic kidney injury during nephron sparing surgery: quantitative assessment by NGAL and KIM-1. World J Urol, 2015;33(12):2053-2062. Doi: 10.1007/s00345-015-1579-3

15. Amasyali AS, Akkurt A, Kazan E, Yilmaz M, Erol B, Yildiz Y, et al. The protective effect of tadalafil on IMA (ischemia modified albumin) levels in experimental renal ischemia-reperfusion injury. Int J Clin Exp Med, 2015;8(9):15766.

16. Salama AAA, Mostafa RE, Omara EA. Ameliorative effects of phosphodiesterase (PDE) inhibitors in potassium dichromate-induced acute renal failure in rats. Int J Pharm Sci Rev Res, 2016;36(2):40-46.

17. Mohammed EM, Elberry AA, Sayed MM, Abdelfatah SF. Evaluation of the effect of administration of tadalafil on gentamicin-induced nephrotoxicity in rats. Egypt J Med Hum Genet, 2022;3(4):114-139. Doi: 10.21608/ejmr.2022.267691

18. Adeneye AA, Benebo AS. Chemopreventive effect of tadalafil in cisplatin-induced nephrotoxicity in rats. Niger J Physiol Sci, 2016;31(1):1-10.

19. Bhatia P, Singh N. Ameliorative effect of phosphodiesterase-5 inhibitor in rat model of vascular dementia. Curr Neurovasc Res, 2019;16(1):27-39. Doi: 10.2174/1567202616666190130153954

20. Rashid M, Kotwani A, Fahim M. Long-acting phosphodiesterase 5 inhibitor, tadalafil, and superoxide dismutase mimetic, tempol, protect against acute hypoxia-induced pulmonary hypertension in rats. Hum Exp Toxicol, 2012;31(6):626-636. Doi: 10.1177/0960327111429138

21. Uhuo EN, Egba SI, Nwuke PN, Odinamadu H. Renoprotective effects of Adansonia digitata leaf extract on renal function and histopathological changes in vancomycin-induced nephrotoxicity in Wistar rats. Comp Clin Path, 2022;31(2):229-242. Doi: 10.1007/s00580-022-03325-5

22. Hamdy MM, Abdel-Rahman MS, Badary DM, Sabra MS. Effects of furosemide and tadalafil in both conventional and nanoforms against adenine-induced chronic renal failure in rats. Eur J Med Res, 2022;27(1):1-17. Doi: 10.1186/s40001-022-00747-3

23. Fawcett J, Scott J. A rapid and precise method for the determination of urea. J Clin Pathol, 1960;13(2):156-159. Doi: 10.1136/jcp.13.2.156

24. Heinegård D, Tiderström G. Determination of serum creatinine by a direct colorimetric method. Clin. Chim. Acta, 1973;43(3):305-310. Doi: 10.1016/0009-8981(73)90466-X

25. Pellicer-Valero ÓJ, Massaro GA, Casanova AG, Paniagua-Sancho M, Fuentes-Calvo I, Harvat M, et al. Neural network-based calculator for rat glomerular filtration rate. Biomedicines, 2022;10(3):610. Doi: 10.3390/biomedicines10030610

26. Aydin S. A short history, principles, and types of ELISA, and our laboratory experience with peptide/protein analyses using ELISA. Peptides (NY), 2015;72:4-15. Doi: 10.1016/j.peptides.2015.04.012

27. Mescher A. L. Histology & Its Methods of Study. In: Junqueira's Basic Histology Text and Atlas. 14th edition. New York: McGraw-Hill Education; 2016. pp. 1-15.

28. Kwiatkowska E, Domański L, Dziedziejko V, Kajdy A, Stefańska K, Kwiatkowski S. The mechanism of drug nephrotoxicity and the methods for preventing kidney damage. Int J Mol Sci, 2021;22(11):6109. Doi: 10.3390/ijms22116109

29. Choi YK, Elaine D, Kwon Y-G, Kim Y-M. Regulation of ROS production and vascular function by carbon monoxide. Oxid Med Cell Longev, 2012;2012. Doi: 10.1155/2012/794237

30. Basile DP, Anderson MD, Sutton TA. Pathophysiology of acute kidney injury. Compr Physiol, 2012;2(2):1303. Doi: 10.1002%2Fcphy.c110041

31. Sadeghi H, Karimizadeh E, Sadeghi H, Mansourian M, Abbaszadeh-Goudarzi K, Shokripour M, et al. Protective effects of hydroalcoholic extract of rosa canina fruit on vancomycin-induced nephrotoxicity in rats. J Toxicol, 2021;2021:5525714. Doi: 10.1155/2021/5525714

32. Uckun Z, Guzel S, Canacankatan N, Yalaza C, Kibar D, Coskun Yilmaz B. Potential protective effects of naringenin against vancomycin-induced nephrotoxicity via reduction on apoptotic and oxidative stress markers in rats. Drug Chem Toxicol, 2020;43(1):104-111. Doi: 10.1080/01480545.2018.1512612

33. Gaucher C, Boudier A, Bonetti J, Clarot I, Leroy P, Parent M. Glutathione: antioxidant properties dedicated to nanotechnologies. Antioxidants, 2018;7(5):62. Doi: 10.3390/antiox7050062

34. Kandemir FM, Yildirim S, Kucukler S, Caglayan C, Mahamadu A, Dortbudak MB. Therapeutic efficacy of zingerone against vancomycin-induced oxidative stress, inflammation, apoptosis and aquaporin 1 permeability in rat kidney. Biomed Pharmacother, 2018;105:981-991. Doi: 10.1016/j.biopha.2018.06.048

35. Yu P, Luo J, Song H, Qian T, He X, Fang J, et al. N-acetylcysteine ameliorates vancomycin-induced nephrotoxicity by inhibiting oxidative stress and apoptosis in the in vivo and in vitro models. Int J Med Sci, 2022;19(4):740-752. Doi: 10.7150%2Fijms.69807

36. Alsawaf S, Alnuaimi F, Afzal S, Thomas RM, Chelakkot AL, Ramadan WS, et al. Plant flavonoids on oxidative stress-mediated kidney inflammation. Biology (Basel), 2022;11(12):1717. Doi: 10.3390/biology11121717

37. Abdel-Wahab BA, Alkahtani SA, Elagab EAM. Tadalafil alleviates cisplatin-induced reproductive toxicity through the activation of the Nrf2/HO-1 pathway and the inhibition of oxidative stress and apoptosis in male rats. Reprod Toxicol, 2020;96:165-174. Doi: 10.1016/j.reprotox.2020.06.015

38. He Y, Huang Y, Mai C, Pan H, Luo H-B, Liu L, et al. The immunomodulatory role of PDEs inhibitors in immune cells: Therapeutic implication in rheumatoid arthritis. Pharmacol Res, 2020;161:105134. Doi: 10.1016/j.phrs.2020.105134

39. Gasanov F, Aytac B, Vuruskan H. The effects of tadalafil on renal ischemia reperfusion injury: an experimental study. Bosn J Basic Med Sci, 2011;11(3):158-162. Doi: 10.17305/bjbms.2011.2567

Acta Pharm. Sci. Vol 62:(2), 2024
Research article
DOI: 10.23893/1307-2080.APS6221

Development and validation of a stability indicating LC method for the analysis of chlordiazepoxide and trifluoperazine hydrochloride in the presence of their degradation products

Payal CHAUHAN[1*], Rakesh PARMAR[2], Anuja TRIPATHI[3]

1 Ramanbhai Patel College of Pharmacy, CHARUSAT Campus, Changa, Gujarat, India
2 Sardar Patel College of Pharmacy, Bakrol, Anand, Gujarat, India
3 Ramanbhai Patel College of Pharmacy, CHARUSAT Campus, Changa, Gujarat, India

ABSTRACT

A novel, accurate, and specific stability-indicating RP-HPLC method for determining Chlordiazepoxide (CLR) and Trifluoperazine HCl (TFP) in drug substances and drug products has been developed. A forced degradation study was performed as per the ICH guideline for both drugs. The degradation of chlordiazepoxide and trifluoperazine HCl in bulk and formulation was tested under a variety of stress conditions, including acidic, alkaline, neutral, oxidative, thermolytic, and photolytic conditions. The Separation was done using a C_{18} (250 mm × 4.6 mm, 5µm) column as a stationary phase and 70:30%(v/v) Acetonitrile: Phosphate buffer (pH 5.5) adjusted with 0.1% Triethaylamine (TEA) as isocratic mobile phase. The flow rate was 1ml/min and the wavelength for detection was 262 nm. The retention time was 4.1min and 7.1min for Chlordiazepoxide and Trifluoperazine HCl respectively. The developed method was validated as per the ICH guideline Q2(R1). Specificity, linearity, accuracy, precision, LOD, LOQ, robustness, and system suitability were checked to meet specified criteria. Specificity, linearity, precision, accuracy, LOD, LOQ,

* Corresponding author: Payal CHAUHAN
E-mail: payalmpharm@gmail.com
ORCIDs:
Payal CHAUHAN: 0000-0001-5456-2509
Rakesh PARMAR: 0000-0003-2441-0461
Anuja TRIPATHI: 0000-0001-8337-841X
(Received 31 Jan 2023, Accepted 8 Aug 2023)

robustness, system suitability, and other criteria were analyzed, Chlordiazepoxide and Trifluoperazine HCl were susceptive to degradation in photolytic and thermal stress conditions. The method was proven to be appropriate for use in the analysis of Chlordiazepoxide and Trifluoperazine HCl formulations in quality-control laboratories.

Keywords: chlordiazepoxide, trifluoperazine hydrochloride, HPLC, stability indicating, degradation products

INTRODUCTION

Chlordiazepoxide

Chlordiazepoxide is a long-acting benzodiazepine approved by the FDA for adults suffering from mild-moderate to severe anxiety, preoperative anxiety, and alcohol withdrawal. It is one of the safer psychopharmacological benzodiazepine compounds. Chlordiazepoxide (CLR) structure is shown in Figure 1, and the IUPAC name is 7-chloro-2-methylamino-5-phenyl-3H-1,4-benzodiazepine 4-oxide having molecular formula is $C_{16}H_4ClN_3O$ and the molecular weight is 299.75g/mol, melting point is 135-138°C. CLR is soluble in water and alcohol[1-3].

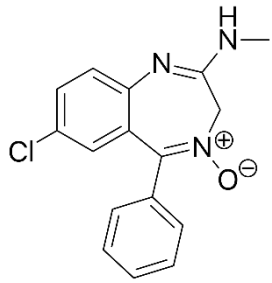

Figure 1. Structure of Chlordiazepoxide

Trifluoperazine hydrochloride

Trifluoperazine, a typical antipsychotic medication, not only blocks dopamine D2 receptors but also stimulates 5-HT2 receptor-mediated behavior. Trifluoperazine was discovered to be superior to a placebo for the treatment of generalized anxiety disorder in a randomized, double-blind, placebo-controlled study. Trifluoperazine also suppresses human purinergic receptor P2X7 responses, which relate inflammation to depression. This action is comparable to that of paroxetine. Trifluoperazine Hydrochloride (TFP) structure is shown in Figure 2, and the IUPAC name is 10 - [3 - (4 - methyl piper zine - 1 - yl) propyl] - 2

- (trifluoromethyl) phenothiazine, hydrochloride. TFP belongs to the phenothiazine class and is used as an antipsychotic for treating schizophrenia and anxiety[4-6].

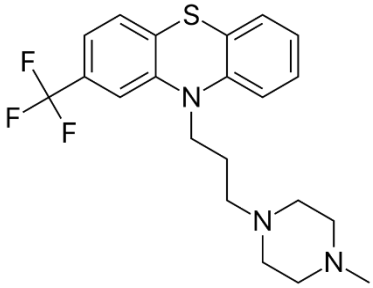

Figure 2. Structure of Trifluoperazine HCL

This two-drug combination is used in the treatment of mental disorders such as schizophrenia, and psychotic disorders. In this combination CLR is acted by enhancing the action of GABA, a chemical messenger that overcomes abnormal and excessive activity of nerve cells in the brain and TFP is an antipsychotic, it acts by blocking the action of dopamine, which affects thoughts and mood.

The literature review revealed that many UV spectrophotometric[7-10] and chromatographic methods[11-18] are available for the estimation of both drugs either alone or in combination with other drugs. One UV visible spectrophotometric method[18] and two RP-HPLC methods[19-21] are available for the determination of both drugs in combination. But there is no reported stability indicating the RP-HPLC method for Simultaneous estimation of CLR and TFP in the combined dosage form. The present RP-HPLC method is specific for the simultaneous quantification of chlordiazepoxide and trifluoperazine HCl in both formulation and bulk in presence of its degradation products in various stressed conditions[22].

METHODOLOGY

Instrumentation

Chromatographic measurement was performed on a Shimadzu corporation LC-2010 HT system (Shimadzu Corporation, Tokyo), consisting of a quaternary pump LC-2010, and a UV-Visible detector LC-2010. For drug substance chromatographic separation, a reverse-phase Phenomenex Luna C18 analytical column (4.6mm×250mm) was used. Chromatographic analysis and data integration were recorded on a Windows computer system using a Shimadzu LC-2010HT LC system with software LC-solution (1.25).

Reagents and materials

Reference Standards for trifluoperazine and chlordiazepoxide were procured from MANUS AKTTEVA BIOPHARMA LLP. Formulations of LIBRA CHEM-T tablets with the labelled dosages of 1 mg and 10 mg of CLR and TFP each were purchased from the local market. All HPLC-grade solvents were bought from Merck (Mumbai, India) and all AR-grade chemicals were bought from Loba Chemie Pvt Ltd.

Chromatographic conditions

Several isocratic elution strategies were employed to assess the optimization of chromatographic parameters. At pH 5.5, the optimised mobile phase was found to be 70:30% (v/v) Acetonitrile: Phosphate buffer adjusted with 0.1% TEA. The wavelength of detection was 262nm, and the flow rate was 1ml/min. The optimized chromatogram gives a sharp and symmetric peak with retention times of 4.17 minutes for CLR and 7.17 minutes for TFP.

Standard solution preparation

A standard solution of CLR (1000µg/ml) and TFP (1000ug/ml) was prepared by dissolving an accurately weighed quantity of CLR 10 mg and TFP 10 mg in 10 mL of mobile phase, and then the same solvent was used to dilute 1 mL of the resultant solution to 10 mL.

Sample solution preparation

Twenty tablets were weighed and then finely powdered (CLR 10 mg, TFP 1 mg). In a 10ml volumetric flask, tablet powder containing 10 mg of CLR and 1 mg of TFP was transferred. In order to create "Sample Stock1," 5ml of methanol was added, sonicated for 10 minutes, diluted with methanol to volume, and then filtered through Whatman filter paper No. 41. 1 ml of the resultant solution was diluted up to 10 ml with mobile phase to produce "Sample Stock2," which contained 100µg/ml CLR and 10µg/ml TFP. Syringe filters were used to filter Sample Stock 2, which was then injected into the HPLC apparatus. The calibration curve formulae y= 20783x+5041.8 and y= 63950x-2270 were used to determine the concentrations of CLR and TFP in the tablets, respectively.

Forced degradation studies[21]

Preparation of test solution for forced degradation study

From the stock solution of CLR and TFP, 20ml and 2ml were pipetted out respectively and made up to 100ml volumetric flask with the mobile phase.

Acid degradation

Accurately weighed and transferred TFP (1mg) and CLR (10mg) into a 50 ml volumetric flask. 10ml of 0.1M HCl was added and thoroughly mixed, and the volumetric flask was set to reflux at 70°C for 3 hrs. After the time period, the reaction was stopped by neutralizing the mixture with 10 ml of 0.1M NaOH. The solution was then diluted to a volume of 50 ml with the mobile phase. The tablet contained 10mg CLR and 1mg TFP was Taken and transferred into 50 ml of volumetric flask. 10 ml of 0.1M HCl was added and thoroughly mixed in. For 3 hours, the volumetric flask was refluxed at 70°C. Following the time period, the mixture was neutralized with 10 ml of 0.1M NaOH to stop the reaction. The solution was then diluted to a volume of 50 ml with the mobile phase.

Base degradation

Accurately weighed and transferred TFP (1 mg) and CLR (10 mg) into a 50 ml volumetric flask. 10 ml of 0.1M NaOH was added and thoroughly mixed, and the volumetric flask was set to reflux at 70 °C for 3 hrs. After the time period, the reaction was stopped by neutralizing the mixture with 10 ml of 0.1 M HCl. The solution was then diluted to a volume of 50 ml with the mobile phase. The tablet contained 10 mg CLR and 1mg TFP was Taken and transferred into 50 ml of volumetric flask. 10 ml of 0.1 M NaOH was added and thoroughly mixed in. For 3 hours, the volumetric flask was refluxed at 70 °C. Following the time period, the mixture was neutralized with 10 ml of 0.1 M HCl to stop the reaction The solution was then diluted to a volume of 50 ml with the mobile phase.

Neutral degradation

Accurately weighed and transferred TFP (1mg) and CLR (10mg) into 50 ml volumetric flask.10ml of water was added and thoroughly mixed, and the volumetric flask was set to reflux at 70°C for 3 hrs. Following the time period, the mixture was diluted to a volume of 50 ml with the mobile phase. The tablet contained 10mg CLR and 1mg TFP was Taken and transferred into 50 ml of volumetric flask. 10 ml of water was added to it and thoroughly mixed in. For 3 hours, the volumetric flask was refluxed at 70°C. Following the time period, the mixture was diluted to a volume of 50 ml with the mobile phase.

Oxidative degradation

Accurately weighed and transferred TFP (1mg) and CLR (10mg) into a 50 ml volumetric flask. 10 ml of 3% H_2O_2 was added and mix well. The volumetric flask was refluxed at a temperature of 70°C for 3 hrs. Following the time period, the mixture was diluted to a volume of 50 ml with the mobile phase. The

tablet contained 10mg CLR and 1mg TFP was Taken and transferred into 50 ml of volumetric flask. 10 ml of 3% H_2O_2 was added to it and mix well. The volumetric flask was refluxed at a temperature of 70° C for 3 hrs. Following the time period, the mixture was diluted to a volume of 50 ml with the mobile phase.

Thermal degradation

Accurately weighed and transferred TFP (1mg) and CLR (10mg) into a petri dish. The Petri dish was then placed in the hot air oven for 12 hours at a temperature of 110 o C. A heated drug sample was transferred to and dissolved in a mobile phase in a 50ml volumetric flask. The heated drug sample was dissolved in the mobile phase in a 50ml volumetric flask. Volume was made up to the mark using the mobile phase. The tablet contained 10mg CLR and 1mg TFP was Taken, powdered, and transferred into a petri dish. The Petri dish was then placed in the hot air oven for 12 hours at a temperature of 110 ° C. A heated drug sample was transferred to and dissolved in a mobile phase in a 50ml volumetric flask. Volume was made up to the mark using the mobile phase.

Photolytic degradation

Accurately weighed and transferred TFP (1mg) and CLR (10mg) into a petri-dish and for 24 hours, a petri dish was placed within the UV chamber. The drug sample was dissolved in a mobile phase in a 50ml volumetric flask. Volume was made up to the mark using the mobile phase. The tablet contained 10mg CLR and 1mg TFP was Taken, powdered, and transferred into a petri dish. A petri dish was put inside the UV chamber for 24 hours. In a 50ml volumetric flask, a UV-Exposed drug sample was transferred and dissolved in the mobile phase. Volume was made up to the mark using the mobile phase.

Method validation

Specificity

It is the ability to analyses unequivocally samples in the presence of other components which are expected to exist or present which can be impurities, degradants, or matrices. Specificity was determined by injecting diluents, standard solution, and sample preparation. Forced degradation was performed on the drug product in addition to establishing specificity.

Linearity and range

Six solutions were prepared in the mobile phase. The range was 50-300 µg/ml and 5-30 µg/ml for CLR and TFP respectively. The calibration plot is obtained

which determines the slope, coefficient correlation and intercept providing the required statistics for linearity.

Accuracy

The accuracy of the method was determined by calculating the recoveries of CLR and TFP by the method of standard addition. The recovery was assessed at three levels 80%,100%, and 120%. The % recovery was calculated.

Precision

The precision was performed by repeatability and inter-day or intra-day precision. For repeatability 6 replicates were injected for CLR and TFP and %RSD was calculated. For inter-day and intra-day precision 3 solutions with different concentration levels solution were prepared for the two drugs and %RSD values were calculated accordingly.

Limit of detection (LOD) and limit of quantification (LOQ)

LOD is defined as "the lowest or smallest concentration of component or sample which can be detected for a specified experimental condition of an analytical method.

LOQ is defined as "an ability to detect and precisely and accurately quantify the least or lowest concentration of compound or sample under the stated experimental parameters of an analytical method.

Robustness

It is a measurement of the ability of any analytical technique to remain unaffected or unchanged by deliberate or known variation in method parameters like in HPLC involving column or sample temperature, flow rate, pH, mobile phase ratio, and injection volume.

System suitability test

It is performed to prove the suitability and reproducibility of the developed method. The test solution was taken in the concentration of CLR and TFP 100µg/ml, and 10µg/ml respectively. Then six replications were injected into the system. Various parameters used for these tests including capacity factor (K NMT 2), resolution (NLT 1.5), tailing factor (NMT 2), column efficiency or number of theoretical plates (N more than 2000), relative standard deviation (% RSD NMT 2%) and separation or relative retention (NLT 2).

RESULTS and DISCUSSION

Development of LC method

The LC method was developed with good peak shape and resolution. Peak characteristics like symmetry and theoretical plates were used to determine the mobile phase. Table 1 shows the optimized conditions, and Figure 3 shows the chromatogram.

Table 1. Optimized LC conditions for the analysis of CLR and TFP

SR NO.	Parameter	Results
1	Mobile phase	Acetonitrile : Phosphate buffer (10mM) (70:30 v/v) (pH-5.5) pH adjust with 0.1%TEA
2	Stationary phase	Luna C_{18} column (4.6mm×250mm)
3	Column oven temperature	40°C
4	Wavelength	262nm
5	Flow rate	1ml/min
6	Elution mode	Isocratic
7	Injection volume	10µl

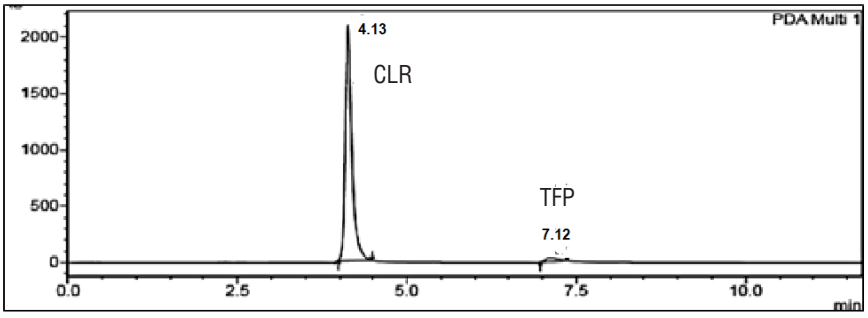

Figure 3. Standard chromatogram of CLR and TFP for degradation study

Forced degradation study

Degradation was observed under various stress conditions such as acidic, basic, photolytic, thermal, oxidation, and neutral. CLR and TFP samples were degraded into acid (Figure 4), base (Figure 5), photolytic (Figure 6), oxidative (Figure 7), Thermal (Figure 8), and neutral (Figure 9) conditions and formed polar impurities. The CLR and TFP sample peaks are homogeneous under all evaluated stress situations, according to peak purity data. The tablet's unaffected sample assay demonstrates the method's accuracy in showing stability (Table 2).

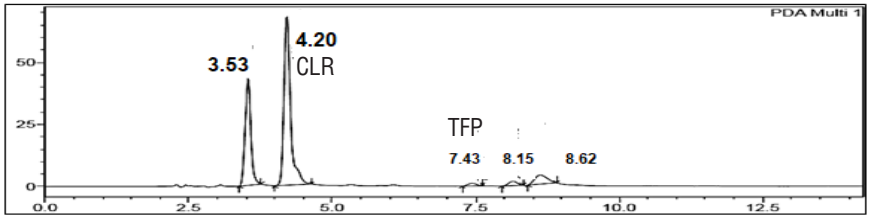

Figure 4. Chromatogram of acidic degradation

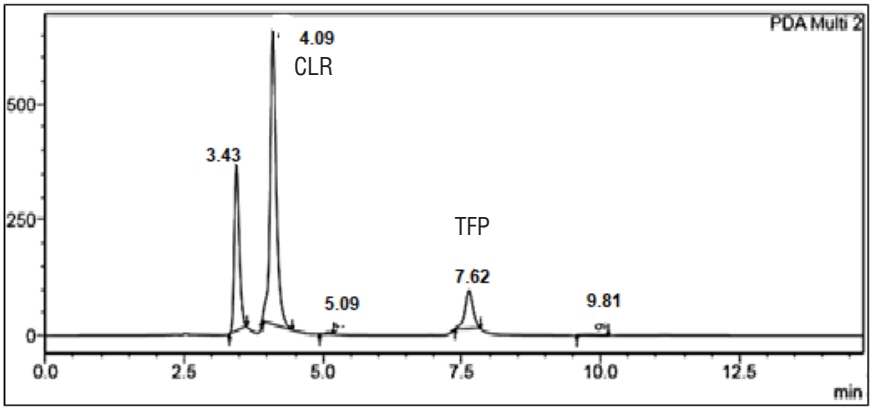

Figure 5. Chromatogram of basic degradation

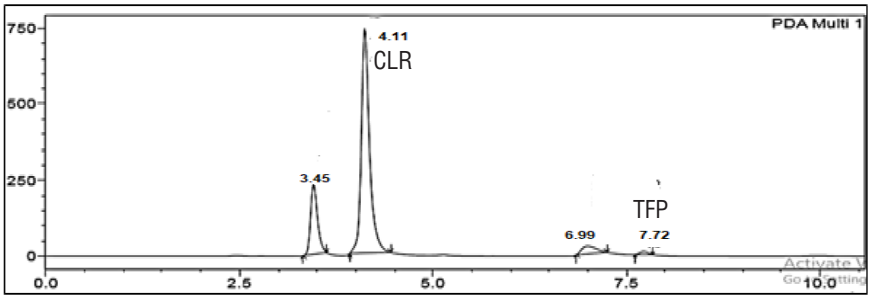

Figure 6. Chromatogram of photolytic degradation

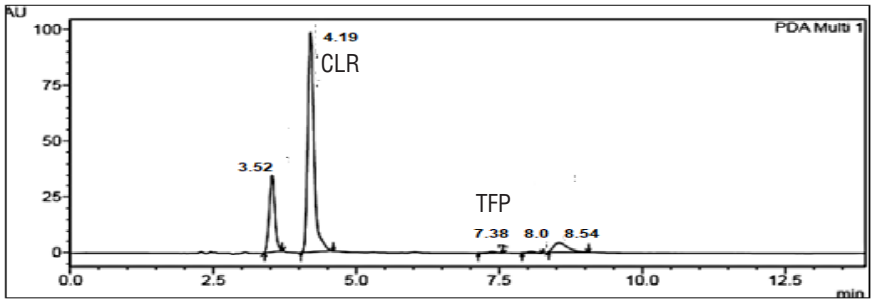

Figure 7. Chromatogram of oxidative degradation

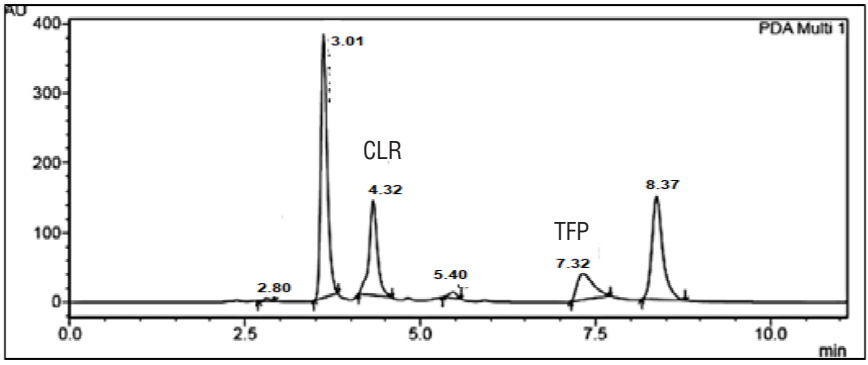

Figure 8. Chromatogram of thermal degradation

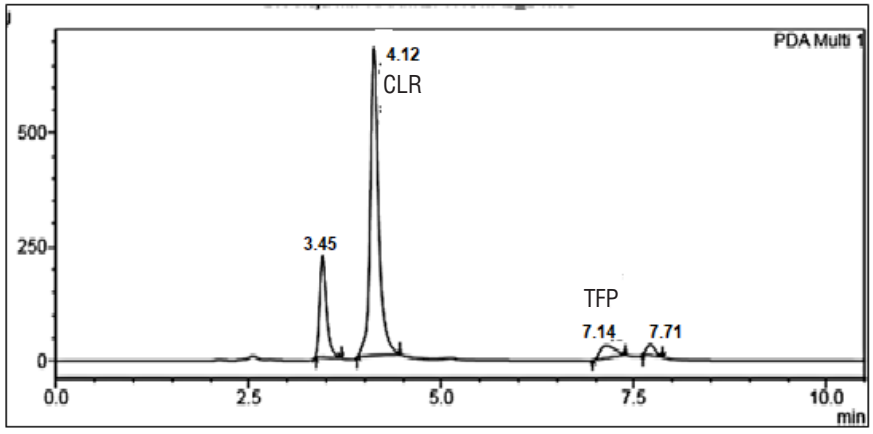

Figure 9. Chromatogram of neutral degradation

Table 2. Summary of force degradation study (CLR and TFP at different stress conditions)

Stress condition	Drugs	Standard area	Degradation area	% degradation
Acid degradation	CLR	14246076	10549619	25%
	TFP	402231	309961	22%
Alkali degradation	CLR	14246076	11356452	20.8%
	TFP	402231	315621	21.5%
Photolytic degradation	CLR	14246076	10452358	26%
	TFP	402231	322345	20%
Oxidative degradation	CLR	14246076	10754411	24.5%
	TFP	402231	316524	21.3%
Thermal degradation	CLR	14246076	10117544	28.2%
	TFP	402231	300979	25.1%
Neutral degradation	CLR	14246076	11558677	18.5%
	TFP	402231	313275	22.1%

Method validation

Method validation is carried out as per ICH guideline Q2(R1). Method validation is a process to ensure that the method was reliable and reproducible.

Specificity

The specificity of the method indicates, there is no interference in the analyte peak. So, there is no other peak was interfering with the standard chromatogram in under different stress conditions and blank. The specificity of the method was tested by subjecting the analyte to various stress conditions, such as light, acid, base, oxidation, heat and determining the extent of degradation and the ability of the method to measure the analyte accurately in the presence of its degradation. Standard chromatogram of CLR and TFP and specificity chromatogram (Blank) are given as Figure 10-11.

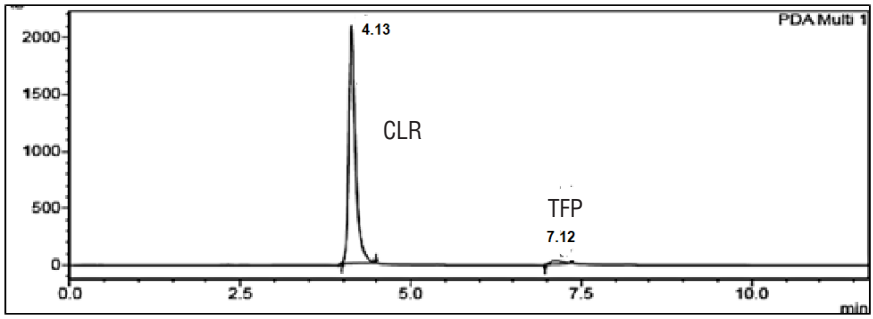

Figure 10. Standard chromatogram of CLR and TFP

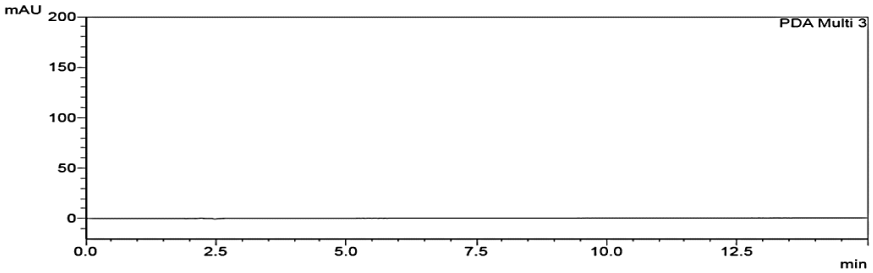

Figure 11. Specificity chromatogram (blank)

Linearity and range

Linear correlation was found between area versus concentration of CLR and TFP in concentration ranges of (50-300) and (5-30) μg/ml respectively. Calibration curves of CLR and TFP are shown in Figures 12 and 13 respectively. The R^2 values were 0.998 and 0.997 for CLR and TFP respectively. So, the method was considered linear at the above-mentioned concentration ranges for the two analytes. Specificity chromatograms belong to photolytic degradation, oxidative degradation, thermal degradation and neutral degradation are given as Figure 14,15,16,17 respectively. Calibration curves of TFP and CLR are also given as Figure 18,19 respectively.

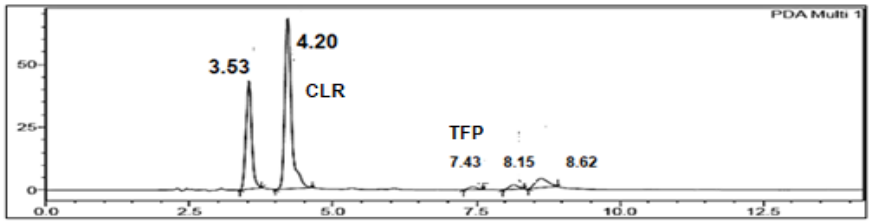

Figure 12. Specificity chromatogram (acid degradation)

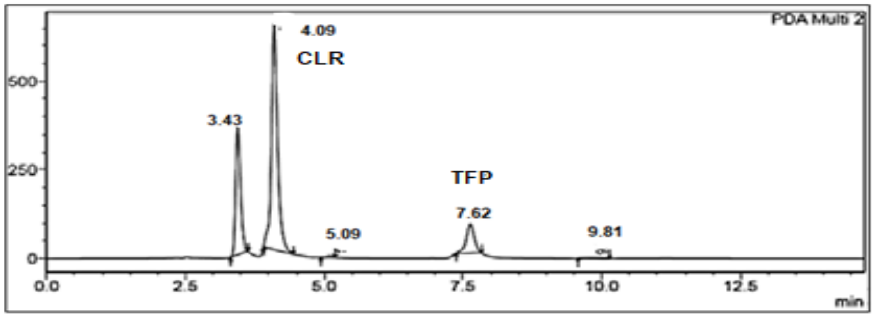

Figure 13. Specificity chromatogram (base degradation)

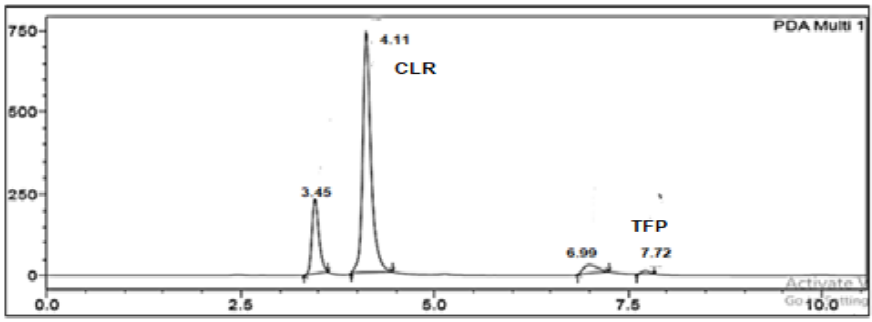

Figure 14. Specificity chromatogram (photolytic degradation)

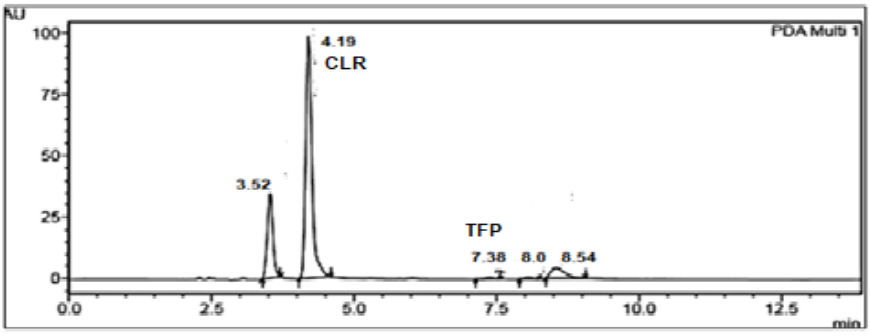

Figure 15. Specificity chromatogram (oxidative degradation)

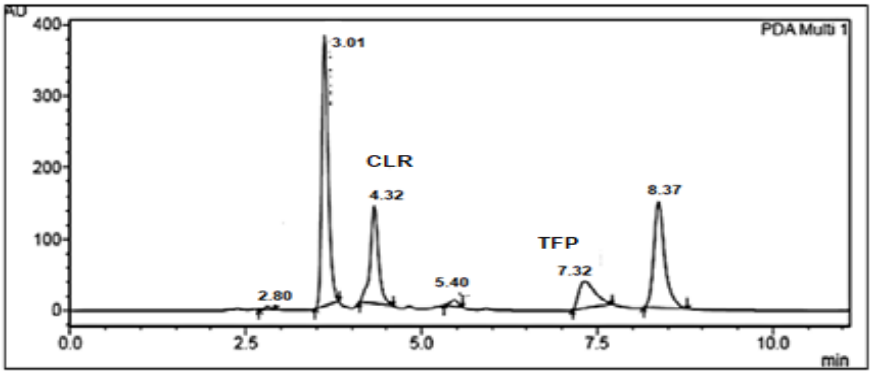

Figure 16. Specificity chromatogram (thermal degradation)

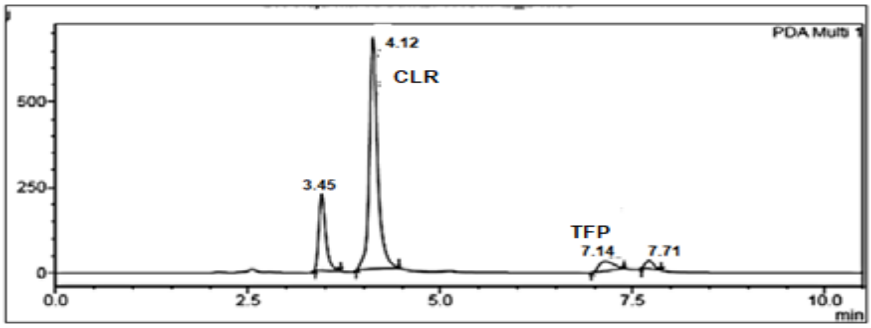

Figure 17. Specificity chromatogram (neutral degradation)

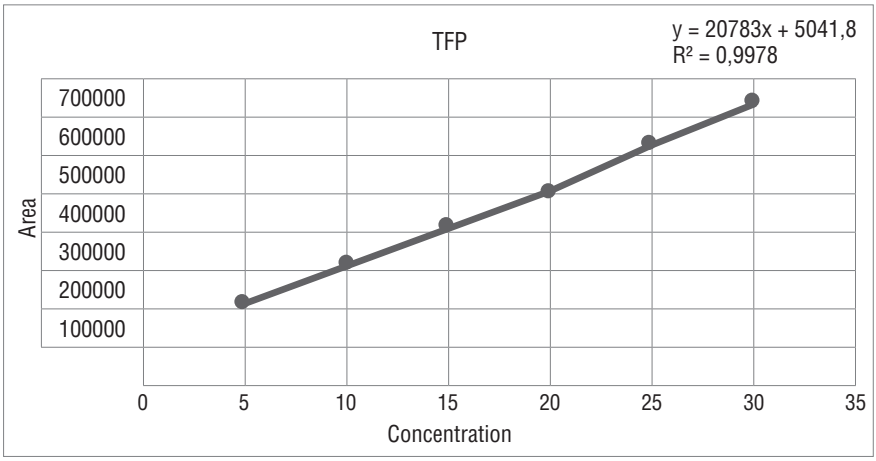

Figure 18. Calibration curve of TFP (5-30 µg/ml)

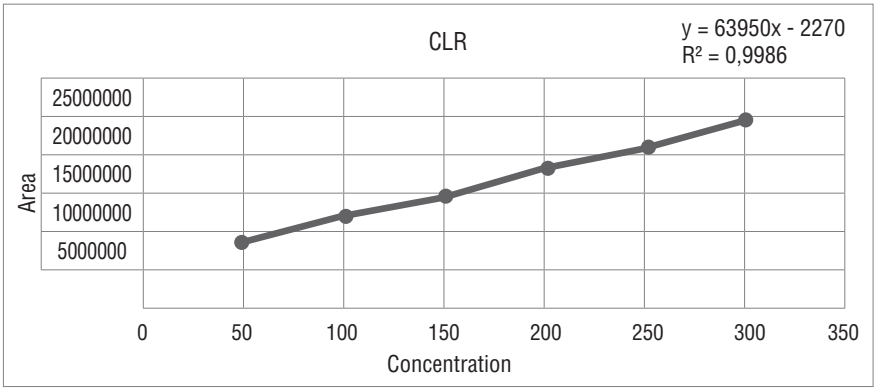

Figure 19. Calibration curve of CLR (50-300 µg/ml)

Accuracy

Accuracy was performed using three different levels 80%, 100%, and 120%. The % recovery was calculated. For both drugs % recovery was 99.8% (Table 3).

Table 3. Accuracy-recovery study of CLR and TFP by standard-addition method

Analyte	Conc. (µg/ml)	Amount of drug added			Amount recovered (µg/ml)	Average area	Average recovery (%)	%RSD
		Level (%)	Spiked amount (µg/ml)	Total conc. (µg/ml)				
CLR	100	80	80	180	179.3	11690936.7	99.6	0.82
		100	100	200	198.9	13038567	99.4	0.62
		120	120	220	219.2	14295238	99.6	0.62
TFP	10	80	8	18	17.9	359346.6	99.8	0.19
		100	10	20	19.8	399812.6	99.4	0.12
		120	12	22	21.8	436232	99.1	0.88

Precision

Repeatability was performed under the same conditions and 6 replicates were injected into the HPLC system. The % RSD was calculated. % RSD value for both drugs was found within the acceptance criteria. The Repeatability Data are shown in Table 4. Interday and intraday precisions were shown in Table 5. The % RSD value less than 2 indicated that the developed method was found to be precise. Table 6 shows data for the inter-day study of CLR and TFP.

Table 4. Data for repeatability study of CLR and TFP (n=6)

Parameters	CLR	TFP
Area 1	13127856	402231
Area 2	13154787	405698
Area 3	13246658	405823
Area 4	13168590	415478
Area 5	13478358	401258
Area 6	13254785	405847
Average	13127856	402231
Standard deviation	128063.3	40566.8
%RSD	0.65	0.87

Table 5. Data for intra-day study of CLR and TFP (n=6)

CLR				TFP			
Conc. (µg/ml)	Mean Area	Standard Deviation	%RSD	Conc. (µg/ml)	Mean Area	Standard Deviation	%RSD
100	6408493	2946.6	0.45	10	214154.7	1660.3	0.77
150	9222194	39320.2	0.52	15	303256.3	2430.5	0.80
200	13050371	68038.4	0.52	20	400527.7	3067.3	0.76

Table 6. Data for inter-day study of CLR and TFP (n=6)

CLR				TFP			
Conc. (µg/ml)	Mean Area	Standard deviation	%RSD	Conc. (µg/ml)	Mean Area	Standard deviation	%RSD
100	6463236	37391.7	0.57	10	213065.5	1333.6	0.62
150	9265818	28941.5	0.31	15	309360	2333.9	0.75
200	13077463	67472.3	0.51	20	403931	2044.7	0.50

LOD and LOQ

Limit of detection and Limit of quantitation were calculated from standard calibration curves. LOD was 1.83 µg/ml and 1.12µg/ml for CLR and TFP respectively. LOQ was 5.54 µg/ml and 3.41µg/ml for CLR and TFP respectively (Table 7). Sensitivity was calculated using following formula:

LOD= 3.3* δ/S

where

δ = standard deviation of response (intercept of calibration/linearity plot)

S=the slope of linearity plot

LOQ= 10* δ/S

where

δ = standard deviation of response (intercept of calibration/linearity plot)

S=the slope of linearity plot

Table 7. LOD and LOQ study CLR and TFP

Parameter	CLR(µg/ml)	TFP(µg/ml)
LOD	1.83	1.12
LOQ	5.54	3.41

Robustness

Robustness was performed by changes in different parameters like wavelength, flow rate, temperature, mobile phase ratio, and pH. The %RSD was calculated. The percentage relative standard deviation was less than 2% which indicates the method was robust (Tables 8-9).

Table 8. Results of robustness study of CLR and TFP

Parameter	Actual value	Changed value(+)	Changed value(-)	%RSD	
				CLR	TFP
Wavelength	262 nm	264 nm	260nm	0.16	0.35
Flow Rate	1ml/min	1.2ml/min	0.8ml/min	0.62	0.74
Temperature	40ºC	45ºC	35ºC	0.19	0.38
Mobile phase ratio	70:30v/v	80:20v/v	60:40v/v	0.25	0.88
pH	5.5	5.7	5.3	0.32	0.74

Table 9. Assay of pharmaceutical formulation

Drugs	Label Claim (mg)	% Amount found ±SD	%RSD
CLR	100	98.21±0.147	0.14
TFP	10	98.80±0.113	0.11

System suitability tests

System suitability parameters such as theoretical plates, peak area, tailing factor, and resolution were investigated, followed by the calculation of % RSD values. Obtained results were found to be close to the system suitability criteria, which indicated that the system was suitable and precise for analysis (Table 10).

Table 10. System suitability results of the proposed HPLC method for separation of CLR and TFP

Parameters	Active pharmaceutical drugs			
			TFP	
Retention time	Average	4.23	Average	7.14
	SD	0.085	SD	0.043
	%RSD	1.04	RSD%	0.76
Peak area	Average	6441595	Average	204185
	SD	49157	SD	2105
	%RSD	0.76	RSD%	1.03
Tailing factor	Average	1.32	Average	1.43
	SD	0.026	SD	0.032
Theoretical plates	Average	6405	Average	3165
Resolution	Average	10.4		
	SD	0.121		
	%RSD	1.16		

Table 11. Assay of CLR and TFP

Tablet (LIBRA CHE-T)	Label Claim (mg)	Conc. (µg/ml)	Mean area	%Assay ±SD	%RSD
CLR	10	100	6490131.6	98.21±0.147	0.14
TFP	1	10	205787.3	98.80±0.113	0.11

Chlordiazepoxide and Trifluoperazine HCl are effectively estimated using an isocratic stability-indicating RP-HPLC method in a combined pharmaceutical formulation. In acid and base degradation, maximum degradation was observed. The drug was also susceptive to degradation under photolytic and thermal conditions. Forced degradation studies indicated that both drugs and degradation products are separated from each other. The method was also validated according to ICH Q2(R1) guidelines. All-important analytical parameters were investigated and found within the Acceptance limit. So, the developed RP-HPLC method is accurate, précised, and robust. Therefore, the proposed method can be successfully employed in routine analysis of these drugs in bulk as well as in pharmaceutical formulation.

STATEMENT OF ETHICS

This study does not require any ethical approval.

CONFLICT OF INTEREST STATEMENT

The authors declare no conflict of interest.

AUTHORS CONTRIBUTIONS

All authors contributed to data collection, processing, writing, revision of the draft, reading and approval of the final manuscript.

FUNDING SOURCES

No funding or other financial support was received for the study.

REFERENCES

1. Zhao Y, Bijlsma EY, Verdouw PM, Garssen J, Groenink L. The contribution of contextual fear in the anxiolytic effect of chlordiazepoxide in the fear-potentiated startle test. Behav Brain Res, 2018;1(353):57-61. Doi: 10.1016/j.bbr.2018.06.035

2. Carlini EA. Plants and the central nervous system. Pharmacol Biochem Behav, 2013;75(3):501-512. Doi: 10.1016/s0091-3057(03)00112-6

3. Indian Pharmacopoeia 2018, Government of India Ministry of Health and Family Welfare, published by the Indian Pharmacopoeia Commission, Ghaziabad. 2018;2:1579-1580.

4. The United States Pharmacopiea. USP 39 NF 40. Rockville MD US A, United states pharmacopoeia convention Inc. 2016;3093-3094.

5. Indian Pharmacopoeia, Government of India Ministry of Health and Family Welfare, published by The Indian Pharmacopoeia Commission, Ghaziabad, 2018;3:3430-3431.

6. The United States Pharmacopiea. USP 39 NF 40. Rockville MD USA, United states pharmacopoeia convention Inc. 2016;6259-6260.

7. Hamzah MJ, Taqi RM, Hasan MM, Al-Timimi RJ. Spectrophotometric Determination of Trifluoperazine HCL in Pure Forms and Pharmaceutical Preparations. Int J Pharm Clin Res, 2017;9(5):337-342. Doi: 10.47743/achi-2022-2-0006

8. Rajitha K, Prasanna NL, Vasundhara G, Kumar RN, Kumar AA. UV spectrophotometric method development and validation for the simultaneous quantitative estimation of mebeverine hydrochloride and chlordiazepoxide in capsules. Int J Pharm Sci, 2014;6(8):345-349. ISSN: 0975-1491

9. Saudagar R, Saraf S, Saraf SJ. Spectrophotometric determination of chlordiazepoxide and trifluoperazine hydrochloride from the combined dosage form. Indian J Pharm Sci, 2007;69(1):149-152. Doi: 10.4103/0250-474X.32135

10. Patel S, Patel NJ. Spectrophotometric and chromatographic simultaneous estimation of amitriptyline hydrochloride and chlordiazepoxide in tablet dosage forms. Indian J Pharm Sci, 2009;71(4):472-476. Doi: 10.4103/0250-474X.57305

11. Sharma D, Shrivastava A, Duggal D, Patel A. Stability indicating RP-HPLC method for the estimation of Trifluoperazine Hydrochloride as API and estimation in tablet dosage forms. Int J Pharm Qual, 2010; 22;2(2):38-41. ISSN: 0975-9506

12. Pattanayak S, Rani YA. A Novel RP-HPLC Method Development and Validation for Simultaneous Estimation of Trifluoperazine and Isopropamide in Tablet Dosage Form. Int J Pharm Sci and Drug Res, 2015;7(1):105-109. ISSN: 0975-248X

13. Kishore MS, Rambabu C. Development and validation of a stability indicating hplc method for the simultaneous analysis of isopropamide and trifluoperazine in fixed-dose combination tablets. Int J Pharm Res, 2017;8(12):5178-5185. Doi: 10.13040/IJPSR.0975-8232.8(12).5178-85

14. Patel B, Marvniya V, Patani P. Analytical method development and validation of the simultaneous estimation of trihexyphenidyl, trifluoperazine and thioridazine in its pharmaceutical dosage form by HPLC method. IJRAR, 2019;6(1):805-813. ISSN: 2349-5138

15. Dhabab JM, Al-Ameri SA, Taufeeq AH. Separation and determination of trifluoperazine and prochlorperazine in pharmaceutical preparations by HPLC. J Assoc Arab Univ Basic Appl Sci, 2013;13(1):14-18. Doi: 10.1016/j.jaubas.2012.08.002

16. Khodadoust S, Ghaedi M. Optimization of dispersive liquid–liquid micro extraction with central composite design for preconcentration of chlordiazepoxide drug and its determination by HPLC-UV. J Sep Sci, 2013;36(11):1734-1742. Doi: 10.1002/jssc.201300085

17. Kattan NJ. Simultaneous determination of Amitriptyline Hydrochloride and chlordiazepoxide in combined dosage forms by high-performance liquid chromatography. Indian J Pharm Sci, 2009;71(4):472-476. Doi: 10.4103/0250-474X.57305

18. M Heneedak H, Salama I, Mostafa S, El-Sadek M. A stability-indicating HPLC method for the simultaneous determination of ccurring hydrochloride and chlordiazepoxide in commercial tablets. Curr Anal Chem, 2014;10(4):565-573. Doi: 10.2174/1573411013099990040

19. Jadhao VM, Gide PS, Kadam VJ. Reverse phase high-performance liquid chromatographic determination of chlordiazepoxide and trifluoperazine hydrochloride in tablets. Indian Drugs, 2006;43:99-101.

20. Patel SK, Patel NJ. Simultaneous RP-HPLC Estimation of Trifluoperazine Hydrochloride and Chlordiazepoxide in Tablet Dosage Forms. Indian J Pharm Sci, 2009;71(5):545-547. Doi: 10.4103/0250-474X.58192

21. Shetti P, Venkatachalam A. Stability indicating HPLC method for simultaneous quantification of trihexyphenidyl hydrochloride, trifluoperazine hydrochloride and chlorpromazine hydrochloride from tablet formulation. J Chem, 2010;7(S1):299-313. Doi: 10.1155/2010/529386

22. Bakshi M, Singh S. Development of validated stability-indicating assay methods – a critical review. J Pharm Biomed Anal, 2002;28(6):1011-1040. Doi: 10.1016/s0731-7085(02)00047-x

Acta Pharm. Sci. Vol 62:(2), 2024
Research article
DOI: 10.23893/1307-2080.APS6222

Natural polymers for targeted drug delivery to the colon: A comparative study of tamarind gum and karaya gum

Jaymin M. PATEL[1,2], Kaushika PATEL[1], Shreeraj SHAH[1*]

1 L. J. Institute of Pharmacy, LJ University, Ahmedabad-382210, India
2 Research Scholar, Gujarat Technological University, Ahmedabad, India

ABSTRACT

The study aimed to create an effective colon-targeted budesonide delivery system using natural polymers. Various natural gums were assessed for their ability to develop a microbial degradation-based colon-targeted drug delivery system. The sensitivity of polymers to colonic enzymes was tested by evaluating viscosity changes in the presence of a prebiotic culture medium simulating rat cecal content. Tamarind gum and Karaya gum exhibited superior viscometric profiles. Compression coating with these gums, followed by an Eudragit S 100 coat, was employed for successful colon delivery. A 3^2-factorial design optimized the system, using variables like polymer to ethyl cellulose (EC) ratio and Eudragit S 100 weight gain. The design-space stipulated less than 10% drug release in 2 hours (h), less than 15% in 5 h, and over 50% in 7 h for colon targeting. The Tamarind gum batch (TM 9) released 8.91% at 5 h and 50.23% at 7 h, achieving optimal drug delivery to the colon.

Keywords: budesonide, tamarind gum, karaya gum, Eudragit S 100, colon targeting

* Corresponding author: Shreeraj SHAH
E-mail: technoresearch2004@gmail.com
ORCIDs:
Jaymin PATEL: 0000-0001-6698-5365
Kaushika PATEL: 0000-0002-5482-9063
Dr. Shreeraj SHAH: 0000-0002-8729-7104
(Received 14 Apr 2023, Accepted 25 Sep 2023)

INTRODUCTION

Both ulcerative colitis and Crohn's disease are forms of inflammatory bowel disease (IBD). They both possess a prolonged, recurrent inflammation of the digestive tract, yet they are distinct things[1]. The colon and rectum are most affected by the continuous inflammation that describes ulcerative colitis. The most effective therapy for moderate to severe ulcerative colitis is corticosteroids (UC)[1,2]

However, undesirable side effects and a lack of potential for maintenance treatment restrict their long-term use. The therapy of choice for active IBD is a new class of anti-inflammatory glucocorticoids, such as budesonide, with greater topical anti-inflammatory impact and less systemic activity[3, 4].

However, budesonide is poorly absorbed in the colon because of its fast presystemic clearance in hepatocytes and small intestine epithelial cells[5,6].

To treat IBD effectively and reduce the common systemic adverse effects of glucocorticoids, an oral colonic drug delivery (CDD) system for budesonide is desperately needed to boost the drug's local concentration in the colon mucosa[7,8].

For colon-specific drug delivery, several strategies including Prodrug, pH-dependent[9] time-dependent[10], and micro flora-activated systems[11] have been developed. Among several approaches, polymers that are biodegraded by colonic bacterial enzymes show the most potential[9,12].

Numerous reductive and hydrolytic enzymes, such as b-glucuronidase, b-xylosidase, b-galactosidase, a-arabinosidase, nitroreductase, azoreductase, urea hydroxylase, etc., are produced by *Bacteroides, Bifidobacterium, Eubacterium, Peptococcus, Lactobacillus, Clostridium,* etc. Di-, tri-, and polysaccharide biodegradation are catalysed by these enzymes[13].

In general, 4% of the rat cecal content is used to imitate the enzymatic environment of the colon in the microbial approach. However, several rats must be killed for this purpose. To prevent this, novel dissolution biorelevant media that function as appropriate media[13,14] were developed using the probiotic culture medium prepared with the bacterial strains of Velgut capsule, and their effectiveness on viscosity of polymeric solution was evaluated and compared to the effectiveness of 4% rat cecal content. On the basis of enzymatic susceptibility, the ideal quantity of probiotic culture medium is determined, and the same amount is used for all dissolution procedures in the research[14].

The colonic drug delivery system was developed utilising novel natural polymers, namely Karaya gum, Khaya gum, Gellan gum, Gum Ghatti, and Tamarind gum[15–17]

Karaya gum is produced by Sterculia urens trees and is one of India's essential forest products. Bacterial enzymes in the colonic region break down Karaya gum, which consists of four galacturonic acid molecules[17,18].

Khaya gum is extracted from the cut stem of the *Khaya grandifoliola* plant, belonging to the Maliaceae family. Khaya gum contains the sugars D-galactose and L-rhamnose as well as the acids D-galacturonic acid and 4-O-methyl-D-glucoronic acid[19].

Gellan gum is an extracellular polymer produced by *Sphingomonas elodea*, formerly known as *Pseudomonas elodea*. Commercial production uses a fermentation process[20].

Gum Ghatti is a non-starch polysaccharide that is indigenous to India and is generated by the Combretaceae plant species *Anogeissus latifolia*[21].

The endosperm of seeds from the tamarind tree (*Tamarindus indica*) may be used to make a gum that has potential health benefits[22]. Tamarind kernel powder is a complex carbohydrate polymer with a high degree of branching, as determined by its chemical composition. Similar to cellulose, its backbone consists of (1-4) b-linked D-glucose units. As an effective excipient in the manufacturing of matrix tablets, Tamarind gum is employed[23].

The 3^2 Full factorial design is a valuable experimental design technique with specific applications in the field of targeted drug delivery. Its advantages include the ability to systematically investigate the effects of multiple variables on drug delivery performance, optimize the formulation parameters for enhanced therapeutic efficacy, reduce side effects, and improve patient compliance[24]. By employing 3^2 Full factorial design, researchers can efficiently explore the design space and identify optimal conditions for targeted drug delivery systems[25].

These systems were meticulously designed and formulated according to predefined selection criteria to achieve colon-targeted drug delivery. The desired drug release profile for the colon-targeted system was defined as the release of no more than 15% of the drug within the initial 5 h, with a minimum of 50% drug release within 7 h.

The study analyzed the impact of the viscosity profile of natural polymers on the release characteristics of formulations, and assessed the ability of the polymer to specifically target drug delivery to the colon[26].

METHODOLOGY

Materials

The budesonide sample was acquired as a gift sample from Zydus Cadila Pharmaceuticals, Ahmadabad. Karaya gum, Khaya gum, Gallan gum and Ghatti gum were purchased from ACS Chemicals, Bombay. The Tamarind gum utilised in this study was acquired as a free sample from H. B. Gum Ltd. Kalol, Gujarat. Eudragit S-100 was obtained as a gift sample from Evonik, Mumbai. The remaining chemicals employed were of analytical quality. The Nutrient Agar media was procured from the Himedia supplier.

Methods

Selection of natural polymers using viscosity measurement

The experiment focused on assessing the viscosity of various natural polymers, namely Khaya Gum, Karaya gum, Gellan gum, Ghatti gum, and Tamarind gum to assess the retardation capacity of gums indirectly. To begin, 1% solutions of each gum were meticulously prepared using a phosphate buffer solution adjusted to a pH of 6.8. These solutions were allowed to rest overnight, enabling the gums to fully soaked within the buffer. The subsequent step involved employing a Brookfield Viscometer, an instrument designed to measure the viscosity of gum solutions. In this case, a standardized approach was adopted, using Spindle No. 63 and a rotation speed of 12 rpm. These adjustment were consistent across all measurements and were chosen to ensure accurate and comparable results[14]. Natural polymers with the significant viscosity were selected.

Core tablet preparation using direct compression technique

The quantified quantity of Budesonide along with all accompanying excipients, underwent sieving through mesh number 60. The dry binding agent employed was polyvinyl chloride (PVP K-30). A suitable measure of Tablettos 100 diluent was incorporated. Talc and magnesium stearate were introduced to the powder formulation to enhance lubrication and augment the flow characteristics of the powder aggregate. The composition of the core tablets containing budesonide is outlined in Table 1. Subsequently, a predetermined mass of the powder aggregate was compacted using an 08/32” flat punch through employment of a double rotating tablet compression machine.

Table 1. Composition of budesonide core tablets

Material	Quantity
Budesonide	9 mg
Tablettos 100	64 mg
PVP K-30	4 mg
Talc	2 mg
Magnesium stearate	1 mg
Total	80 mg

Quantitative determination of drug content in a core tablet of budesonide

A drug content assessment was executed on the budesonide-containing core tablets. Ten tablets were pulverized into a fine powder, and an accurately measured amount of this powder, corresponding to 100 mg of budesonide, was introduced into 100 mL volumetric flasks containing 50 mL of methanol. Following a six-hour period of intermittent sonication to ensure full drug solubility, the solutions underwent sequential dilution and subsequent filtration. The quantification of drug concentration transpired at a wavelength of 245 λ_{max}, employing a UV spectrophotometer, to ascertain the accurate content of the drug within the tablets[27]

Compression coating of the core tablets of budesonide

Using 10/32" D Tooling Concave punches, a compression coating procedure was executed. Approximately one-third of the powder was introduced into the die cavity, followed by precise placement of budesonide core tablets, previously prepared using an 8/32" flat punch, positioned at the center of the cavity. The remaining powder was then added, facilitating the compression process for creating budesonide core tablets with an outer coating. The total mass of the coat formulations employed in the Karaya gum/Tamarind gum (KR/TM) batches was meticulously set at 165 mg. Detailed compositions for compression coating utilizing Tamarind gum and Karaya gum are presented in Table 2.

Table 2. Composition of coating formulation using Karaya gum or Tamarind gum

Ingredients	Coating Composition (mg)
Karaya Gum/ Tamarind Gum and EC	150
PVP K 30	15
Total	165

This study encompassed the comprehensive assessment of various attributes of compression-coated tablets, encompassing aspects such as hardness, friability, weight variation, drug content, and drug release kinetics. Furthermore, the compression-coated tablets underwent a subsequent super-coating step using Eudragit S 100 coating solution containing triethyl citrate (TEC) as plasticizers, accomplished through the pan coating technique[28].

Preparation of different batches using 3^2 full factorial designs

Tablets intended for colonic delivery underwent optimization employing a comprehensive 3^2 full factorial design via Design Expert 11.0 software. This design encompassed a systematic assessment of the main, interaction, and quadratic effects of two independent variables, namely the Proportion of Natural Polymer to EC and the percentage weight gain by Eudragit S100, each at three distinct levels. The selected responses, which represented the dependent variables, were % drug release at 2 h, % drug release at 5 h, and % drug release at 7 h, as precisely detailed in Table 3.

Table 3. Independent and dependent variables and the levels used for factorial design

Factors (Independent variables)	LEVELS			Responses (Dependent variables)
	-1	0	+1	
X1- Proportion of Natural Polymer to EC (mg) (Compression coating)	125:25	100:50	75:75	Y_2= % Cumulative Drug release at 2 h
X2- Coating level of Eudragit S 100 (% Weight Gain) Pan coating	0%	2.5%	5%	Y_5= % Cumulative Drug release at 5 h
				Y_7 % Cumulative Drug release at 7 h

The resultant formulations of Tamarind gum and Karaya gums were succinctly compiled and presented in both Table 4 and Table 5, offering a comprehensive overview of the variables' impact on the colonic delivery performance of the formulated tablets.

Table 4. Composition of experimental formulations of Karaya gum

Batch	Amount of Karaya Gum in Compression Coating (mg)	Amount of Ethyl cellulose in Compression Coating (mg)	Coating level of Eudragit S 100 (% Weight gain)
KR 1	125	25	0
KR 2	100	50	0
KR 3	75	75	0
KR 4	125	25	2.5
KR 5	100	50	2.5
KR 6	75	75	2.5
KR 7	125	25	5
KR 8	100	50	5
KR 9	75	75	5

Table 5. Composition of experimental formulations of Tamarind gum

Batch	Amount of Tamarind gum in Compression Coating (mg)	Amount of Ethyl cellulose in Compression Coating (mg)	Coating level of Eudragit S 100 (% Weight gain)
TM 1	125	25	0
TM 2	100	50	0
TM 3	75	75	0
TM 4	125	25	2.5
TM 5	100	50	2.5
TM 6	75	75	2.5
TM 7	125	25	5
TM 8	100	50	5
TM 9	75	75	5

Preparation of probiotic culture medium

In the context of probiotic culture media preparation, the utilisation of the velgut prebiotic and probiotic capsule (manufactured by Eris Life Science Ltd.) is recommended. The velgut probiotics comprise a diverse range of 5 billion bacterial species, namely *Bifidobacterium breve, Bifidobacterium longum, Bifidobacterium infantis, Lactobacillus acidophilus, Lactobacillus plantarum, Lactobacillus casei, Lactobacillus rhamnosus, Streptococcus thermophilus, and Saccharomyces boulardi*[14].

Fluid Thioglycollate Medium (FTM) was used for the incubation and activation of anaerobic bacteria in the probiotic capsule. 8.94 grammes of FTM were mixed with 300 mL of deionized water. The mixture was autoclaved for fifteen minutes at 121 °C and 15 pounds of pressure. Subsequently, the medium was subjected to an inoculation process involving 325 mg of a probiotic combination taken out of a capsule. The medium was then incubated for 48 h at a temperature of 35 °C while being maintained under anaerobic conditions[13,14].

In vitro dissolution testing

In vitro drug release of colon-specific budesonide tablets was conducted in a United State Pharmacopeia (USP) Type II (Paddle) apparatus at a rotation speed of 50 rpm and at 37±0.5 °C. Initially, the test was done in 0.1 N HCl for 2 h to mimic the environment of stomach[29]. The test was then conducted for three hours in phosphate buffer pH 7.4, which mimics the milieu of the small intestine[29]. In reality, the small intestine can be categorized into three distinct segments: the duodenum, which exhibits a pH range of 5 to 6; the jejunum, with a pH of approximately 6.63±0.53; and the ileum, which maintains a pH level of around 7.49±0.46. The ileum is the longest section of the small intestine, and as a result, its mean pH is 7.3±0.34[30,31]. The remaining investigation was conducted in biorelevant medium with a pH of 6.8, which is comparable to the mean pH of the large intestine (6.63±0.04)[30,31], and CO_2 aeration to create a favorable environment for anaerobic bacteria[13]. Samples were extracted at regular intervals and analyzed spectrophotometrically at a wavelength of 243 nm.

Statistical analysis

The assessment of the data pertaining to the percentage of drug released at the completion of each dissolution test was a pivotal step in understanding the drug delivery behavior of the formulated dosage forms. To elucidate the relationship between the independent variables X1 and X2 and the dependent variables Y2, Y5, and Y7, a comprehensive statistical model was constructed. This model was predicated on a second-order polynomial equation, embody-

ing both main and interaction effects of the variables:

Dependent Variable = b0 + b1X1 + b2X2 + b11X1^2 + b22X2^2 + b12X1X2

Here, b0 represents the intercept, b1 and b2 denote the coefficients for X1 and X2 respectively, while b11, b22, and b12 represent the quadratic and interaction coefficients.

To individually capture the relationship between the response variables (Y2, Y5, and Y7) and the independent variables, the Design Expert 11.0 software facilitated the fitting of a second-order polynomial model for each response variable.

In order to assess whether the response variables exhibited statistically significant differences, the Dunnett test was performed. A P-value of less than 0.05 was established as the criterion for declaring a result as statistically significant. This threshold was chosen to indicate a high level of confidence in the observed differences.

RESULTS and DISCUSSION

The literature has documented the utilisation of guar gum as a carrier for targeted drug release in the colon, either through a matrix tablet or a compression coat enveloping a central drug core tablet[32]. On account of that knowledge, the capacity of different polysaccharides to deliver the drug to the colonic environment was evaluated[12].

The viscosity profile was used to screen natural gums for their ability to delay drug release in the upper gastrointestinal tract, since this lag time is assessed by the viscosity profile.

Figure 1 depicts the viscosity of 1% solutions of various natural polymers produced in a 6.8 pH phosphate buffer.

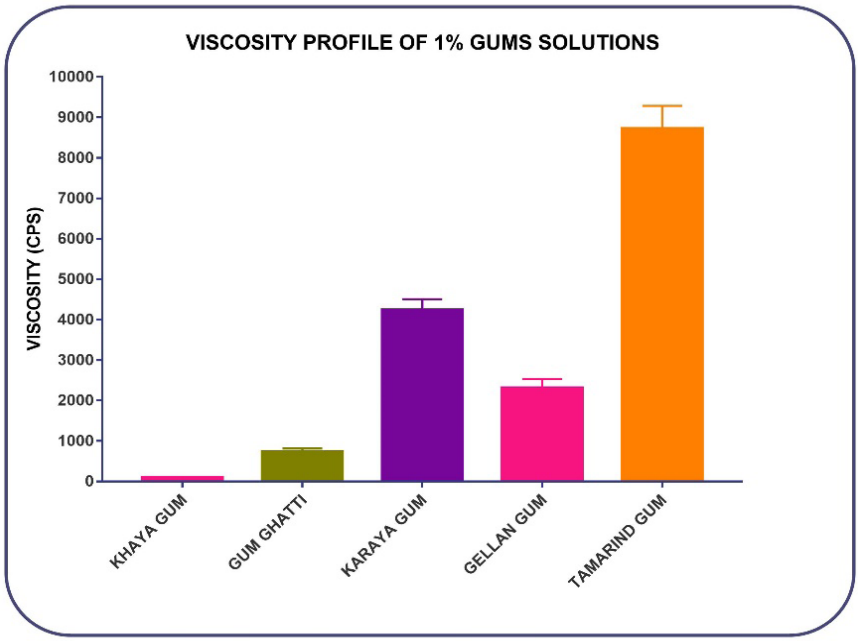

Figure 1. Viscosity profile of 1% solutions of various natural polymers

The viscosity profiles of Tamarind gum and Karaya gum were found to be statistically significant in achieving the desired lag time. On the basis of viscosity profiling, formulations including Tamarind gum and Karaya gum were designed to evaluate the efficacy of a polymer in delivering the drug to the colon. Tamarind gum is also used as a matrix-former in the formulation of matrix tablets and as controlled drug release carriers for a number of different pharmaceuticals[22,33]. In addition, it is employed in the development of oral[34], buccal[35], colon[36], nasal[37], and ocular[38] drug delivery systems. Karaya gum was effectively tested for its appropriateness in the development of colon-specific drug carriers[18], gastro-retentive drug delivery systems[17], sustained release matrices[17], etc.

The study indicates that the core tablet formulations that were prepared have successfully passed the Indian Pharmacopiea (IP)-96 test for weight variation and friability. 3^2 full factorial designs were used to evaluate the impact of independent factors, Proportion of Natural Polymers relative to EC and % weight growth, on dependent variables, % drug release at 5 h and % drug release at 12 h. Table 6 displays the dependent variables of the compression-coated tablets that were produced in accordance with the experimental design.

Table 6. Experimental runs obtained from 3^2 Factorial design and their responses for Tamarind and Karaya formulations

Batch No.	Amount of Tamarind gum	% Weight Gain	% CDR at 2 h	% CDR at 5 h	% CDR at 7 h	Batch No.	Amount of Karaya gum	% Weight Gain	% CDR at 2 h	% CDR at 5 h	% CDR at 7 h
1	-1	-1	34.43	99.05	99.01	1	-1	-1	47.38	99.05	99.95
2	0	-1	30.66	74.2	100.01	2	0	-1	28.86	100.45	100.01
3	1	-1	22.73	60.55	89.8	3	1	-1	21.5	72.52	100.67
4	-1	0	11.18	49.32	83.82	4	-1	0	17.32	99.25	99.92
5	0	0	7.36	38.41	73.19	5	0	0	15.35	72.72	99.67
6	1	0	5.08	33.66	69.65	6	1	0	14.13	61.94	92.81
7	-1	1	3.38	26.65	62.71	7	-1	1	3.43	42.64	74.41
8	0	1	2.98	16.89	51.23	8	0	1	2.59	32.91	59.57
9	1	1	2.93	8.91	50.23	9	1	1	2.28	22.87	47.03

The post compression parameters for the core tablets and coated tablets are summarized in Table 7 demonstrating that all batches satisfy the required standards of all parameters.

Table 7. Post-compression parameters for Tamarind and Karaya formulations

Batch No.	Tamarind Gum based formulation					Karaya Gum based formulation				
	V	F	D	H (kg/ cm^2)	C	V	F	D	H (kg/ cm^2)	C
1	Pass	0.92	4	4.5	98.45	Pass	0.91	3	4.1	98.52
2	Pass	0.76	5	4.3	99.25	Pass	0.82	6	4.5	99.45
3	Pass	0.67	4.5	4.2	98.23	Pass	0.65	4	4.1	99.67
4	Pass	0.89	6	4.5	98.19	Pass	0.96	3	4.2	98.15
5	Pass	0.78	5.5	4.1	99.36	Pass	0.82	4	4.3	99.43
6	Pass	0.69	5	4.2	98.45	Pass	0.62	5	4.2	99.72
7	Pass	0.91	6	4.6	98.45	Pass	0.94	3.5	4.5	98.45
8	Pass	0.71	4	4.2	100.08	Pass	0.76	6	4.6	99.15
9	Pass	0.65	5	4.3	98.16	Pass	0.62	5	4.2	99.45

V: weight variation, F: friability, D: Disintegration (core tablet) in min,
H: hardness, C: Drug content (core tablet)

Figures 2 (a and b) show the results of the dissolution test of coated budesonide tablet prepared from Karaya gum and Tamarind gum respectively. The predetermined *in vitro* release profile for colon-specific targeting requires restricting drug release to no more than 5% within the first 2 h, no more than 10% by the end of the small intestine (5 h) and achieving a release of over 50% within 7 h. Actually, gastro-intestinal (GI) tract transit time is 15–30 h yet a third dependent variable determined that more than 50% of the drug should be released within 7 h because the main function of the colon is absorption of water. The reduction of water content in the colon has the potential to hinder the release of drugs from the dosage form over time. Therefore, a time duration of 7 h was deemed appropriate for achieving drug release of over 50% from the colon-targeted drug delivery system.

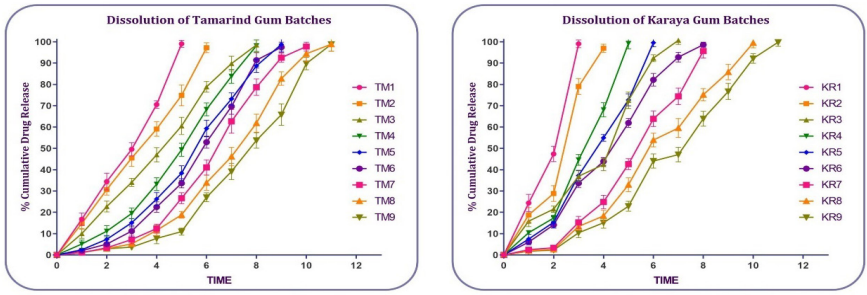

(a) (b)

Figure 2. Mean (±S.D.) Percent of budesonide released from compression-coated tablets (n=3) containing different amount of Karaya gum (a) and Tamarind gum (b)

Upon exposure to dissolution fluids, the Eudragit S 100 super-coating would impede the release of the drug in the upper gastrointestinal tract. Subsequently, the Eudragit S 100 coat would dissolve in the lower section of the small intestine, and the Karaya gum or Tamarind gum would undergo hydration, forming a dense gel layer. This layer, in the form of a compression coat, would serve the dual purpose of safeguarding the drug from release in the small intestine's physiological environment and facilitating its release in the colon with the aid of colonic bacteria. Consequently, experiments were conducted to investigate drug release using *in vitro* methods. The pH of the phosphate-buffered solution was adjusted to 6.8, and 4.5 mL of probiotic culture medium was added to the solution to mimic colonic environment.

As per the findings of the dissolution studies (Figure 2), it has been observed that all batches of Tamarind gum-based formulation (TM1-TM8) and Karaya gum-based formulation (KR1-KR8) exhibit a drug release rate of over 10%

within a period of 5 h. Karaya gum with KR 9 batch exhibited a drug release of 22.87 % in 5 h, while Tamarind gum having TM 9 batch exhibited a drug release of 8.91 %. This indicates that Tamarind gum with batch TM 9 has a greater capacity to protect the drug release in the upper portion of the GI tract and to transport the drug in intact form to the colonic milieu.

Regression analysis of formulations by 3^2 factorial designs

The result of ANOVA analysis (Table 8) yielded helpful findings regarding the significance and predictive power of the model. The Model F-value of 249.53 highlighted the model's significance for Y2 (% cumulative drug release at 2 h)[24], with P-values below 0.05 of tamarind formulation indicating the statistical significance of the model terms.

Table 8. Analysis of variance (ANOVA) for three dependent variables for Tamarind and Karaya formulation batches

Source	Dependent Variable (For TM Formulations)			Dependent Variable (For KR Formulations)		
Source	Y2- % CDR at 2 h	Y5- % CDR at 5 h	Y7- % CDR at 7 h	Y2- % CDR at 2 h	Y5- % CDR at 5 h	Y7- % CDR at 7 h
Sum of Squares	1253.432	6575.982	2862.32	1638.35	6187.93	3364.281
df	5	5	3	3	2	5
Mean Square	250.6863	1315.196	954.11	546.12	3093.97	672.8563
F-value	249.5313	66.69654	101.37	41.99	23.5	99.1675
p-value	0.000398	0.002835	< 0.0001	0.0006	0.0015	0.001575
R^2	0.9976	0.9911	0.9838	0.9618	0.8868	0.9940
Adjusted R^2	0.9936	0.9762	0.9741	0.9389	0.8491	0.9840
Predicted R^2	0.9757	0.8913	0.9309	0.7932	0.7280	0.9368
Adeq Precision	39.4191	23.2825	26.4859	17.5431	12.9431	26.0538

The quadratic models representing Y2 exhibited an adjusted R^2 of 0.9976, indicating a strong representation of variance. The predicted R^2 of 0.9757 indicated the model's accuracy in predicting future data, with the minimal difference between adjusted R^2 and predicted R^2 supporting the model's predictive capability[39].

For TM formulation (% CDR at 2 h) = 8.12556 – 3.04167X1 – 13.0883X2 + 2.812X1X2 – 0.37833X1^2 + 8.31167*X2^2

Analysis of the polynomial equation, the 3D response curve (Figure 3a), and the contour plot (Figure 3b) revealed that the percentage weight gain due to Eudragit S 100 coating (X2) significantly influenced Y2. As coating level (X2) increased, Y2 (drug release at 2 h) decreased substantially. Tamarind gum amount (X1) had a similar negative impact on Y2, but it less pronounced than that of X2.

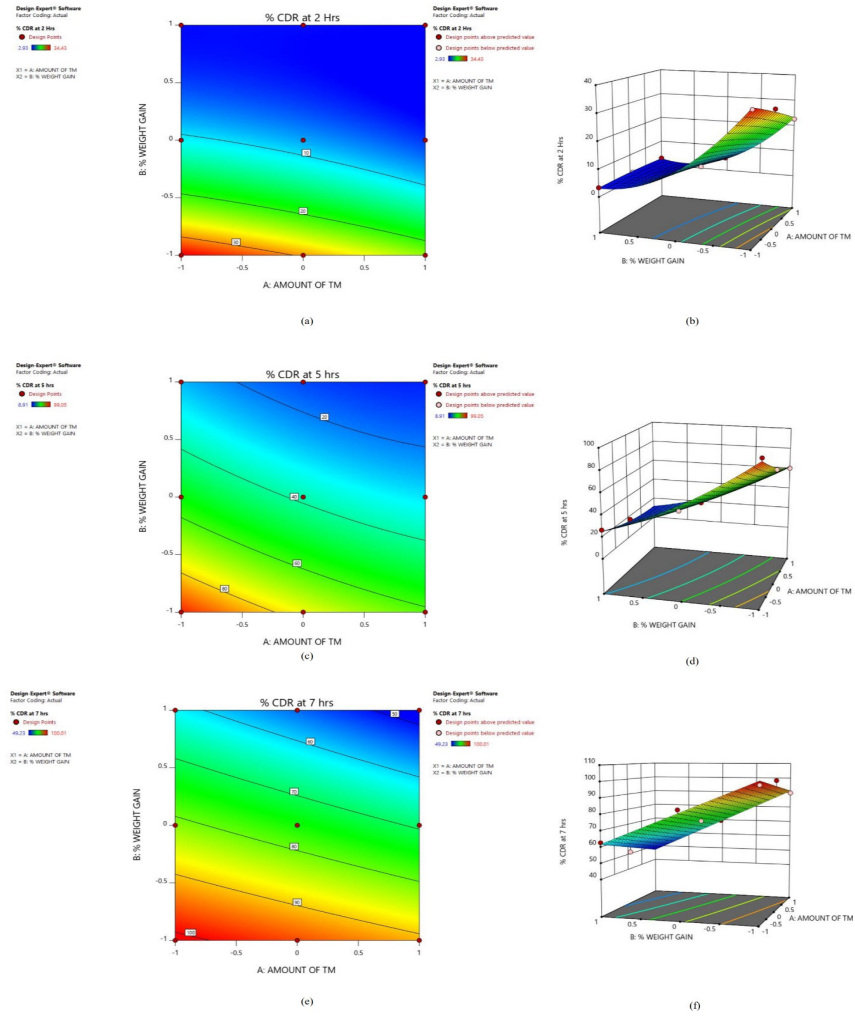

Figure 3. Contour Plot and 3D Response Plot for Tamarind formulation for Y2 (% CDR at 2 h – (a and b)), Y5 (% CDR at 5 h – (c and d)), Y7 (% CDR at 7 h – (e and f))

A comparable trend was observed in the formulation containing Karaya gum. The model F-value of 41.99 highlighted the statistical significance of the model. This conclusion is further substantiated by considering the adjusted R^2 (0.9389) and predicted R^2 (0.7932) values, which demonstrate the model's

robust predictive power.

For KR formulation (% CDR at 2 h) = 16.9822 – 5.03667*X1* – *14.9067*X2 + 6.1825*X1X2

Analysing the polynomial equation for Y2, in conjunction with the 3D response curve (Figure 4a) and contour plot (Figure 4b), it becomes evident that the effect observed in the Karaya gum formulation is even more pronounced than what was noted in the Tamarind formulation. The greater impact on Y2, as demonstrated by these graphical representations, signifies that the variables exert a stronger influence in the case of Karaya gum-containing formulations compared to those with Tamarind gum.

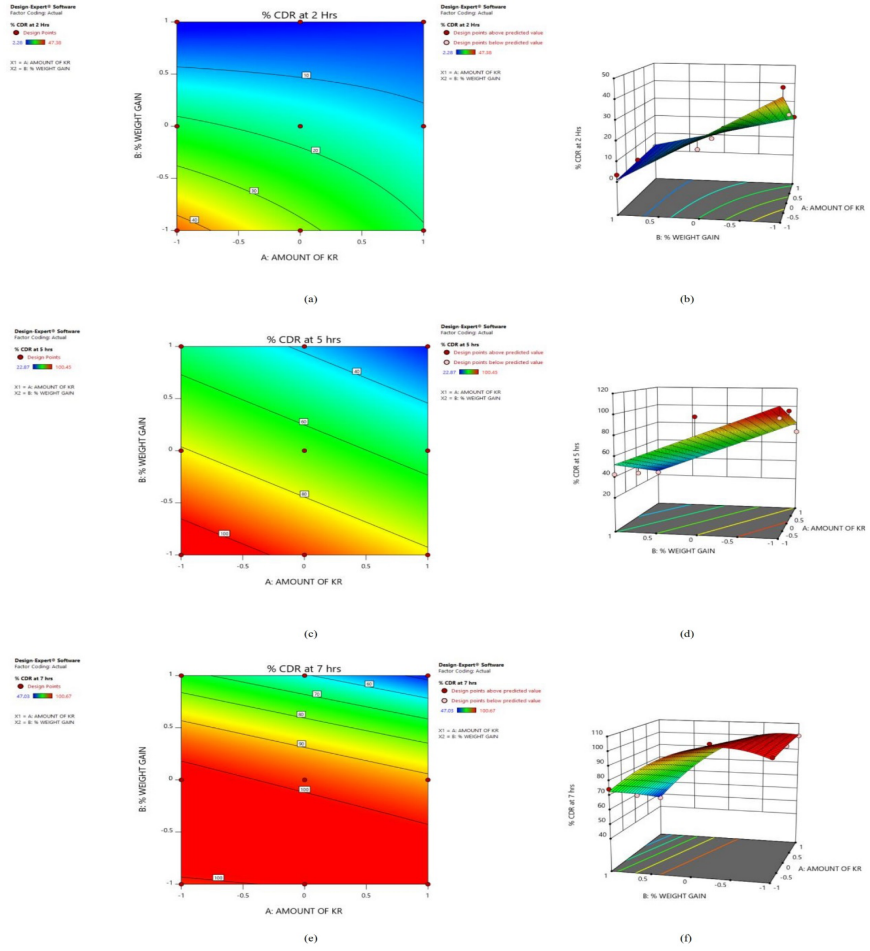

Figure 4. Contour Plot and 3D Response Plot for Karaya Formulations for Y2 (% CDR at 2 h – (a and b)), Y5 (% CDR at 5 h – (c and d)), Y7 (% CDR at 7 h – (e and f))

The Model F-value of 66.69 indicate the model's notable significance for Y5, which represents the percentage cumulative drug release at 5 h. The presence of P-values below 0.05 for the Tamarind formulation emphasized the statistical significance of the model terms in this context. The quadratic models used to depict Y5 produced an adjusted R^2 value of 0.9762, suggesting a strong and reliable representation of the observed variance. The theoretical analysis demonstrated the model's proficiency in describing variations in the response, as shown by the predicated R^2 value of 0.8913. The small differences observed between the adjusted and predicted R^2 values provides additional evidence to support the claim that the model displays an adequate capacity for prediction.

For the TM formulation: % CDR at 5 h = 38.3367 – 11.9833*X1* – *30.225*X2 + 5.19*X1X2* + *3.19*X1^2 + 7.245*X2^2

Analysing the polynomial equation, the 3D response curve (Figure 3c), and the contour plot (Figure 3d) revealed that the percentage weight gains due to Eudragit S 100 coating (X2) exerted a significant influence on Y5. As the coating level (X2) increased, Y5 (drug release at 5 h) exhibited a considerable decrease. Similarly, the amount of tamarind gum (X1) also negatively impacted Y5, although to a lesser extent compared to X2.

This comparable trend extended to the Karaya gum-containing formulation. A model F-value of 23.5 improved the statistical significance of the model, confirming its importance. The small difference between adjusted R^2 (0.8491) and predicted R^2 (0.7280) values further showed to the model's reliable predictive capacity.

For the KR formulation: % CDR at 5 h = 67.15 – 13.935X1 – 28.9333X2

Analysing the polynomial equation for Y5 within the context of the 3D response curve (Figure 4c) and contour plot (Figure 4d) indicate that more pronounced effect in the karaya gum formulation compared to the tamarind formulation. The sharp impact on Y5, as demonstrated by these graphical representations, underlined the increased influence of variables within Karaya gum-containing formulations.

The Model F-value of 101.37 served as a prominent indicator of the model's significance in relation to Y7 (% cumulative drug release at 7 h) for the tamarind formulation. The presence of P-values below 0.05 highlighted the statistical significance of the model terms, solidifying their relevance. The quadratic models representing Y7 displayed an adjusted R^2 of 0.9741, signifying a robust representation of variance. Meanwhile, the predicted R^2 of 0.9309 testified to the model's precision in forecasting future data. This alignment between ad-

justed R^2 and predicted R^2 confirmed the model's exceptional predictive capability.

For the Tamarind formulation: % CDR at 7 h = 75.4056 – 6.14333 * X1-20.9417*X2 -1.0675*X1X2

Evaluation of the polynomial equation, coupled with scrutiny of the 3D response curve (Figure 3e) and contour plot (Figure 3f), showed the substantial impact of quantity of tamarind gum (X1) on Y7. Additionally, the percentage of Eudragit S 100 (X2) yielded a comparable, yet less pronounced, negative effect on Y7 as compared to X1.

A similar trend was observed in the formulation containing Karaya gum. The model F-value of 99.16 underscored the statistical significance of the model, emphasizing its relevance. This conclusion is buttressed by the adjusted R^2 (0.9840) and predicted R^2 (0.9368) values, both of which highlighted the model's robust predictive capability.

For the Karaya formulation: % CDR at 7 h = 97.8789 – 5.62833*X1-19.9367*X2-7.025*X1X2-0.618333*$X1^2$-17.1933*$X2^2$

A comprehensive analysis of the polynomial equation for Y5, coupled with the insights gained from examining the 3D response curve (Figure 4e) and contour plot (Figure 4f), affirmed that the effect witnessed in the Karaya gum-containing formulation exhibited even more pronounced characteristics than those observed in the tamarind formulation. This heightened impact on Y5 signified that the variables exerted a more substantial influence within the context of Karaya gum-containing formulations, setting them apart from those formulated with Tamarind gum.

The figures shown in this study, namely Figure 5a for Tamarind gum and Figure 5b for Karaya gum formulations, clearly demonstrate that tamarind gum has the potential to create a design space that is favorable for developing optimized formulations. In contrast, it might be stated that Karaya gum does not provide a comparable range of design options that are ideal for this particular objective.

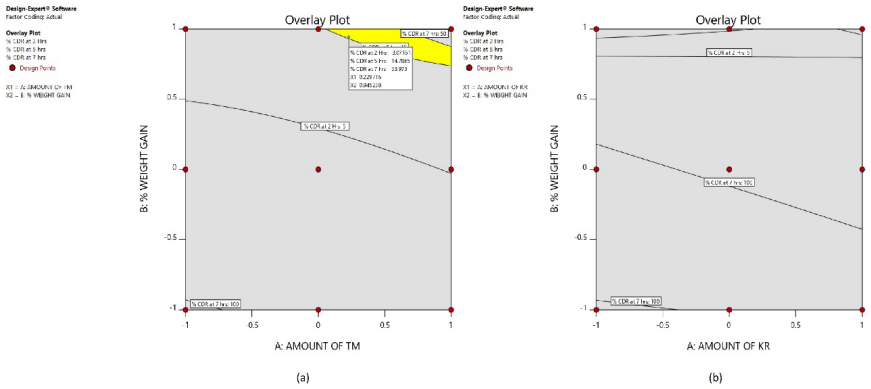

Figure 5. Design space generated by 3^2 factorial design (a) Tamarind formulations (b) Karaya formulations

Graphs in Figure 6a and 6b illustrate the correlation between the observed values in the actual world and the expected values produced by the model.

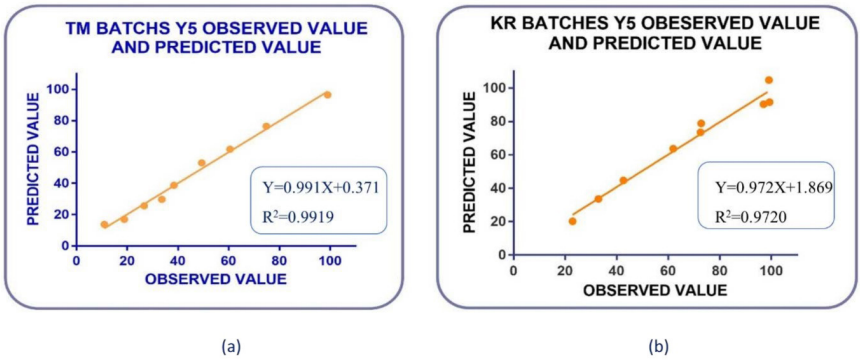

Figure 6. The predicted and actual values of Y5 responses for Tamarind gum (a) and Karaya gum (b) containing formulations

These predictions are based on the independent variables within the TM and KR formulations, respectively. The strong correlation between the observed and projected results provides evidence of the model's significant predictive capability. The alignment seen between the observed and anticipated values provides empirical evidence supporting the model's dependability in properly predicting future outcomes.

Based on the results, Tamarind gum was found to be superior to Karaya gum in delivering the drug to the colon, with TM 9 batch showing the highest concentration of intact drug released in the colon among all the batches. The op-

timized Tamarind-based formulation was able to meet the necessary selection criteria, ensuring not more than 15% of the substance is released in five hours and not less than 50% in seven hours.

Moreover, the results obtained from the Dunnett test revealed a statistically significant disparity in the in vitro release data of the optimized sample when compared to the other batches. The P-value associated with this difference was found to be less than 0.001. The notable discrepancy in the patterns of release shows the efficacy of the optimization procedure, providing further validation for the practicality of the developed model in predicting actual effects.

In conclusion, the study provides insights into the use of natural polymers in the development of colon-targeted drug delivery systems. Further research could explore the potential of other natural polymers and super-coating agents to improve the efficiency of colon-specific drug delivery systems. With the continuous advancements in technology, it is hoped that natural polymer-based colon-targeted drug delivery systems could be developed and used to treat various colon-related diseases effectively.

STATEMENT OF ETHICS

Not applicable as no human or animal subjects were involved in the study.

CONFLICT OF INTEREST STATEMENT

Authors declare no conflict of interest.

AUTHOR CONTRIBUTIONS

Jaymin Patel contributed to the article's conception/design and data analysis/interpretation. Kaushika Patel wrote/edited the article with major intellectual input. Dr. Shreeraj Shah provided substantial support for the argument/analysis and finalized for publication.

ACKNOWLEDGMENTS

The authors, JP is thankful to Dr. Shreeraj Shah for valuable guidance and to the L. J. Institute of Pharmacy, LJ University, Ahmedabad for providing the research facilities which is a part of Doctor of Philosophy (Ph.D.) research work of Mr. Jaymin Patel, to be submitted to Gujarat Technological University, Ahmedabad

REFERENCES

1. Mishra S, Sharma N, Jain S. Formulation development and evaluation of colon targeting nanosponges of deflazacort using box behnken design. J Pharm Res Int, 2021;33(63A):451-459. Doi: 10.9734/jpri/2021/v33i63A35961

2. Akhil Gupta, Anuj Mittal AKG. Colon targeted drug delivery systems – a review. Asian J Pharm Res, 2017;1(2):25-33. Doi: 10.5001/omj.2010.24

3. Turanlı Y, Acartürk F. Fabrication and characterization of budesonide loaded colon-specific nanofiber drug delivery systems using anionic and cationic polymethacrylate polymers. J Drug Deliv Sci Technol, 2021;63:102511. Doi: 10.1016/j.jddst.2021.102511

4. Song IH, Finkelman RD, Lan L. A pharmacokinetic bridging study to compare systemic exposure to budesonide between budesonide oral suspension and ENTOCORT EC in healthy individuals. Drugs R D, 2020;20(4):359-367. Doi: 10.1007/s40268-020-00324-1

5. Kane SV, Schoenfeld P, Sandborn WJ, Tremaine W, Hofer T, Feagan BG. Systematic review: the effectiveness of budesonide therapy for Crohn's disease. Aliment Pharmacol Ther, 2002;16(8):1509-1517. Doi: 10.1046/j.1365-2036.2002.01289.x

6. Rutgeerts P, Lofberg R, Malchow H, Lamers C, Olaison G, Jewell D, et al. A comparison of budesonide with prednisolone for active Crohn's disease. N Engl J Med, 1994;331(13):842-845. Doi: 10.1056/nejm1994092933113047

7. Sairenji T, Collins KL, Evans D V. An opdate on inflammatory bowel disease. Prim Care - Clin Off, 2017;44(4):673-692. Doi: 10.1016/j.pop.2017.07.010

8. Ramos GP, Papadakis KA. Mechanisms of disease: inflammatory bowel diseases. Mayo Clin Proc, 2019;94(1):155-165. Available from: 10.1016/j.mayocp.2018.09.013

9. García MA, Varum F, Al-Gousous J, Hofmann M, Page S, Langguth P. In vitro methodologies for evaluating colon-targeted pharmaceutical products and industry perspectives for their applications. Pharmaceutics, 2022;14(2):291. Doi: 10.3390/pharmaceutics14020291

10. Turanlı Y, Acartürk F. Preparation and characterization of colon-targeted pH/Time-dependent nanoparticles using anionic and cationic polymethacrylate polymers. Eur J Pharm Sci, 2022;171:106122. Doi: 10.1016/j.ejps.2022.106122

11. Casati F, Melocchi A, Moutaharrik S, Uboldi M, Foppoli A, Maroni A, et al. Injection molded capsules for colon delivery combining time-controlled and enzyme-triggered approaches. Int J Mol Sci, 2020;21(6):1917. Doi: 10.3390/ijms21061917

12. De Anda-Flores Y, Carvajal-Millan E, Campa-Mada A, Lizardi-Mendoza J, Rascon-Chu A, Tanori-Cordova J, et al. Polysaccharide-based nanoparticles for colon-targeted drug delivery systems. Polysaccharides, 2021;2(3):626-647. Doi: 10.3390/polysaccharides2030038

13. Wahlgren M, Axenstrand M, Håkansson Å, Marefati A, Lomstein Pedersen B. In vitro methods to study colon release: state of the art and an outlook on new strategies for better in-vitro biorelevant release media. Pharmaceutics, 2019;11(2):95. Doi: 10.3390/pharmaceutics11020095

14. Yadav A, Sadora M, Singh S, Gulati M, Maharshi P, Sharma A, et al. Novel biorelevant dissolution medium as a prognostic tool for polysaccharide-based colon-targeted drug delivery system. J Adv Pharm Technol Res, 2017;8(4):150. Doi: 10.4103/japtr.japtr_70_17

15. Mali K, Dhawale S, Dias R, Ghorpade V. Delivery of drugs using tamarind gum and modified tamarind gum: a review. Bull Fac Pharm Cairo Univ, 2019;57(1):1-24. Doi: 10.21608/BFPC.2019.47260

16. Huanbutta K, Sittikijyothin W. Use of seed gums from *Tamarindus indica* and *Cassia fistula* as controlled-release agents. Asian J Pharm Sci, 2018;13(5):398-408. Doi: 10.1016/j.ajps.2018.02.006

17. Silva JSF da, Oliveira AC de J, Soares MF de LR, Soares-Sobrinho JL. Recent advances of Sterculia gums uses in drug delivery systems. Int J Biol Macromol, 2021;193:481-490. Doi: 10.1016/j.ijbiomac.2021.10.145

18. Nath B, Nath LK. Design, development, and optimization of sterculia gum-based tablet coated with Chitosan/Eudragit RLPO mixed blend polymers for possible colonic drug delivery. J Pharm, 2013;2013:1-9. Doi: 10.1155/2013/546324

19. Prabhu P, Ahamed N, Matapady HN, Ahmed MG, Narayanacharyulu R, Satyanarayana D, et al. Investigation and comparison of colon specificity of novel polymer khaya gum with guar gum. Pak J Pharm Sci, 2010;23(3):259-265.

20. Villarreal-Otalvaro C, Coburn JM. Fabrication methods and form factors of gellan gum-based materials for drug delivery and anti-cancer applications. ACS Biomater Sci Eng, 2023;9(7):3832-3842. Doi: 10.1021/acsbiomaterials.1c00685

21. Sharma K, Kaith BS, Kalia S, Kumar V, Swart HC. Gum ghatti-based biodegradable and conductive carriers for colon-specific drug delivery. Colloid Polym Sci, 2015;293(4):1181-1190. Doi: 10.1007/s00396-015-3505-z

22. Malviya R, Sundram S, Fuloria S, Subramaniyan V, Sathasivam KV, Azad AK, Sekar M, et al. Evaluation and characterization of tamarind gum polysaccharide: the biopolymer. Polymers, 2021;13(18):3023. Doi: 10.3390/polym13183023

23. Nayak AK, Pal D. Functionalization of tamarind gum for drug delivery. Functional Biopolymers. Springer; 2018. 25-56. Available from: 10.1007/978-3-319-66417-0_2

24. Pandit AP, Waychal PD, Sayare AS, Patole VC. Carboxymethyl tamarind seed kernel polysaccharide formulated into pellets to target at colon. Indian J Pharm Educ Res, 2018;52(3):363-373. Doi: 10.5530/ijper.52.3.42

25. Muley SS, Nandgude T, Poddar S. Formulation and optimization of lansoprazole pellets using factorial design prepared by extrusion-spheronization technique using carboxymethyl tamarind kernel powder. Recent Pat Drug Deliv Formul, 2017;11(1):54-66. Doi: 10.2174/1872211316661701131502 48

26. Zhang H, Neau SH. In vitro degradation of chitosan by bacterial enzymes from rat cecal and colonic contents. Biomaterials, 2002;23(13):2761-2766. Doi: 10.1016/s0142-9612(02)00011-x

27. Varshosaz J, Emami J, Tavakoli N, Minaiyan M, Rahmani N, Ahmadi F, et al. Development and validation of a rapid HPLC method for simultaneous analysis of budesonide and its novel synthesized hemiesters in colon specific formulations. Res Pharm Sci, 2011;6(2):107-116.

28. Martín-Illana A, Cazorla-Luna R, Notario-Pérez F, Rubio J, Ruiz-Caro R, Tamayo A, et al. Eudragit® L100/chitosan composite thin bilayer films for intravaginal pH-responsive release of Tenofovir. Int J Pharm, 2022;616:121554. Doi: 10.1016/j.ijpharm.2022.121554

29. Ren Y, Jiang L, Yang S, Gao S, Yu H, Hu J, et al. Design and preparation of a novel colon-targeted tablet of hydrocortisone. Braz J Pharm Sci, 2017;53(1). Doi: 10.1590/s2175-97902017000115009

30. McCoubrey LE, Favaron A, Awad A, Orlu M, Gaisford S, Basit AW. Colonic drug delivery: Formulating the next generation of colon-targeted therapeutics. J Control Release, 2023;353:1107-1126. Doi: 10.1016/j.jconrel.2022.12.029

31. Evans DF, Pye G, Bramley R, Clark AG, Dyson TJ, Hardcastle JD. Measurement of gastrointestinal pH profiles in normal ambulant human subjects. Gut, 1988;29(8):1035-1041. Doi: 10.1136/gut.29.8.1035

32. Hanmantrao M, Chaterjee S, Kumar R, Vishwas S, Harish V, Porwal O, et al. Development of guar gum-pectin-based colon targeted solid self-nanoemulsifying drug delivery system of Xanthohumol. Pharmaceutics, 2022;14(11):2384. Doi: 10.3390/pharmaceutics14112384

33. Guntaka PR, Sriram N, Bukke SPN, Kiran Kumar Y, Parameshwar H, Jaganathan S, et al. Formulation and evaluation of sustained release matrix tablets of glimipride using natural polymers tamarind seed mucilage and guar gum. J Pharm Negat, 2022;13(9):5256-5267. Doi: 10.47750/pnr.2022.13.S09.645

34. Nayak AK, Pal D, Malakar J. Development, optimization, and evaluation of emulsion-gelled floating beads using natural polysaccharide-blend for controlled drug release. Polym Eng Sci, 2013;53(2):238-250. Doi: 10.1002/pen.23259

35. Avachat AM, Gujar KN, Wagh K V. Development and evaluation of tamarind seed xyloglucan-based mucoadhesive buccal films of rizatriptan benzoate. Carbohydr Polym, 2013;91(2):537-542. Doi: 10.1016/j.carbpol.2012.08.062

36. Newton AMJ, Indana VL, Kumar J. Chronotherapeutic drug delivery of tamarind gum, chitosan and okra gum controlled release colon targeted directly compressed propranolol HCl matrix tablets and in-vitro evaluation. Int J Biol Macromol, 2015;79:290-299. Doi: 10.1016/j.ijbiomac.2015.03.031

37. Kumar A, Garg T, Sarma GS, Rath G, Goyal AK. Optimization of combinational intranasal drug delivery system for the management of migraine by using statistical design. Eur J Pharm Sci, 2015;70:140-151. Doi: 10.1016/j.ejps.2015.01.012

38. Rawooth M, Qureshi D, Hoque M, Prasad MPJG, Mohanty B, Alam MA, et al. Synthesis and characterization of novel tamarind gum and rice bran oil-based emulgels for the ocular delivery of antibiotics. Int J Biol Macromol, 2020;164:1608-1620. Doi: 10.1016/j.ijbiomac.2020.07.231

39. Ranch KM, Maulvi FA, Naik MJ, Koli AR, Parikh RK, Shah DO. Optimization of a novel in situ gel for sustained ocular drug delivery using Box-Behnken design: In vitro, ex vivo, in vivo and human studies. Int J Pharm, 2019;554:264-275. Doi: 10.1016/j.ijpharm.2018.11.016

Acta Pharm. Sci. Vol 62:(2), 2024
Research article
DOI: 10.23893/1307-2080.APS6223

The applicability of bioluminescent bacteria for preliminary screening of antibacterial activity: Comparative analysis of aqueous and ethanol extracts from plant raw material

Yuliia Yu HAVRYCHENKO*, Andrei M. KATSEV, Sergei L. SAFRONYUK, Dhruv VASHISHT

Institute of Biochemical Technologies, Ecology and Pharmacy of Vernadsky CFU, Medicinal and Pharmaceutical Chemistry, Russian Federation

ABSTRACT

This study aimed to assess the effectiveness of whole-cell luminous biosensors in detecting the antibacterial activity of plant extracts. The biosensors included bioluminescent genetically modified *Escherichia coli* MG1655 pXen7 and naturally occurring *Aliivibrio fischeri* F1 bacterial strains. Initially, chemical substances known for their antibacterial properties, such as ethanol, quercetin, and zinc sulfate, were used to evaluate the functionality of the biosensors. Subsequently, 17 herbal extracts were screened for antibacterial activity in both aqueous and ethanol forms. As a result, extracts from *Coreopsis grandiflora*, *Thymus vulgaris*, and *Monarda x hybrida* demonstrated significant antibacterial potential, resulting in a 50% reduction in bioluminescence. Notably, *A. fischeri* F1 exhibited higher sensitivity compared to recombinant *E. coli* MG1655 pXen7 in detecting antimicrobial compounds at lower concentrations. The variations in the effects of extracts from different species within the same and different plant families were observed, utilizing both biosensors. These findings align with existing literature data regarding the antibacterial activity of the investigated plant species against pathogenic bacteria.

*Corresponding author: Yuliia Yu HAVRYCHENKO
E-mail: havrychenkoyuliia@gmail.com
ORCIDs:
Yuliia Yu HAVRYCHENKO: 0000-0002-5651-3169
Andrei M. KATSEV: 0000-0002-7762-3818
Sergei L. SAFRONYUK: 0000-0002-6276-7755
Dhruv VASHISHT: 0009-0005-5614-987X
(Received 5 Aug 2023, Accepted 25 Sep 2023)

Overall, the results underscore the efficacy of bioluminescent bacteria for the rapid screening of antibacterial properties in crude plant extracts.

Keywords: antibacterial activity, *lux*-biosensors, *Aliivibrio fischeri* F1, *Escherichia coli* MG1655, crude plant extracts

INTRODUCTION

One of the most pressing problems in the modern world is that microorganisms are adjusting to antibacterials faster than these are being developed by pharmaceutical companies, which results in an enormous rise in the death rate all over the globe from earlier treatable infections[1]. However, this problem can potentially be addressed by expanding the scope of investigation to explore novel active compounds and optimizing the time and financial requirements associated with the initial screening stages.

By broadening the investigation area, researchers can explore a wider range of sources, including natural substances, synthetic compounds, and their combinations, which may possess potent antibacterial properties. In this regard, medical plants continue to hold immense potential as a source of future medications. Plants are rich in secondary metabolites such as tannins, terpenoids, alkaloids, flavonoids, and other compounds known for their antibacterial characteristics[2]. Moreover, utilizing natural sources can help reduce the cost of developing and producing medicines. Notably, The World Health Organization highlights that 50% of prescribed medications worldwide originate from plants, and traditional medicine still plays a prominent role in illness prevention and treatment, with approximately 80% of the population relying on it[3-4].

On the other hand, the current methods used to test antibacterial activity are often time-consuming and inadequate for screening certain bioactive substances, especially those of plant origin. The widely used diffusion into agar method, commonly employed for evaluating antimicrobial activity[5-6], has its limitations, particularly in measuring the antibacterial effects of plant extracts. The water-based agar matrix used in diffusion methods hampers the diffusion of non-polar substances into its layers compared to polar compounds, resulting in incomplete diffusion of complexes with intermediate polarity, which are considered to possess the highest antibacterial activity[7-8]. Moreover, this method requires a significant investment of time and resources, posing constraints on conducting efficient screening tests[9]. Therefore, there is a need for more uniform methods to measure antibacterial activity. One potential solution lies in incorporating widely utilized in toxicological studies methodologies based on bacterial luminescence

into the screening of potential antibacterial compounds. Above all, biotests utilizing bioluminescent bacteria have long been used in environmental and toxicological studies, demonstrating their high sensitivity to various biologically active substances[10-12]. In recent years, these methods have also shown promise in the field of pharmacy, indicating their potential applicability[13-15]. Furthermore, the sensitivity of bioluminescent bacteria allows the examination of hundreds of samples within several hours, whereas traditional procedures often require days or even weeks to achieve comparable results. By reducing screening time, valuable resources such as consumables and personnel are conserved, resulting in cost savings for the study. Consequently, with decreased time and funding requirements, the development and production of treatments can be accelerated, potentially saving countless lives[11-13].

The aim of this study was to assess the applicability of whole-cell bacterial bioluminescent biosensors for the preliminary evaluation of the antimicrobial activity of aqueous and ethanol extracts derived from raw materials of medicinal plants.

METHODOLOGY

This study assessed the antibacterial activity of extracts from seventeen plant species including *Echinacea purpurea* (L.) Moench, *Echinacea pallida* (Nutt.). Nutt., *Echinacea angustifolia* A.Heller, *Echinacea tennessesnsis* (Beadle) Small, *Calendula officinalis* L.*, Coreopsis grandiflora* Hogg ex Sweet, *Hyssopus officinalis* L., *Monarda fistulosa* L., *Monarda didyma* L., *Monarda* x *hybrida* hort., *Myrtus communis* cv. Yuzhnoberezhny, *Satureja montana* L.*, Thymus serpyllym* L., *Thymus vulgaris* cv. Fantasia, *Thymus striatus* cv.Yubileynyy, *Rosmarinus officinalis* cv. Gorizont, *Vitex agnus-castus* L. These species were harvested within the territory of the Federal State Budgetary Institution "Nikitsky Botanical Garden – National Scientific Center of the Russian Academy of Sciences" in Yalta, Republic of Crimea, Russia. Aqueous and ethanol extracts of these plant species were obtained following established pharmacopoeial methods for tinctures and decoctions[16]. Biosensors used for the testing of antimicrobial activity of plant extracts included naturally ccurring bioluminescent strain of *Aliivibrio fischeri* F1 from the collection of the Institute "S.I. Georgievsky Medical Academy" FSAOU VO "V.I. Vernadsky CFU", and genetically engineered luminescent strain of *Escherichia coli* MG1655 pXen7[17-18]. Bacterial strain cultivation and inoculum preparation were carried out in accordance with previously described techniques[18-20]. To assess the functionality of the bacterial bioluminescent strains, ethanol (OAO Flora Kavkaza, RF), quercetin (Quercetin >95%, Sigma-Aldrich), and zinc sulfate (LenReaktiv, Russia) was used as positive controls in the study.

Ethanol solutions were prepared at a 70% concentration, similar to the ethanol concentration used for the preparation of herbal tinctures. An ethanol solution of quercetin was prepared by dissolving quercetin powder in 70% ethyl alcohol to achieve a concentration of 10 mg/mL. A zinc sulfate solution was prepared by dissolving it in distilled water to reach a concentration of 0.175 mg/mL[21-22]. The assessment of antibacterial activity was conducted in accordance with established eco-toxicity testing standards[23], which, notably, demonstrated remarkable efficacy in evaluating the antimicrobial properties of substances from diverse sources, including those of plant origin[24-26]. The testing was conducted as follows: Aqueous solutions of sodium chloride at concentrations of 3% and 1% were prepared for *A. fischeri* F1 and *E. coli* pXen7, respectively, and dispensed into the bioluminometer cuvettes in volumes of 950, 940, 930, and 910 μL. To these sodium chloride solutions, samples of plant extracts were added in quantities of 10, 20, and 40 μL, resulting in dilutions of 1:25, 1:50, and 1:100, respectively. Positive control samples contained solutions of quercetin, ethanol, and zinc sulfate in the same volumes as the tested plant extracts. The negative control consisted of suspensions of bacterial cultures in sodium chloride solutions, excluding the test samples. The resulting systems were thoroughly mixed at 100 rpm for 15 minutes using an orbital shaker (OS-20, biosan, Latvia) to ensure an even distribution of substances in the sample. After that, 50 μL of bacterial suspension was added with a cell concentration corresponding to 0.5 McFarland turbidity standard. The prepared samples were incubated at 25°C and 37°C in a thermostat (TCO -1/80 SPU, Russia) for *A. fischeri* F1 and *E. coli* pXen7, respectively, for 30 minutes with constant stirring, after which the intensity of bioluminescence of the systems was measured using a biochemiluminometer (BHL-06, Nizhny Novgorod, Russia). The results of measuring the bioluminescence of the test strains were presented as the bioluminescence intensity index (I), which was calculated by the formula: $I = Io/Ic \times 100\%$ (expressed as a percentage), where Io – is the luminescence intensity of the test strain in the test sample after a certain time of incubation (30 min), and Ic – is the intensity luminescence of the test strain in the control sample after a certain time of incubation (30 min)[21,26]. The antimicrobial activity of plant extracts was assessed by the effective dilutions of the plant extracts, which reduced the luminescence of microorganisms by 50% (ED_{50}). Statistical processing of the research results was carried out in accordance with the pharmacopoeial standards “Statistical processing of experimental results” using Microsoft Excel 2003.

RESULTS and DISCUSSION

The sensitivity evaluation of *A. fischeri* F1 and *E. coli* pXen7 to quercetin, ethanol, and zinc sulfate demonstrated that both strains exhibited sensitivity to all tested agents, displaying a dose-dependent response. However, a difference in sensitivity was distinguished between the natural strain, *A. fischeri* F1 (Figure 1), and the genetically engineered strain, *E. coli* pXen7 (Figure 2), with the natural strain showing higher sensitivity to the tested agents. The minimum concentration of zinc sulfate solution required to inhibit bioluminescence by 50% in both *A. fischeri* F1 and *E. coli* pXen7 strains was 0.0035 mg/mL. In contrast, *A. fischeri* F1 strain showed greater sensitivity to ethanol solution, inhibiting bioluminescence at a dilution of 1:25 (corresponding to a 2.8% concentration in the sample). Ethanol solution caused a slight dose-dependent inhibition of *E. coli* bioluminescence, but none of the used in the study concentrations reduced it by 50% or more. Notably, *A. fischeri* F1 strain exhibited significantly higher sensitivity to the quercetin solution, with complete inhibition of luminescence starting from a minimum tested concentration of 0.1 mg/mL. In comparison, the same concentration of quercetin inhibited bioluminescence in *E. coli* pXen7 by 51.43%, without a significant dose-dependent increase within the applied concentrations in the experiment.

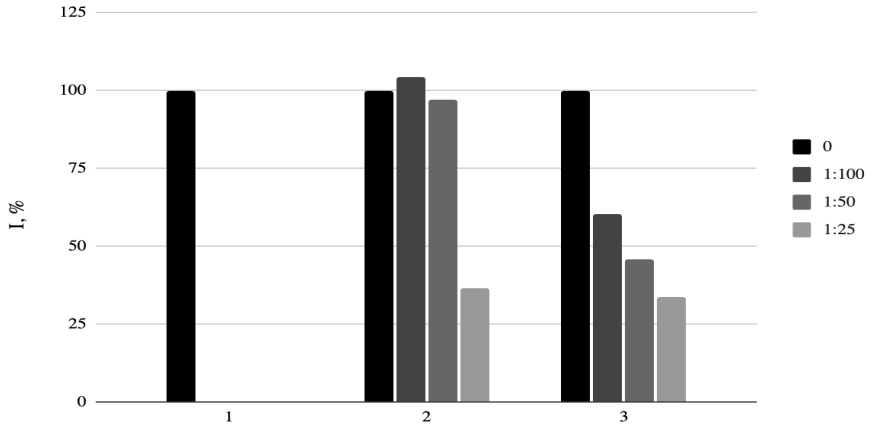

1- quercetin solution 10 mg/mL, 2- ethanol solution 70%, 3- zinc sulfate solution 0.175 mg/mL. I-bioluminescence intensity index, calculated by the formula: I = Io/Ic × 100%, where Io – is the luminescence intensity of the test strain in the test sample, and Ic – the bioluminescence intensity of the test strain in the negative control sample.

Figure 1. The effect of different concentrations of quercetin, ethanol and, zinc sulfate solutions on the bioluminescence of *A. fischeri* F1 strain

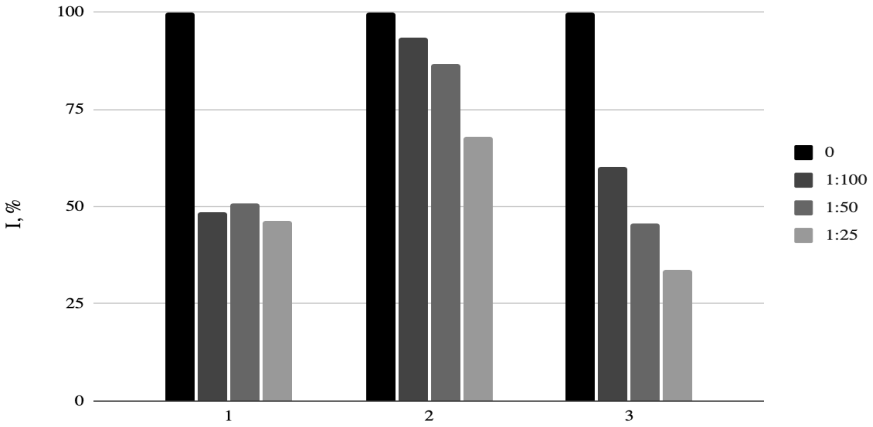

1- quercetin solution 10 mg/mL, 2- ethanol solution 70%, 3- zinc sulfate solution 0.175 mg/mL. I-bioluminescence intensity index, calculated by the formula: I = Io/Ic × 100%, where Io – is the luminescence intensity of the test strain in the test sample, and Ic – the bioluminescence intensity of the test strain in the negative control sample

Figure 2. The effect of different concentrations of quercetin, ethanol, and zinc sulfate solutions on the bioluminescence of *E. coli* pXen7 strain

The next step involved utilizing natural and genetically engineered bioluminescent biosensors to evaluate the antibacterial properties of aqueous and ethanol plant extracts. The assessment of the effects of aqueous plant extracts on the bioluminescence of the natural marine strain *A. fischeri* F1 revealed that extracts from *E. purpurea, E. pallida, E. angustifolia, E. tennessesnsis, C. officinalis*, and *Vítex agnus-castus* did not reduce the luminescence intensity of the test strain by more than 50% at a minimum dilution of 1:25 (Figure 3).

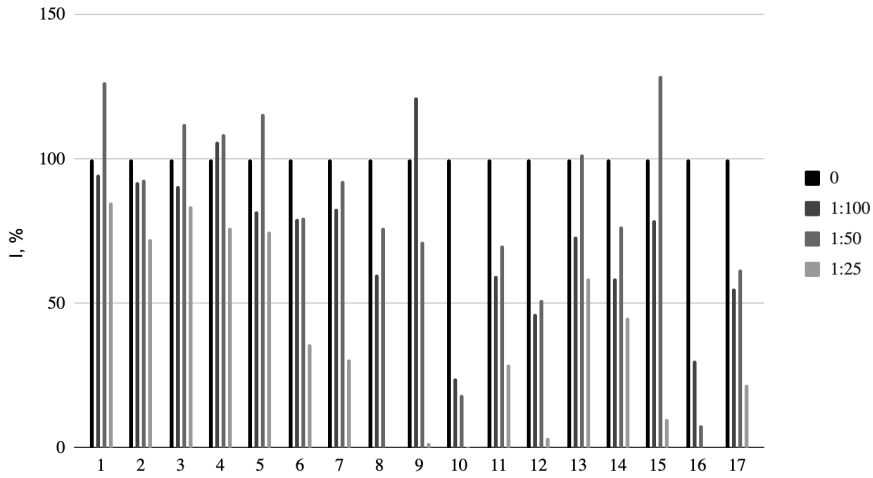

1– *E. purpurea* (L.) Moench; 2– *E. pallida* (Nutt.). Nutt.; 3– *E. angustifolia* A.Heller; 4– *E. tennessesnsis* (Beadle) Small; 5– *Calendula officinalis* L.*;* 6– *Thymus serpyllym* L.; 7– *Satureja montana* L.*,* 8– *Monarda fistulosa* L.; 9– *Myrtus communis* cv. Yuzhnoberezhny; 10– *Coreopsis grandiflora* Hogg ex Sweet; 11– *Rosmarinus officinalis* cv. Gorizont; 12 – *Thymus vulgaris* L.; 13– *Vítex agnus-castus* L.*,* 14– *Hyssopus officinalis* L.; 15– *Monarda didyma* L.; 16– *Monarda* x *hybrida* hort.; 17– *Thymus striatus* cv. Yubileynyy. I- bioluminescence intensity index, calculated by the formula: I = Io/Ic × 100%, where Io – is the luminescence intensity of the test strain in the test sample, and Ic – the bioluminescence intensity of the test strain in the negative control sample.

Figure 3. The effect of different dilutions of aqueous plant extracts on the bioluminescence of *Aliivibrio fischeri* F1

Aqueous extracts of *T. serpyllym*, *S. montana*, *M. fistulosa*, *M. communis* cv. Yuzhnoberezhny; *R. officinalis* cv. Gorizont, *Hyssopus officinalis*, *Monarda didyma* и *Thymus striatus* cv. Yubileynyy reduced the intensity of bioluminescence by 50% or more at a dilution of 1:25. Aqueous extracts of *C. grandiflora*, *T. vulgaris* cv. Fantasia and *Monarda* x *hybrida* hort. Inhibited the bioluminescence of the *A. fischeri* F1 strain by 50% or more at the highest dilution of 1:100. As a result of the testing of the ethanol extracts, it was found that all the extracts were inhibiting the intensity of bioluminescence of *A. fischeri* F1 by 50% or more (Figure 4). At the same time, ethyl alcohol in similar dilutions did not reduce bioluminescence intensity by more than 35.64% of the control values.

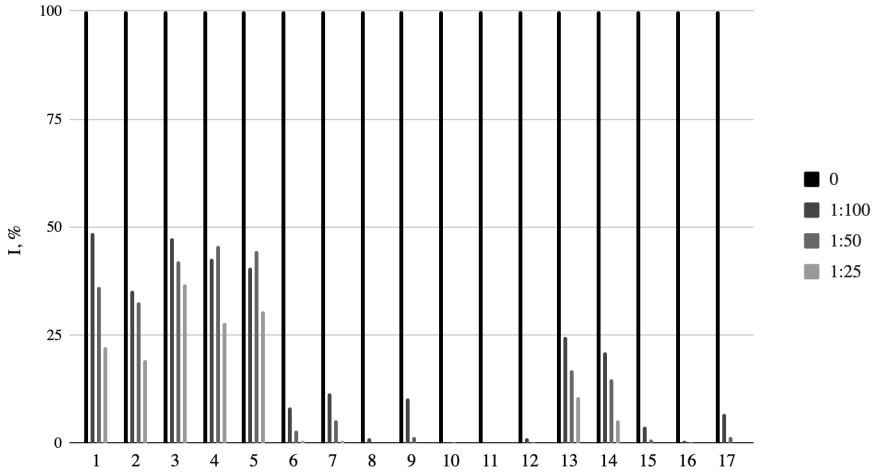

1– *Echinacea purpurea* (L.) Moench; 2– *Echinacea pallida* (Nutt.). Nutt.; 3– *Echinacea angustifolia* A.Heller; 4– *Echinacea tennessesnsis* (Beadle) Small; 5– *Calendula officinalis* L.*;* 6– *Thymus serpyllym* L.; 7– *Satureja montana* L.*,* 8– *Monarda fistulosa* L.; 9– *Myrtus communis* cv. Yuzhnoberezhny; 10– *Coreopsis grandiflora* Hogg ex Sweet; 11– *Rosmarinus officinalis* cv. Gorizont; 12– *Thymus vulgaris* cv. Fantasia; 13– *Vítex agnus-castus* L.; 14– *Hyssopus officinalis* L.; 15– *Monarda didyma* L.; 16– *Monarda* x *hybrida* hort.; 17– *Thymus striatus* cv. Yubileynyy. I- bioluminescence intensity index, calculated by the formula: I = Io/Ic × 100%, where Io – is the luminescence intensity of the test strain in the test sample, and Ic – the bioluminescence intensity of the test strain in the negative control sample.

Figure 4. The effect of different dilutions of ethanol plant extracts on the bioluminescence of *Aliivibrio fischeri* F1

Ethanol extracts of *T.serpyllym*, *S. montana*, *M. fistulosa*, *M. communis* cv. Yuzhnoberezhny, *C. grandiflora*, *R. officinalis*, *T. vulgaris*, *Vítex agnus-castus*, *H. officinalis*, *M. didyma*, *Monarda* x *hybrida* hort., *T. striatus* cv. Yubileynyy was reducing bioluminescence intensity by more than 75% at a maximum dilution of 1:100. When comparing the complete dataset of the effect of aqueous and alcohol extracts on the *A. fischeri* F1 test strain, a moderate linear positive correlation was observed with a Pearson correlation coefficient of 0.65. This finding suggests a general similarity in the effects of aqueous and ethanol extracts from plants. However, it is important to note that differences were identified in the overall action of the components extracted using different solvents. For instance, it was determined that ethanol extracts from *E. purpurea*, *E. pallida*, *E. Angustifolia, E. tennessesnsis, C. grandiflora*, *T. vulgaris*

cv. Fantasia had no considerable difference in effect with the aqueous extracts of these plants. For alcohol extracts of *E. purpurea*, *E. pallida*, *E. angustifolia*, *E. tennessesnsis*, ED_{50} was only 1:25, which indicates their low antimicrobial potential in both aqueous and alcohol forms. The activity of *C. grandiflora*, *T. vulgaris* cv. Fantasia was up to 4 times more both in alcohol and aqueous forms, their ED_{50} was 1:100, which indicates their higher antimicrobial potential. The differences were found in the action of aqueous and ethanol extracts from *C. officinalis, T.serpyllym*, *S. montana*, *M. fistulosa*, *M. communis* cv. Yuzhnoberezhny, *R. officinalis* cv. Gorizont, *Vítex agnus-castus, H. officinalis*, *M. didyma* и *M.* x *hybrida* hort., *T. striatus* cv. Yubileynyy. Ethanol extracts of these plants inhibited bioluminescence up to 4 times more than aqueous extracts. The ED_{50} of alcohol extracts was 1:100, and of aqueous extracts – 1:25.

As a result of studies on the effect of aqueous plant extracts on the bioluminescence of *E. coli* pXen7, it was found that aqueous extracts of *E. purpurea*, *E. pallida*, *E. angustifolia*, *E. tennessesnsis*, *C. officinalis*, *T. serpyllym*, *S. montana,* and *M. communis* cv. Yuzhnoberezhny did not reduce bioluminescence intensity by more than 50% at a minimum dilution of 1:25 (Figure 5). Aqueous extracts from *M. fistulosa*, *R. officinalis* cv. Gorizont, *Vítex agnus-castus*, *H. officinalis*, *M.* x *hybrida* hort., and *T. striatus* cv. Yubileynyy reduced bioluminescence genetically engineered test strain by 50% or more at a dilution of 1:25. Aqueous extracts from *T. vulgaris* cv. Fantasia, *M. didyma*, reduced bioluminescence intensity at ED_{50} = 1:50 and only an aqueous extract from *C. grandiflora* inhibited the bioluminescence of the *E. coli* pXen7 at a dilution of 1:100.

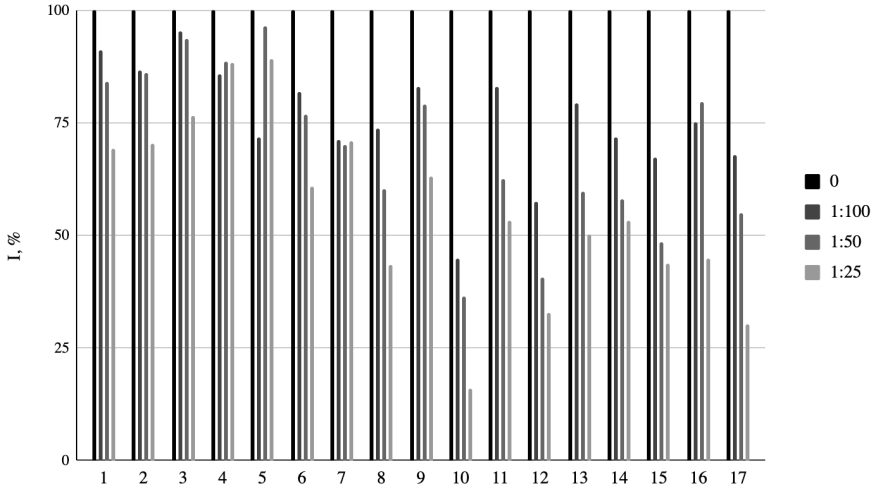

1– *Echinacea purpurea* (L.) Moench; 2– *Echinacea pallida* (Nutt.). Nutt.; 3– *Echinacea angustifolia* A.Heller; 4– *Echinacea tennessesnsis* (Beadle) Small; 5– *Calendula officinalis* L.*;* 6– *Thymus serpyllym* L.; 7– *Satureja montana* L.*;* 8– *Monarda fistulosa* L.; 9– *Myrtus communis* cv. Yuzhnoberezhny; 10– *Coreopsis grandiflora* Hogg ex Sweet; 11– *Rosmarinus officinalis* cv. Gorizont; 12– *Thymus vulgaris* cv. Fantasia; 13– *Vítex agnus-castus* L.*;* 14– *Hyssopus officinalis* L.; 15– *Monarda didyma* L.; 16– *Monarda* x *hybrida* hort.; 17– *Thymus striatus* cv. Yubileynyy. I- bioluminescence intensity index, calculated by the formula: I = Io/Ic × 100%, where Io – is the luminescence intensity of the test strain in the test sample, and Ic – the bioluminescence intensity of the test strain in the negative control sample.

Figure 5. The effect of different dilutions of aqueous plant extracts on the bioluminescence of *Escherichia coli* pXen7 strain

As a result of testing of ethanol extracts on the bioluminescence of the *E. coli* pXen7 strain, it was found that 15 extracts reduced intensity of bioluminescence by 50% or more at a maximum dilution of 1:100, and only *E. angustifolia* and *C. officinalis* reduced I at ED_{50} = 1:50, and the alcohol extract from *E. purpurea* was characterized by ED_{50} = 1:25, despite the fact that alcohol in similar dilutions did not reduce bioluminescence by more than 8.69% of the control values (Figure 6).

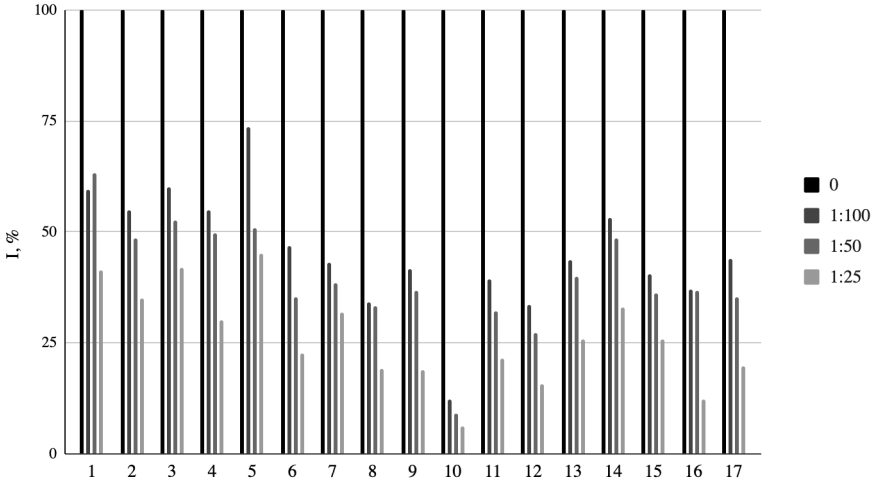

1– *Echinacea purpurea* (L.) Moench; 2– *Echinacea pallida* (Nutt.). Nutt.; 3– *Echinacea angustifolia* A.Heller; 4– *Echinacea tennessesnsis* (Beadle) Small; 5– *Calendula officinalis* L.*;* 6– *Thymus serpyllym* L.; 7– *Satureja montana* L.*;* 8– *Monarda fistulosa*; 9– *Myrtus communis* cv. Yuzhnoberezhny; 10– *Coreopsis grandiflora* Hogg ex Sweet; 11– *Rosmarinus officinalis* cv. Gorizont,

12– *Thymus vulgaris* cv. Fantasia; 13– *Vitex agnus-castus* L.*;* 14– *Hyssopus officinalis* L.; 15– *Monarda didyma* L.; 16– *Monarda* x *hybrida* hort.; 17 – *Thymus striatus* cv. Yubileynyy. I – bioluminescence intensity index, calculated by the formula: I = Io/Ic × 100%, where Io – is the luminescence intensity of the test strain in the test sample, and Ic – the bioluminescence intensity of the test strain in the negative control sample.

Figure 6. The effect of different dilutions of ethanol plant extracts on the bioluminescence of *Escherichia coli* pXen7 strain

A moderate linear positive correlation (Pearson correlation coefficient = 0.78) was observed when comparing the effects of aqueous and ethanol extracts on the test strain *E. coli* pXen7. This suggests a general similarity in the results, although the differences were noted between the effects of the two extract types. For example, when evaluating the effect of alcohol and aqueous extracts on the luminescence of the test strain *E. coli* pXen7, it was found that when using 70% ethyl alcohol as a solvent, the ED_{50} value for *E. purpurea, E. pallida*, *E. angustifolia*, *E. tennessesnsis, C. officinalis* increased to 1:100 compared to aqueous extracts, for *T. serpyllym* increased to 1:50. For *M. fistulosa*, *R. officinalis* cv. Gorizont, *V. agnus-castus, M.* x *hybrida* hort.*, T. striatus* cv. Yubileynyy ED_{50} has changed from 1:25 to 1:100. The strength of the effect has not changed for *C. grandiflora a*nd *H. officinalis*. ED_{50} for *T. vulgaris* cv. Fantasia and *M. didyma* became 1:100. And only for *S. montana* and *M. communis* cv. Yuzhnoberezhny ED_{50} change occurred up to 1:100. The data obtained confirm that ethanol is more optimal for extracting the amount of substances with antimicrobial activity. When the overall data on the effect of aqueous extracts on the *A. fischeri* F1 test strain and the *E. coli* pXen7, strain were compared, a moderate linear direct correlation with a Pearson correlation coefficient of 0.67 was obtained. This indicates that the results obtained from both strains were similar. When comparing the data on the effect of alcohol extracts on the test strain *A. fischeri* F1 and the strain *E. coli* pXen7, a moderate linear direct correlation was established with a Pearson correlation coefficient of 0.77, which indicates that both strains were similarly more sensitive to the action of ethanol extracts of plants then aqueous.

The experimental results are supported by literature data regarding the activity of the plants tested in the experiment. For instance, Echinacea, which extracts have not shown high inhibitory activity in the experiments, is known to contain polysaccharides and hydroxycinnamic acids as the main bioactive compounds. When using water as a solvent, the proportion of polysaccharides is 72%, and hydroxycinnamic acids 53% in the samples. When water-alcohol

mixtures are used as a solvent, 77% of polysaccharides and 46% of hydroxycinnamic acids are extracted[27]. Therefore, the choice of the solvent can considerably impact the activity of the plant extract. Echinacea purpurea extracts, the main action of which is immunomodulatory[28], according to modern scientific studies, inhibit the growth of *Candida albicans, Saccharomyces cerevisiae, Streptococcus pyogenes, Haemophilus influenzae*, *Legionella pneumophila*. However, many pathogens such as *Acinetobacter baumannii, Bacillus cereus, Bacillus subtilis, Enterococcus faecalis, Aspergillus niger, Escherichia coli, Klebsiella pneumoniae*, *Pseudomonas aeruginosa,* and *Candida albicans* were found to be insensitive to Echinacea preparations[29]. The Coreopsis extracts have demonstrated a significant inhibitory effect on bacterial luminescence in both aqueous and alcohol forms. This outcome can be attributed to the presence of phenolic compounds and phlavonoids, including chalcones, aurones, anthocyanins, flavanones, flavonols, and phenylpropanoids within *C. grandiflora*, which are found to possess diverse pharmacotherapeutic properties, such as antioxidant, antibacterial, antiviral, and anti-inflammatory[30]. Flavonoids' antibacterial mechanism of action involves forming complexes with bacterial cell walls. Additionally, flavonoids that are highly lipophilic have the capacity to disrupt bacterial membranes. The most common flavonoid – quercetin, which is also present in Coreopsis grandiflora has shown high inhibitory activity against Streptococcus pyogenes, and mild activity against various Gram-positive and Gram-negative bacteria. Its mechanism of action includes the inhibition of biofilm and Beta-lactamase formation. The average minimum inhibitory concentration (MIC) of quercetin is reported to be 58.7 μg/mL[31-33]. According to the research data Coreopsis extracts exhibit high activity against pathogenic flora, with *Enterococcus faecalis* and *Bacillus cereus* being the most sensitive[33].

High inhibitory activity in both aqueous and ethanol forms was noted for *T. vulgaris* cv. Fantasia, with an ED50 of 1:50 for the aqueous extract and 1:100 for the alcohol extract. While *T. serpyllym* produced a significant inhibitory effect only in the ethanol form, ED_{50} = 1:100. Thyme is approved for use as an antimicrobial, antiseptic, antifungal, expectorant, enveloping, antispasmodic, and reducing gas formation in the intestine. In plants of the genus *Thymus* L., the main active substances are phenolic compounds, essential oils, and triterpene compounds. The difference in the manifested biological effects is confirmed by the data on the chemical composition of these species. It has been reported that most of the thyme species are superior to *T. serpyllym* in terms of the total content of essential oil[34]. The MIC of the thymol, the major component of Thyme species, varies from 2-10 μg/mL[35]. Calendula flowers

are used in official medicine as an anti-inflammatory agent for diseases of the gastrointestinal tract, kidneys, and urinary tract[36]. Carotenoids and polysaccharides are the major components of Calendula flowers; its aqueous extract's major components are flavonoids and saponins, and alcohol extracts contain alkaloids, flavonoids, and saponins[37]. 70% ethanol extracts of *Calendula officinalis* had a strong inhibitory effect on bacterial luminescence with ED_{50} = 1:100, while aqueous extracts had no inhibitory effect even at a minimum dilution of 1:25. This effect can be explained by the fact that 70% ethanol solution is considered to be more suitable for extracting the sum of flavonoids contained in calendula flowers[38].

The main biologically active compounds of the investigated species of the genus *Monarda* are thymol, carvacrol, paracymol, and their derivatives[39]. The known biological activity of these compounds against pathogens is consistent with the traditional use of *Monarda* L. species for the treatment of wounds, skin infections, colds, and fevers. The significant antibacterial activity of *Monarda* species is supported by literature data[40]. According to the study's findings, the species *Monarda x hybrida* hort., which belongs to the chemotype with a higher content of geraniol, demonstrated stronger activity among the *Monarda* samples tested. *Satureja montana* (savory) contains as main components terpenes and terpenoids, which are known to play a key role in antibacte'©al action. Studies have shown that savory extracts are active against both Gram-positive (*Listeria monocytogenes*, *Staphylococcus aureus*, *Staphylococcus haemolyticus*) and Gram-negative (*Escherichia coli*, *Klebsiella pneumoniae*, *Pseudomonas aeruginosa* и *Serratia marcescens*) bacterial strains[41]. The primary constituents of *V. agnus-castus*are are essential oils with a predominance of 1,8-cineol and α-pinene, flavonoids, iridoids, diterpenoids, and steroids[42].

Vtex is currently utilized as a dietary supplement for estrogen hormone imbalances. A number of studies have noted a high antibacterial activity of *V. agnus-castus*, including antibiotic-resistant strains of *Pseudomonas aeruginosa* and *Escherichia coli*[43]. The literature review on the biologically active components of Hyssopus showed the presence of polyphenolic compounds, primarily flavonoids, apigenin, quercetin, diosmin, luteolin, and their glucosides, followed by other phenolic compounds, such as chlorogenic, protocatechin, ferulic, syringic, p-hydroxybenzoic and caffeic acid. In essential oils isolated from the aerial part of *H. officinalis*, several major components have been identified, including the terpenoids pinocamphone, isopinocamphone, and β-pinene. Hyssop has moderate antioxidant and antimicrobial activity against gram-positive and negative bacteria, as well as antifungal, insecticidal, and antiviral properties *in*

vitro. This plant has been found in animal experiments to exhibit muscle relaxant, antiplatelet, and alpha-glucosidase inhibitory properties[44-45].

Summarising the experimental data, it can be concluded that both strains displayed sensitivity to individual substances and plant extracts in the form of tinctures and decoctions. The natural bacterial strain A. *fischeri* F1 exhibited higher sensitivity to both aqueous and ethanol plant extracts compared to the recombinant strain *E. coli* pXen7, although the data on the effect of plant extracts correlated between the two strains. The study specifically identified extracts from *C. grandiflora*, *T. vulgaris* cv. Fantasia, and *M. x hybrida* hort as having the strongest inhibitory effect (ED_{50} = 1:100) in the forms of decoctions and tinctures. Extracts from *T. serpyllym, S. montana, M. fistulosa, M. communis* cv. Yuzhnoberezhny, *R. officinalis* cv. Gorizont, *H. officinalis, M. didyma, T. striatus* cv. Yubileynyy, and *Vitex agnus-castus* showed moderate inhibitory activity (ED_{50} = 1:25 to 1:100). *E. purpurea, E. pallida, E. angustifolia,* and *E. tennessesnsis* exhibited weak inhibitory activity with minimal ED_{50} values ranging from 1:25 to 1:50. Notably, the inhibitory activity of most plant extracts was enhanced when using 70% ethanol as a solvent. However, their inhibitory activity exceeded that of the 70% ethanol solution at the same dilutions. These findings align with the literature data, further affirming the confirmation of the validity of the obtained results.

Overall, the investigation demonstrated the potential of whole-cell bacterial bioluminescent biosensors for evaluating the antimicrobial activity of aqueous and ethanol extracts from medicinal plant raw materials, with *A. fischeri* F1 strain exhibiting higher sensitivity and the ability to detect variations in the antibacterial action of different plant species.

STATEMENT OF ETHICS

This study did not involve experiments on animals or humans, and, therefore, ethical approval was not required. Nevertheless, the research methods employed adhered to ethical standards, ensuring data integrity, compliance with professional codes of conduct, and adherence to institutional policies regarding research practices.

CONFLICT OF INTEREST STATEMENT

The authors declare no conflict of interest.

AUTHOR CONTRIBUTIONS

Yuliia Yu Havrychenko designed and carried out the experimental work and wrote the article with support from Andrei M. Katsev. Andrei M Katsev super-

vised the findings of this work and contributed to the final manuscript. Sergei L Safronyuk contributed to the analysis of the results. Dhruv Vashisht contributed to sample preparation and designed the figures.

FUNDING SOURCES

This work was supported by the Russian Science Foundation, Project No 22-25-20206, https://rscf.ru/en/project/22-25-20206/.

ACKNOWLEDGMENTS

The plant extract samples utilized in this scientific article were acquired from the Federal State Budgetary Institution "Nikitsky Botanical Garden – National Scientific Center of the Russian Academy of Sciences," situated in Yalta, Republic of Crimea, Russia. We extend our gratitude to O. M. Shevchuk, L.A. Logvinenko, and S.A. Feskov for their valuable contributions in obtaining these samples from the garden's location at Nikitsky descent 52, town of Nikita. Their assistance greatly enriched the scope and quality of our research.

REFERENCES

1. Oyebode O, Kandala NB, Chilton PJ, Lilford RJ. Use of traditional medicine in middle-income countries: a WHO-SAGE study. Health Policy Plan, 2016;31(8):984-991. Doi: 10.1093/heapol/czw022

2. Fabricant DS, Farnsworth NR. The value of plants used in traditional medicine for drug discovery. Environ Health Perspect, 2011;109(1):69-75. Doi:10.1289/ehp.01109s169

3. National Action Plans and Monitoring and Evaluation, Surveillance, Prevention and Control. Global action plan on antimicrobial resistance. 2015. Available from: https://www.who.int/en/news-room/fact-sheets/detail/antimicrobial-resistance

4. Cowan MM. Plant products as antimicrobial agents. Clin Microbiol Rev, 1999;12(4):564-582. Doi: 10.1128/cmr.12.4.564

5. Balouiri M, Sadiki M, Ibnsouda SK. Methods for in vitro evaluating antimicrobial activity: a review. J Pharm Anal, 2016;6(2):71-79. Doi: 10.1016/j.jpha.2015.11.005

6. State Pharmacopoeia of the Russian Federation XIV edition. OFS.1.2.4.0010.15. Available from: https://pharmacopoeia.ru/ofs-1-2-4-0010-15-opredelenie-antimikrobnoj-aktivnosti-antibiotikov-metodom-diffuzii-v-agar/

7. Kotze M, Eloff JN. Extraction of antibacterial compounds from *Combretum microphyllum* (Combretaceae). S Afr J Bot, 2002;68:62-67. Doi: 10.1016/S0254-6299(16)30456-2

8. Eloff JN, Angeh IE, McGaw LJ. Solvent-solvent fractionation can increase the antifungal activity of a *Melianthus comosus* (Melianthaceae) acetone leaf extract to yield a potentially useful commercial antifungal product. Ind Crop Prod, 2017;110:103-112. Doi: 10.1016/j.indcrop.2017.11.014

9. Eloff JN. Avoiding pitfalls in determining antimicrobial activity of plant extracts and publishing the results. BMC Complement Med Ther, 2019;19:106. Doi: 10.1186/s12906-019-2519-3

10. Bolelli L, Ferri EN, Girotti S. The management and exploitation of naturally light-emitting bacteria as a flexible analytical tool: a tutorial. Anal Chim Acta, 2016;934:22-35. Doi: 10.1016/j.aca.2016.05.038

11. Poikulainen E, Tienaho J, Sarjala T, Santala V. A panel of bioluminescent whole-cell bacterial biosensors for the screening for new antibacterial substances from natural extracts. J Microbiol Methods, 2020;178:106083. Doi: 10.1016/j.mimet.2020.106083

12. Kovats N, Acs A, Goloncser F, Barabas A. Quantifying of bactericide properties of medicinal plants. Plant Signal Behav, 2011;6(6):777-779. Doi: 10.4161/psb.6.6.15356

13. Kotova Vyu, Ryzhenkova KV, Manukhov IV, Zavilgelsky GB. Inducible specific lux-biosensors for the detection of antibiotics: Construction and main parameters. Appl Biochem Microbiol, 2014;50:112-117. Doi: 10.1134/S0003683814010074

14. Thorn RM, Robinson GM, Reynolds DM. Comparative antimicrobial activities of aerosolized sodium hypochlorite, chlorine dioxide, and electrochemically activated solutions evaluated using a novel standardized assay. Antimicrob Agents Chemother, 2013;57(5):2216-2225. Doi: 10.1128/aac.02589-12

15. Safronjuk SL, Sharipov JT, Katsev AM. Identification of luminous bacteria isolated from the Black and the Azov seas. Aspirantskij vestnik Povolzh'ja. 2017;5(6):19-23. Available from: https://elibrary.ru/item.asp?id=35551502

16. State Pharmacopoeia of the Russian Federation XIV edition. OFS.1.5.1.0002.15. Available from: https://pharmacopoeia.ru/ofs-1-5-1-0002-15-travy/

17. Safronyuk SL, Gavrichenko YuYu, Katsev AM. Applicability of recombinant lux-biosensors for the identification of some antibacterial activity mechanisms of directly synthesized derivatives 2-((2-oxo-3-phenyl-2H-[1,2,4]triazino[2,3-c]quinazolin-6-yl)thio) acetic acid. Russ J Biopharm, 2020;12(5):26-32. Doi: 10.30906/2073-8099-2020-12-5-26-32

18. Safronyuk SL, Milova VV, Havrichenko YuYu, Katsev AM. Assessment of the applicability of primarily identified natural luminescent bacteria, isolated from the Azov and the Black seas, to determine the antimicrobial activity of antibiotics. Aspirantskiy Vestnik Povolzhiya, 2020;20(5-6): 175-183. Doi: 10.17816/2072-2354.2020.20.3.175-183

19. Safronyuk SL, Havrichenko YuYu, Katsev AM. Applicability of recombinant lux-biosensors for the identification of some antibacterial activity mechanisms of directly synthesized derivatives 2-((2-oxo-3-phenyl-2h-[1,2,4]triazino[2,3-c]quinazolin-6-yl)thio) acetic acid. Russ J Biopharm, 2020;12(5):26-32.

20. Safronyuk SL, Gavrichenko YuYu, Katsev AM. Applying of the Bioluminescent Bacteria for Estimation of Antibiotic Effects of Medicinal Preparations. Proceedings of Voronezh State University. Series: Systems Analysis and Information Technologies, 2018;(1):194-203. Available from: http://www.vestnik.vsu.ru/pdf/chembio/2018/01/2018-01-25.pdf

21. Kurvet I, Ivask A, Bondarenko O, Sihtmäe M, Kahru A. LuxCDABE—transformed constitutively bioluminescent *Escherichia coli* for toxicity screening: comparison with naturally luminous *Vibrio fischeri*. Sensors, 2011;11(8):7865-7878. Doi: 10.3390/s110807865

22. Menz J, Schneider M, Kümmerer K. Toxicity testing with luminescent bacteria–characterization of an automated method for the combined assessment of acute and chronic effects. Chemosphere, 2013;93(6):990-996. Doi: 10.1016/j.chemosphere.2013.05.067

23. ISO 11348-3:2007. Water quality — Determination of the inhibitory effect of water samples on the light emission of *Vibrio fischeri* (Luminescent bacteria test) — Part 1: Method using freshly prepared bacteria. Available from: https://www.iso.org/obp/ui/es/#iso:std:iso:11348:-3:ed-2:v1:en

24. Bazhenov SV, Novoyatlova US, Scheglova ES, Prazdnova EV, Mazanko MS, et al. Bacterial lux-biosensors: constructing, applications, and prospects. Biosens Bioelectron: X, 2023;(13)100323. Doi: 10.1016/j.biosx.2023.100323

25. Shukla DM, Bajwa V, Gajic D, Saxena PK. Quorum sensing inhibition in *Vibrio fischeri*: an efficient system to assess antibacterial properties of medicinal plants and their volatile compounds. Integr Food Nutr Metab, 2020;(7):1-9. Doi: 10.15761/IFNM.1000281

26. Peng Y, Wang Q, Zhu K, Ding W. Application of the Luminescent luxCDABE gene for the rapid screening of antibacterial substances targeting *Pseudomonas aeruginosa*. Foods, 2023;12(2):392. Doi: 10.3390/foods12020392

27. Maltseva VA, Tarasov VE. Development of an integrated technology for the processing of *Echinacea purpurea*. News of higher educational institutions. Food Technology, 2008;(4):57-59. Available from: https://cyberleninka.ru/article/n/razrabotka-kompleksnoy-tehnologii-pererabotki-ehinatsei-purpurnoy/viewer

28. Manayi A, Vazirian M, Saeidnia S. *Echinacea purpurea*: pharmacology, phytochemistry and analysis methods. Pharmacogn Rev, 2015;9(17):63-72. Doi: 10.4103/0973-7847.156353

29. Hudson JB. Applications of the phytomedicine *Echinacea purpurea* (Purple Coneflower) in infectious diseases. Biomed. Res Int, 2010;2012(8-9):563-568. Doi: 10.1155/2012/769896

30. Kumar S, Pandey AK. Chemistry and biological activities of flavonoids: an overview. Sci World J, 2013:162750. Doi: 10.1155/2013/162750

31. Shahzad M, Millhouse E, Culshaw S, Edwards CA, Ramage G, Combet E. Selected dietary (Poly)phenols inhibit periodontal pathogen growth and biofilm formation. Food Funct, 2015;6(3):719-729. Doi: 10.1039/C4FO01087F

32. Dey D, Ray R, Hazra B. Antimicrobial activity of pomegranate fruit constituents against drug-resistant *Mycobacterium tuberculosis* and β-lactamase producing *Klebsiella pneumoniae*. Pharm Biol, 2015;53(10):1474-1480. Doi: 10.3109/13880209.2014.986687

33. Cushnie TP, Lamb AJ. Antimicrobial activity of flavonoids. Int J Antimicrob Agents, 2005;26(5):343-356. Doi: 10.1016/j.ijantimicag.2005.09.002

34. Vinokurova OA, Trineeva OV, Slivkin AI. Comparative characteristics of different types of thyme: the composition, properties and application (review). Development and Registration of Medicines, 2016;4:134-150. Available from: https://www.pharmjournal.ru/jour/article/view/167/165?locale=en_US

35. Nikolić M, Glamočlija J, Ferreira CFR, Calhelha RC, Fernandes Â, Marković T, et al. Chemical composition, antimicrobial, antioxidant and antitumor activity of *Thymus serpyllum* L., *Thymus algeriensis* Boiss. And Reut and *Thymus vulgaris* L. essential oils. Ind Crops Prod, 2014;(52):183-190. Doi: 10.1016/j.indcrop.2013.10.006

36. Kurkin VA, Kurkina AV, Zaitseva EN, Dubischev AV, Afanaseva PV. Investigation of diuretic activity of phytopreparations of *Calendula officinalis* L. flowers. Bull Sib Med, 2016;15(2):51-57. Doi: 10.20538/1682-0363-2016-2-51-57

37. Kumar N, Sharma J, Sharma S. Pharmacognostical and phytochemical investigation of *Calendula officinalis*. J Adv Sci Res, 2010;1(1):61-66. Available from: https://sciensage.info/index.php/JASR/article/view/9

38. Dong J, Zhou K, Ge X, Xu N, Wang X, He Q, et al. Effects of extraction technique on the content and antioxidant activity of flavonoids from *Gossypium hirsutum* Linn. flowers. Molecules, 2022:27(17):5627. Doi: 10.3390/molecules27175627

39. Lawson SK, Satyal P, Setzer WN. The volatile phytochemistry of *Monarda* Species growing in South Alabama. Plants, 2021;10(3):482. Doi: https://doi.org/10.3390/plants10030482

40. Hong L, Tian Y, Fei-Yan L, Yan Y, Zhong-Min S. Antibacterial activity and mechanism of action of *Monarda punctata* essential oil and its main components against common bacterial pathogens in respiratory tract. Int J Clin Exp Pathol, 2014;7(11):7389-7398. Available from: https://pubmed.ncbi.nlm.nih.gov/25550774/

41. Maccelli A, Vitanza L, Imbriano A, Fraschetti C, Filippi A, Goldoni P, et al. *Satureja montana* L. Essential oils: chemical profiles/phytochemical screening, antimicrobial activity and O/W nanoemulsion formulations. Pharmaceutics, 2019;12(1):7. Doi: 10.3390/pharmaceutics12010007

42. Chen SN, Friese JB, Webster D, Nikolic D, Van Breemen RB, Wang ZJ, et al. Phytoconstituents from *Vitex agnus-castus* fruits. Fitoterapia, 2011;82(4):528-533. Doi: 10.1016/j.fitote.2010.12.003

43. Arokiyaraj S, Perinbam K, Agastian P, Mohan Kumar R. Phytochemical analysis and antibacterial activity of *Vitex agnus-castus*. Int J Green Pharm, 2009;3(2):162-164. Doi: 10.4103/0973-8258.54912

44. Fathiazad F, Hamedeyazdan S. A review on *Hyssopus officinalis* L.: composition and biological activities. Afr J Pharm Pharmacol, 2011;5(17):1959-1966. Doi: 10.5897/AJPP11.527

45. Renzini G, Scazzocchio F, Lu M, Mazzanti G, Salvatore G. Antibacterial and cytotoxic activity of *Hyssopus officinalis* L. oils. J Essential Oil Res, 1999;11(5):649-654. Doi: 10.1080/10412905.1999.9701232

Acta Pharm. Sci. Vol 62:(2), 2024
Research article
DOI: 10.23893/1307-2080.APS6224

HPLC investigation of hidden danger deoxynivalenol (vomitoxin) in baby foods from grain sources in Türkiye

Ozan Emre EYUPOGLU[1]*, Duygu YAZICIOGLU[2], Gizem Sena ELAGÖZ[3]
Mücteba Eşref TATLIPINAR[3], Gülden Zehra OMURTAG[4]

1 Department of Biochemistry, School of Pharmacy, Istanbul Medipol University, Istanbul, Türkiye
2 Deparment of Pharmaceutical Toxicology, School of Pharmacy, Istanbul Medipol University, Istanbul, Türkiye
3 Department of Pharmaceutical Toxicology, Faculty of Pharmacy, Istanbul University, Istanbul, Türkiye
4 Department of Pharmaceutical Toxicology, School of Pharmacy, Istanbul Medipol University, Istanbul, Türkiye

ABSTRACT

The Food and Agricultural Organization (FAO) declared that at minimum, one quarter of the earth's food supply is infected with mycotoxins. Deoxynivalenol (DON) is the most common *Fusarium* mycotoxin in maize, wheat, rice oats, and barley. The goal of this study is to explore the incidence of DON in cereal-based baby foods in Turkey by using high-performance liquid chromatography (HPLC) with C_{18} column and UV detector at 220 nm. The results were statistically significant ($p< 0.05$) in terms of standard deviation (in parallel analysis). The highest amount of detected DON in baby foods was 0.17 ppm. The samples with DON by HPLC were also confirmed with LC-MS detection (positive and negative mode). Forty-eight commercial cereal-based baby foods were analyzed, and four samples were contaminated (8.3%). DON analysis results show that baby foods containing cereal sources sold in Turkish markets are a significant threat for human health and baby health.

Keywords: deoxynivalenol (DON), LC-MS analysis, baby foods, mycotoxin

*Corresponding Author: Ozan Emre EYUPOĞLU
E-mail: oeeyupoglu@medipol.edu.tr
ORCIDs:
Ozan Emre EYUPOĞLU: 0000-0002-4449-0537
Duygu YAZICIOĞLU: 0000-0003-0787-0685
Gizem Sena ELAGÖZ: 0009-0009-5614-1877
Mucteba Eşref TATLIPINAR: 0000-0001-8422-3188
Gülden Zehra OMURTAG: 0000-0002-2018-9619
(Received 15 Sep 2023, Accepted 28 Sep 2023)

INTRODUCTION

Mycotoxins are easily affected raw materials used in foods, in both the pre-harvest and storage periods. Trichothecenes are produced by several types of fungi such as *Fusarium*, *Myrothecium*, *Trichoderma* and *Cephalosporium*. Deoxynivalenol (DON), commonly referred to vomitoxin, is widely dispersed trichothecene caused especially by *F. graminearium* and *F. culmorum*. The most widespread and frequently recognized mycotoxins that threaten human health are trichothecenes and fumonisins. DON occurs frequently in cereal-based foodstuffs. The possible influence of DON on human health may occur after the consumption of infected foodstuffs. Acute, chronic dietary admission of contaminated food is dangerous. The occurrence of DON in processed cereals and pulses in Turkey were previously researched in Omurtag and Beyoglu[1].

In Turkey, the most recent guideline for DON limits in baby infant supplemental foods is 0.2 ppm[2].

The increase in DON amounts in wheat products also occurs at harvest time since wheat cultivation, Good Agricultural Practices (GAPs) usage, mold strains, temperature, water activity, nutriment accessibility, uses synthesized methods. As is the case for every natural material, mycotoxins may be infected by mold and produce mycotoxins if the environmental conditions (e.g. temperature, moisture) are conducive to it. Human exposure may be through cereals or via animal-based foods (kidneys, liver, milk, eggs). DON's role in the infection is a result of *Tri5* gene disruption leading to a drop in wheat contamination since it cannot generate DON.

Mycotoxins accumulate within the membranes of vegetables, and cereals; then they negatively affect or impede human and animal functions. Studies indicate that temperature, water activity, and development time, have a clear influence on DON exhibition in *F. graminearum, F. culmorum,* as well as *F. meridionale*. The ideal temperature of DON is between 25 °C and 30 °C[3]. Llorens et al.[4], declared that *F. graminearum*, *F. culmorum* growth temperature is between 20 °C and 32 °C, and that fungal growth is reduced at temperatures below at 15 °C. For *F. graminearum,* minimum water activity for growth is 0.90 and the maximum limit is recorded as in excess of 0.99[5]. The highest water activity for DON occurred at 0.97 and 0.99 in wheat[6].

Subjection to trichothecenes is referred to in Southeast Asia as "yellow rain". DON, nivalenol, DAS (diacetoxyscirpenol) and T-2 toxin are parts of this airborne substance and can be detected in tissue, blood, and urine samples of sufferers. The above-mentioned toxins were found in many gastrointestinal

disease epidemics in China and India after the absorption of bread with infected flour, and in rice[7].

DON was proven to be the reason for vomiting (hence the term "vomitoxin"), under-nourishment, diminished weight gain, anorexia, and an impaired immune system. The symptoms described for DON in humans consist of abdominal pain, nausea, vomiting, dizziness, headache, throat irritation, diarrhea, and blood in the stool[7]. Effects on the immune system, especially on IgA were demonstrated with experimental animal studies. Humoral and cellular immunity, as well as a tendency for infectious diseases, were demonstrated in studies on experimental mice[8]. Reports of vomiting caused by the consumption of moldy cereal grains, even when baked into bread in the form of flour, have been reported for animals and humans since 1916 by numerous investigators in various parts of the world. The causative agents that had previously eluded detection were identified in a new trichothecene vomitoxin from corn contaminated in the field with *F. graminearum* by Vesonder et al.[9].

DNA damage in human hepatoma cells (Hep G2) via DON-influenced oxidative stress was shown by Stepanova et al.[10] who demonstrated that the temporary intrauterine subjection of DON results in its durable availability in piglets' plasma, causing the alteration of the body's immune system. DON impairs protein synthesis and is toxic for the body's immune system in a variety of animals, resulting in gastrointestinal diseases, lower growth, and a growing threat of contagious illness. The Codex Alimentarius Commission manages food sourced mycotoxins that are risky for people, have set the maximum tolerable levels (MTLs) of DON as 0.2 ppm of cereal-based foods for children. 1 ppm of flour, meal, semolina, or flakes sourced from wheat, maize or barley, 2 ppm of wheat, maize and barley for additional treatment can diminish levels of DON before usage within foods. The Food and Drug Administration (FDA) put the limit for DON in processed human food as 1 ppm. Health Canada set DON levels for wheat as 2 ppm for raw foods and 1 ppm for children's foodstuffs. The European Union (EU)'s DON standards are in line with the American and Canadian regulations. The Codex Alimentarius Commission (CAC) set the allowed limit as 2 ppm of DON in raw wheat, barley, and maize. EU countries are applying a 0.75 ppm DON limit in flour intended for raw materials for several years[5]. The European Union set the highest levels for DON as 0.2 ppm in infant and baby foodstuffs. The lowest limit of quantification (LOQ) is 0.2 ppm for DON for baby food in EU[11].

The NOAEL in the study with mice is 1 ppm feed, equal to 0.1 ppm b.w. / day[12]. In another trial, the results of DON on humoral and cellular defense systems in

mice was investigated; a 'no effect' level for immune system related outcomes in mice was demonstrated between 0.25 ppm and 0.50 ppm b.w. / day[13]. For single mycotoxins, the approximate daily subjection compared with the toxicological thresholds of mycotoxins without carcinogenic potency, i.e. tolerable daily intake (TDI) or highest tolerable daily intake (PMTDI) was: DON (TDI 1000 ng kg^{-1}.$bw.day^{-1}$)[14]. For DON, a tolerable daily intake (TDI) was shown as 1 μg DON / kg.bw/ day by the European Food and Safety Authority (EFSA) for people[11]. *Fusarium* toxin exposure in the diets of children and adults were assessed worldwide, but no data on baby foods and baby biscuits is available for DON in Turkey. This study will address the lack of data for the DON limitation in the healthy growth of those populations. The HPLC and clean-up procedures were adapted by Omurtag and Beyoglu[1].

LC-MS / MS development and validation were used for the coincident detection of *Fusarium* mycotoxins in single chromatographic runs in cereals and cereal-derived foods[15].

Pereira et al.[16] evaluated DON in processed cereal-based baby food by GC-MS. Scott et al.[17] first evaluated DON in wheat and grains by GLC-EC. DON in concentrations of 0.01-4.3 mg / g revised for recovery were reaffirmed in 15 positive samples by GLC-MS (SIM). Omurtag and Beyoglu[1] evaluated the incidence of DON in 83 processed cereals and pulses in Turkey and concluded that 6 out of 68 cereal contain significant amounts of DON, with the highest level being 2.67 ppm.

The objective of this research was to investigate the possible health risks of DON in baby foods while raising a healthy generation.

METHODOLOGY

Materials

All the baby food samples were purchased from stores and pharmacies from Istanbul, Turkey. Only 4 of 48 total samples were baby foods and the remaining of them were in the food supplement category with grain and fruit additives (Table 1). Each sample (1 kg) was blended by an Erwaka blender. A 50-g aliquot of 250 g subsample was taken for analysis and stored at -20°C until analysis.

Table 1. Deoxynivalenol in baby foods processed with cereal sources determined by HPLC

Samples From Turkey	Processed baby foods with cereals sources		
	DON by HPLC (positive / total)	DON level by HPLC (LOD-LOQ) (ppm)	Mean of DON (ppm)
Baby Food (A)	0/2[p]	-	-
Baby Food with Milk, Rice (B_1)	0/2[p]	-	-
Baby Food with Organic Grain Rice ©	½[m]	0.05-0.17	0.13*
Baby Food with Milk, Rice (B_2)	0/2[m]	-	-
Baby Food with Milk, Rice (B_3)	0/2[p]	-	-
Baby Food with Cereal (D_1)	½[m]	0.05-0.17	0.12*
Baby Food (D_2)	0/2[m]	-	-
Baby Food with Milk ©	0/2[m]	-	-
Baby Food with Milk, Biscuit (F)	0/2[p]	-	-
Baby Food with Milk, Honey, Semolina (G1)	½[p]	0.05-0.17	0.07*
Baby Food with Organic Grain, Oat (H)	0/2[m]	-	-
Baby Food with Grain, Fruit, Yogurt (J)	½[m]	0.05-0.17	0.17**
Baby Food with Organic Grain, Apple, Milk (K)	0/2[m]	-	-
Baby Food with Whole Grain with Milk (L)	0/2[p]	-	-
Baby Food with Milk, Five Fruits (M)	0/2[p]	-	-
Baby Food with Apple, Seven Grain (N)	0/2[p]	-	-
Baby Food with Milk, Banana, Apricot (O)	0/2[p]	-	-
Baby Food with Organic Grains (P)	0/2[m]	-	-
Baby Food with Milk, Fennel, Grains ©	0/2[m]	-	-
Baby Food with, Milky, Apple, Grains (S)	0/2[m]	-	-
Baby Food with Milk, Banana, Rice (T)	0/2[m]	-	-
Baby Food with Milk, Honey, Semolina (G_2)	0/2[m]	-	-
Baby Food with Milk, Pear (U)	0/2[p]	-	-
Baby Food with Milk, Honey, Semolina (G_3)	0/2[p]	-	-
A, C, E, F, H, J, K, L, M, N, O, P, R, S, T, U: Different brands' baby food samples' codes.			

B_1, B_2, B_3, D_1, D_2, G_1, G_2, G_3: Different brands with similar ingredients' codes

DON, deoxynivalenol; [m] received from retailer; [p] received from pharmacy, *: > LOD, **: =LOQ, >LOD.

Chemicals

All solvents were of high purity and were purchased from Carlo Erba (methanol) and Merck (acetonitrile), while the DON standard was purchased from Sigma-Aldrich. Ultra-pure water purified by an Elgaflex-3-Ultra-Purified Water Machine was used in all the solution preparation steps and HPLC separation.

Preparation of stock solutions

A DON stock standard solution was prepared as a 1 mg / mL concentration in acetonitrile and from this stock solution, the 40 ng / mL mother liquor, which served as a source for dilutions, was diluted to 5 different concentrations with a methanol: water (20:80 v/v) mixture, and standard solutions of the calibration chart for HPLC analysis were created with them.

Sample preparation

After baby food samples (50 g) were blended with acetonitrile: aqua (21:4 v/v), a suspension mixture was decanted by a filtering process with Whatman no:4. The filtrate was evaporated with a vacuum dryer under inert atmosphere at 60°C. After sample extracts were dissolved acetonitrile: aqua (21:4 v/v), they were loaded to Alumina–Celite–Charcoal clean-up disposable column for stabilizing the DON composition. After collecting the elations, they were evaporated with inert vacuum atmosphere at 60°C (Extract A)[18].

HPLC procedure

Extract A was solved with a methanol: aqua (20:80 v/v) solution mixture (1 mL). After it was filtered to vials with IsoLab Syringe filters (cellulose acetate 0.22 μm) PVDF cartridge, vial samples (50 μL) were auto injected to the HPLC system from a 100-vial tray into an autosampler unit. For the calibration graph, diluted DON standards of five different concentrations (3-40 ng / mL) were qualitatively and quantitatively analysed for 15 min in triplicate with HPLC. DON was detected at retention time of 6.2 min at UV 220 nm. Detected DON contents were verified with further LC-MS analysis on negative and positive mass fragment mode (Figure 1). All of the peak areas from standards and samples were recorded for quantitative analysis. Concentrations of baby food samples were calculated with the linear equation obtained from the calibration graph ($y = 2.402x + 3.416$ (r= 0.9770))[18]. The detection limits of DON contents at baby foods were found to be 3 times and 10 times of mean standard deviation of noise. The method linearity was measured as of 0.05-3 ppm in recognized DON compounds. Chemwindow detection limit analysis data were found to be highly significant.

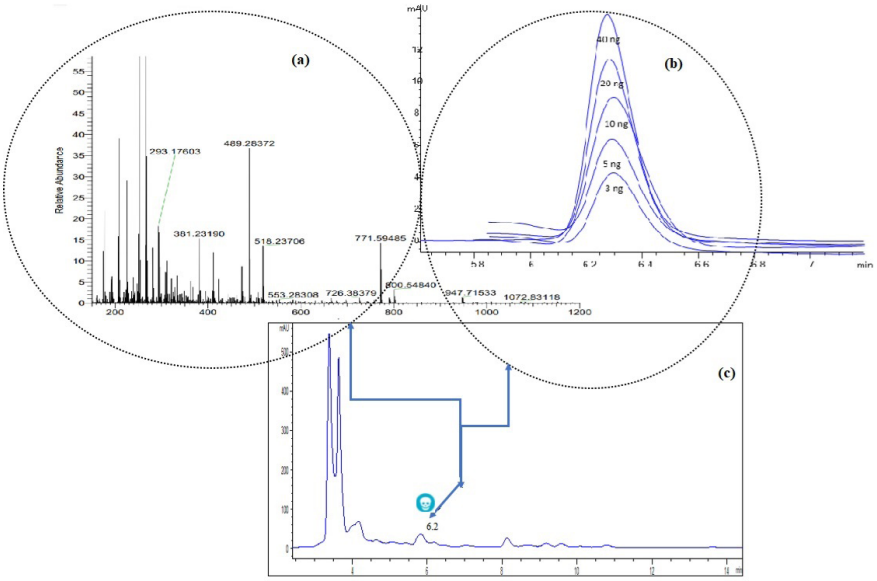

Figure 1. (a): DON chromatogram with MS, (b): Overlapped peaks for DON standards (3-40 ng), (c): DON detected in baby food samples' UV chromatogram (0.17 ppm)

HPLC apparatus

The Shimadzu LC-2010C-HT HPLC compact system (Japan) utilized in the analysis consisted of a degasser, a thermostable column unit, a gradient manager pump, an autosampler unit, and a UV detector. UV wavelength was set at 220 nm. The experiments were performed using an encapped purospher star reverse phase- C_{18} column with guard column (4.6 × 250 mm, 5 µm) (Merck, Germany). Data procurement (peak area, retention time) was carried out with the use of the Shimadzu Chemwindow Program. An auto-injection receptacle with 50 µL loop volume ensured the correct concentration of the baby food samples.

Operating conditions

The isocratic mobile phase was methanol: aqua (70:30 v/v), and flow rate was 0.7 $ml.min^{-1}$. The column temperature was set at 25-30°C with a column oven. The mobile phase was purchased ultra purely and the isocratic solvent flow was secured with the degasser system and filter cartridge system[18].

Confirmation with LC-MS

A Thermo Orbitrap Q-Exactive system of LC-MS was utilized for the confirmation of DON. The detector was applied in electron spray ionization (ESI) mode, with an electron spray voltage equivalent to 3.8 kV. Operating conditions were as follows: the column was a Fortis C_{18} – 150 x 3.0 mm of 3 μm film thickness; gradient pump flow rate and carrier gas flow rate were 0.35 mL / min and 10 mL / min, respectively. Initially (for the first 3 min.), dual gradient flow consisting of 50% mobile phase A (1% Formic acid – H_2O), 50% mobile phase B (1% Formic acid – MeOH) was completed with 100% mobile phase B while DON detection was performed. The temperatures of the capillary and heater ion source gas were adjusted to 320°C. The quantification was performed using a mass fragment scan range of 150-1200 *m/z* from the component library for DON, and its retention time was 6.2 min. The temperature and relative humidity under which the analysis was applied, were respectively[19]: (22.0 ± 5.0) °C, (50 ± 15) rh%.

RESULTS and DISCUSSION

DON occurrence in cereal grains and processed products was found to be an important food safety and global health concern, especially in developing countries. The intake risk evaluation of DON for baby foods was not known.

DON was the most abundant toxin in processed cereal-based foodstuffs for children and toddlers, with an incidence of 21.3%. The maximum DON found in the EU was as 0.2 ppm in only one sample[20]. DON was analyzed in 35 samples of commercial baby foods. Herrera et al.[19], noticed that DON was found in higher amounts in baby foods with organic sources. DON was detected in 20% of all samples (one of them was exceeded the EU limit of 0.2 ppm). In a survey where cereal based baby and infant foods were evaluated, DON was found in 71% of all samples. DON was also tested in commercial baby foods from Qatar. 27% of samples were found to contain DON, and this mycotoxin was the only one exceeding EU limits[21]. The occurrence of DON in beer in Turkey was investigated by HPLC[22]. DON was detected from urine after exposure. Sarkanj et al.[23], firstly, analyzed DON with LC–ESI–MS / MS in samples collected from 40 pregnant Croatian women, and it was found that 97.5% of the urine samples exceeded the limit of detection. Huybrechts et al.[24] detected DON and its derivative with an LC–MS / MS method.

DON levels exceeding legal limits were found in several cereal-based baby foods[25]. In our study, the highest amount of detected DON in baby foods was 0.17 ppm. Recovery (%) was 101.4 (SD: 2.17, n=5). Detected baby food samples

were those made with grain, semolina, rice and cereals. The rice sample was of organic origin. Cuce[26] investigated DON with ELISA and could detect it in tarhana, lentils, wheat and wheat flour in Turkey; it was concluded that temperature and humidity have a direct relationship with DON growth. LOD and LOQ validation criteria for DON were set in line with the International Conference on Harmonization guidelines[18].

Baby foods and baby biscuits are largely consumed as matter of convenience and saving time. Many countries consume high amounts of baby foods and baby biscuits; it is important to test DON presence in those products too.

As a result of the pandemic, securing immune system support with healthy foods gained importance. The Food and Agriculture Organization of the United Nations (FAO) declared 2021 the "International Year of Fruits and Vegetables". Uncontaminated dietary products from the source are in focus worldwide. Growing with clean food is a fundamental for a healthy generation. For sustainable secure food access, the results of this study on baby food contamination levels by DON will lead to set criteria on this era.

The previous sentence is beyond repair. Also, dietary DON intake in chicken affected the body defense response to virus vaccines and influenced the serum clinical parameters[27]. Thus, during baby and children's vaccinations, the effect of chronic exposure to DON should be considered for its effect on vaccine responses as well as immune system responses.

STATEMENT OF ETHICS

This study does not require any ethical permission.

CONFLICT OF INTEREST STATEMENT

The authors declare that they have no conflict of interests that could have appeared to influence the work reported in this paper.

AUTHOR CONTRIBUTIONS

O.E.E. and D.Y. conceived and wrote the original draft. G.Z.O provided advice and supervision. O.E.E., G.S.E. and M.E.T. collected the data that shown in the Figure 1 and Table 1. D.Y. and O.E.E. summarized the data of published articles. O.E.E., G.Z.O., and D.Y. finally revised the manuscript.

ACKNOWLEDGMENTS

Special thank you to Assistant Prof. Dr. Pınar Sinem Omurtag Ozgen for all her contributions to the analysis of samples.

REFERENCES

1. Omurtag GZ, Beyoglu D. Occurrence of deoxynivalenol (vomitoxin) in processed cereals and pulses in Turkey. Food Addit Contam, 2003;20(4):405-409. Doi: 10.1080/0265203031000082512

2.Turkish Official Gazette, 29 December 2011; 28157. Available from: https://www.resmigazete.gov.tr/eskiler/2011/12/20111229M3.htm

3. Perincherry L, Lalak-Kańczugowska J, Stępień Ł. *Fusarium*-produced mycotoxins in plant-pathogen interactions. Toxins (Basel), 2019;11(11): 664. Doi: 10.3390/toxins11110664

4. Llorens A, Mateo R, Hinojo MJ, Logrieco A, Jimenez M. Influence of the interactions among ecological variables in the characterization of zearalenone producing isolates of *Fusarium spp*. Syst. Appl Microbiol, 2004;27(2):253-260. Doi: 10.1078/072320204322881871

5. Food and Agriculture Organization (FAO), 26 January 2021. Available from: https://www.fao.org/3/cb4476en/cb4476en.pdf

6. Cambaza E, Koseki S, Kawamura S. *Fusarium graminearum* colors and deoxynivalenol synthesis at different water activity. Foods, 2020;8(1):7. Doi: 10.3390/foods8010007

7. Peraica M, Radić B, Lucić A, Pavlović M. Toxic effects of mycotoxins in humans. Bull. World Health Organ, 1999;77(9):754-766. PMID: 10534900

8. Cai G, Sun K, Xia S, Feng Z, Zou H, Gu J, et al. Decrease in immune function and the role of mitogen-activated protein kinase (MAPK) overactivation in apoptosis during T lymphocytes activation induced by zearalenone, deoxynivalenol, and their combinations. Chemosphere, 2020;255. Doi: 10.1016/j.chemosphere.2020.126999

9. Vesonder RF, Ciegler A, Jensen AH. Isolation of the emetic principle from *Fusarium*-infected corn. Appl Microbiol, 1973;26(6):1008-1010. Doi: 10.1128/am.26.6.1008-1010.1973

10. Štěpánová H, Hlavová K, Štastný K, Gopfert E, Levá L, Faldyna M. Maternal exposure results in long-term deoxynivalenol persistence in piglets' plasma and modulates the immune system. Toxins, 2020;12(10):615. Doi: 10.3390/toxins12100615

11. EFSA (European Food Safety Authority). Risks to human and animal health related to the presence of deoxynivalenol and its acetylated and modified forms in food and feed. EFSA J, 2017;15. Doi: 10.2903/j.efsa.2017.4718

12. Iverson F, Armstrong C, Nera E, Truelove J, Fernie S, Scott P, et al. Chronic feeding study of deoxynivalenol in B6C3F1 male and female mice. Teratog Carcinog Mutagen, 1995;15(6):283-306. Doi: 10.1002/tcm.1770150606

13. Tryphonas H, Iverson F, So Y, Nera EA, McGuire PF, O'Grady L, et al. Effects of deoxynivalenol (vomitoxin) on the humoral and cellular immunity of mice. Toxicol Lett, 1981;30(2):137-150. Doi: 10.1016/0378-4274(86)90096-2

14. Scientific Committee on Food (SCF). Safety and efficacy of a feed additive consisting of butylated hydroxyanisole (BHA) for use in cats (FEDIAF). EFSA Journal, 2021;19(7):6714. Doi: 10.2903/j.efsa.2021.6714

15. De Boevre M, Di Mavungu JD, Maene P, Audenaert K, Deforce D, Haesaert G, et al. Development and validation of an LC-MS / MS method for the simultaneous determination of deoxynivalenol, zearalenone, T-2-toxin and some masked metabolites in different cereals and cereal-derived food. Food Addit Contam Part A Chem Anal Control Expo Risk Assess, 2012;29(5):819-835. Doi: 10.1002/tcm.1770150606

16. Pereira VL, Fernandes JO, Cunha SC. Comparative assessment of three cleanup procedures after QuEChERS extraction for determination of trichothecenes (type A and type B) in processed cereal-based baby foods by GC-MS. Food Chem, 2015;182:143-149. Doi: 10.1002/tcm.1770150606

17. Scott PM, Lau PY, Kanhere SR. Gas chromatography with electron capture and mass spectrometric detection of deoxynivalenol in wheat and other grains. J Assoc Off Anal Chem, 1981;64(6):1364-1371. Doi: 10.1093/jaoac/64.6.1364

18. Armbruster DA, Pry T. Limit of blank, limit of detection and limit of quantitation. Clin Biochem Rev, 2008; 29 (1): 49-52. PMID: 18852857

19. Herrera M, Bervis N, Carramiñana JJ, Juan T, Herrera A, Ariño A, et al. Occurrence and exposure assessment of aflatoxins and deoxynivalenol in cereal-based baby foods for infants. Toxins, 2019;11(3):150. Doi: 10.3390/toxins11030150

20. Kirimker SE, Turksoy S, Kabak B. Assessment of dietary exposure to deoxynivalenol and fumonisin in the population of infants and toddlers in Turkey. Food Chem Toxicol, 2020;140. Doi: 10.1016/j.fct.2020.111304

21. Ul Hassan Z, Al Thani R, Atia F, Al Meer S, Migheli Q, Jaoua S. Co-occurrence of mycotoxins in commercial formula milk and cereal-based baby food on the Qatar market. Food Addit Contam Part B Surveill, 2018;11(3):191-197. Doi: 10.1080/19393210.2018.1437785

22. Omurtag GZ, Beyoglu D. Occurrence of deoxynivalenol (vomitoxin) in beer in Turkey detected by HPLC. Food Control, 2007;18(2):163-166. Doi: 10.1016/j.foodcont.2005.09.007

23. Šarkanj B, Warth B, Uhlig S, Abia WA, Sulyok M, Klapec T, et al. Urinary analysis reveals high deoxynivalenol exposure in pregnant women from Croatia. Food Chem Toxicol, 2013;62:231-237. Doi: 10.1016/j.fct.2013.08.043

24. Huybrechts B, Martins JC, Debongnie P, Uhlig S, Callebaut A. Fast and sensitive LC-MS / MS method measuring human mycotoxin exposure using biomarkers in urine. Arch Toxicol, 2015;89(11):1993-2005. Doi: 10.1007/s00204-014-1358-8

25. Pascari X, Marin S, Ramos AJ, Molino F, Sanchis V. Deoxynivalenol in cereal-based baby food production process A review. Food Control, 2019;99:11-20. Doi: 10.1016/j.foodcont.2018.12.014

26. Cuce M. Incidence of aflatoxins, ochratoxin A, zearalenone, and deoxynivalenol in food commodities from Turkey. J Food Saf, 2020;40(6):1-13. Doi: 10.1111/jfs.12849

27. Ghareeb K, Awad WA, Böhm J. The toxicity of *Fusarium* mycotoxin deoxynivalenol in poultry feeding. Worlds Poult Sci J, 2012;68(4):651-668. Doi: 10.1017/S0043933912000797

Acta Pharm. Sci. Vol 62:(2), 2024
Research article
DOI: 10.23893/1307-2080.APS6225

Chemical composition and biological activities of seed butter extracted from *Garcinia gummi-gutta* (L.) Roxb.

Neenthamadathil Mohandas KRISHNAKUMAR[1*], George SHINEY[2]

1 Department of Biosciences, Rajagiri College of Social Sciences (Autonomous), Rajagiri P. O., Kalamassery, Cochin, 683104, Kerala, India

2 Department of Biotechnology, Presentation College of Applied Sciences, Puthenvelikkara, Ernakulam, 683594, Kerala, India

ABSTRACT

Garcinia gummi-gutta (L.) Roxb. is a commercially viable fruit crop and it is a rich source of valuable edible fat known as seed butter. In the present study, the cytotoxic, antiproliferative and antimicrobial properties of *G. gummi-gutta* seed butter (GGSB) were investigated. The cytotoxic effects of the seed butter were assessed with Dalton's Lymphoma Ascites (DLA) and Ehrlich's Ascites Carcinoma (EAC) cell lines, and also on normal splenocytes. The seed butter was found to be cytotoxic for DLA an EAC and it exhibited a dose dependent effect and IC_{50} value of 289.04 μg/mL and 299.18 μg/mL for DLA and EAC respectively while less toxic to normal spleen cells. Further, human triple negative breast cancer (MDA-MB-231) and hepatocellular carcinoma (HepG2) cell lines in culture exhibited reduction in cell viability revealing its antiproliferative effect. The IC_{50} value of GGSB against MDA-MB-321 and HepG2 were determined as 66.70±2.60 μg/mL and 110.98 μg/mL respectively. The antimicrobial effect of the seed butter was determined by broth dilution method. The gas chromatography mass spectrometry (GC-MS) and gas chromatography with flame ionization detection (GC-FID) analysis revealed the presence fatty acids as the major phytochemical compounds responsible its bioactivities.

Keywords: *garcinia gummi-gutta*, cytotoxicity, antiproliferative effect, antimicrobial activity

*Corresponding author: Neenthamadathil Mohandas KRISHNAKUMAR
E-mail: krishnakumarnmohandas@gmail.com
ORCIDs:
Neenthamadathil Mohandas KRISHNAKUMAR: 0000-0002-8510-5391
George SHINEY: 0009-0001-2575-4760
(Received 11 May 2023, Accepted 29 Sep 2023)

INTRODUCTION

The regular consumption of dairy butter has increased risks of weight gain and coronary diseases and therefore search for alternate plant based butter viz., seed butter is important. The seeds and nuts are consumed in various ways as ingredients recipe, spreads, snacks and as a delicacy[1]. Plant based butters are made from plant nuts like cashew butter, peanut butter, almond butter, sunflower butter, soy butter, sesame butter and pumpkin seed butter[2]. The previous reports suggested that nut or seed butter consumption protects against lifestyle diseases like diabetes, coronary heart diseases, metabolic syndrome and gall stone disease[3]. The plant based seed butters contain higher percentage of unsaturated fats, essential fatty acids and minerals like magnesium, calcium, zinc etc. The phytocompounds present in seed butters exhibited protection against breast, prostate and colon cancer[4]. The efficacy of anticancer drugs improves when combined with natural compounds like curcumin, resveratrol, apigenin, cyclopamine, quercetin, tetrandrine etc. The anticancer effect is achieved through perturbing various cellular signaling pathways in cancer development. The phytocompounds prevent tumor cell proliferation, development and metastasis by various mechanisms such as induced cell cycle arrest, reactive oxygen species generation, activating intrinsic and extrinsic apoptotic pathways and down regulating the activated signaling pathways[5]. It has been reported that dietary polyphenols exhibited cancer chemoprevention effect through the epigenetic regulation of cancer associated genes via noncoding RNAs (ncRNAs) and long noncoding RNA (lncRNA)[6].

Only some limited literature is available on the therapeutic effects of plant based seed butters. *Cucurbita pepo* (pumpkin) seeds alleviated the signs of benign prostatic hyperplasia by decreasing protein binding prostate (PBP) levels and weight of ventral prostate[7]. In another study, Ortiz et al. (2019) reported the cytotoxic and antiproliferative activities of grape seed and extracts of grape pomace on colon cancer cells (Caco-2) and the effect was achieved through the down- regulation of Mfc gene expression levels[8]. In addition, the roasted almond butter significantly lowered total cholesterol and low density lipoprotein levels in healthy volunteers suggesting cardiac protective effect of the butter[9].

Garcinia gummi-gutta (L.) Roxb. (Family: Clusiaceae) commonly called 'Malabar Tamarind', is a small tree up to 25 m height. It is an under exploited, economically important tree species, tropically distributed and found in the evergreen forests of Western Ghats from Konkan to Kerala of the Indian peninsula. It is also common in the home gardens and fields of Kerala. The fruit rind of *G. gummi-gutta* is acidic and used in fish and meat curries as a souring

condiment[10]. *G. gummi-gutta* is traditionally used against constipation, delayed menstruation, edema, fever, hemorrhoids, dysentery and diarrhea. It is an established plant for reducing body weight[11]. The dried seeds yield edible fat commonly known as 'seed butter', due to its solid state in room temperature, and it is a rich source of protein and fat. The physicochemical characteristics such as acid value, saponification value and peroxide value of the seed butter are within the range of domestic oils used for cooking purposes and therefore it forms an important source for edible oil[12].

A closely related species of the family *Garcinia indica* is a good source of edible fat known as 'Kokum butter'. It is used by the people of coastal Konkan region of the states of Goa and Maharashtra, India for cooking purposes. The butter is also used in cosmetic industries and a better substitute for cocoa butter in chocolate industries[13]. Earlier, *G. gummi-gutta* seeds were considered as waste product of post-harvest operations. The seed oil *G. gummi-gutta* is traditionally used against skin diseases[14] and recently it has been explored as a source of biodiesel[15]. Rani et al. (2021) evaluated the toxicity by acute oral toxicity and acute dermal toxicity studies *in vivo* and the results showed that there was no significant change in the bodyweight, no mortality, morbidity or clinical signs of dermal responses[16]. The importance of the present study is to find out the chemical composition of GGSB from *G. gummi-gutta* seeds. The therapeutic efficacy of the seed butter has not been scientifically validated and the present study was undertaken to investigate the cytotoxic, anti-proliferative and antimicrobial properties of *G. gummi-gutta* seed butter. Furthermore, GC-MS and GC-FID analyses were performed to understand the chemical composition of GGSB.

METHODOLOGY

Chemical reagents

RPMI-1640, Trypan blue, fetal bovine serum, penicillin and streptomycin were purchased from Sigma Aldrich, USA. Commercial kit for MTT assay was purchased from Merck, Germany. All the other chemicals used were of analytical reagent grade.

Cell cultures

DLA (Dalton's Lymphoma Ascites) and EAC (Ehrlich's Ascites Carcinoma) cell lines were obtained from Amala Cancer Research Centre, Thrissur, India. Human triple negative breast cancer cell line (MDA-MB-231) (RRID: CVCL_0062) and hepatocellular carcinoma (HepG2) (RRID: CVCL_0027) cell lines were procured from National Centre for Cell Sciences, Pune, India.

Animals

Sprague-Dawley rats, males (200–250g) and Swiss albino mice, males (25-30 g) were obtained from the Animal House of Amala Cancer Research Centre, Thrissur, Kerala, India. They were housed in polyacrylic cages under standard conditions of temperature (24–28◦C), relative humidity (60–70%) and 12h dark–light cycles), fed commercial rat feed (Lipton India Ltd., Mumbai, India) and boiled water *ad libitum*. Animals were acclimatized for 1 week before starting the experiments. All experiments involving animals were carried out according to guidelines of Committee for the Purpose of Control and Supervision of Experiments on Animals (CPCSEA), New Delhi, after getting the approval of the Institute's Animal Ethics Committee.

Extraction of the seed butter

The seeds of *G. gummi-gutta* were collected from the homesteads of Mala locality, Thrissur District, Kerala, India and it was authenticated by the plant taxonomist. A voucher specimen (PCASH-01 dated 15/05/2017) was deposited in the herbarium of Biotechnology Department of the College for future reference. The seed butter was extracted according to the standardized method[12]. The seeds were separated from the succulent aril of fresh ripen fruits, washed thoroughly and dried in oven at 60°C. The seed kernels were separated from the seed coat and second level of drying was carried out. 100 g of the kernels were washed in hot water to remove the impurities and they were slightly roasted in gentle heat in a pan and grinded, boiled with 1 L distilled water in an open container for 2 to 3 h. The oily upper layer was separated and decanted into a clean vessel and allowed to evaporate water content. The yield (%) was noted and the *G. gummi-gutta* seed butter (GGSB) was stored in dry and air tight containers.

Short term *in vitro* cytotoxicity studies on normal rat spleen cells

The seed butter was evaluated for short term cytotoxicity effect *in vitro* in rat spleen tissues collected from male Sprague-Dawley rats according to the standard protocol. It was then smashed to single cell suspension in RPMI complete medium containing antibiotics and filtered using mesh cloth. The collected cells were washed thrice and suspended in known volume of RPMI complete medium containing antibiotics and counted. Viable cell suspension ($1x10^6$ cells in 0.1 mL) was added to tubes containing various concentrations of GGSB and the volume was made up to 1 mL using RPMI media. Control tubes contained only cell suspension (without additives). These tubes were incubated for 3h at 37°C. At the end of incubation cell suspension in the tubes were mixed with 0.1 mL of 1% trypan blue and kept for 2-3 minutes and loaded on a haemocy-

tometer. Dead cells take up the blue colour of trypan blue while live cells did not take up the dye. The number of stained cells were counted separately and percentage cytotoxicity was determined[17,19].

$$\% \text{ Cytotoxicity} = \frac{\text{No. of dead cells} \times 100}{\text{No. of live cells} + \text{No. of dead cells}}$$

Evaluation of cytotoxicity effect

The cytotoxic effect of the seed butter GGSB was evaluated by determining the percentage viability of DLA and EAC cell lines *in vitro* using Trypan blue exclusion method[18]. The tumor cells were aspirated aseptically from the peritoneal cavity of tumor bearing male Swiss albino mice after 15 days of inoculation. The aspirated tumour cells were washed thrice with phosphate buffered saline (PBS) and centrifuged at 1500 rpm for 3 min. Cell viability was determined by trypan blue exclusion method. The pellets of cells were re-suspended and the count was adjusted to a concentration of 1×10^7 cells/mL. The different concentrations (10, 20, 50, 100 and 200 µg/mL) of GGSB in 1 mL PBS were added to test tubes containing approximately 1×10^6 cells. Control tube contained only cell suspension. These assay mixtures were incubated at 37°C for 3 h. Further cell suspension was mixed with 0.1 mL of 1% trypan blue and kept for 2-3 minutes and then loaded on haemocytometer to evaluate the cell viability. The percentage viability and IC_{50} of GGSB against tumour cells were calculated[18].

Antiproliferative activity *in vitro* using MTT assay

Antiproliferative activity of GGSB dissolved in dimethyl sulphoxide (DMSO) was evaluated in human triple negative breast cancer cell line (MDA-MB-231) and human hepatocellular carcinoma (HepG2) cell lines, using 3-(4, 5-dimethylthiazol-2-yl) - 2, 5-diphenyltetrazolium bromide (MTT) assay[20]. All the cell lines were maintained in DMEM media, supplemented with 10% fetal bovine serum, 100 µg /mL penicillin and 100 µg/mL streptomycin and kept at 37°C in an incubator with 5% CO_2. The cells were passaged at 80-90% confluency and medium was changed every third day. Cytotoxicity of the test materials was performed by MTT assay. Approximately $1x10^5$ cells/mL were seeded in a 24 well plate, with complete growth medium (DMEM) and allowed to attach and grow. At 80% confluency, the medium was replaced with fresh medium containing different concentrations of GGSB (0-120 µg/mL) and incubated for 48 hrs. At the end of incubation period, the medium was again replaced with

fresh medium containing 40 µL of 5mg/ mL MTT and incubated for 4 hrs. The formazan crystals formed were dissolved in dimethyl sulfoxide and the absorbance was measured at 570 nm in ELISA microplate reader (BioTek, USA). All the experiments were performed in triplicate and the average of the percentage absorbance was plotted against concentration and IC_{50} was calculated[21]. The percentage viability was calculated using the formula:

$$\% \text{ Viability} = \frac{\text{Absorbance of sample} \times 100}{\text{Absorbance of control}}$$

Evaluation of antimicrobial activity

The seed butter GGSB was dissolved in 1% DMSO to get a final concentration of 1 mg/mL and evaluated for antimicrobial effects. A total of seven microbial strains were tested for their susceptibility to GGSB. These strains include one yeast: *Candida albicans* (ATCC 90028); one filamentous fungus: *Aspergillus niger* (ATCC 9029); three Gram-negative bacteria: *Pseudomonas aeruginosa* (ATCC 27853), *Escherichia coli* (ATCC 25292) and *Salmonella typhimurium* (ATCC 14028); and two Gram-positive bacteria: *Staphylococcus aureus* (ATCC 29213) and *Bacillus subtilis* (ATCC 6051). These strains were maintained on agar slant at 4°C and sub-cultured on fresh and appropriate agar plates 24 h prior to the experiment. The broth dilution method was carried out to evaluate the antimicrobial effect of the sample[22].

Fatty acid methyl esters (FAMEs) preparation from GGSB

Lipids extracted from the seed butter were methylated and converted to their respective fatty acid methyl esters (FAMEs), according to the modified method of Moss et al. (1974)[23]. Further, 2 mL of 0.5 M NaOH in 2% (w/v) methanol was added to a 100 mL flask containing the lipid with stirring and heating to 100°C for 5 min under reflux. Boron trifluoride reagent (BF_3) (3 mL) was added, followed by stirring for 2 min for acid catalysis to occur, after which 3 mL of NaCl solution was added at 20% (w/v). The sample was transferred to a separating funnel with containing 20 mL hexane. The organic phase was separated and dried using anhydrous sodium sulfate (2 g). The solvent was evaporated under stream of N_2 on steam bath and the samples were weighed for further analysis.

GC-MS and GC-FID analysis

The seed butter of *G. gummi-gutta* (GGSB) 1 µL (mg/mL) was employed in GC-MS for various phytoconstituents. The analysis was performed on a capillary system, GC Varian CP-3800, containing Combi PAL auto-sampler and a gas chromatograph interfaced to a mass spectrometer (Saturn 2200 MS) provided with a VF-5ms, a Factor Four column, (0.25mm × 30m ID × 0.25µm df). The average peak area to the total areas of each component was compared and relative percentage amount of compound was calculated. Ion trap is the mass-detector used in the analysis. The software used for the analysis of mass spectra and chromatograms was MS work station with National Institute Standard and Technology (NIST) library, Gaithersburg, Maryland, USA. The NIST database, having more than 62,000 patterns was used for the identification of each component by comparing the spectrum of the unknown compounds with the spectrum of known compounds. GC-FID analysis was employed for quantitation of the constituent fatty acids. A gas chromatograph GC-FID with GC6890N equipped with a fused-silica capillary column (SP 2560, dimensions of 100 m x 0.2 mm x 0.25 µm film thickness) was used for quantitative analysis. An analytical curve from FAME MIX-37 standard and internal standardization was used to analyze them qualitatively and quantitatively. An internal standard solution containing non adecanoate (Sigma Aldrich) was prepared at 2 mg/mL concentration.

Statistical analysis

All the analyses were performed in triplicate. Analysis of Variance (ANOVA) was used to find out the statistical significance between the samples. The data were indicated as mean ± standard deviation (SD), and $p \leq 0.05$ was considered to be statistically significant. Dunnett's multiple comparison test was used to determine the significant differences between means. The IBM SPSS Statistics, version 20 (USA) was the computer software used for the analysis.

RESULTS and DISCUSSION

The yield of *G. gummi-gutta* seed butter (GGSB) was estimated as 15%. The isolated butter was yellowish brown in color without any characteristic odor and comparatively high yield of the fixed oil indicated presence of fatty acids in the seeds.

Cytotoxic and antiproliferative effects of *G. gummi-gutta* seed butter (GGSB)

In the present study, the cytotoxicity of GGSB towards DLA and EAC were evaluated in a short-term *in vitro* assay. It was carried out by Trypan blue dye exclusion method and the viable cells remained unstained by the dye and they were counted by using a haemocytometer. The intact membranes of live cells exclude the dye, whereas the dead cells do not. *In vitro* cytotoxic study showed that GGSB exhibited dose dependent cytotoxic effect towards DLA and EAC (Figure 1). The IC_{50} values obtained are 289.04 µg/mL and 299.18 µg/mL for DLA and EAC respectively. The oil GGSB was found non-cytotoxic to rat splenocytes *in vitro* with IC_{50} value above 200 µg/mL concentrations (Figure 1).

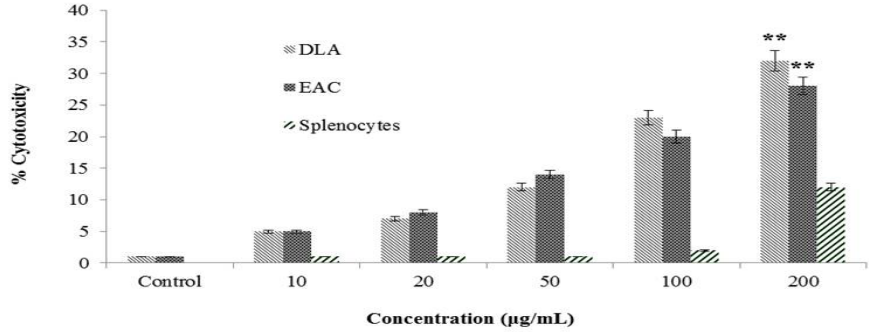

**Significance $p \leq 0.05$ compared to the control

Figure 1. Cytotoxicity effect *in vitro* of *Garcinia gummi-gutta* seed butter (GGSB) on Dalton's Lymphoma Ascites (DLA), Ehrlich Ascites Carcinoma cells (EAC) and normal spleen cells. Values are expressed as mean ± SD of at least three consecutive experiments, Analysis of Variance (ANOVA) followed by Dunnett's multiple comparison test.

Anti-proliferative effect *in vitro* of GGSB was estimated by MTT assay and the relative cell proliferative activities of human triple negative breast cancer cell line (MDA-MB-231) and human hepatocellular carcinoma (HepG2) cell lines following exposure with GGSB are summarized in Figure 2. The seed butter exhibited a dose dependent anti-proliferative effect on MDA-MB-231 and HepG2 cell lines (Figure 2). The IC_{50} value of GGSB against MDA-MB-321 was determined as 66.70±2.60 µg/mL. Significant cytotoxicity was observed towards HepG2 cell line with an IC_{50} of 110.98 µg/mL. The cells in cultures have a proliferating population which is shown to be inhibited by GGSB. In MTT assay GGSB exhibited cytotoxicity towards MDA-MB-231 and HepG2. Photomicrographs of cell at 20, 40 and 100 µg/ mL concentration are shown in Figure 3 and the images were taken under 20 x magnification (total 200 x) of phase contrast microscope (Magnus INVI, Chennai, India).

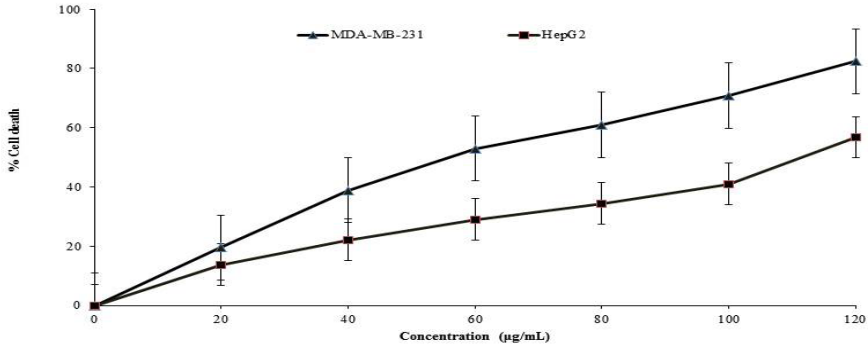

**Significance p≤0.05 compared to the control

Figure 2. Antiproliferative effect *in vitro* of *Garcinia gummi-gutta* seed butter (GGSB) on human triple negative breast cancer (MDA-MB-231) and human hepatocellular carcinoma (HepG2) cell lines following exposure with GGSB. Values represent mean ± SD of at least 3 replica cultures. Analysis of Variance (ANOVA) followed by Dunnett's multiple comparison test.

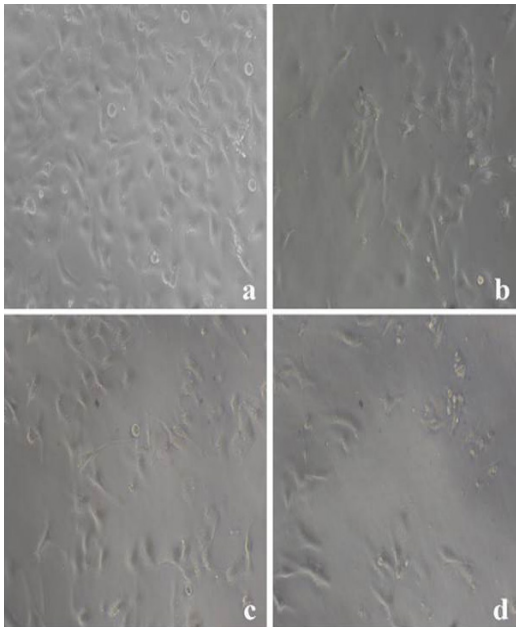

**Significance p≤0.05 compared to the control

Figure 3. Antiproliferative effect *in vitro* of GGSB on Human triple negative breast cancer cell line (MDA-MB-231) (a) Control (b) 20 µg/mL (c) 40 µg/mL and (d) 100 µg/mL concentration treatments. The images were taken under (magnification 200 x) Phase contrast microscope (Magnus INVI, Chennai, India)

Cytotoxic and antiproliferative compounds of plant origin, that are known to target specific oncogenes or malignant cells and interrupt carcinogenesis process and prevent tumor growth. Ursolic acid, corosolic acid, conophylline, kaempferide and campesterol are some of the plant-based chemopreventive agents[24]. The chemopreventive effects of natural compounds is achieved by mechanisms such as antioxidant effect, anti-inflammatory pathways, ability to induce phase II enzymes, cell cycle arrest and apoptosis[25]. The plant species coming under *Garcinia* genus are very important due to its therapeutic effects and it contains phytocompounds having antitumor effects. Prenylxanthones isolated from leaves of *Garcinia bracteata*[26] and garcinol, a polyisoprenylated chalcone from *Garcinia indica*[27] showed cytotoxic effects against different cancer cell lines and exhibited potent antitumor activity. The cytotoxic effect of the seed butter may be achieved by making pores on the cell membrane, through which Trypan blue dye enters and the dead cells stained blue and viable cells were excluded from the staining[28]. Most of the currently using allopathic chemotherapeutic agents have significant immune-suppressing effect. The result is significant that the seed butter is non-cytotoxic to rat splenocytes and as spleen cell population represent the immune cell population. In view of this, it is assumed that the differential toxic potential of GGSB may be an advantage and it can be considered as a good candidate for anticancer drug development.

MTT assay is a colorimetric assay based on the principle of the ability of nicotinamide adenine dinucleotide phosphate (NADPH) dependent cellular oxidoreductase to reduce the tetrazolium to its insoluble purple colored formazan. It measures cell viability in terms of reductive activity as enzymatic conversion of tetrazolium to water insoluble formazan by dehydrogenases present in mitochondria and endoplasmic reticulum. A solubilizing agent was added to dissolve the formazan product and absorbance of the solution was noted[29]. MDA-MB-231 cells are aggressive and invasive triple negative breast cancer cells that are resistant to several anticancer agents[30]. HepG2 cells have high proliferation rates, adherent properties and grow as monolayers in small aggregates in cultures[31]. The cytotoxicity and antiproliferative effects of GGSB may be achieved by inducing apoptosis, cell cycle arrest at sub G_0/G_1 phase and anti-angiogenesis[32]. Several mechanisms have been proposed by the researchers for explaining the antiproliferative effect of unsaturated fatty acids.

One of the major compounds detected in GGSB is oleic acid, which is a monounsaturated omega-9 fatty acid. Oleic acid has been shown in numerous reports to inhibit cellular proliferation in several cancer cell lines. It plays crucial role in intracellular calcium signaling pathways related to apoptosis and growth

induction. The mechanisms related to apoptosis are linked to the rise in intracellular caspase-3 activity and development of reactive oxygen species[33]. It can suppress the over expression of human epidermal growth factor receptor-2 (HER-2/erbB-2), an oncogene which is involved in the development and metastasis of numerous human cancers[34]. Autophagy dependent anticancer effect of oleic acid has been reported in human hepatocellular carcinoma cell lines[35].

Antimicrobial activity of *G. gummi-gutta* seed butter (GGSB)

The antimicrobial property of GGSB was evaluated with concentration range 10-100 µg/mL and the results showed that GGSB inhibited the microbial growth after 24 h of incubation. It significantly ($p \leq 0.05$) inhibited the growth of pathogens such as *E. coli*, *S. aureus* and *B. subtilis* (Figure 4). The maximum microbial growth inhibition percentage (94.19%) was observed in *S. aureus* by GGSB (100 µg/mL) treatment. The minimum inhibition percentage was observed in the case of *A. niger*. The seed butter exhibited a dose dependent growth-inhibitory effect on the microorganisms selected for the study. Amongst the pathogens screened, *E. coli*, *S. aureus* and *B. subtilis* were found to be more sensitive to GGSB, which exhibited the percentage of inhibition of microbial growth ranged between 94.19% to 87.75%. Moderate level of activity was showed by GGSB against *P. aeruginosa* and *S. typhi* compared to the control. The seed butter (100 µg/mL) showed maximum growth inhibition percentage of 27.40% and 36.36% against *A. niger* and *C. albicans* respectively compared to the control (Figure 5). The IC_{50} values of 78.03 µg/mL, 25.43 µg/mL, 58.75 µg/mL, 73.40 µg/mL and 51.78 µg/mL were obtained with GGSB against *P. aeruginosa*, *E. coli*, *S. aureus*, *S. typhimurium* and *B. subtilis* respectively.

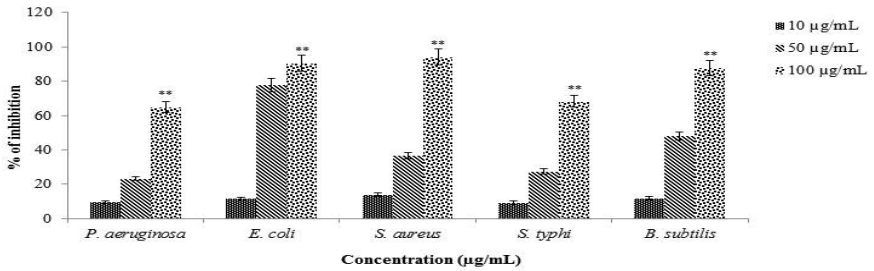

**Significance $p \leq 0.05$ compared to the control.

Figure 4. Antibacterial effect *in vitro* of GGSB (10-100 µg/mL) by broth dilution method. Values are the mean ± SD, n=6 in each group, Analysis of Variance (ANOVA) followed by Dunnett's multiple comparison test.

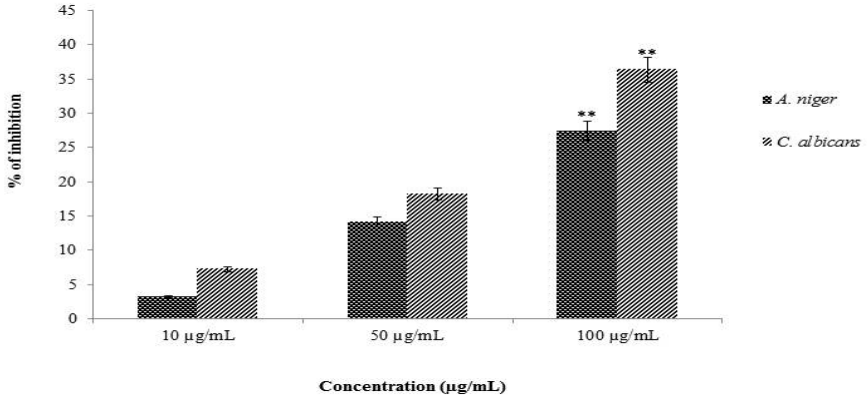

**Significance p≤0.05 compared to the control.

Figure 5. In vitro antifungal effect of GGSB (10-100 µg/mL) by broth dilution method. Values are the mean ± SD, n=6 in each group, Analysis of Variance (ANOVA) followed by Dunnett's multiple comparison test.

Chemical composition of *G. gummi-gutta* seed butter (GGSB)

In the present study, the chemical composition of the seed butter GGSB was investigated using both GC-FID and GC-MS. GC-MS analysis was used for the chemical characterization of GGSB (Figure 6) and the main compound classes identified were fatty acids. The identified compounds are listed in Table 1.

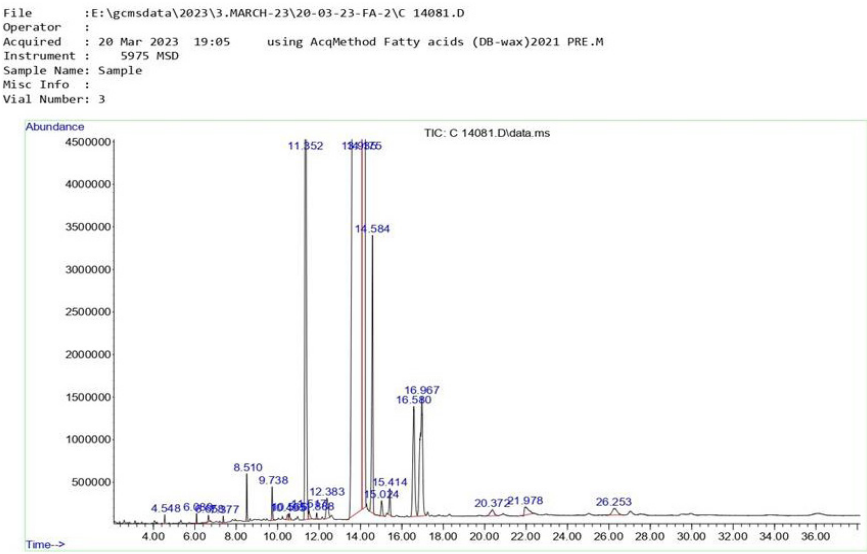

Figure 6. Phytocompounds detected in GC-MS Total Ion Chromatogram of *Garcinia gummi-gutta* seed butter (GGSB)

Table 1. Phytocompounds detected in GC-MS spectrum of *Garcinia gummi-gutta* seed butter (GGSB)

Compound Name	Peak Number	Retention Time RT (min)	Molecular Formula	Molecular Weight	Area (%)
Caprylic acid	1	15.108	$C_8H_{16}O_2$	144.21	0.02
Capric acid	2	18.143	$C_{10}H_{20}O_2$	172.26	0.02
Lauric acid	3	21.926	$C_{12}H_{24}O_2$	200.32	0.14
Myristic acid	4	25.963	$C_{14}H_{28}O_2$	228.37	0.13
Pentadecanoic acid	5	27.948	$C_{15}H_{30}O_2$	242.40	0.03
Palmitic acid	6	29.891	$C_{16}H_{32}O_2$	256.42	4.34
Heptadecanoic acid	7	31.758	$C_{17}H_{34}O_2$	270.50	0.20
Stearic acid	8	33.689	$C_{18}H_{36}O_2$	284.50	63.81
Elaidic acid	9	34.379	$C_{18}H_{34}O_2$	282.50	43.40
Oleic acid	10	34.839	$C_{18}H_{34}O_2$	282.50	26.31
Linoleic acid	11	36.503	$C_{18}H_{32}O_2$	280.40	1.51
Arachidic acid	12	37.068	$C_{20}H_{40}O_2$	312.50	1.06
Cis-11-Eicosenoic acid	13	38.282	$C_{20}H_{38}O_2$	310.50	0.30
Gamma-Linolenic acid-	14	38.593	$C_{18}H_{30}O_2$	278.40	0.06
Cis-11, 14-Eicosadienoic acid-	15	40.105	$C_{20}H_{36}O_2$	308.50	0.28
Behenic acid	16	40.723	$C_{22}H_{44}O_2$	340.60	0.11
Lignoceric acid	17	44.928	$C_{24}H_{48}O_2$	368.60	0.16
Cis-4, 7, 10, 13, 16, 19-Docosahexaenoic acid-	18	53.522	$C_{22}H_{32}O_2$	328.50	0.19

The gas chromatography analysis of GGSB fatty acid composition (Figure 7) showed that the main compounds with high proportions were stearic acid, C18:0 (47.74%), oleic acid, C18:1n9c (43.29%) and palmitic acid, C16:0 (2.53%) as the major compounds (Table 2).

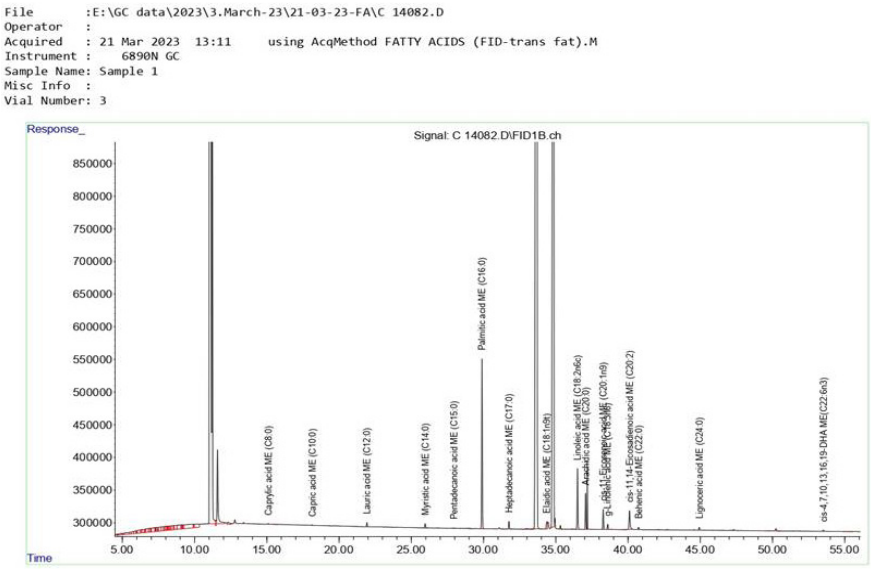

Figure 7. GC-FID chromatogram of *Garcinia gummi-gutta* seed butter (GGSB)

Table 2. The fatty acid composition of *G. gummi-gutta* seed butter (GGSB) determined by GC-FID

Fatty Acid Composition	Concentration (%)	Molecular Formula	Molecular Weight
C16:0 (Palmitic acid)	2.530	$C_{16}H_{32}O_2$	256.42
C17:0 (Heptadecanoic acid)	0.103	$C_{17}H_{34}O_2$	270.50
C18:0 (Stearic acid)	47.740	$C_{18}H_{36}O_2$	284.50
C20:0 (Arachidic acid)	0.438	$C_{20}H_{40}O_2$	312.50
C18:1n9c (Oleic acid)	43.290	$C_{18}H_{34}O_2$	282.50
C18:1n9t (Elaidic acid)	0.144	$C_{18}H_{34}O_2$	282.50
C18:2n6c (Linoleic acid)	0.825	$C_{18}H_{32}O_2$	280.40
C20:2 (cis-11, 14-Eicosadienoic acid)	0.393	$C_{20}H_{36}O_2$	308.50

The presence of phytocompounds such as heptadecanoic acid, arachidic acid, elaidic acid, linoleic acid and cis-11, 14-eicosadienoic acid was also detected.

The nuclear magnetic resonance (NMR) spectroscopy analysis of *G. gummi-gutta* seed oil helps to evaluate the quality of the edible oils by identifying the fatty acids compounds present in it. Rani et al. (2021) carried out the NMR spectroscopy analysis of the seed oil extracted from *G. gummi-gutta*[16] and the study revealed the tentative presence of compounds like stearic acid, 9-octadecenoic acid and the saturated fatty acid such as oleic acid was detected in the oil.

Stearic acid ($C_{18}H_{36}O_2$) is saturated long chain fatty acid with 18 carbon backbone and 9-octadecenoic acid ($C_{18}H_{34}O_2$) is monounsaturated fatty acid. The composition of GGSB is similar to the seed oil from a closely related species, *G. indica*[36]. The previous phytochemical studies conducted in the petroleum ether extract of *G. gummi-gutta* seeds reported to contain margaric acid and oleic acid as the major fatty acid compounds[37]. However, in the present study, it was not detected in the seed butter. The combination of monounsaturated fatty acids and long chain saturated fatty acids provides higher levels of melting temperature, heat of combustion and oxidation stability[38]. Due to the stable and solid nature at room temperature, stearic acid is widely used in food industries and cosmetic products. It is used to increase the hardness and heat resistance property of the chocolates by using along with cocoa butter. In hot climatic conditions the butter helps to prevent softening and loss of consistency of chocolates caused by heat[39]. GGSB is in the solidified form at room temperature, suggesting it as a better component for chocolates.

Garcinia seed kernel consists of fixed oil (30-40%) compared to other seed fats like coconut (60%), palm kernel (36%), sunflower (32%), castor seed (50%), mustard (35%), sesame (50%) and ground nut kernel (42%). *Garcinia* butter is rich in stearic acid and it is considered as demulcent, nutritive, emollient and astringent[40]. Stearic acid reduces blood pressure, improves cardiac function and reduces the risk for cancer[41]. It had been reported that the compounds stearic acid and oleic acid exhibited anticancer and antimicrobial effects[42]. According to Li et al. (2011), stearic acid can induce apoptosis of breast cancer cells[43] by arresting the cell cycle and dietary stearic acid has the potential to decrease the incidence of mammary tumor in carcinogenesis models[44]. Cell culture studies indicated that stearic acid showed anti-cancer activities including inhibition of the invasion and proliferation of cancer cells, changes in cell morphology and inducing apoptosis[45]. Dietary stearate delayed tumor development and decreased tumor incidence in experimental animals by inhibited metastasis to the lungs through a mechanism independent of primary tumor size[46]. It has been reported that oleic acid promoted antitumor effect against prostate, breast and colorectal cancers through inducing apoptosis and increased production of reactive oxygen species[47]. Stearic acid showed antibacterial activity against both Gram positive and Gram negative bacteria. The antibacterial effect of stearic acid derivative isolated from the hexane-soluble fraction of the leaf and stem extracts of *Stemodia foliosa* has been reported[48]. Oleic acid is a component of omega-9-unsaturated fatty acid and it reported to exhibit antifungal and antibacterial effects[49]. Liposomal oleic acid loaded (LipoOA) antibiotics were reported to exhibit enhanced antimicrobial activity against multidrug-resistant *Pseudomonas aeruginosa*. Thus, LipoOA could be utilized to encapsulate antibiotics for the development of novel and more effec-

tive methods to tackle emerging multidrug resistance in pathogenic microbes[50]. The phytochemical compounds present in GGSB are responsible for its therapeutic effects. In the present study, the *in vitro* cytotoxic and antiproliferative effects are reported and pharmacological studies using *in vivo* models should be carried out to understand the effects of GGSB on biological system.

In conclusion, the present study deals with the evaluation of cytotoxic, antiproliferative and antimicrobial effects of *G. gummi-gutta* seed butter. The seed butter exhibited dose dependent cytotoxic and antiproliferative effects *in vitro*. But at the same time, it was found non-cytotoxic to normal splenocytes and GGSB showed significant antimicrobial effect also. The GC-MS and GC-FID analysis revealed the presence of fatty acid compounds in the seed butter and these compounds are responsible for its therapeutic effects. Detailed *in vivo* studies, molecular gene expression analysis and detailed phytochemical studies are warranted for the isolation of bioactive compounds from GGSB. Future research in this field should be carried out to understand the exact mechanism of action of the compounds isolated from the seed butter.

STATEMENTS OF ETHICS

All experiments involving animals were carried out according to guidelines of Committee for the Purpose of Control and Supervision of Experiments on Animals (CPCSEA), New Delhi, after getting the approval of the Institute's Animal Ethics Committee.

CONFLICT OF INTEREST STATEMENT

Authors declare to have no conflict of interest.

AUTHOR CONTRIBUTIONS

Concept: GS, NMK; Design: GS, NMK; Data Collection or Processing: NMK; Analysis or Interpretation: GS, NMK; Literature Search: GS, NMK; Writing: NMK; Revision and Proofreading: GS, NMK.

FUNDING SOURCES

This study obtained financial support from the State Science and Technology programme of the Department of Science and Technology (DST), Ministry of Science and Technology, Govt. of India, New Delhi (DST/SSTP/Kerala/453).

ACKNOWLEDGMENTS

The authors thank Rajagiri College of Social Sciences (Autonomous), Kalamassery and Presentation College of Applied Sciences, Puthenvelikkara for the research support.

REFERENCES

1. King JC, Blumberg J, Ingwersen L, Jenab M, Tucker KL. Tree nuts and peanuts as components of a healthy diet. J Nutr, 2008;138:1736-1740. Doi: 10.1093/jn/138.9.1736S

2. Gorrepati K, Balasubramanian S, Chandra P. Plant based butters. J Food Sci Technol, 2015;52:3965-3976. Doi: 10.1007/s13197-014-1572-7

3. Jenkins DJA, Hu FB, Tapsell LC. Possible benefit of nuts in type-2 diabetes. J Nutr, 2008;138:1752-1756. Doi: 10.1093/jn/138.9.1752S

4. Mangels R. Guide to nut and nut butters. Vegetarian J, 2001;21:20-23.

5. Rahman MM, Sarker MT, Tumpa MAA, Yamin M, Islam T, Park MN, et al. Exploring the recent trends in perturbing the cellular signaling pathways in cancer by natural products. Front Pharmacol, 2022;13. Doi: 10.3389/fphar.2022.950109

6. Shah D, Gandhi M, Kumar A, Martins NC, Sharma R, Nair S. Current insights into epigenetics, noncoding RNA interactome and clinical pharmacokinetics of dietary polyphenols in cancer chemoprevention. Crit Rev Food Sci Nutr, 2021;63(12):1755-1791. Doi: 10.1080/10408398.2021.1968786

7. Rahman KMA. Effect of Pumpkin seed (*Cucurbita pepo* L.) diets on benign prostatic hyperplasia (BPH): Chemical and morphometric evaluation in rats. World J Chem, 2006;1:33-40.

8. Ortiz JMP, Alguacil LF, Salas E, Gutiérrez IH, Alonso SG, Martin CG. Antiproliferative and cytotoxic effects of grape pomace and grape seed extracts on colorectal cancer cell lines. Food Sci Nutr, 2019;7:2948-2957. Doi: 10.1002/fsn3.1150

9. Spiller GA, Miller A, Olivera K, Reynolds J, Miller B, Morse SJ, et al. Effects of plant-based diets high in raw or roasted almonds or roasted almond butter on serum lipoproteins in humans. J Am Coll Nut, 2003;22:195-200. Doi: 10.1080/07315724.2003.10719293

10. Abraham Z, Malik SK, Rao GE, Narayanan SL, Biju S. Collection and characterization of Malabar tamarind [*Garcinia cambogia* (Gaertn.) Desr.]. Genet Resour Crop Evol, 2006;53:401-406. Doi: 10.1007/s10722-004-0584-y

11. Madappa MB, Bopaiah AK. Preliminary phytochemical analysis of the leaf of *Garcinia gummi-gutta* from Western Ghats. IOSR J Pharm Biol Sci, 2012;4:17-27.

12. George S, Krishnakumar NM, Vincent L, Rini KT, Athira S, Agnesjini PJ, Ramesh B. Physicochemical characterization of *Garcinia gummi-gutta* (L.) Robs. seed oil. Int J Applied Biol Pharmaceut Technol, 2018;9:5-12. Doi: 10.21276/Ijabpt

13. Maheshwari B, Reddy YS. Application of Kokum (*Garcinia indica*) fat as cocoa butter improver in chocolate. J Science Food Agri, 2005;85:135-140. Doi: 10.1002/jsfa.1967

14. Sharmila KP, Vijaya R, Pushpalatha KC, Kumari NS. Phytochemical profile and *in vitro* antioxidant activity of *Garcinia gummi*-gutta (L.) peel extracts. J Biol Scientific Opinion, 2015;3:7-12.

15. Janakiraman S, Lakshmanan T, Chandran V, Subramani L. Comparative behavior of various nano additives in a diesel engine powered by novel *Garcinia gummi-gutta* biodiesel. J Cleaner Prod, 2020; 245:118940. Doi: 10.1016/j.jclepro.2019.118940

16. Rani MP, Raj MRG, Rameshkumar KB. *Garcinia gummi-gutta* seeds: a novel source of edible oils. J Sci Food Agri, 2021;102:3475-3479. Doi: 10.1002/jsfa.11671

17. Moldeus P, Hogberg J, Orrenius S. Isolation and use of liver cells. Methods Enzymol, 1978;52:60-71. Doi: 10.1016/s0076-6879(78)52006-5

18. Talwar GP. Hand Book of Practical Immunology. New Delhi: National Book Trust;1974.

19. Ramavarma SK, Unnikrishnan AP, Babu TD, Achuthan CR. *In vitro* cytotoxic and antiproliferative activities of *Uvaria narum* seed oil (UNSO). Int J Advanced Res, 2018;6:912-916. Doi: 10.21474/IJAR01/7751

20. Mosmann T. Rapid colorimetric assay for cellular growth and survival: application to proliferation and cytotoxicity assays. J Immunol Methods, 1983:65:55-63. Doi: 10.1016/0022-1759(83)90303-4

21. Cree IA. Cancer Cell Culture-Methods and Protocols. 2nd ed., New Jersey: Humana Press; 2011.

22. Nagalakshmi S, Saranraj P, and Sivasakthivelan P. Determination of minimum inhibitory concentration (MIC) and percentage bacterial growth inhibition of essential oils against gram positive bacterial pathogens. J Drug Deliv Ther, 2019;9:33-35. Doi: 10.22270/jddt.v9i3.2596

23. Moss CW, Lambert MA, Merwin WH. Comparison of rapid methods for analysis of bacterial fatty acids. Applied Microbiol, 1974;28:80-85. Doi: 10.1128/am.28.1.80-85.1974

24. Mazumder K, Biswas B, Raja IM, Fukase K. A review of cytotoxic plants of the Indian subcontinent and a broad-spectrum analysis of their bioactive compounds. Molecules, 2020;25:1904. Doi: 10.3390/molecules25081904

25. Wu SJ, Lin YX, Ye H. Prognostic value of alkaline phosphatase, gamma-glutamyl transpeptidase and lactate dehydrogenase in hepatocellular carcinoma patients treated with liver resection. Int J Surg, 2016;36:143-151. Doi: 10.1016/j.ijsu.2016.10.033

26. Thoison O, Fahy J, Dumontet V, Chiaroni A, Riche C, Tri MV, Sevenet T. Cytotoxic phenylxanthones from *Garcinia bracteata*. J Nat Prod, 2000; 63: 441-446. Doi: 10.1021/np9903088.

27. Saadat N, Gupta SV. Potential role of garcinol as an anticancer agent. J Oncol, 2012;2012:647206. Doi: 10.1155/2012/647206

28. Latha PG, Panikkar KR. Cytotoxic and antitumor principles from *Ixora coccinea* flowers. Cancer Lett, 1998;130:197-202. Doi: 10.1016/S0304-3835(98)00140-2

29. Kuete V, Karaosmanoglu O, Sivas H. Medicinal spices and vegetables from Africa. In: Kuete, V. ed. Medicinal Species and Vegetables from Africa: Therapeutic Potential against Metabolic, Inflammatory, Infectious and Systemic Diseases. 1st ed. USA: *Academic Press*, 2017.

30. Gest C, Joimel U, Huang L, Pritchard LL, Petit A, Dulong C, et al. Rac3 induces a molecular pathway triggering breast cancer cell aggressiveness: Differences in MDA-MB-231 and MCF-7 breast cancer cell lines. *BMC Cancer*, 2013;13:63. Kuete V, Karaosmanoglu O, and Sivas, H. Medicinal spices and vegetables from Africa. In: Kuete, V. ed. Medicinal Species and Vegetables from Africa: Therapeutic Potential against Metabolic, Inflammatory, Infectious and Systemic Diseases. 1st ed. USA: *Academic Press*, 2017. Doi: 10.1186/1471-2407-13-63

31. Chang TT, Fulford MH. Monolayer and spheroid culture of human liver hepatocellular carcinoma cell line cells demonstrate distinct global gene expression patterns and functional phenotypes. Tissue Engineering, 2009;15:559-567. Doi: 10.1089/ten.tea.2007.0434

32. Razak NA, Abu N, Ho WY, Zamberi NR, Tan AW, Alitheen NB, et al. Cytotoxicity of eupatorin in MCF-7 and MDA-MB-231 human breast cancer cells via cell cycle arrest, antiangiogenesis and induction of apoptosis. Sci Rep, 2019;9:1514. Doi: 10.1038/s41598-018-37796-w

33. Farag MA, Gad MZ. Omega-9 fatty acids: Potential roles in inflammation and cancer management. J Genet Engg Biotechnol, 2022;20:48. Doi: 10.1186/s43141-022-00329-0

34. Nelson R. Oleic acid suppresses over expression of ERBB2 oncogene. Lancet Oncol, 2005;6:69. Doi: 10.1016/s1470-2045(05)01722-5

35. Giulitti F, Petrungaro S, Mandatori S, Tomaipitinca L, de Franchis V, D'Amore A, et al. Anti-tumor effect of oleic acid in hepatocellular carcinoma cell lines via autophagy reduction. Front Cell Develop Biol, 2021;9. Doi: 10.3389/fcell.2021.629182

36. Nagavekar N, Kumar A, Dubey K, Singhal RS. Supercritical carbon dioxide extraction of kokum fat from *Garcinia indica* kernels and its application as a gelator in oleogels with oils. Ind Crops Prod, 2019;138:111459. Doi: 10.1016/j.indcrop.2019.06.022

37. Choppa T, Selvaraj CI, Zachariah A. Evaluation and characterization of Malabar tamarind [*Garcinia cambogia* (Gaertn.) Desr.] seed oil. J Food Sci Technol, 2015;52:5906-5913. Doi: 10.1007/s13197-014-1674-2

38. Nikolskaya E, Hiltunen Y. Determination of carbon chain lengths of fatty acid mixtures by time domain NMR. Appl Magnetic Resonance, 2018;49:185-193. Doi: 10.1007/s00723-017-0953-2

39. Utpala P, Nandakishore OP, Senthil KR, Nirmal BK. Chromatographic fingerprinting and estimation of organic acids in selected *Garcinia* species. Int J Innov Hortic, 2012;1:68-73.

40. Rameshkumar KB. Diversity of *Garcinia* Species in the Western Ghats: *Phytochem. Persp*. 1st ed. Jawaharlal Nehru Tropical Botanic Garden and Research Institute, Thiruvananthapuram, India. 2016.

41. Senyilmaz TD, Pfaff DH, Virtue S, Schwarz KV, Fleming T, Altamura S, et al. 9-dietary stearic acid regulates mitochondria *in vivo* in humans. Nat Commun, 2018;9:3129. Doi: 10.1038/s41467-018-05614-6

42. Gheda SF, Ismail GA. Natural products from some soil cyanobacterial extracts with potent antimicrobial, antioxidant and cytotoxic activities. Bras Academic Sci, 2020;92: e20190934 Doi: 10.1590/0001-3765202020190934

43. Li C, Zhao X, Toline EC, Seigal GP, Evans LM, Hashim AI, et al. Prevention of carcinogenesis and inhibition of breast cancer tumor burden by dietary stearate. Carcinogenesis, 2011;32:1251-1258. Doi: 10.1093/carcin/bgr092

44. Bennett AS. Effect of dietary stearic acid on the genesis of spontaneous mammary adenocarcinomas in strain A/ST mice. Int J Cancer, 1984;34:529-533. Doi: 10.1002/ijc.2910340416

45. Evans LM, Cowey SL, Siegal GP, Hardy RW. Stearate preferentially induces apoptosis in human breast cancer cells. Nutrition and Cancer, 2009; 61: 746-753. Doi: 10.1080/01635580902825597

46. Habib NA, Wood CB, Apostolov K, Barker W, Hershman MJ, et al. Stearic acid and carcinogenesis. British J Cancer, 1987;56:455-458. Doi: 10.1038/bjc.1987.223

47. Carrillo C, Cavia MM, Alonso TSR. Antitumor effect of oleic acid; mechanisms of action: a review. Nutrici Hospi, 2012;27:1860-1865. Doi: 10.3305/nh.2012.27.6.6010

48. da Silva LD, Nascimento M, Silva DHS, Furlan M, Bolzani VS. Antibacterial activity of a stearic acid derivative from *Stemodia foliosa*. Planta Med, 2002; 68:1137-1139. Doi: 10.1055/3-2002-36346

49. Shobier AH, Ghan, SAA, Barakat KM. GC/MS spectroscopic approach and antifungal potential of bioactive extracts produced by marine macroalgae. Egyptian J Aqu Res, 2016;42: 289-299. Doi: 10.1016/j.ejar.2016.07.003

50. Selvadoss PP, Nellore J, Ravindrran MB, Sekar U, Tippabathani J. Enhancement of antimicrobial activity by liposomal oleic acid-loaded antibiotics for the treatment of multidrug-resistant *Pseudomonas aeruginosa*. Artificial Cells, Nanomed Biotechnol, 2017; 46:268-273. Doi: 10.1080/21691401.2017.130720

Acta Pharm. Sci. Vol 62:(2), 2024
Research article
DOI: 10.23893/1307-2080.APS6226

Neuroprotective application of *Hemidesmus indicus* root extract and its silver nanoparticles implication against monosodium glutamate-induced neurotoxicity in albino rats

Mahesh CHINTHALA[1], Syed Sagheer AHMED[1], Ajay BANKAD VENKATESH[1]
Pooja RANGENAHALLI CHIDANANDA MURTHY[1], Ramesh BEVINHALLI[2]
Bharathi DODDLA RAGHUNATHANAIDU[1*]

1 Department of Pharmacology, Sri Adichunchanagiri College of Pharmacy, Adichunchanagiri University, B G Nagara, Karnataka, India

2 Department of Pharmaceutical Chemistry, Sri Adichunchanagiri College of Pharmacy, Adichunchanagiri University, B G Nagara, Karnataka, India

ABSTRACT

Monosodium glutamate (MSG) induced neurotoxicity is a typical experimental model used to lower memory in laboratory animals. *Hemidesmus indicus* (*H. indicus*) has been used to treat neurotoxicity in Ayurvedic and Unani medicines. The study aimed to assess the neuroprotective efficacy of *H. indicus* root extract and nanoparticles against MSG-induced neurotoxicity in albino rats. The effects of MSG on the brain include neurotoxicity, decreased acetylcholine in rat brains, increased oxidative stress, and increased acetylcholinesterase (AChE) levels after MSG administration. The behavioral, biochemical, and neuroanatomical abnormalities caused by MSG were reduced after treatment with *H. indicus* root extract and its silver nanoparticles (AgNPs) for 21 days. Our study reveals that both the extract and NPs were protecting the rat brain

*Corresponding author: Bharathi DODDLA RAGHUNATHANAIDU
E-mail: rambha.eesh@gmail.com
ORCIDs:
Mahesh CHINTHALA: 0009-0008-4432-875X
Syed Sagheer AHMED: 0000-0001-9817-9747
Ajay BANKAD VENKATESH: 0009-0002-4446-693X
Pooja RANGENAHALLI CHIDANANDA MURTHY: 0000-0003-2625-3711
Ramesh BEVINHALLI: 0000-0002-2551-234X
Bharathi DODDLA RAGHUNATHANAIDU: 0000-0002-5250-9760
(Received 12 Jul 2023, Accepted 3 Oct 2023)

against the harmful effects of MSG such as loss of memory and cognitive decline by controlling AChE activity and oxidative stress. AgNPs of *H. indicus* root extract proved extremely significant activity as compared to the extract alone.

Keywords: monosodium glutamate, behavioral impairment, acetylcholinesterase, *Hemidesmus indicus*

INTRODUCTION

Neurotoxicity usually alters the functioning of the central nervous system. It may result in permanent or reversible nerve tissue damage that finally leads to neuronal death.

Grey matter diseases known as neurodegenerative diseases are defined by the progressive death of neurons from particular brain regions. This disorder causes major medical and social issues[1].

Neuroprotection is the body's defense mechanisms and strategies designed to protect the central nervous system from injury caused by both acute and chronic neurological conditions, such as dementia, Parkinson's disease, Alzheimer's disease and epilepsy. Dementia, also known as Alzheimer's disease, is a long-term cognitive and emotional condition that affects a person's ability to function normally[2]. The prevalent type of dementia is Alzheimer's disease, which is characterized as a neurotoxin disorder that most frequently causes memory loss and cognitive deterioration[3]. Alzheimer's disease affects an estimated 50 million people globally and is projected to affect 152 million people by 2050[4]. Monosodium glutamate (MSG) is one of the most commonly used flavor enhancers and a controversial food additive, found in almost all types of fast foods, packed Chinese food, soups, canned vegetables and processed meats. MSG is sodium salt of a naturally occurring non-essential amino acid L glutamic acid and is the most abundant amino acid found in nature[5]. Monosodium glutamate administration led to acute increase in intracerebroventricular and hippocampal glutamate concentrations. Glutamate, which is released from about 40% of synapses in the central nervous system, is the most prevalent excitatory neurotransmitter in the brain. Along with playing a crucial role as a neurotransmitter, glutamate may also act as a powerful neurotoxin to neurons when levels are too high. It is still unknown how cells die, despite the fact that glutamate-induced cell death is linked to both apoptotic and necrotic changes. The excitotoxic pathway and the oxidative pathway are two distinct pathways for glutamate-induced cell death that have each been described. The excito-

toxic pathways involve excessive glutamate receptor activation, which causes both quickly triggered and gradually triggered cytotoxic events[6]. The extract and nanoparticles of *H. indicus* prevents monosodium glutamate induced neurotoxicity due to its anti-oxidative property. The neuroprotective activity of *H. indicus* might be due to the presence of various phytochemical constituents such as β-sitosterol, tannins, saponins, flavonoids, alkaloids and higher content of phenols and free amino acids[7].

The multidisciplinary nature of nanotechnology makes it one of the fastest-growing fields of science[8].As AgNPs have attracted significant attention because of their unique properties and potential uses in a wide spectrum of application and various features such as stable morphology, less particle size, high surface-to-volume ratio, high bioavailability and useful chemical properties relating to surface and cell penetration capability which can be useful for many purposes[9]. AgNPs are found to be metal nanoparticles with a large absorption band[10]. Due to their specific physical and chemical characteristics, AgNPs are used in many kinds of industrial and medicinal applications. AgNPs have attractive physicochemical properties, low toxicities, the ability to generate a wide range of nano structure, and low manufacturing costs. Additionally, AgNPs have electronegativity, optical properties, and biological properties[11,12]. Indian Sarsaparilla, also known as *H. indicus* (Asclepiadaceae), is a popular plant that may be found in India. It is frequently utilised in Indian traditional medicine, and its medicinal uses have been studied extensively[13]. *H. indicus* is widely used as a traditional folk remedy and is also an ingredient of Ayurveda and Unani medicinal products aganist various diseases such as rheumatism, kidney and urinary disorders, diarrhoea, skin issues and asthma. It has also been reported for its neuroprotective activity[14]. A systematic literature survey has not yielded scientific evidence to prove the neuroprotective activity of AgNPs of *H. indicus* root. So, the present study aims to evaluate the neuroprotective efficacy of *H. indicus* root extract and its AgNPs in MSG-induced neurotoxicity in albino rats.

METHODOLOGY

Plant material

The roots of *H. indicus* were collected From the Bellary district. The roots were authenticated by Dr. Pradeep, Department of Dravyaguna, Sri Dharmasthala Manjunatheshwara college of Ayurveda and Hospital, Hassan, Karnataka, India (Voucher Number of the plant: SDMCAH-DG/2023/03). The collected roots were washed, dried, subjected for size reduction into a coarse powder and stored in an airtight container at room temperature for further usage.

Preparation of extract

The roots of *H. indicus* were extracted by cold maceration method using 70% ethanol. Roots residue was removed from the extract using Whatman No. 1 filter paper. The obtained clear extract was stored in a refrigerator for further investigation[15].

Preparation of nanoparticles

A 250 mL volumetric flask contains 180mL of silver nitrate solution (1mM) and 20mL of *H. indicus* root extract was swirled twice for 5min at room temperature using a magnetic stirrer. After one week, the colour change indicates the presences of AgNPs. Then, a UV-spectrophotometer was used to assess absorbance (200 to 700 nm). After the reaction was finished, the solution was centrifuged at 5000rpm for 15min at 40°C. The pellet that had collected in the tubes bottoms was removed and dried for 5hrs in a hot air oven at 80°C[16].

Zeta potential

A zeta potential study was conducted to determine the surface charge of the prepared material and its stability *H. indicus* AgNPs. Method used to determine the Zeta potential is dynamic light scattering (DLS) with Malvern-Model Zeta sizer Nano ZSP which is used to control the stability of the sample[17].

Fourier Transform Infrared Spectroscopy (FTIR)

In order to identify the sample functional groups, we used the (Shimadzu 8400S, Shimadzu, Kyoto Japan) FTIR, and the FTIR measurements were made to determine the silver ions and compounds responsible for reducing silver nitrate to AgNPs. The sample was then placed on ATR and analyzed using FT-IR[18].

Scanning Electron Microscopy (SEM) analysis

SEM was utilized to determine the surface structure of the bio-generated AgNPs (Hitachi s3400n, Japan)[10].

Experimental animals

This study involved female Wistar rats that weighed between 150-180 gms. The rats were taken from an approved breeder and kept at a temperature of 24 to 28°C. The cages were sterilized, and the animals were kept for 21 days. They were given a regular pellet diet with water *adlibtum*[19]. The Institutional Animal Ethics Committee approved the study, which was done at the Sri Adichunchanagiri college of Pharmacy in Karnataka, India (Approval No: SACCP-IAEC/2022-02/66).

Experimental design

Fourth two animals were divided into seven groups with six in each group.

Group 1- Normal control (received vehicle)

Group 2- Received MSG (2g/kg) from 8th to 21days with no extract

Group 3- Received Piracetam (140mg/kg) + MSG (2g\kg) for 21 days

Group 4- Received *H. indicus* root extract for 21 days (300mg\kg) + MSG (2 g\kg) from 8th to 21st day

Group 5- *H. indicus* root extract for 21 days (150mg\kg) +MSG (2 g\kg) from 8th to 21st day

Group 6- AgNPs of *H. indicus* root extract for 21 days (50mg\kg) + MSG (2 g\kg) from 8th to 21st day

Group 7- AgNPs of *H. indicus* root extract for 21 days (100mg\kg) + MSG (2 g\kg) from 8th to 21st day

Morris Water Maze (MWM) (San Diego Instruments, United States)

Before the research began, all laboratory animals were given 3days of training. Within the study target quadrant (Q4) of this pool, a submerged platform was positioned 1cm below the water surface. Each rat was dropped into the water in a different spot between the quadrants, facing the wall of the pool. They were then given 120sec to find the submerged platform. The platform location remained stable during the event. For 4days (days 5, 8 and 14) each animal had two consecutive trials with a 5min gap between them. During these trials, the animal was allowed to run onto the hidden platform and remain there for 20sec. On the 21st day, the platform was removed and rats were assigned a position in any one of the three quadrants (Q1, Q2, or Q3) and given 120 sec to explore the target quadrant. As a measure of memory, the typical amount of time spent in the target quadrant (Q4) in search of the missing platform was recorded[20].

Novel object recognition

The experimental set-up for the object recognition task includes an open field box made of black acrylic that is 40 by 40 by 40 cm in size. The behavior test was conducted under low red-light illumination. Before the initiation of the project, all laboratory animals underwent training, each with a different starting position for 1week. MSG was given to lab animals on day 8 for 21 days, and then *H. indicus* was given on day 1 to 21 days. The things to be distinguished

were a toy Lego set, a novel object and two identical clear cultured flasks with water. The day before the trial, each rat got habituated to the open field box for 10min without any objects. On the day of the experiment, each rat was allowed to investigate two identical objects (transparent cultured flasks filled with water) for 5min in the 1st trial. One of the training session old objects was swapped out for a new one, and the rat was given 2min to investigate the new ones. The time spent near each object was recorded. When they were shown during the test session, the two items had different textures, colors, and sizes. Between runs, the open field box was cleaned with 70% ethanol to reduce fragrance remnants. The formula [TB / (TA + TB)*100] was used to determine the recognition index, where TA and TB stand for the length of time spent examining known object A and novel object B respectively. A rat was considered to have explored an object when it touched it with its forepaws or nose[21].

Preparation of brain supernatant

On day 22, animals were sacrificed by cervical dislocation and the brain was isolated. The brain was cleaned with 0.9% saline and stored on ice. The brain was then blotted with filter paper. The brain and hippocampus were extracted, and the cerebrum was homogenized (20% w/v) in cold phosphate buffer. The homogenate (pH 8 = 0.1M) was centrifuged at 3000rpm for 10min at 4°C. The cloudy supernatant fluid was used to calculate brain acetylcholinesterase activity[22].

Estimation of acetyl cholinesterase (AChE) activity

The Ellman method was used to evaluate the AChE activity. The test sample contains 0.05mL of supernatant. 3mL of sodium phosphate buffer Acetylthiocholine iodine 0.1 mL of acetylthioquinolone DTNB 1mL of Ellman reagent. Perkin Elmer lambda 20 spectrophotometer was used to measure the change in absorbance at 412nm for 2min at 30sec intervals[23].

Histopathological analysis

For histopathological studies, the brain was separated and preserved in a 10% formalin solution[24].

Statistical analysis

The data were presented as Mean ± SEM and statistically significant ($p < 0.001$). ANOVA (analyses of variance) was used to compare groups and Tukey's test was used to determine *p*-values.

RESULTS and DISCUSSION

Around 50 million people worldwide suffer from Alzheimer's disease and by 2050, the total population is projected to triple every five years to reach 152 million[4]. Monosodium glutamate produces a specific taste called umami through activation of the TAS1R1-TAS1R3 in the tongue. Due to its unique taste, the use of MSG is increased worldwide. Monosodium glutamate is problematical so it should be used with limitations according to the permissible amounts stated by different organizations to avoid its adverse effects[25]. The presence glutamic acid is responsible for triggering neuronal migration and differentiation, synaps remodeling and long-term potentiating, yet excessive concentration of this compound may cause neuronal death. In the recovery trial of the Morris water maze test, the MSG-induced rat took longer to find the hidden platform, which is a sign of memory impairment, according to our findings. The Novel objective recognition test suggested that the Piracetam, *H. indicus* root extract, nanoparticles group rats significantly reduced the amount of time spent in the novel object when compared to the MSG-treated group. Levels of acetylcholinesterase in *H. indicus* demonstrated that MSG administration substantially increased the activity of acetylcholinesterase in rats compared to the control group. Additional evidence came from the abnormal brain structure, which also shows that MSG has caused memory impairment and the involvement of certain brain regions in cognitive functions. In Treatment with *H. indicus* extract, nano-particles resulted in an increase in pyramidal cells and a decrease in cytoplasm vacuolation. Our results showed that *H. indicus* extract and its nano-particles, treated the memory impairment caused by MSG, while maintaining brain structure and preventing neurodegeneration, by reducing brain AChE activity and oxidative stress. Histological analysis of the brains of the MSG-treated rats revealed observable vacuolar changes, oedema and modest signs of inflammation in cortical regions in comparison with the control group. When compared to *H. indicus* extract and silver nanoparticles, the silver nanoparticles have higher levels of neuroprotective action.

Fourier Transfer Infra-Red rays

The FTIR spectrum was observed within a range of 4000-500 cm^{1} and it indicates that the *H. indicus* AgNPs contains numerous functional groups that serve as reducing and stabilizing agents before the synthesis of NPs. The different peaks of *H. indicus* are represented in Figure 1 and Table 1.

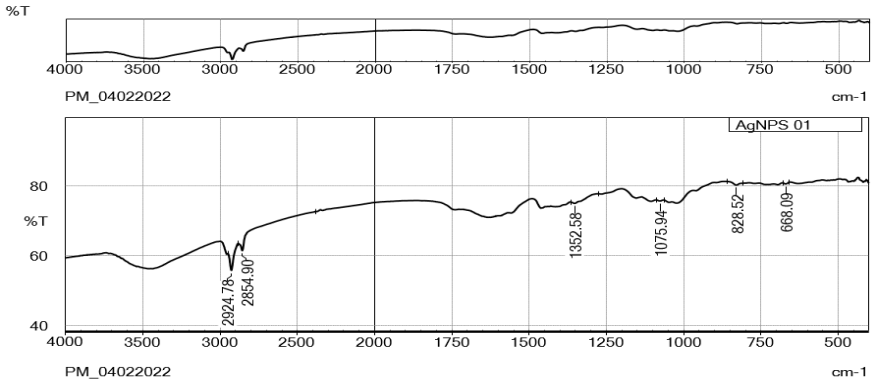

Figure 1. Structural features of the *H. indicus*AgNPs by FTIR spectrum

Table 1. Wave number and functional groups of *H. indicus*AgNPs

Wave numbers (cm-1)	Assignments
2924.78	OH(Broad)
2854.90	C6H6O
1351.16	C≡C (week)
1075.61	Mononuclear aromatics
828.52	Oxirane ring
668.09	Benzene (Ring bending bands)

Zeta potential

The surface charge of the produced NPs and the stability of the synthesized NPs were determined in a zetapotential investigation. A clear signal was observed at -8mv, which can be observed in Figure 2, suggesting that the synthesized NPs had good stability. This indicates that intermediate stability is attributed to the presence of capping molecules on the surfaces of biosynthesis-based Ag-NPs, which are predominantly composed of negatively-charged groups (Table 2). It is speculated that the incorporation of components such as proteins or flavonoids into AgNPs is responsible for the reduction in metal ions and the successful stabilization of the AgNPs.

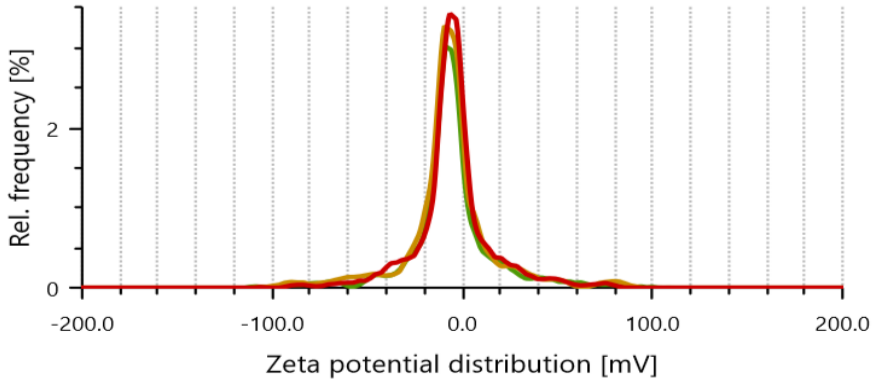

Figure 2. Zeta potential of the *H. indicus*AgNPs

Table 2. Mean zeta potential, conductivity, adjusted voltage and processed runs

Sl.No	Mean zeta pot. [mV]	Electroph. Mobil. [µm*cm/ Vs]	Conductivity [mS/cm]	Adjusted voltage [V]	Processed runs
1	-8.0	-0.4137	3.707	10.0	140
2	-8.3	-0.4332	3.704	10.0	100
3	-7.7	-0.4015	3.706	10.0	120

Scanning electron microscopy

The SEM analysis of the AgNPs from *H. indicus* showed morphological homogeneity in the AgNPs distribution on the grid surface. Although spherical NPs of various sizes tend to prevail, SEM displays an abundance of NPs with a range of shapes. The synthesized AgNPs were found to have an average size of 73.2 nm as shown in Figure 3.

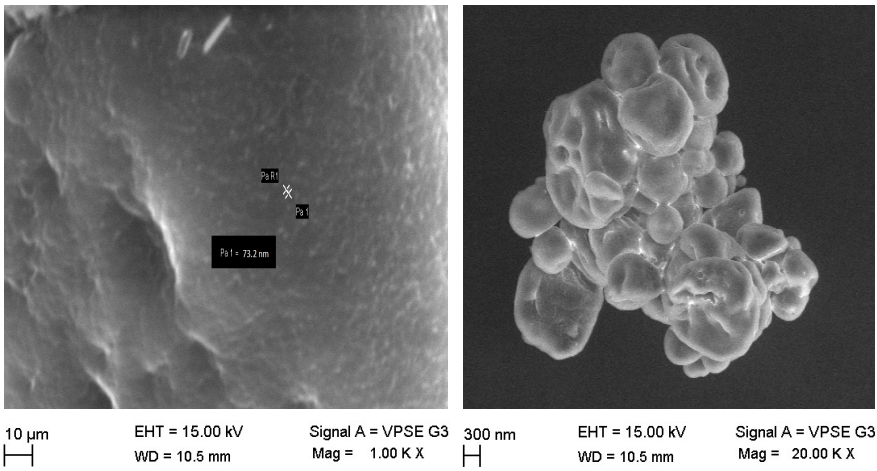

Figure 3. SEM image shows the shape of variable size of AgNPs

Morris Water Maze

The acquisition latency for reaching the visual platform was considerably delayed in MSG-treated rats is compared to the control group, demonstrating memory impairments. On days 5, 8 and 14, the *H. indicus* extract (150 and 300mg/kg) and its AgNPs (50 and 100mg/kg) treatment enhanced memory function (reduced mean acquisition latency) in the MSG-treated group significantly. After training, the visible platform was maintained 1cm below the waterline. In comparison with the control group, the MSG treatment significantly increased the mean acquisition latency and retention latency (days 5, 8 and 14 respectively) to reach the hidden platform which has been depicted in Figure 4 and Figure 5. These findings imply that MSG significantly impaired cognitive function. Furthermore, compared to animals treated with MSG, *H. indicus* roots extract and AgNPs administration significantly boosted memory recall on days 5, 8 and 14 respectively. On the 21st daytime spent in the target quadrant by the NPs-treated group showed highly significant activity as compared with inducer alone. The activity is highly significant in *H. indicus* AgNPs as compared to *H. indicus* extract alone. The data is given in Table 3 and Table 4.

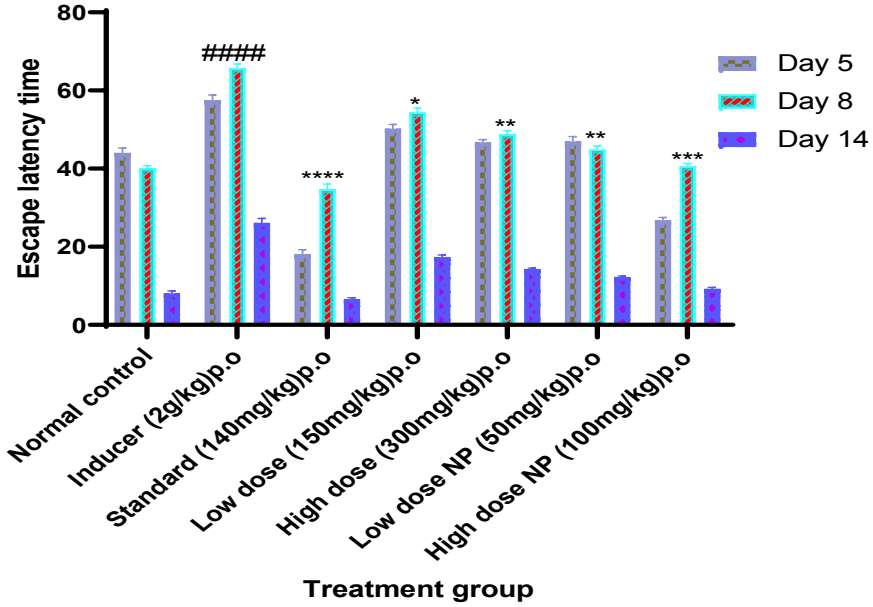

Figure 4. Effect of *H. indicus* on escape latency time (ELT) of rats by using Morris Water Maze on the 5, 8 and 14 days

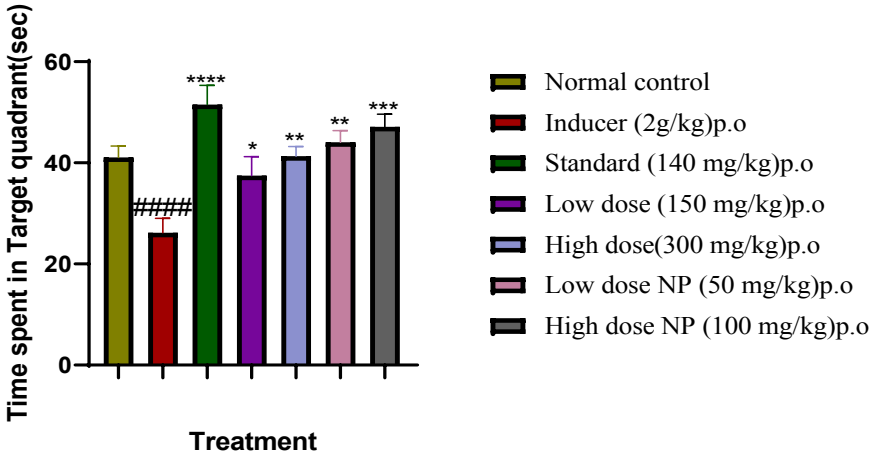

Figure 5. The effect of *H. indicus* on time spent in the target quadrant of rats by using MWM on 21th day

Table 3. Effect of *H. indicus* on escape latency time (ELT) of rats by using Morris Water Maze on the 5, 8, 14 days

Group No	Treatment	ELT (sec) Mean±S.E.M [n=6]		
		On 5th day	On 8th day	On 14th day
1	Control	44.0 ± 1.309	40.13 ± 0.6331	8.117 ± 0.5755
2	Monosodium glutamate (2g/kg)	57.52 ± 1.295	65.68 ± 1.093	26.13 ± 1.152
3	Piracetam (140mg/kg) + MSG (2g/Kg)	18.10 ± 1.179****	34.77 ± 1.279****	6.583 ± 0.3635****
4	Plant extract treated (150 mg/kg) + MSG (2g/Kg)	50.23 ± 1.099*	54.37 ± 1.144 *	17.37 ± 0.4888*
5	Plant extract treated (300 mg/kg) + MSG (2g/Kg)	46.70 ± 0.7131**	48.87± 0.8582**	14.28 ± 0.2354**
6	AgNPs treated (50mg/Kg) + MSG (2g/Kg)	46.93 ± 1.262**	44.87± 0.8982**	12.28 ± 0.2354**
7	AgNPs treated (100mg/Kg) + MSG (2g/Kg)	26.77 ± 0.6965***	40.60 ± 0.6814***	9.250 ± 0.3293***

The behavioral analysis was compared to an inducer control group (monosodium glutamate). The data are presented as Mean ± SEM, n = 6, and statistical analysis is conducted using a Two-way (ANOVA) followed by a Tukey's test. *p<0.05, **p<0.01 ***p<0.001compared to an inducer control group (monosodium glutamate).

Table 4. Effect of *H. indicus* on time spent in the target quadrant of rats by using Morris Water Maze on the 21st day

Group No	Treatment	TSTQ Mean±S.E.M [n=6]
1	Control	41.05 ± 0.8660
2	Monosodium glutamate (2g/kg)	26.18 ± 1.066
3	Piracetam (140mg/kg) + MSG (2g/kg)	51.50 ± 1.443****
4	Plant extract treated (150mg/kg) +MSG (2g/kg)	37.48 ± 1.412*
5	Plant extract treated (300mg/kg) + MSG (2g/kg)	41.33 ± 0.7127**
6	AgNPs treated (50mg/kg) + MSG (2g/kg)	44.07 ± 0.8706**
7	AgNPs treated (100mg/kg) + MSG (2g/kg)	47.13 ± 0.9349***

The behavioural analysis was compared to an inducer control group. The data are presented as Mean ± SEM, n = 6, and statistical analysis is conducted using a Two-way (ANOVA) followed by a Tukey's test. *p<0.05, **p<0.01 ***p<0.001compared to an inducer control group (monosodium glutamate).

Novel object recognition

Piracetam, *H. indicus* extract and *H. indicus* AgNPs significantly decreased the time spent by the rat near the novel object when compared to the MSG-treated group, as depicted in Figure 6. Rat's acceptance of novelty is usually measured using the discrimination index, as depicted in Figure 7. The MSG-treated group of rats showed poor object recognition as compared to the normal control group. MSG-induced rats treated with piracetam, *H. indicus* extract and its AgNPs spent more time near the novel object. Treatment also increased the object recognition ability in rats. *H. indicus*AgNPs possess highly marked activity as compared to extract alone. The data is shown in Table 5 and Table 6.

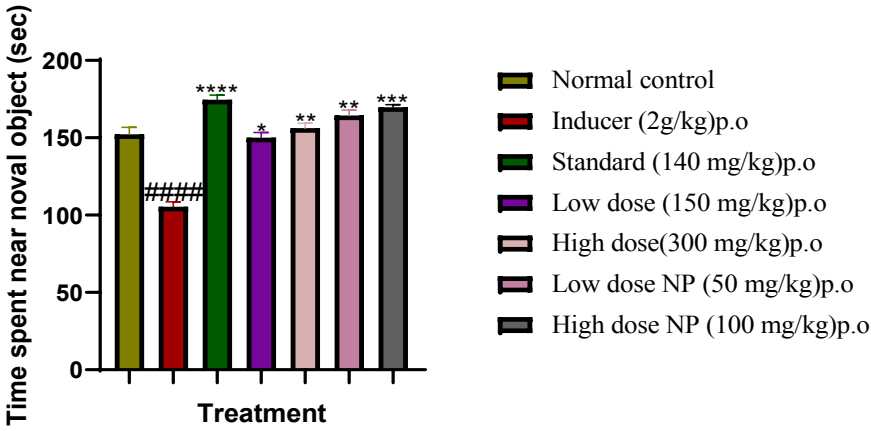

Figure 6. Effect of *H. indicus* on Time spent near novel object of rats by using NOR test

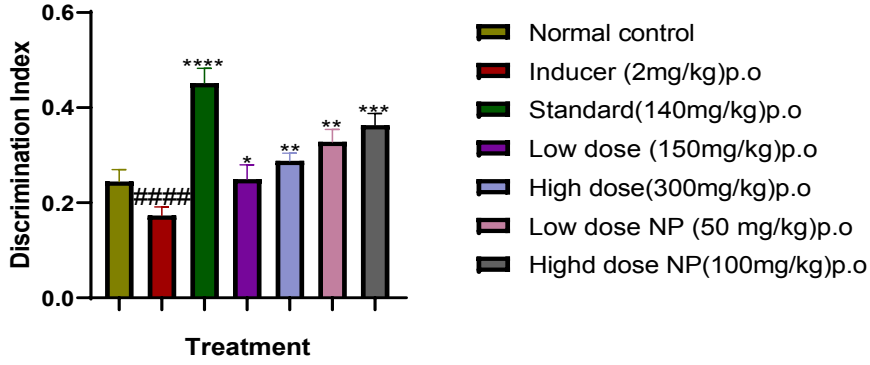

Figure 7. Effect of *H. indicus* on Discrimination index of rats by using NOR test

Table 5. Effect of *H. indicus* on time spent near novel object of rats by using Novel Objective Recognition test

Group No	Treatment	Time spent near novel object Mean±S.E.M [n=6]
1	Control	152.2 ± 1.751
2	Monosodium glutamate (2g/kg)	105.4 ± 1.218
3	Piracetam (140mg/kg) + MSG (2g/kg)	174.6 ± 1.132****
4	Plant extract treated (150mg/kg) +MSG (2g/kg)	150.1 ± 1.235*
5	Plant extract treated (300mg/kg) + MSG (2g/kg)	156.3 ± 1.159**
6	AgNPs treated (50mg/kg) + MSG (2g/kg)	164.4 ± 1333**
7	AgNPs treated (100mg/kg) + MSG (2g/kg)	169.8 ± 0.5378****

The behavioral analysis was compared to an inducer control group (monosodium glutamate). The data are presented as Mean ± SEM, n = 6, and statistical analysis is conducted using a Two-way (ANOVA) followed by a Tukey's test. *p<0.05, **p<0.01 ***p<0.001 compared to an inducer control group (monosodium glutamate).

Table 6. Effect of *H. indicus* on discrimination index of rats by using Novel Objective Recognition test

Group No	Treatment	Discrimination (DI) Mean ± S.E.M [n=6]
1	Control	0.2450 ±0.0094
2	Monosodium glutamate (2g/kg)	0.1733 ±0.0067
3	Piracetam (140mg/kg) + MSG (2g/kg)	0.4517 ±0.01184****
4	Plant extract treated (150mg/kg) +MSG (2g/kg)	0.2500 ±0.0059*
5	Plant extract treated (300mg/kg) + MSG (2g/kg)	0.2883 ±0.00594**
6	AgNPs treated (50mg/kg) + MSG (2g/kg)	0.3283 ±0.00986**
7	AgNPs treated (100mg/kg) + MSG (2g/kg)	0.3633 ±0.009172***

The behavioral analysis was compared to an inducer control group (monosodium glutamate). The data are presented as Mean ± SEM, n = 6, and statistical analysis is conducted using a Two-way (ANOVA) followed by a Tukey's test. *p<0.05, **p<0.01 ***p<0.001compared to an inducer control group (monosodium glutamate).

Acetylcholine assays

The Acetylcholine esterase activity was greatly increased in MSG treated rats as compared to normal control rats. In comparison to MSG induced rats, *H. indicus* root extract and its nanoparticles therapy continuously reduced acetylcholine esterase activity as shown in Figure 8 and Table 7.

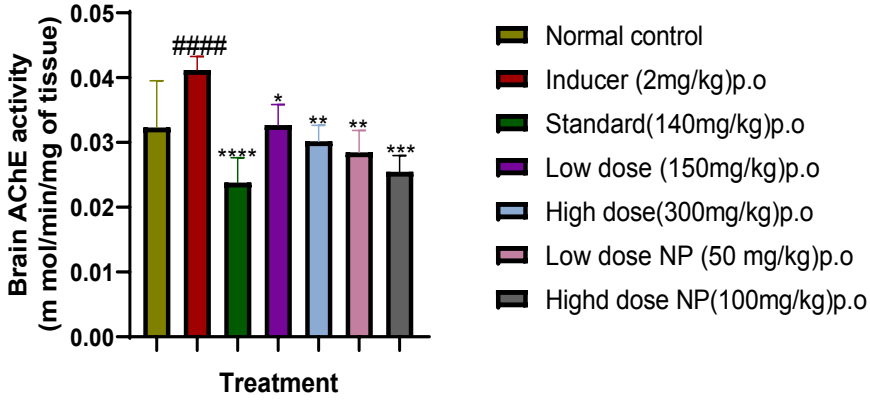

Figure 8. Effect of HI on AChE on rat brain

Table 7. Effect of *H. indicus* on AChE of rats

Group No.	Treatment	AChE Mean ± S.E.M [n=6]
1	Control	0.0323 ± 0.00272
2	Monosodium glutamate (2g/kg)	0.04117 ± 0.00079
3	Piracetam (140mg/kg) + MSG (2g/kg)	0.02383 ± 0.00143****
4	Plant extract treated (300mg/kg) +MSG (2g/kg)	0.03267 ± 0.001208*
5	Plant extract treated (150mg/kg) + MSG (2g/kg)	0.03017 ± 0.0009365**
6	AgNPs treated (100mg/kg) + MSG (2g/kg)	0.02850 ± 0.001268**
7	AgNPs treated (50mg/kg) + MSG (2g/kg)	0.0255 ± 0.0009449***

The behavioral analysis was compared to an inducer control group (monosodium glutamate). The data are presented as Mean ± SEM, n = 6, and statistical analysis is conducted using a Two-way (ANOVA) followed by a Tukey's test. *p<0.05, **p<0.01 ***p<0.001compared to inducer control (monosodium glutamate).

Histopathological examination (Brain cell)

- Normal Control-there are no intracellular spaces, cells are linearly arranged, no shrunken cells and well-organized pyramidal cells were observed (Figure 9-A).
- Inducer (MSG)-there are more intracellular spaces, cells are not linearly arranged, pyramidal cells are unorganized, and cells are more shrunken (Figure 9-B).

- Standard (piracetam)-no intracellular spaces, cells are linearly arranged, no shrunken cells observed, pyramidal cells are well organized (Figure 9-C).
- *H. indicus* extract low dose-there are adequate intercellular spaces were observed and cells are well organized, less shrunken cells (Figure 9-D).
- *H. indicus* extract High dose-there are adequate intercellular spaces were observed and cells are well organized, less shrunken cells (Figure 9-E).
- *H. indicus*AgNPs low dose-there are adequate intercellular spaces were observed and cells are well organized, less shrunken cells (Figure 9-F).
- *H. indicus*AgNPs low dose-adequate intercellular spaces were observed and cells are well organized, less shrunken cells, and cell morphology changes are not seen (Figure 9-G).

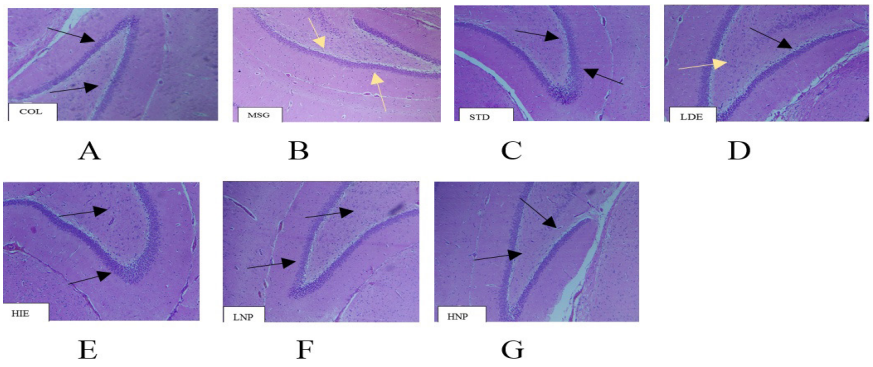

Figure 9. Histopathological Observation, (A):normal control, (B):Monosodium glutamate (inducer 2g/kg(p.o)), (C):Piracetam (standard 140mg/kg(p.o)), (D):Low Dose 150mg/kg(p.o), (E):High dose 300mg/kg(p.o), (F):Low dose nanoparticle 50mg/kg(p.o), (G):High dose Nanoparticle 100mg/kg(p.o).

Black- Normal pyramidal cells observed, less intercellular spaces and the cells are linearly arranged, no apoptosis is observed. Yellow- Pyramidal cells are shrunken, more intercellular spaces are observed, and cells morphology changes are shown.

This study shows that MSG treatment in rats causes behavioral and cognitive abnormalities as well as histological and biochemical alterations in the brain. Our results showed that therapy with *H. indicus* roots extract and nano-particles lowers MSG-induced behavioral and cognitive impairment and reduces neurotoxicity. *H. indicus* root extract and nano-particles also help to decrease the effects of MSG-induced oxidative stress and AChE activity in the brain. These results suggest that *H. indicus* enhances cholinergic transmission and

decreases oxidative stress to protect against neurodegeneration in the brain and maintain memory and cognitive functioning. The neuroprotective potential of *H. indicus* silver nanoparticles were higher than the extract alone. Further study is required to exactly understand how the phytoconstituents of *H. indicus* roots interact with biochemical pathways in the brain to the presence of its neuroprotective activity.

STATEMENT OF ETHICS

The animal experiments were approved by the Institutional Animal Ethics Committee (IAEC) at Sri Adichunchanagiri College of Pharmacy, B.G Nagara, under the approval number SACCP-IAEC/2022-02/66. The procedures adhered to the guidelines set forth by the Committee for the Control and Supervision of Experiments on Animals (CCSEA), India.

CONFLICT OF INTEREST STATEMENT

The authors declare that they have no competing interests.

AUTHOR CONTRIBUTIONS

MC: Design, acquisition of data, analysis of data, drafting of manuscript, statistical analysis. PRC: Design, acquisition of data. SSA: Design, critical review of manuscript, supervision. ABV: Design, plant collection and authentication. BDR, BR: Design, critical review of manuscript, supervision.

ACKNOWLEDGMENTS

We thank the management of Sri Adichunchanagiri College of Pharmacy, Adichunchanagiri University for providing infrastructural support.

REFERENCES

1. Crofton KM, Bassan A, Behl M, Chushak YG, Fritsche E, Gearhart JM, et al. Current status and future directions for a neurotoxicity hazard assessment framework that integrates in silico approaches. Comput Toxicol, 2022;22:100223. Doi: 10.1016/j.comtox.2022.100223

2. Piers R, Albers G, Gilissen J, De Lepeleire J, Steyaert J, Van Mechelen W, et al. Advance care planning in dementia: recommendations for healthcare professionals. BMC Palliat Care, 2018;17:1-7. Doi: 10.1186/s12904-018-0332-2

3. DeTure MA,Dennis WD. The neuropathological diagnosis of alzheimer's disease. Mol Neurodegener,2019;14:1-18. Doi: 10.1186/s13024-019-0333-5

4. Pooja RC,BharathiDR. Elementary pathophysiology, treatment, risk factor of alzheimer's sisease. Int Res J Mod Eng Technol Sci, 2022;4:1381-1398. Doi: 10.56726/IRJMETS30873

5. Hashem HE,El-Din Safwat MD,Algaidi S.The effect of monosodium glutamate on the cerebellar cortex of male albino rats and the protective role of vitamin C. J Mol Hist, 2012;43:179-186. Doi: 10.1007/s10735-011-9380-0

6. Khalil RM, Khedr NF. Curcumin protects against monosodium glutamate neurotoxicity and decreases NMDA2B and mGluR5 expression in rat hippocampus. Neurosignals, 2018;24(1):81-87. Doi: 10.1159/000442614

7. Das S, Bisht SS. The bioactive and therapeutic potential of *Hemidesmus indicus* root. Phytother Res, 2013;27:791-801. Doi: 10.1002/ptr.4788

8. Sheikh FA, Barakat NA, Kanjwal MA, Nirmala R, Lee JH, Kim H, et al. Electrospun titanium dioxide nanofibers containing hydroxyapatite and silver nanoparticles as future implant materials. J Mater Sci Mater Med, 2010;21:2551-2259. Doi: 10.1007/s10856-010-4102-9

9. Marin S, Mihail Vlasceanu G, Elena Tiplea R, Raluca Bucur I, Lemnaru M, Minodora Marin M, Mihai Grumezescu A. Applications and toxicity of silver nanoparticles: a recent review. Curr Top Med Chem, 2015;15(16):1596-1604. Doi: 10.2174/1568026615666150414142209

10. NagarajaS, Ahmed SS, GoudanavarP, Fattepur S, Meravanige G, Shariff A, et al. Green Synthesis and Characterization of Silver Nanoparticles of *Psidium Guajava* Leaf Extract and Evaluation for Its Antidiabetic Activity. Molecules, 2022;27:4336. Doi: 10.3390/molecules27144336

11. Zhang XF, Liu ZG, Shen W, Gurunathan S. Silver Nanoparticles: Synthesis, Characterization, Properties, Applications, and Therapeutic Approaches. Int J Mol Sci, 2016;17(9):1534. Doi: 10.3390/ijms17091534

12. Almatroudi A. Silver nanoparticles: Synthesis, characterization and biomedical applications. Open Life Sci, 2020;15(1):819-839. Doi: 10.1515/biol-2020-0094

13. Das S, Singh Bisht S. The bioactive and therapeutic potential of *Hemidesmus indicus* root. Phytother Res, 2013;27:791-801. Doi: 10.1002/ptr.4788

14. Lakshman K, Shivaprasad HN, Jaiprakash B, Mohan S. Anti-inflammatory and antipyretic activities of *Hemidesmus indicus* root extract. Afr J Tradit Complement Altern Med, 2006;3(1):90-94. Doi: 10.4314/ajtcam.v3i1.31143

15. Mehta A, Sethiya NK, Mehta C, Shah GB. Anti–arthritis activity of roots of *Hemidesmus indicus* in rats. Asian Pac J Trop Med, 2012;5(2):130-135. Doi: 10.1016/S1995-7645(12)60011-X

16. Keshari AK, Srivastava R, Singh P, Yadav VB, Nath G. Antioxidant and antibacterial activity of silver nanoparticles synthesized by *Cestrum nocturnum*. J Ayurveda Integr Med, 2020;11(1):37-44. Doi: 10.1016/j.jaim.2017.11.003

17. Heflish AA, Hanfy AE, Ansari MJ, Dessoky ES, Attia AO, Elshaer MM, et al. Green biosynthesized silver nanoparticles using *Acalypha wilkesiana* extract control root-knot nematode. J King Saud Univ Sci, 2021;33(6):101516. Doi: 10.1016/j.jksus.2021.101516

18. Hussein UK, Hassan NE, Elhalwagy ME, Zaki AR, Abubakr HO, Nagulapalli Venkata KC, et al. Ginger and propolis exert neuroprotective effects against monosodium glutamate-induced neurotoxicity in rats. Molecules, 2017;22(11):1928. Doi: 10.3390/molecules22111928

19. Hamza RZ, Al-Salmi FA, El-Shenawy NS. Evaluation of the effects of the green nanoparticles zinc oxide on monosodium glutamate-induced toxicity in the brain of rats. Peer J, 2019;23:7460. Doi: 10.7717/peerj.7460

20. Hamza RZ, Al-Salmi FA, Laban H, El-Shenawy NS. Ameliorative role of green tea and zinc oxide nanoparticles complex against monosodium glutamate-induced testicular toxicity in male rats. Curr Pharm Biotechnol, 2020;21(6):488-501. Doi: 10.2174/138920102066619 1203095036

21. Bhuvanendran S, Kumari Y, Othman I, Shaikh MF. Amelioration of cognitive deficit by embelin in a scopolamine-induced Alzheimer's disease-like condition in a rat model. Front Pharmacol, 2018;9:665. Doi: 10.3389/fphar.2018.00665

22. Pooja RC, Bharathi DR. *Benincasa hispida* reversed D-galactose-induced oxidative stress and neurodegeneration-mediated cognitive impairment in aged rats. Int J in Pharm Sci, 2023;1:150-164. Doi: 10.21203/rs.3.rs-3387639/v1

23. Hazarika I, Mukundan GK, Sundari PS. Neuroprotective effect of *Hydrocotyle sibthorpioides* against monosodium glutamate-induced excitotoxicity. J Nat Prod, 2022;36(23):6156-6159. Doi: 10.1080/14786419.2022.2057493

24. Pandey A. A glimpse into the Indian traditional medicine with special reference to use of *Hemidesmus indicus* in Southern India: A review. Inter J Theor Appl Sci, 2021;13(1):73-79.

25. Niraimathee VA, Subha V, Ravindran RE, Renganathan S. Green synthesis of iron oxide nanoparticles from *Mimosa pudica* root extract. Int J Environ Sci, 2016;15(3):227-240. Doi: 10.1504/IJESD.2016.077370

Acta Pharm. Sci. Vol 62:(2), 2024
Research article
DOI: 10.23893/1307-2080.APS6227

Evaluation of fluconazole-loaded nanocellulose-reinforced xanthan gum film for drug delivery applications

Vipin JAIN[1], Rimpy PAHWA[2], Rashmi SHARMA[1], Munish AHUJA[1*]

1 Drug Delivery Research Laboratory, Department of Pharmaceutical Sciences, Guru Jambheshwar University of Science and Technology, Hisar-125001, Haryana, India

2 Amity Institute of Pharmacy, Amity University, Noida-201303, Uttar Pradesh, India

ABSTRACT

The purpose of the present study is to prepare xanthan films reinforced with nanocellulose and to evaluate them for drug delivery applications using fluconazole as the model drug. The preparation of films by solvent casting method was optimized using a central composite design. It was observed that increasing the concentration of nanocellulose and polyethylene glycol 4000 increases the tensile strength and delays the release of fluconazole from xanthan gum films. The optimal formulation was composed of nanocellulose (100 mg), polyethylene glycol 4000 (50 mg), and xanthan gum (100 mg) which exhibited the tensile strength of 4220 mN and 100% release of the drug over 24 h. The film had a fibrous surface. The film released fluconazole by zero-order kinetics by super case II transport mechanism. It can be concluded based on the present study that reinforcement of nanocellulose in xanthan gum films improves their tensile strength and imparts sustained release character.

Keywords: fluconazole, nanocellulose, film, xanthan gum, sustained drug delivery

*Corresponding Author: Munish AHUJA
E-mail: munishahuja17@yahoo.co.in
ORCIDs:
Vipin JAIN: 0009-0003-8569-5496
Rimpy PAHWA: 0000-0003-2087-1105
Rashmi SHARMA: 0000-0002-9364-9188
Munish AHUJA: 0000-0001-6723-140X
(Received 23 May 2023, Accepted 9 Oct 2023)

INTRODUCTION

Xanthan gum is an extracellular microbial heteropolysaccharide produced by the bacterium *Xanthomonas campestris*. It is composed of dual pentameric units including two glucose units, two mannose units, and a glucuronic acid in the ratio of 2.8:2.0:2.0[1,2]. Xanthan gum is a high molecular weight long-chain polysaccharide with functional groups[3-5]. Due to its special rheological properties, it has been widely used as stabilizing, suspending, thickening, and emulsifying agent in various industries. Xanthan gum is also used in film formation with appropriate gloss[6]. Various researchers have focused on preparing the xanthan gum-based composite films using sodium alginate, carrageenan, gum Arabic, polyvinyl alcohol, pullulan, and hydroxypropyl methylcellulose[6-9]. Xanthan gum-based film formulations have been employed for a number of applications such as mucoadhesive buccal film[10,11], buccal patch[2], orodispersible film[12], mouth dissolving films[13], transdermal patch[14], dermal dressings[15], and as antibacterial film[1].

Nanocellulose is defined as the nano-scaled cellulosic material having a diameter in the range of 1-100 nm. Depending upon the method of synthesis, source, dimension, composition, and properties, the nanocellulose is referred to as cellulose nanofibers, bacterial cellulose, and cellulose nanocrystals[16,17]. A great number of reported articles show that nanocellulose-reinforced polymeric composite films have a lot of properties like design flexibility, tolerability, high mechanical strength of the film, and easy processing which makes these composites highly usable in food packaging, automotive, biotechnological, and pharmaceutical industries[18-23]. As per earlier reports nanocellulose, as reinforcing agent in the starch-based composites provided the high aspect ratio, improved mechanical properties, and high Young's modulus[24,25]. Most of the studies of nanocellulose reinforced chitosan films, emphasized on enhancement of mechanical properties and preservation of the antibacterial property of the films[26,27]. It is also reported that when alginate-based films were reinforced with nanocellulose, the tensile strength, and thermal stability were increased while water vapor permeability was decreased[28]. Gelatin films with nanocellulose reinforcement showed an improvement in mechanical properties as well as oxygen gas barrier properties[29]. The incorporation of nanocellulose in polyvinyl alcohol-based composite films much improved the barrier properties and mechanical strength of the films[30,31]. In one of the research projects, nanocellulose reinforcement in polyvinyl alcohol film exhibited outstanding UV-blocking property[32]. Some crystalline nanocellulose products have also shown sustained drug release behaviour[16]. Xanthan gum and nanocellulose are reported to possess mucoadhesive properties[10,20,23].

Nanocellulose-reinforced xanthan gum film may be potentially useful as food packaging material, UV-blocking film, antimicrobial film, transdermal patch, mucoadhesive buccal or vaginal film, buccal patch, and dermal dressing. To the best of our comprehension, no report has been made on the nanocellulose-reinforced xanthan gum film. Therefore, the purpose of this study was to observe the changes in the physicochemical characteristics and release behaviour of xanthan gum by reinforcing with nanocellulose using fluconazole as the model drug. The two-factor three-level central composite experimental design was employed to obtain the optimized batch of film. The prepared polymeric films were characterized further utilizing many characterization techniques such as thickness, tensile strength, surface pH, swelling capability, Fourier transform-infrared spectroscopy (FT-IR), X-ray diffraction (XRD), scanning electron microscopy (SEM), and *in vitro* drug release study for drug delivery applications.

METHODOLOGY

Materials

Rice nanocellulose (α-cellulose = 91.78%, mol. wt. = 1.16 x 10^7 g/mol, particle size = 441.7 nm) was isolated from rice straw as per the previously reported literature and used for the present study[33]. Fluconazole was received as a gift sample from Hetero Drugs Ltd. (Hyderabad, India). Xanthan gum, sodium hydroxide, and glacial acetic acid were purchased from Sisco Research Laboratories Pvt. Ltd. (Maharashtra, India). Sodium hypochlorite was obtained from Loba Chemie Pvt. Ltd. (Mumbai, India). Polyethylene glycol 4000 (PEG) was procured from Thomas Baker (Chemicals) Pvt. Ltd. (Mumbai, India). Disodium hydrogen orthophosphate and sodium dihydrogen orthophosphate were purchased from High Purity Laboratory Chemicals Pvt. Ltd. (Mumbai, India). Glycerine and oxalic acid were procured from Central Drug House Pvt. Ltd. (Delhi, India).

Extraction of rice nanocellulose

Initially, rice straws were collected from agricultural land and washed properly using water to remove dirt and other impurities. The extraction process of nanocellulose consists of three steps. In the first step, 10 g of rice straws were taken and cut into small pieces. The pieces of straws were placed into a 1000 mL beaker and then treated with sodium hydroxide solution (5% w/v) for 6 h under mechanical stirring. The slurry was filtered and washed with distilled water. The washing step was repeated five times for the complete removal of lignin and hemicellulose. In the next step, the rice pulp was treated with 10 mL of sodium hypochlorite and 1 mL of glacial acetic acid under mechanical stirring for 6 h, followed by washing with distilled water. This step was repeated till the pulp be-

came white in color. In the last step, the obtained white pulp was treated with 5 g of oxalic acid and stirred continuously for the time interval of 6 h. Thus, the obtained nanocellulose was washed with distilled water for 2 to 3 times to remove any other chemical impurities and subjected to deep freezing at -40 °C for drying. The dried nanocellulose was stored in an airtight container for further use[33].

Preparation of fluconazole-loaded xanthan-nanocellulose film

The fluconazole-loaded polymeric film was prepared by employing the solvent casting method. Initially, a definite amount of xanthan gum was weighed and swelled in distilled water for 24 h. In an aqueous solution of fluconazole, a pre-weighed quantity of nanocellulose and PEG was added and stirred up to 4 h. Then, the nanocellulose dispersion was mixed with swelled xanthan gum and stirred continuously for 2 h. The prepared fluconazole-loaded xanthan-nanocellulose solution was poured into a Petri dish and dried in a hot air oven at 50 °C for 36 h. The obtained fluconazole-loaded xanthan-nanocellulose film (XNF) was stored in a desiccator for further characterization and evaluation. For comparative evaluation, native fluconazole-loaded xanthan film (XF) and fluconazole-loaded nanocellulose film (NF) were also prepared.

Experimental design

A two-factor, three-level central composite experimental design was applied to examine the effect of different parameters in preparation for appropriate formulation by using Design Expert Software (trial version 11.0.0, Stat-Ease Inc., Minneapolis, MN). The amount of nanocellulose (25-100 mg, X_1) and amount of PEG (15-50 mg, X_2) were selected as independent variables whereas, tensile strength (Y_1) and *in vitro* release (Y_2) were taken as response variables. Thirteen batches were prepared as per the software and entries of independent variables were coded as low (-1), medium (0), and high (+1). Analysis of variance (ANOVA) was used to determine the R^2 value (coefficient of determination), adjusted R^2 value, predicted R^2 value, adequate precision, coefficient of variance, and lack of fit values.

Characterizations of film

Physicochemical properties

Percent moisture content

To calculate the percentage of moisture absorbed by the formulation, the precise weight of a dried film was measured (W_0). The pre-weighed film was introduced into a chamber with a constant relative humidity of 75% at a temperature of 40 °C, where it remained for a period of 72 h[34]. Then the weight of the film was calculated again (W_t). Then, the percentage of moisture content was determined using the following equation 1:

$$\% \text{ Moisture content} = \frac{W_t - W_o}{W_o} \times 100 \qquad (1)$$

Average weight

Three pieces of the film (2 cm × 2 cm) were cut and weighed individually using a digital weighing balance. The average weight was calculated and expressed as mean ± standard deviation.

Film thickness

The thickness of the film is the important parameter that ensures the content uniformity of the prepared film. The thickness was measured at different edges by using Vernier Caliper (YAMAYO® Classic, Japan) and the average thickness was calculated[35].

Tensile strength

The tensile strength measures the maximum force applied to the point at which the film breaks. The film (2×2 cm^2) was taken and hung between two clamps attached with a hardness tester (VG-500, Vin Syst Technologies, India), and load or force was applied at the lower end. The force was noted at which the film broke. This test was performed three times for accurate results and an average reading was noted.

Surface pH

The pH of the surface was identified by selecting the random sections of films (1 cm^2) and allowing them to swell in 5 mL of distilled water. Then the pH was measured by using a digital pH meter (pH Testr 10, Eutech Instruments, Singapore)[36].

Swelling study

The swelling property of XF, NF, and XNF was determined in distilled water, HCl buffer (pH 1.2), and phosphate buffer (pH 6.8)[37]. The prepared films were cut into small pieces, weighed (W_1), and placed individually into solvent-containing Petri dishes. The weights of swelled films (W_2) were measured at different time intervals by removing excess surface liquid with the help of tissue paper and the swelling percentage was calculated using the following equation 2:

$$\text{Swelling } \% = \frac{W_2 - W_1}{W_1} \times 100 \qquad (2)$$

Fourier-Transform Infrared Spectroscopy (FT-IR)

The FT-IR spectra of fluconazole, XF, NF, and XNF were estimated using an FT-IR spectrophotometer (Spectrum Two, PerkinElmer Spectrum®, US) for the detection of the functional groups in the prepared film. The sample was mixed with potassium bromide with the help of a mortar and pestle. The pellet was prepared by direct compression using an IR hydraulic press at the pressure of 50 kg/cm^2 (IR Hydraulic Press CAP-15T, PCI Analytics, Mumbai, India). The IR spectrum was recorded in the range of 4000-400 cm^{-1}.

X-Ray Diffraction (XRD)

XRD is used to determine the nature of a solid whether it is crystalline, amorphous, or semicrystalline. XRD of fluconazole, XF, NF, and XNF were investigated by using different kinds of radiations (Cu, Kα, Kβ) at room temperature (25 °C) by using an XRD instrument (Miniflex 600, Rigaku Corporation, Tokyo, Japan). The XRD pattern was analyzed at a range of scattering angle 2θ (10° to 80°) at a speed of 2°/min.

Scanning Electron Microscopy (SEM)

SEM was used for the determination of the surface topography and morphology of the film. XNF was coated with gold in a sputter coater (DII-29030SCTR, Smart Coater, JEOL, USA) to suppress the charging effects in an electron microscope. The micrographs of the film were captured at different magnifications (100X, 500X, 5000X, and 10000X) in JSM-7610FPLUS, JEOL, Japan.

Drug content (%)

An accurately weighed amount of film (25 mg) was dissolved in 25 mL of distilled water, followed by filtration. The filtrate was diluted appropriately and the drug content in the filtrate was determined by measuring the absorbance in a UV spectrophotometer at λ_{max} 260 nm[33,38].

In vitro release study

The *in vitro* release study of fluconazole was performed by using a paddle-type apparatus (USP Type II). A weighed amount of film (50 mg) was placed at the bottom of beakers separately and covered with wire mesh of stainless steel to avoid film floating at the dissolution surface. A definite amount of phosphate buffer (pH 6.8, 900 mL) was taken as the dissolution medium, and the temperature was maintained at 37 ± 0.5 °C with a dissolution speed of 50 rpm for 24 h. An aliquot of 5 mL was withdrawn at different time intervals and replaced with a fresh dissolution medium to maintain the sink condition. The collected

samples were analyzed using a UV spectrophotometer (USP-II, TDI-08L, Electrolab, Mumbai, India) at a wavelength of 260 nm, absorbance was noted and the cumulative percentage of drug release was calculated. The release data was fitted into four different drug release kinetic models i.e., zero-order (% cumulative release vs time), first-order [log(100-% cumulative release) vs time], Higuchi model (% cumulative release vs square root time), and Korsmeyer Peppas model (log % cumulative release *vs* log time). Further, the obtained equation of the plots and the value of the coefficient of determination (R^2) were compared.

RESULTS and DISCUSSION

Preparation of fluconazole-loaded xanthan-nanocellulose film

In this study, the isolated nanocellulose and xanthan gum were utilized further to develop a sustained-release film of fluconazole. As per the earlier literature, cellulose has been widely used in drug delivery applications due to its various properties like biocompatibility, biodegradability, hydrophilicity, rheological properties, and high mechanical strength. Various cellulose derivatives such as cellulose ethers (methylcellulose, hydroxypropyl methyl cellulose, and ethyl cellulose) and nanocellulose are being used as strengthening or reinforcing agents in different studies. However, cellulose ethers are chemically modified cellulose while nanocellulose is nano-sized cellulose free from lignin and hemicellulose[16]. The literature also shows that the presence of hydrogen bonds in nanocellulose enhances the material stiffness and postpones the initiation and evolution of damage with a somewhat reduction in the brittleness of the polymer[33]. In the earlier reports, rice nanocellulose was evaluated for the *in-vitro* cytotoxicity property by using HeLa and SiHa cell lines and results showed 100% cell viability of HeLa and SiHa cells revealing the non-cytotoxicity of rice nanocellulose[39]. In this study, the polymeric films were prepared by employing the solvent casting method. In the xanthan gum film, extracted nanocellulose was utilized as reinforcing material, and PEG and fluconazole were used as a plasticizer and antifungal model drug respectively. The films were prepared by drying at 50 °C, as the films do not dry properly at low temperature. Moreover, it is also mentioned in the literature that drying of nanocellulose-based composite films at high temperature (50-100 °C) improves the tensile strength of the films as compared to the films dried at low temperatures[40]. The experimental design was also implemented for getting an optimized batch of the XNF. XF and NF were also prepared by the same process for the comparative study. The diagrammatic representation of the preparation of XNF has been shown in Figure 1.

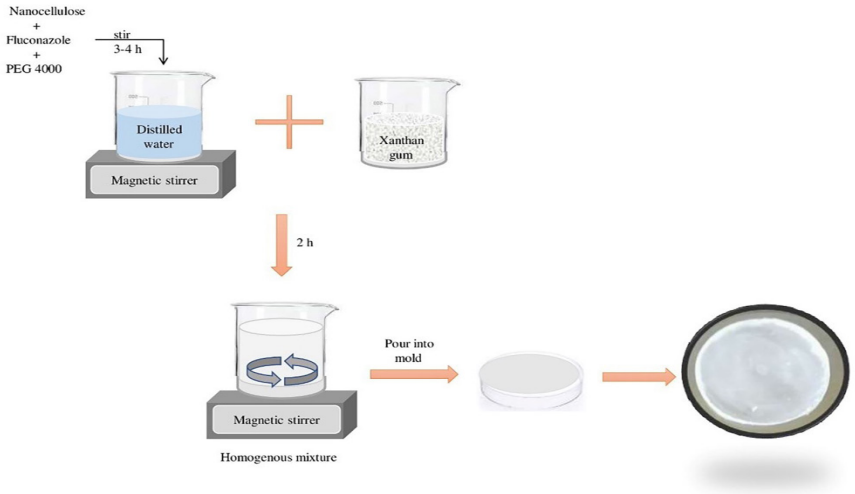

Figure 1. Schematic representation of preparation of fluconazole-loaded xanthan-nanocellulose film

Experimental design

The preliminary trials suggested that the concentration of nanocellulose and PEG highly influenced the drug release property and tensile strength of the composite film. Therefore, in this study, the amount of nanocellulose and PEG were taken as independent variables while drug release (%) and tensile strength (mN) were taken as dependent variables. Table 1 shows the responses obtained from thirteen trial runs generated by the two-factor three-level central composite experimental design.

Table 1. Experimental values of the tensile strength (mN) and cumulative drug release (%) of XNF

Formulations	X_1 (mg)	X_2 (mg)	Y_1 (mN)	Y_2 (%)
F1	25	15	1100	79.27
F2	25	32.5	1330	76.6
F3	25	50	2100	72.73
F4	62.5	15	2200	63.79
F5	62.5	32.5	2800	57.82
F6	62.5	50	2860	59.46
F7	100	15	2330	50.74
F8	100	32.5	3230	53.7
F9	100	50	4580	46.76
F10	62.5	32.5	2360	57.5
F11	62.5	32.5	2430	59.77
F12	62.5	32.5	2400	58.84
F13	62.5	32.5	2700	65.39

X_1-amount of nanocellulose, X_2- amount of PEG, Y_1-tensile strength (mN), Y_2-cumulative drug release (%)

The responses were fitted into multiple polynomial models using Design Expert® software. It was found that response Y_1 (tensile strength) was best fitted into the two-factor interaction (2FI) model while response Y_2 (% release) was best fitted into the quadratic model without transformation. Equations 3 and 4 showed the relationship between independent variables and response variables.

$$Y_1 = 60.72 - 12.40X_1 - 2.98X_2 - 0.1125X_1X_2 + 3.26X_2^2$$

$$Y_2 = 2493.85 + 935.00X_1 + 651.76X_2 + 312.50X_1X_2$$

Table 2 represents the ANOVA results which indicate that polynomial models are significant with a '*non-significant*' lack of fit. The R^2 values of both models were found more than 0.9, depicting the better quality of models, and the difference between adjusted and predicted R^2 values was found less than 0.2, showing the reasonable difference between actual and predicted values.

Table 2. ANOVA results

Response factor	Model					Lack of fit	
	R^2	Adjusted R^2	Predicted R^2	Adequate precision	C.V.%	F-value	p-value
Y_1	0.9342	0.9122	0.8105	22.5994	10.15	2.1300	0.2414
Y_2	0.9546	0.9221	0.8547	17.2934	04.22	0.4772	0.7152

Figure 2 (a) and (b) showed the effect of nanocellulose and PEG on tensile strength and % drug release. As shown in Figure 2a, an increase in tensile strength was observed by increasing the concentration of nanocellulose and PEG. However, the cumulative drug release of formulation decreases as the amount of nanocellulose and PEG increases as depicted in Figure 2b. This may be due to the high surface area and porous nature of nanocellulose[25].

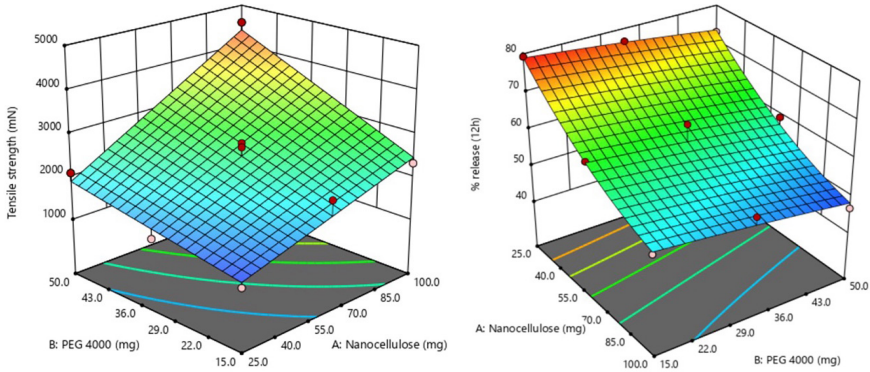

(a) **(b)**

Figure 2. Response surface plots showing the combined effect of the amount of nanocellulose and PEG on (a) tensile strength and (b) % release.

The numerical optimization tool suggested the optimal concentration of nanocellulose and PEG to formulate an optimized batch of XNF (batch F9). The optimized batch of XNF containing nanocellulose (100 mg), PEG (50 mg), xanthan gum (100 mg), and fluconazole (30 mg) releases the fluconazole (46.76%) in a sustained manner (12 h) with high tensile strength (4580 mN). The batches of XF (xanthan gum – 100 mg, PEG – 50 mg, fluconazole – 30 mg) and NF (nanocellulose – 100 mg, PEG – 50 mg, fluconazole – 30 mg) were also prepared for comparative analysis and further characterized.

Characterization of films

Various physicochemical, structural, and mechanical characterization studies

of XF, NF, and XNF such as thickness, tensile strength, surface pH, swelling index, drug content, and *in vitro* release of films were performed for drug delivery applications.

Physicochemical characterizations

The results of physicochemical characterizations of XF, NF, and XNF are given in Table 3. As shown in Table 3, no significant difference was observed in terms of weight uniformity, thickness, and surface pH. The % moisture content of XF, NF, and XNF was calculated to be 10 ± 1.5%, 1 ± 0.4%, and 2 ± 0.7% respectively, indicating that reinforcing the xanthan film with nanocellulose reduces the moisture absorption. The average weight of XF, NF, and XNF was found to be in range of 48.9-51.2 mg. The thickness of XF, NF, and XNF was found in the range of 2.12-2.68 mm whereas the surface pH of the polymeric film was found in the range of 6.7-7.0. However, the tensile strength of the nanocellulose-reinforced polymeric film was found more than six-fold in contrast to native xanthan and nanocellulose films which revealed the high mechanical strength of XNF due to the incorporation of nanocellulose.

Table 3. Physiochemical characterization of films

Batch	Moisture content (%)	Average weight (mg)	Thickness (mm)	Tensile strength (mN)	Surface pH
XF	10 ± 1.5	51.2±1.5	2.44±0.2	700±10.1	6.7±0.2
NF	01 ± 0.4	48.9±0.4	2.12±0.1	230±4.5	7.0±0.1
XNF	02 ± 0.7	50.3±0.6	2.68±0.2	4220±15.7	6.9±0.2

Figure 3 (a-c) shows the results of a swelling study of XF, NF, and XNF in 0.1 N HCl (1.2 pH), phosphate buffer solution (6.8 pH), and distilled water. The XF showed faster swelling in water (1 h) and 0.1 N HCl (2 h) with swelling in the range of 3300-3400% and then started to erode while in phosphate buffer pH 6.8, film swelled continuously up to 7 h with swelling of 2800% and then remained constant up to 20 h. After 20 h, XF started to erode in the phosphate buffer. Film erosion may be due to the hydrophilic property of both xanthan gum and nanocellulose which tends to dissolve or disperse in the swelling medium[41]. The swelling pattern of NF was found to be similar to XF, with a high percent swelling in water and 0.1 N HCl than phosphate buffer pH 6.8. In water and 0.1 N HCl film swelled up to 2 h and then started to erode but in buffer solution film swelled up to 10 h and then became constant. XNF swelling pattern was similar in all media -water, 0.1 N HCl, and buffer solution with swelling up

to 1h followed by a slight drop in swelling up to 3 h and then remained stable up to 24 h. The swelling percentage of XNF was higher in water as compared to 0.1 N HCl and buffer solution. Further, it can be observed that reinforcing the xanthan films with nanocellulose limited their erosion.

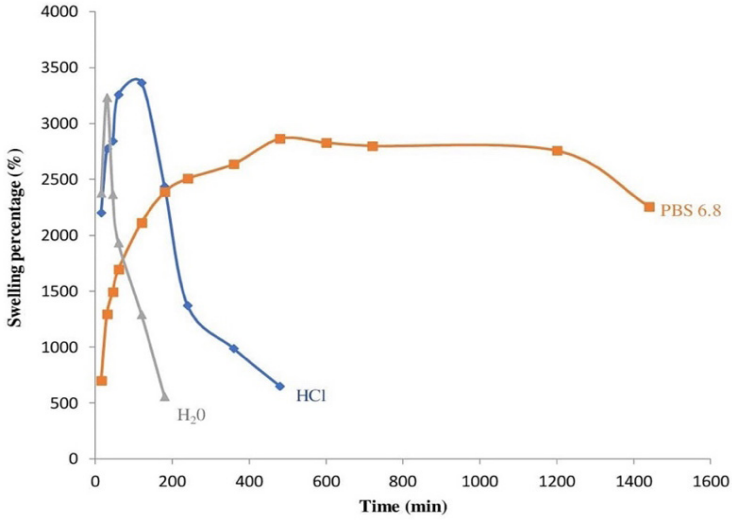

(a)

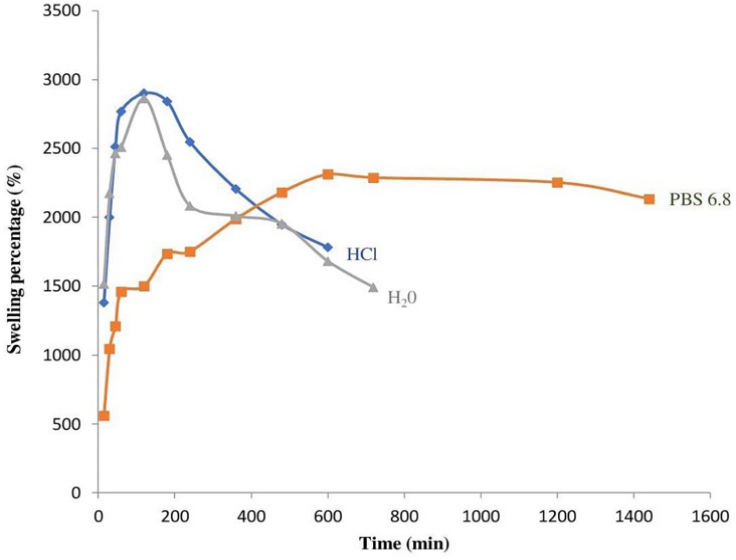

(b)

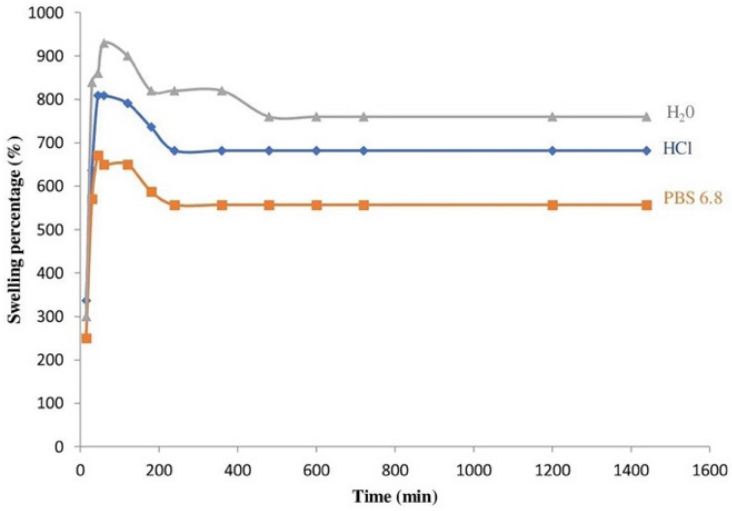

(c)

Figure 3. Swelling property of (a) XF, (b) NF, and (c) XNF in distilled water, HCl, and phosphate buffer

FT-IR

The FT-IR spectra of fluconazole, XF, NF, and XNF have been shown in Figure 4. Fluconazole shows an absorption band at 3444.16 cm^{-1} due to O-H stretching vibrations. Peaks at 1621.29 cm^{-1} and 1515.77 cm^{-1} occurred due to the C=C stretching. The sharp peaks at 1503.48 cm^{-1} and 1418.55 cm^{-1} represented the triazole ring stretching. Peaks at 1272.93 cm^{-1}, 1138.68 cm^{-1} and 1074.82 cm^{-1} exhibited the C-F stretch, triazole ring stretch, and ring bending mode of fluconazole respectively. The peak at 1020.18 cm^{-1} indicated the presence of a C-H aromatic ring. The peaks at 967.66 cm^{-1} and 846.59 cm^{-1} depicted the C-H of the triazole ring present in fluconazole[33]. FT-IR spectrum of XNF showed a characteristic peak at 3447.77cm^{-1} which represents the O-H stretching. The peaks at 1640.15 cm^{-1}, 1566.39 cm^{-1}, and 1415.05 cm^{-1} occurred due to C=O stretching of the carboxylate group, C=O of enols, and –COO stretch respectively. These peaks are also present in XF and NF spectra with slight differences in the peak positions. The peak shown at 1021.18 cm^{-1} at the low depth indicated that fluconazole was incorporated with xanthan gum. A peak at 643.92 cm^{-1} is also associated with -COO stretch[33,42,43]. The spectrum of XNF confirms the presence of fluconazole and reinforcement with rice nanocellulose.

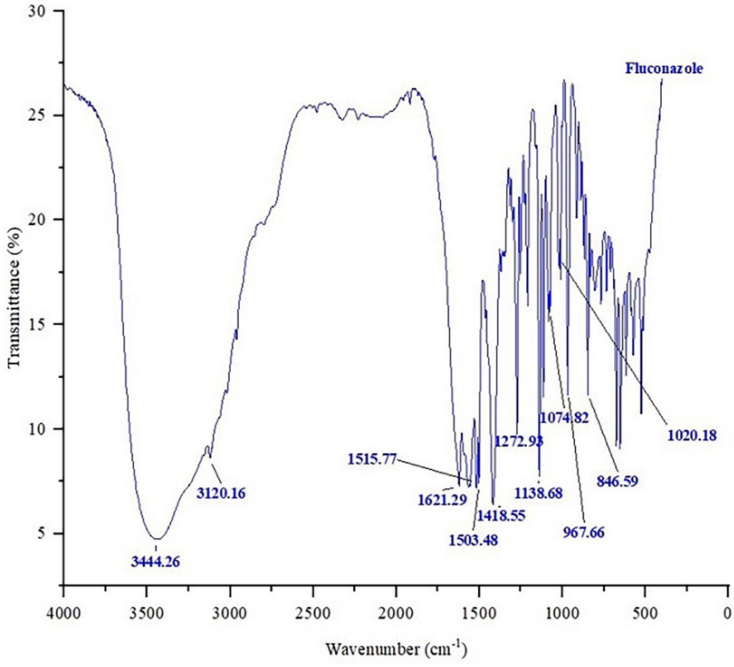
Fluconazole
Transmittance (%)
Wavenumber (cm-1)
3444.26
3120.16
1515.77
1621.29
1503.48
1418.55
1272.93
1138.68
1074.82
967.66
846.59
1020.18

(a)

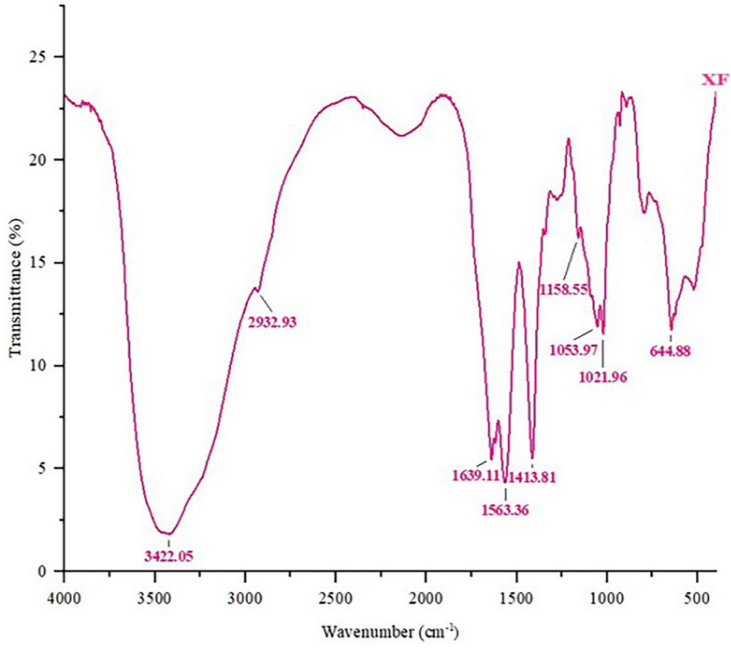
XF
Transmittance (%)
Wavenumber (cm-1)
3422.05
2932.93
1639.11
1563.36
1413.81
1158.55
1053.97
1021.96
644.88

(b)

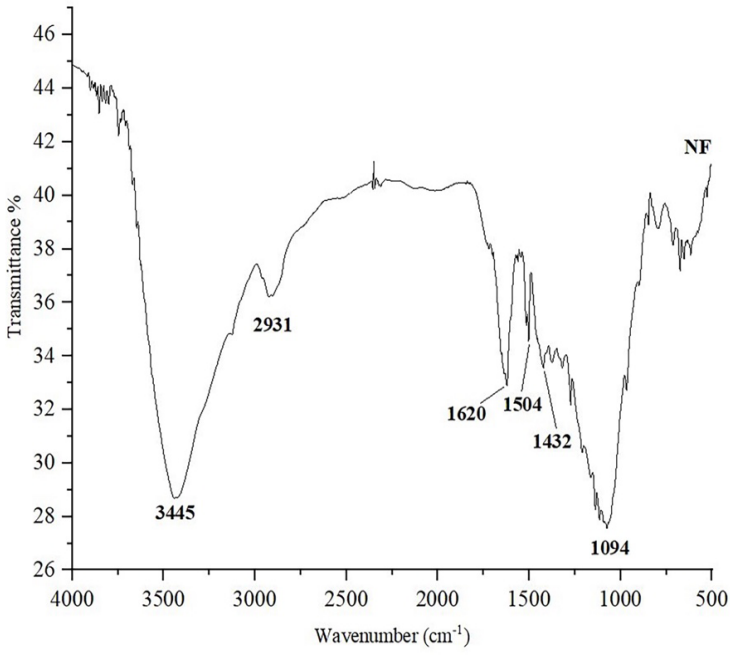

Figure 4. FT-IR spectrum of (a) Fluconazole, (b) XF, (c) NF, and (d) XNF

XRD

The X-ray diffractogram of fluconazole, XF, NF and XNF has been shown in Figure 5. Fluconazole diffractogram depicted the intense peaks at 2θ values of 10.08°, 13.68, 16.66°, 20.10°, 21.18°, 25.72°, 29.36 and 27.5° indicating the crystalline nature of fluconazole. The diffractogram of XF showed sharp peaks at 2θ values of 20.02°, 31.62°, and 45.44° and NF exhibited sharp peaks at 16.58° and 22.56° representing that both XF and NF are amorphous in nature. XNF diffractogram presented the peaks at 2θ values of 17.6°, 18.5°, and 22.5° revealing the amorphous nature of the film. Hence, it can be seen that the diffractograms of XF, NF and XNF are showing the amorphous nature and there is no significant difference in their diffraction patterns.

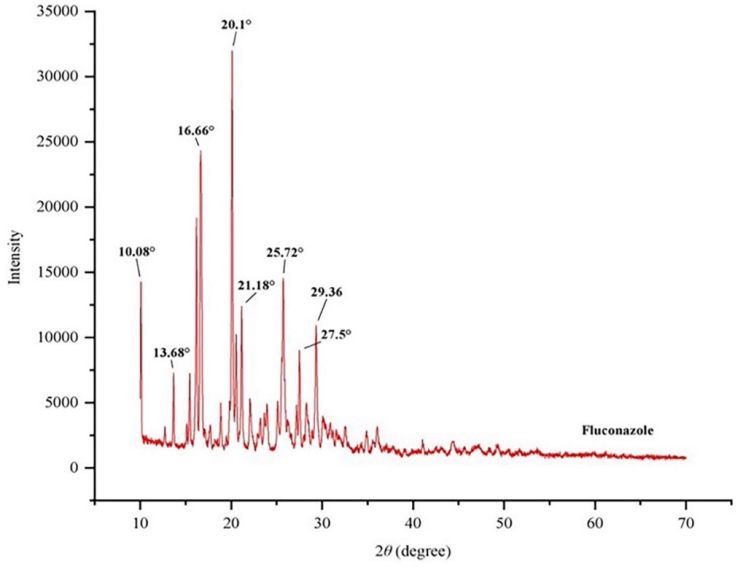

(a)

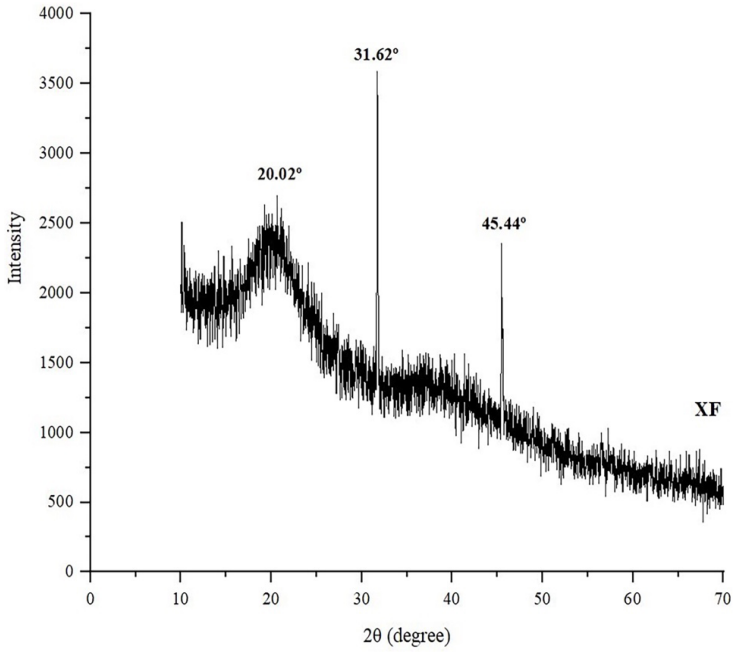
31.62°
20.02°
45.44°
XF
Intensity
2θ (degree)

(b)

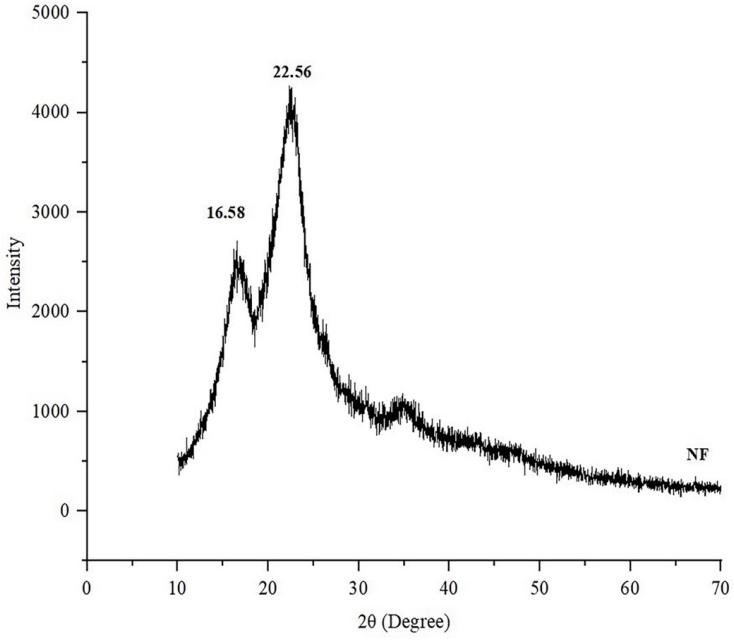
22.56
16.58
NF
Intensity
2θ (Degree)

(c)

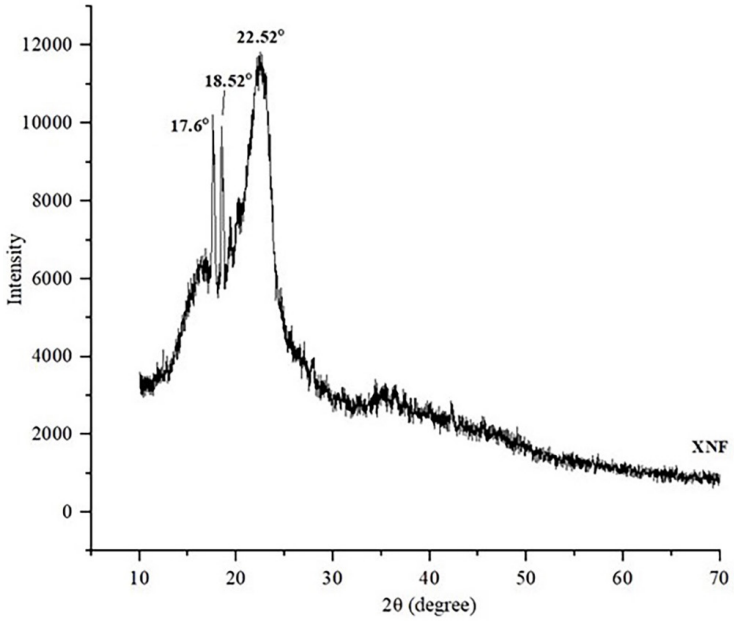

(d)

Figure 5. XRD diffractogram of (a) Fluconazole, (b) XF, (c) NF and (d) XNF

SEM

The scanning electron micrograph of an optimized batch of XNF was captured at 200x. As shown in Figure 6, the fibrous surface of XNF was observed. The cylindrical-shaped nanocellulose fibers embedded in the xanthan gum film were present on the surface of the polymeric film.

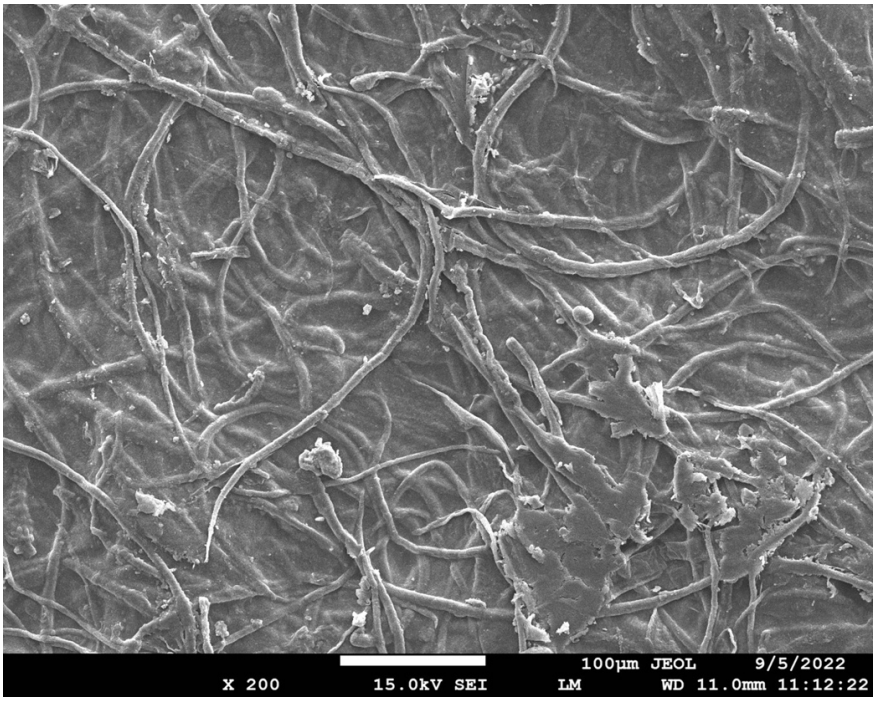

Figure 6. SEM image of XNF

In vitro release study

Initially, the amount of fluconazole drug present in the film was estimated by measuring absorbance using a UV spectrophotometer at wavelength 260 nm. The drug content was calculated and found to be 97.83%, 99.14%, and 102.89% of XF, NF, and XNF respectively. Then, the *in-vitro* release of fluconazole from XF, NF, and XNF was performed up to 24 h in phosphate buffer at pH 6.8. The plot of cumulative release (%) vs time (h) of XF, NF, and XNF is shown in Figure 7. It can be observed that almost all of the fluconazole was released from NF in 8 h, while it took 16 h to release 100% of fluconazole from XF. On the other hand, nanocellulose-reinforced XNF could sustain the release for up to 24 h. It can be concluded that after the reinforcement of nanocellulose in xanthan gum, the release of fluconazole was more sustained compared to native xanthan gum film. The *in vitro* release data of XF, NF, and XNF was also fitted into various kinetics models to recognize the release mechanism of fluconazole (Table 4). The kinetic data analysis of XF, NF, and XNF revealed that the release of fluconazole from XF and NF follows the Higuchi model while XNF follows the zero-order kinetics[44]. The Higuchi model describes the release of less

soluble or very soluble drugs from a solid matrix system through the porosity of the matrix. In the case of XNF, due to its high tensile strength, XNF showed a delay in disintegration and resulted in a very slow drug release. When the release is time-dependent and concentration-independent it means zero-order kinetics has been followed by the formulation. This drug release method is ideal for achieving prolonged pharmacological action. The release exponent, '*n*' values of the Korsmeyer-Peppas model indicated that the mechanism of drug release for both XF and NF ($0.5<n<0.89$) is anomalous transport while release from XNF ($n > 1$) represents super case II transport[45-47]. Anomalous transport shows that mechanism of drug release is controlled by swelling and diffusion while super case II transport represents the diffusion and relaxation of polymer chains[48].

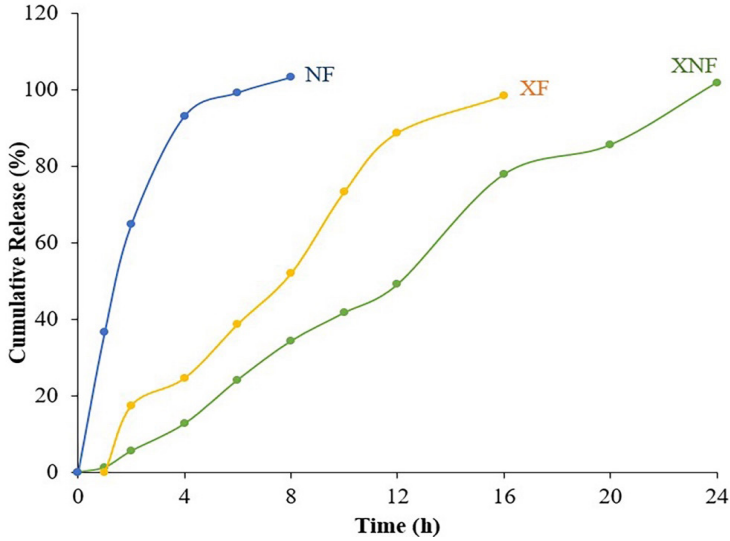

Figure 7. *In-vitro* drug release profile of XF, NF, and XNF

Table 4. Data of kinetic models

Sr. No.	Batch	Zero-order (R^2)	First-order (R^2)	Higuchi (R^2)	Korsmeyer-Peppas	
					(R^2)	n
1.	XF	0.9514	0.8281	0.9623	0.9843	0.7061
2.	NF	0.8118	0.9268	0.9611	0.9284	0.6736
3.	XNF	0.9908	0.9336	0.963	0.982	1.3368

In this study, fluconazole-loaded nanocellulose-reinforced xanthan film was prepared by solvent casting method using nanocellulose as a reinforcing agent, xanthan gum as film-forming polymer, PEG as a plasticizer, and fluconazole as a model drug. The optimization technique, a two-factor three-level central composite experimental design was employed to find out the optimized formulation of the film. Thirteen batches of films were prepared and evaluated for their physical and chemical characteristics. The obtained results revealed that all prepared films had sufficient tensile strength with sustained drug-release properties. The optimized batch (nanocellulose = 100 mg, xanthan gum = 100 mg, PEG = 50 mg, and fluconazole = 30 mg) was selected as the best formulation, and it was further characterized. FT-IR study revealed that no interaction takes place between the drug and other excipients while the XRD study confirmed the amorphous nature of the film. The *in vitro* dissolution study showed a fluconazole release of 100% in 24 h. Xanthan gum and nanocellulose possess mucoadhesive properties. Based on the findings of the present study, it can be concluded that reinforcement of xanthan film with nanocellulose improves the mechanical strength and prolongs the *in-vitro* release of the drug. However, further *ex-vivo* and *in-vivo* studies are needed to explore the potential of fluconazole-loaded nanocellulose-reinforced xanthan films for mucoadhesive or topical drug delivery applications.

STATEMENT OF ETHICS

This study does not require any ethical permission.

CONFLICT OF INTEREST STATEMENT

No conflicts of interest.

AUTHOR CONTRIBUTIONS

All the authors contributed to the study design, and preparation of the manuscript, and all have read and approved the final version. The specific activities of them were Vipin Jain: methodology, acquisition of data, drafting of the manuscript. Rimpy Pahwa and Rashmi Sharma: sample analysis, discussion, data analysis, and paper preparation. Munish Ahuja: design of methodology, planning, data discussion, and mentorship.

FUNDING SOURCES

This research did not receive any specific grant from funding agencies in the public, commercial or not-for-profit sectors.

REFERENCES

1. Meydanju N, Pirsa S, Farzi J. Biodegradable film based on lemon peel powder containing xanthan gum and TiO_2-Ag nanoparticles: Investigation of physicochemical and antibacterial properties. Polym Testing, 2022;106(12). Doi: 10.1016/j.polymertesting.2021.107445

2. Shiledar RR, Tagalpallewar AA, Kokare CR. Formulation and in vitro evaluation of xanthan gum-based bilayered mucoadhesive buccal patches of zolmitriptan. Carbohydr Polym, 2014;101:1234-1242. Doi: 10.1016/j.carbpol.2013.10.072

3. Jadhav M, Pooja D, Adams DJ, Kulhari H. Advances in xanthan gum-based systems for the delivery of therapeutic agents. Pharmaceutics, 2023;15(2):1-27. Doi: 10.3390/pharmaceutics15020402

4. Rimpy, R, Ahuja M. In Polysaccharide-based Biomaterials: Delivery of Therapeutics and Biomedical Applications. The Royal Society of Chemistry, 2022, pp. 361-396.

5. Zheng M, Chen J, Tan KB, Chen M, Zhu Y. Development of hydroxypropyl methylcellulose film with xanthan gum and its application as an excellent food packaging bio-material in enhancing the shelf life of banana. Food Chem, 2022;374. Doi: 10.1016/j.foodchem.2021.131794

6. Wen Q, Wang X, Liu B, Lu L, Zhang X, Swing CJ, et al. Effect of synergism between sodium alginate and xanthan gum on characteristics of composite film and gloss of areca nut coating. Food Biosci, 2022;50. Doi: 10.1016/j.fbio.2022.102113

7. Hazirah MN, Isa MI, Sarbon NM. Effect of xanthan gum on the physical and mechanical properties of gelatin-carboxymethyl cellulose film blends. Food Packag Shelf Life, 2016;9:55-63. Doi: 10.1016/j.fpsl.2016.05.008

8. Chen J, Zheng M, Tan KB, Lin J, Chen M, Zhu Y. Polyvinyl alcohol/xanthan gum composite film with excellent food packaging, storage and biodegradation capability as potential environmentally-friendly alternative to commercial plastic bag. Int J Biol Macromol, 2022;212:402-411. Doi: 10.1016/j.ijbiomac.2022.05.119

9. Zheng M, Zhu Y, Zhuang Y, Tan KB, Chen J. Effects of grape seed extract on the properties of pullulan polysaccharide/xanthan gum active films for apple preservation. Int J Biol Macromol, 2023;241. Doi: 10.1016/j.ijbiomac.2023.124617

10. Singh M, Tiwary AK, Kaur G. Investigations on interpolymer complexes of cationic guar gum and xanthan gum for formulation of bioadhesive films. Res Pharm Sci, 2010;5(2):79-87.

11. Shipp L, Liu F, Kerai-Varsani L, Okwuosa TC. Buccal films: a review of therapeutic opportunities, formulations & relevant evaluation approaches. J Control Release, 2022;352:1071-1092. Doi: 10.1016/j.jconrel.2022.10.058

12. Gil MC, Park SJ, Lee BS, Park C, Lee BJ. Dual thermal stabilizing effects of xanthan gums via glycosylation and hydrogen bonding and in vivo human bioavailability of desmopressin in orodispersible film. Int J Pharm. 2023;637. Doi: 10.1016/j.ijpharm.2023.122879

13. Deshkar SS, Mahore JG. Herbal bioactive–based vaginal and rectal drug delivery systems. Herbal Bioactive-Based Drug Delivery Systems. Academic Press; 2022. 111-168. Available from: 10.1016/B978-0-12-824385-5.00017-0

14. Dimofte A, Dinu MV, Anghel N, Doroftei F, Spiridon I. Xanthan and alginate-matrix used as transdermal delivery carrier for piroxicam and ketoconazole. Int J Biol Macromol, 2022;209:2084-2096. Doi: 10.1016/j.ijbiomac.2022.04.189

15. Singh S, Nwabor OF, Sukri DM, Wunnoo S, Dumjun K, Lethongkam S, et al. Poly (vinyl alcohol) copolymerized with xanthan gum/hypromellose/sodium carboxymethyl cellulose dermal dressings functionalized with biogenic nanostructured materials for antibacterial and

wound healing application. Int J Biol Macromol, 2022;216(24):235-250. Doi: 10.1016/j.ijbiomac.2022.06.172

16. Sun B, Zhang M, Shen J, He Z, Fatehi P, Ni Y. Applications of cellulose-based materials in sustained drug delivery systems. Curr Med Chem, 2019;26(14):2485-2501. Doi: 10.2174/0929867326661707051433 08

17. Pahwa R, Ahuja M. Nanocellulose-gellan cross-linked scaffolds for vaginal delivery of fluconazole. Int J of Biol Macromol, 2023;229:668-683. Doi: 10.1016/j.ijbiomac.2022.12.273

18. Aitomäki Y, Oksman K. Reinforcing efficiency of nanocellulose in polymers. React Funct Polym, 2014;85:151-156. Doi: 10.1016/j.reactfunctpolym.2014.08.010

19. Jonoobi M, Mathew AP, Oksman K. Producing low-cost cellulose nanofiber from sludge as new source of raw materials. Ind Crop Prod, 2012;40:232-238. Doi: 10.1016/j.indcrop.2012.03.018

20. Kargarzadeh H, Mariano M, Huang J, Lin N, Ahmad I, Dufresne A, et al. Recent developments on nanocellulose reinforced polymer nanocomposites: a review. Polym, 2017;132:368-393. Doi: 10.1016/j.polymer.2017.09.043

21. Lee KY, Aitomäki Y, Berglund LA, Oksman K, Bismarck A. On the use of nanocellulose as reinforcement in polymer matrix composites. Comp Sci Technol, 2014;105:15-27. Doi: 10.1016/j.compscitech.2014.08.032

22. Mahardika M, Amelia D, Syafri E. Applications of nanocellulose and its composites in bio packaging-based starch. Mater Today, 2023;74(3):415-418. Doi: 10.1016/j.matpr.2022.11.138

23. Kargarzadeh H, Huang J, Lin N, Ahmad I, Mariano M, Dufresne A, et al. Recent developments in nanocellulose-based biodegradable polymers, thermoplastic polymers, and porous nanocomposites. Prog Polym Sci, 2018;87:197-227. Doi: 10.1016/j.progpolymsci.2018.07.008

24. Lu Y, Weng L, Cao X. Biocomposites of plasticized starch reinforced with cellulose crystallites from cottonseed linter. Macromol Bio Sci, 2005;5:1101-1107. Doi: 10.1002/mabi.200500094

25. Liu D, Zhong T, Chang PR, Li K, Wu Q. Starch composites reinforced by bamboo cellulosic crystals. Bioresour Technol, 2010;101(7):2529-2536. Doi: 10.1016/j.biortech.2009.11.058

26. Li Q, Zhou J, Zhang L. Structure and properties of the nanocomposite films of chitosan reinforced with cellulose whiskers. J Polym Sci Part B, 2009;47(11):1069-1077. Doi: 10.1002/polb.21711

27. Khan A, Sp Salmieri, Fraschini C, Bouchard J, Riedl B, Lacroix M. Genipin cross-linked nanocomposite films for the immobilization of antimicrobial agent. ACS Appl Mater Interfaces, 2014;6(17):15232-15242. Doi: 10.1021/am503564m

28. Huq T, Salmieri S, Khan A, Khan RA, Le Tien C, Riedl B, et al. Nanocrystalline cellulose (NCC) reinforced alginate based biodegradable nanocomposite film. Carbohydr Polym, 2012;90(4):1757-1763. Doi: 10.1016/j.carbpol.2012.07.065

29. Mondragon G, Pena-Rodriguez C, Gonzalez A, Eceiza A, Arbelaiz A. Bionanocomposites based on gelatin matrix and nanocellulose. Eur Polym J, 2015;62:1-9. Doi: 10.1016/j.eurpolymj.2014.11.003

30. Pereira ALS, do Nascimento DM, Morais JPS, Vasconcelos NF, Feitosa JPA, Brígida AIS, et al. Improvement of polyvinyl alcohol properties by adding nanocrystalline cellulose isolated from banana pseudo stems. Carbohydr Polym, 2014;112:165-172. Doi: 10.1016/j.carbpol.2014.05.090

31. Ilyas RA, Azmi A, Nurazzi NM, Atiqah A, Atikah MS, Ibrahim R, et al. Oxygen permeability properties of nanocellulose reinforced biopolymer nanocomposites. Mater Today Proc, 2022;52(5):2414-2419. Doi: 10.1016/j.matpr.2021.10.420

32. Feng Z, Xu D, Shao Z, Zhu P, Qiu J, Zhu L. Rice straw cellulose microfiber reinforcing PVA composite film of ultraviolet blocking through pre-cross-linking. Carbohydr Polym, 2022;296. Doi: 10.1016/j.carbpol.2022.119886

33. Rimpy, Ahuja M. Fluconazole-loaded TEOS-modified nanocellulose 3D scaffolds–Fabrication, characterization and its application as vaginal drug delivery system. J Drug Del Sci Technol, 2022;75. Doi: 10.1016/j.jddst.2022.103646

34. Sharma R, Pahwa R, Ahuja M. Iodine-loaded poly (silicic acid) gellan nanocomposite mucoadhesive film for antibacterial application. J Appl Polym Sci, 2021;138(2). Doi: 10.1002/app.49679

35. Shaikh R, Singh TR, Garland MJ, Woolfson AD, Donnelly RF. Mucoadhesive drug delivery systems. J Pharm Bioallied Sci, 2011;3(1):89-100. Doi: 10.4103/0975-7406.76478

36. Nair AB, Shah J, Jacob S, Al-Dhubiab BE, Patel V, Sreeharsha N, et al. Development of mucoadhesive buccal film for rizatriptan: in vitro and in vivo evaluation. Pharmaceutics, 2021;13(5):1-16. Doi: 10.3390/pharmaceutics13050728

37. Ahuja M, Thakur K, Kumar A. Amylopectin-g-poly (N-vinyl-2-pyrrolidone): synthesis, characterization and in vitro release behavior. Carbohydr Polym, 2014;108:127-134. Doi: 10.1016/j.carbpol.2014.03.007

38. Almehmady AM, El-Say KM, Mubarak MA, Alghamdi HA, Somali NA, Sirwi A, et al. Enhancing the antifungal activity and ophthalmic transport of fluconazole from PEGylated polycaprolactone loaded nanoparticles. Polymers, 2022;15(1):209. Doi: 10.3390/polym15010209

39. Pahwa R, Ahuja M. Design and Development of fluconazole-loaded nanocellulose-eudragit vaginal drug delivery system. J Pharm Innov, 2023;18:1065-1083. Doi: 10.1007/s12247-022-09705-2

40. Zhou L, Wang K, Bian L, Chang T, Zhang C. Improving properties of curdlan/nanocellulose blended film via optimizing drying temperature. Food Hydrocoll, 2023;137. Doi: 10.1016/j.foodhyd.2022.108421

41. Baniasadi H, Kimiaei E, Polez RT, Ajdary R, Rojas OJ, Österberg M, et al. High-resolution 3D printing of xanthan gum/nanocellulose bio-inks. Int J Biol Macromol, 2022;209:2020-2031. Doi: 10.1016/j.ijbiomac.2022.04.183

42. Zhu L, Feng L, Luo H, Dong RS, Wang MY, Yao G, et al. Characterization of polyvinyl alcohol-nanocellulose composite film and its release effect on tetracycline hydrochloride. Ind Crops Prod, 2022;188. Doi: 10.1016/j.indcrop.2022.115723

43. Prado KS, Spinacé MA. Isolation and characterization of cellulose nanocrystals from pineapple crown waste and their potential uses. Int J Biol Macromol, 2019;122:410-416. Doi: 10.1016/j.ijbiomac.2018.10.187

44. Qureshi MA, Arshad N, Rasool A, Rizwan M, Rasheed T. Guar gum-based stimuli responsive hydrogels for sustained release of diclofenac sodium. Int J Biol Macromol, 2023;250. Doi: 10.1016/j.ijbiomac.2023.126275

45. Verma S, Rimpy, Ahuja M. Carboxymethyl modification of *Cassia obtusifolia* galactomannan and its evaluation as sustained release carrier. Int J Biol Macromol, 2020;164:2823-2834. Doi: 10.1016/j.ijbiomac.2020.08.231

46. Costa P, Lobo JM. Modeling and comparison of dissolution profiles. Eur J Pharm Sci, 2001;13(2):123-133. Doi: 10.1016/s0928-0987(01)00095-1

47. Bruschi ML. Strategies to modify the drug release from pharmaceutical systems. Woodhead Publishing; 2015. 63-86. Available from: 10.1016/B978-0-08-100092-2.00005-9

48. Karthikeyan M, Deepa MK, Bassim E, Rahna CS, Raj KS. Investigation of kinetic drug release characteristics and in vitro evaluation of sustained-release matrix tablets of a selective COX-2 inhibitor for rheumatic diseases. J Pharm Innov, 2021;16:551-557. Doi: 10.1007/s12247-020-09459-9

Acta Pharm. Sci. Vol 62:(2), 2024
Research article
DOI: 10.23893/1307-2080.APS6228

Anti-anemic potential of *Moringa oleifera* flower extract against phenylhydrazine-induced anemia in rats

Nikitha MANJEGOWDA[1], Mani Rupesh KUMAR[1], Bharathi Doddla RAGHUNATHANAIDU[1], Anjali BABU[1], Karthik SRIDHARA[1], Bevinhalli RAMESH[2] Syed Sagheer AHMED[1*]

1 Adichunchanagiri University, College of Pharmacy, Department of Pharmacology, Sri Adichunchanagiri, B G Nagara, Karnataka, India

2 Adichunchanagiri University, College of Pharmacy, Department of Pharmaceutical Chemistry, Sri Adichunchanagiri, B G Nagara, Karnataka, India

ABSTRACT

The present study was focused to evaluate the anti-anemic activity in hydro-alcoholic extract of *Moringa oleifera* flower extract against phenylhydrazine induced anemic rats. Anemia was induced by administration of (40 mg/kg b.w.) intraperitoneally in rats for two days. The animals were divided into 6 groups containing 6 animals each. Group 1 received normal saline as a control, and all other groups received phenylhydrazine for two days in order to cause anaemia. Group 3 served as the standard group and received ferrous sulphate treatment (100 mg/kg). The remaining groups 4, 5, 6 received *M. oleifera* flower extract at three different doses (200 mg/kg, 400 mg/kg, and 800 mg/kg) orally for 14 days. On 15th day blood was withdrawn, through cardiac puncture and subjected to the estimation of RBC, Hb and HCT. The anemic parameters were reversed after treatment with *Moringa oleifera* flower at different doses for 15 days when compared with phenylhydrazine-induced anemic rats.

Keywords: anemia, phenylhydrazine, *Moringa oleifera* flower extract, ferrous sulphate

*Corresponding author: Syed Sagheer AHMED
E-mail: sysaha6835@gmail.com
ORCIDs:
Nikitha MANJEGOWDA: 0009-0008-0447-6600
Mani Rupesh KUMAR: 0000-0002-4736-8123
Bharathi Doddla RAGHUNATHANAİDU: 0000-0002-5250-9760
Anjali BABU: 0009-0006-4107-7065
Karthik SRIDHARA: 0009-0002-9224-4696
Bevinhalli RAMESH: 0000-0002-2551-234X
Syed Sagheer AHMED: 0000-0001-9817-9747
(Received 13 Jul 2023, Accepted 10 Oct 2023)

INTRODUCTION

A common public health issue known as anaemia is defined as a decrease in haemoglobin concentration or erythrocyte mass in the blood, which results in a reduction in the blood's ability to carry oxygen[1]. When haemoglobin levels in the blood fall below the normal range of less than 12 g/dL for female adults and less than 13 g/dL for male adults, anaemia has occurred[2]. Anaemia tends to be three to four times more common in developing nations than it is in developed nations. Anaemia has an impact on a person's physical and mental growth, which reduces their capacity for work and has an impact on the nation's development[3]. The behavioural effects of anaemia are extremely relevant because a nation's technological and economic development heavily depends on its trained human resources. Consequently, a nation's intellectual and economic potential may be significantly hampered if anaemia is highly prevalent there[4]. Although synthetic drugs are frequently used to treat a particular disease, due to their high cost and unwanted side effects, attention is now being paid to the use of medicinal plant products to manage or prevent various diseases or ailments in both humans and animals [5]. For the treatment of various types of anaemia, medicinal plants are used around the world, particularly in the tropics [6].

At the end of the 19th century, phenylhydrazine (PHZ) and its derivatives were first prescribed as antipyretics, but their use was hazardous due to their toxic effects on red blood cells. Rats were given injections of phenylhydrazine (40 mg/kg), which caused anaemia[7]. Haemoglobin experiences oxidative denaturation when oxygen is present, and the first step in this process is a bimolecular reaction, likely a two-electron transfer from phenylhydrazine to oxyhemoglobin; the reaction product is neither methemoglobin nor deoxyhemoglobin[8]. Red blood cells (RBC) membrane skeleton experiences oxidative degradation of spectrin, peroxidation of lipids, and the formation of reactive oxygen species as a result of PHZ. The red blood cell proteins appear to undergo oxidative changes that cause the PHZ-induced hemolytic injury [9].

Moringa oleifera Lam (*M. oleifera*) is a cruciferous plant in the *Moringaceae* family. *M. oleifera*, also known as the horseradish tree or drumstick tree by locals, is well-liked throughout the world[10]. Because of its many applications, exceptional nutritional value, and potential for use in nutraceutical, *M. oleifera* is known as "The Miracle Tree". This plant has been recognized as the "Botanical of the Year-2007" by the National Institutes of Health (NIH)[11]. *Moringa* flower is a rich reservoir of bioactive phytochemical and crude flower extracts showed promising antibacterial, antifungal, anti-larval, antioxidant, antiinflammatory and anticancer properties[12]. It contains A, B, C, D, E, and

K are among the vitamins that are found in the highest concentrations in this plant. Among other necessary minerals, *Moringa* contains calcium, copper, iron, potassium, magnesium, manganese, and zinc. There are several notable studies on the antioxidant properties of aqueous and ethanol extracts of flower. More than 40 natural antioxidants are reported in *Moringa oleifera* flower extract[13]. The total Antioxidant content is higher in flower than other parts of *Moringaoleifera*[14]. Traditionally, *M. oleifera* plant has been used in the treatment of diuretic, analgesic, antipyretic, vermifuge, anti-ulcer, hypoglycemic, hypolipidemic, laxative, and asthma diseases. *Moringa oleifera* also possesses antiviral, antioxidant, antimicrobial, anti-inflammatory, antipyretic, anthelmintic, antifungal, hepatoprotective, antihyperglycemic, hypolipidemic, antidiabetic, antiviral, antihyperlipidemic and cardioprotective activity[15]. The leaf of *M. oleifera* is reported for its antianemic property due to the presence of significant amount of iron and vitamin C[16]. Such contents are also found in *M. oleifera* flower. In the current study the flower of *M. oleifera* showed potent antianemic property. It might be due to the presence of iron and vitamin C[17].

METHODOLOGY

Procurement of chemicals and reagents

Phenylhydrazine was obtained from Loba Chemie Pvt. Ltd, jehangir villa, 107, Wodehouse Rd., colaba, Mumbai (India). Ferrous sulphate was obtained from s d fine-chem. limited, 1502, marathon icon, lower parel, Mumbai. Other chemicals utilized in this work are of analytical grade.

Instrumentation

Sonicator (Ana Matrix Instrument Technologies Pvt Ltd, LMUC-3, India), Water bath (Shital Scientific Industries, India), Heating mantel (Techno Scientific Products, S.S 104, India), Rotary evaporator (Rotavapor R-3, Buchi, India).

Plant material

The *Moringa oleifera* flowers were collected from surrounding area of B G Nagar, Mandya. The collected flowers were cleaned, dried in the shade, ground into a coarse powder, and then kept at room temperature in an airtight container. Dr. Pradeep, Associate Professor, Department of Dravyaguna, and Sri Dharmasthala Manjunatheshwara College of Ayurveda & Hospital verified the authenticity of the flowers. (No: SDMCAH-DG/2022/56)

Preparation of extract

In a conical flask, 1500ml of hydro alcohol (70-30%) was used to soak the fine powder (300g) for 72 hours. After 72 hours, the mixture is concentrated using simple distillation in a water bath and filtered using a fine muslin cloth followed by filter paper (Whatman No. 1)[18].

Experimental animals

Female albino Wistar strain rats weighing 100–150g were chosen for the study. Individual polypropylene cages were used to house each animal under sanitary and typical environmental conditions (22±3 °C, humidity 30–70%, 12h light/dark cycle). The animals were given free access to standard feed and water. Before being used in the experiment, they spent a week getting familiar to the surroundings. Experiments were conducted with the approval of both the Committee for the Purpose of Control and Supervision of Experiments on Animals (CPCSEA). The animal experimentations were approved by IAEC of SACCP, B.G Nagara. (IAEC Approval number: SACCP-IAEC/2022-02/68)

Experimental design

Induction of anemia

Phenylhydrazine (40 mg/kg) intraperitoneal injections were given once daily for two days to induce anaemia. Anemia was confirmed by the reduction of red blood cells (RBC) and hemoglobin concentration of the blood reduced by 40%[19].

Phenylhydrazine induced anemia model in rats

Rats were divided into six groups containing six rats in each group and treated for 15days.

Group 1: Normal control (received vehicle).

Group 2: Anemic group (treated with phenylhydrazine 40 mg/kg).

Group 3: Received standard drug ferrous sulfate, 100 mg/kg.

Group 4: Phenylhydrazine + Treatment with *Moringa oleifera* flower extract 200 mg/kg.

Group 5: Phenylhydrazine +Treatment with *Moringa oleifera* flower extract 400 mg/kg.

Group 6: Phenylhydrazine + Treatment with *Moringa oleifera* flower extract 800 mg/kg.

Blood collection and analysis

About (1-2 ml) of blood was collected from tail vein after the induction of anemia and blood was collected by cardiac puncher after the treatment with standard and plant extract. Blood was thoroughly mixed with EDTA to avoid coagulation and used for haematological test. The cyanomethaemoglobin method was used to estimate haemoglobin[20].

Analysis of haematological parameter

The concentrations of red blood cells (RBCs), haemoglobin (Hb), hematocrit (HCT), packed cell volume (PCV), mean corpuscular haemoglobin (MCH), mean corpuscular haemoglobin concentration (MCHC), and mean corpuscular volume (MCV) in the blood were determined[21].

Histopathological analysis

For histopathological studies, the kidney and spleen were separated and preserved in a 10% formalin solution.

Statistical analysis

Data were expressed as the mean ±SEM, and statistical analysis of variance (ANOVA) and Tukey's test were used to identify differences between the groups. ***P0.001 p-values were regarded as statistically significant.

RESULTS and DISCUSSION

The present study was aimed to evaluate the anti-anemic activity of *Moringa oleifera* flower extract against phenylhydrazine induced anemic rats. The ability of phenylhydrazine to induce hemolysis *in vivo* through the production of aryl and hydroxyl radicals, which have been linked to its interaction with erythrocytes, is well known. Hemolysis is largely caused by erythrocyte oxidative stress. Chronic hemolysis results in haemoglobin loss[22]. In rats, phenylhydrazine administration reduces hematocrit, red blood cell count and haemoglobin concentration[23]. The anemia which was resulted due early lysis of the blood cells was treated with hydroalcoholic extract of *Moringa oleifera* flower at different doses. This study used six groups of female rats which are consisting of six rats per group. The dose variation which is used in this study is determined to know which dose of *Moringa oleifera* flower extract that has significant effect on various parameters of anemia was observed.

Phenylhydrazine induced anemia model in rats

The aim of the current study was to evaluate the *Moringa oleifera* flowers ability to treat anaemia. The following comparisons were made between anemic induced animal groups and control animal group.

Table 1 represents the impact of *Moringa oleifera* flower extract on Wistar albino rats RCB, Hb, and HCT counts. When compared to Group I rats, Group II phenylhydrazine-intoxicated rats displayed a significant decline in RBC, Hb, and HCT count. Rats treated with regular ferrous sulphate who had consumed Group III phenyl hydrazine had higher levels of RBC, Hb, and HCT than those who had consumed Group II. Rats treated with *Moringa oleifera* flower extract at different doses of 200 mg/kg, 400 mg/kg, and 800 mg/kg each showed a significant rise in RBC, Hb, and HCT levels compared to group II intoxicated with phenylhydrazine, group IV, group V, and group VI. The higher dose of (800 mg/kg) showed highly significant activity as compared to low doses (200 mg/kg and 400 mg/kg). Effect of *M. oleifera* flower extract might due to the presence of vitamins and iron content in them.

Table 1. Effect of hydroalcoholic extract of *Moringa oleifera* flower on blood levels of RBCs, hemoglobin, and HCT in anemia-induced rats

Groups	Complete Haemogram		
	RBCs count (10^6/µl)	Hemoglobin count (g/dl)	HCT count (%)
Normal control	5.135±0.9	13.03 ± 0.26	39.5 ± I.83
PHZ - induces	3.441 ± 0.8	9.463 ± 0.4	23 ± 0.9
Standard	4.555 ± 1.2***	13.315 ± 0.5***	34.83 ± 1.81***
PHZ + Low dose	4.123 ± 0.9*	11.465 ± 0.9*	32 ± 1.98*
PHZ + Medium dose	4.240 ± 0.8**	11.811 ± 0.6**	33.166 ± 1.57**
PHZ + High dose	4.425 ± 1.1***	12.323 ± 0.9***	35.33 ± 1.98***

The inducer control group was used as a comparison point for the haematological parameters. Data are presented as Mean + SEM, n = 6, with two-way ANOVA and Tukey's test used for statistical analysis. When compared to the inducer control, ***$p<0.001$.

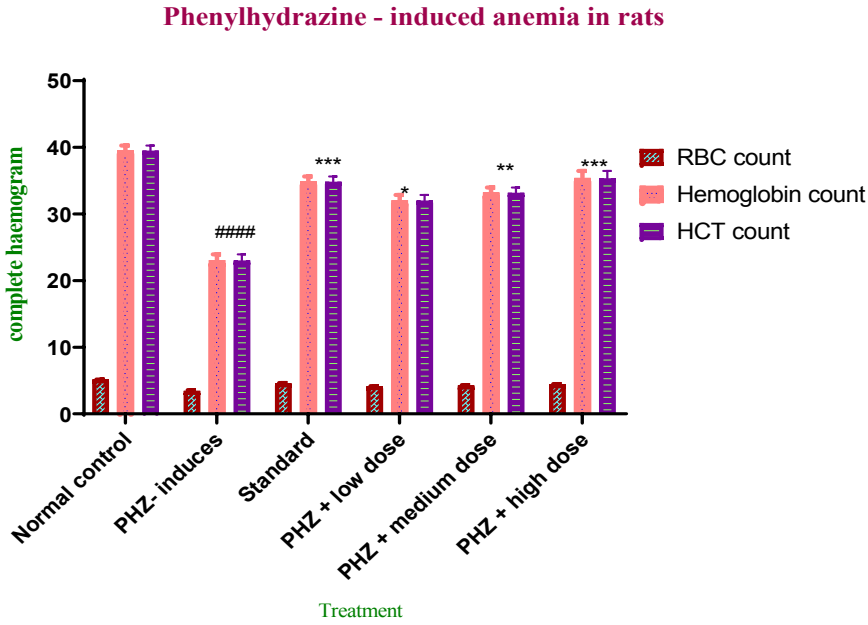

Figure 1. Effect of hydroalcoholic extract of *Moringa oleifera* flower on blood levels of RBCs, hemoglobin, and HCT in anemia-induced rats

Table 2 represents the impact of *Moringa oleifera* flower extract on Wistar albino rats PCV, MCH, MCHC, and MCV counts. Comparing Group II phenylhydrazine-intoxicated rats to Group I rats, the PCV, MCH, MCHC, and MCV count significantly decreased. When compared to Group II, rats treated with standard ferrous sulphate who had been intoxicated with phenyl hydrazine in Group III showed a significantly higher level of PCV, MCH, MCHC, and MCV. When compared to group II, group IV, group V, and group VI phenylhydrazine-intoxicated rats received doses of 200 mg/kg, 400 mg/kg, and 800 mg/kg of *Moringa oleifera* flower extract, respectively. These doses resulted in a significant rise in PCV, MCH, MCHC, and MCV levels. The higher dose of (800 mg/kg) showed highly significant activity as compared to low doses (200 mg/kg and 400 mg/kg). Effect of *M. oleifera* flower extract might due to the presence of vitamins and iron content in them.

Table 2. Effect of hydroalcoholic extract of *Moringa oleifera* flower on PCV, MCH, MCHC, and MCV

Groups	Differential Count			
	PCV	MCH	MCHC	MCV
Normal Control	46.4±0.121	29.305±0.137	44.456±0.159	84.691±0.137
PHZ – induces	31.611±0.175	21.09±0.234	31.118±0.276	68.386±0.151
Standard	45.57 ± 0.129***	28.31±0.234***	40.308±0.146***	78.471±0.171***
PHZ + Low dose	41.66±0.137*	26.33± 0.128*	36.351± 0.117*	74.418± 0.117*
PHZ + Medium Dose	42.211±0.051**	26.68± 0.139**	37.336± 0.103**	77.203± 0.045**
PHZ + High Dose	44.306± 0.140***	27.37± 0.157***	38.51±0.151***	78.595± 0.149***

The inducer control group was used as a comparison point for the haematological parameters. Data are presented as Mean + SEM, n = 6, with two-way ANOVA and Tukey's test used for statistical analysis. When compared to the inducer control, ***p<0.001.

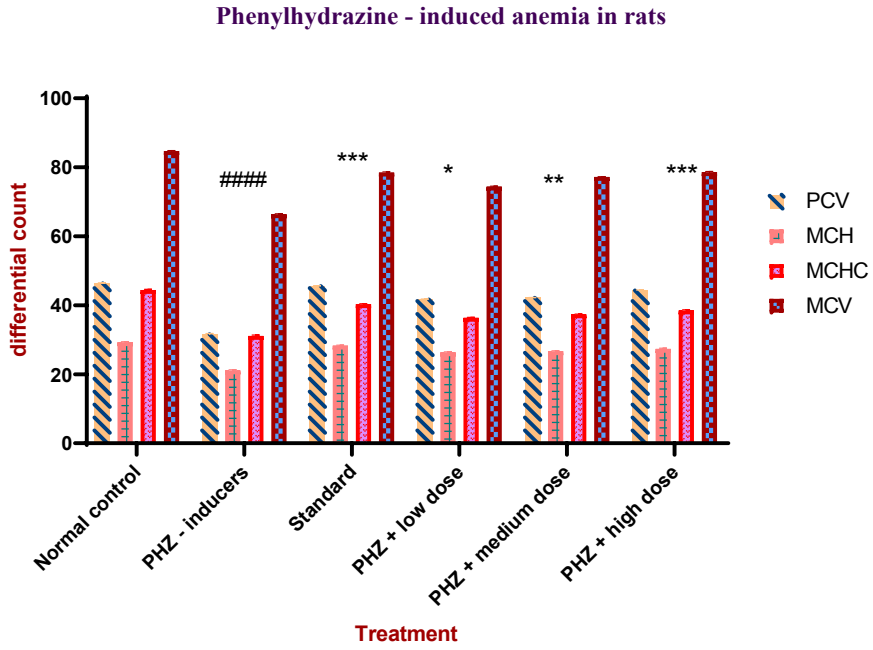

Figure 2. Effect of hydroalcoholic extract of *Moringa oleifera* flower on PCV, MCH, MCHC and MCV

Histological examination

Kidney

The kidney of the control group had intact basement membranes, normal glomeruli, and renal tubules. The renal blood vessels in the anemic group were congested, and the renal tubular epithelium had deteriorated. The groups given *Moringa oleifera* flower extract showed minimal to undetectable glomeruli or tubular degeneration in the kidneys. The renal tubular epithelial vacuolation and mild glomeruli and inter-tubular capillary congestion were seen in the ferrous sulphate group. Effect of *M. oleifera* flower extract might due to the presence of vitamins and iron content in them.

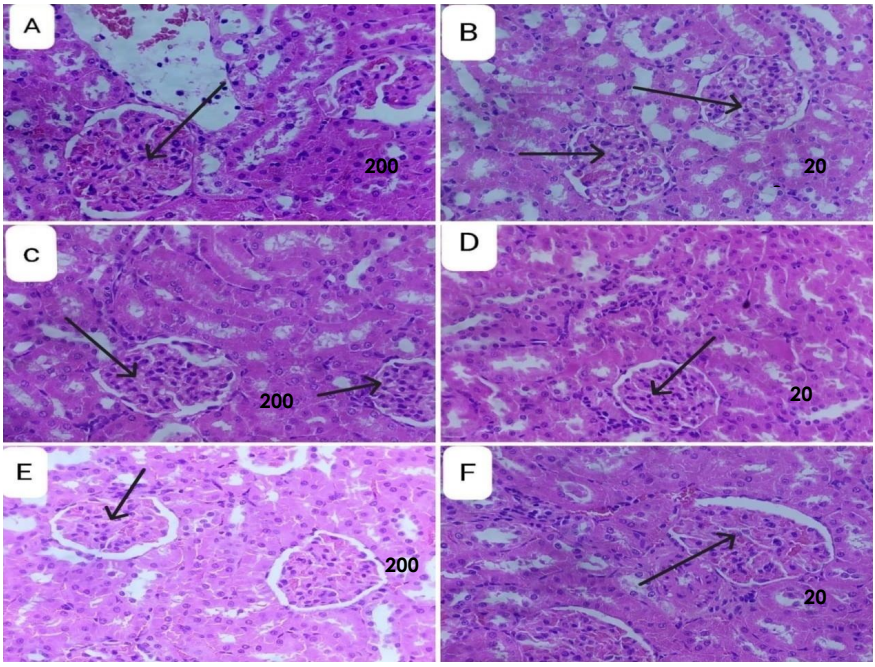

Figure 3. Histopathology of Kidney

The kidney section of histology was stained with hematoxylin and eosin (Scale bar 10X magnification).

(a) Normal control (Vehicle),

(b) Standard (Ferrous sulphate 100 mg/kg (p.o)),

(c) Inducer (Phenylhydrazine 4 0mg/kg (i.p)),

(d) Low dose (200 mg/kg (p.o)),

(e) Middle dose (400 mg/kg (p.o)),

(f) High dose (800 mg/kg (p.o)).

(g) Where A & B showed normal glomeruli and renal tubules with intact basement membranes and C showed congestion of renal blood vessels and degenerative changes of renal tubular epithelium and D, E & F showed improvement in degeneration of renal tubules or glomeruli.

Spleen

The control group's spleen displayed typical white and red pulps with a small number of megakaryocytes and minimal hemosiderin pigment deposition. The anemic group displayed hyperplasia of megakaryocytes, congested sinusoids and blood vessels, and significant hemosiderin deposition. The best outcomes were seen in the *Moringa oleifera* flower extract groups, while the other treated groups showed varying degrees of improvement as represented by a decrease in the number of megakaryocytes and deposition of hemosiderin pigments. Effect of *M. oleifera* flower extract might due to the presence of vitamins and iron content in them.

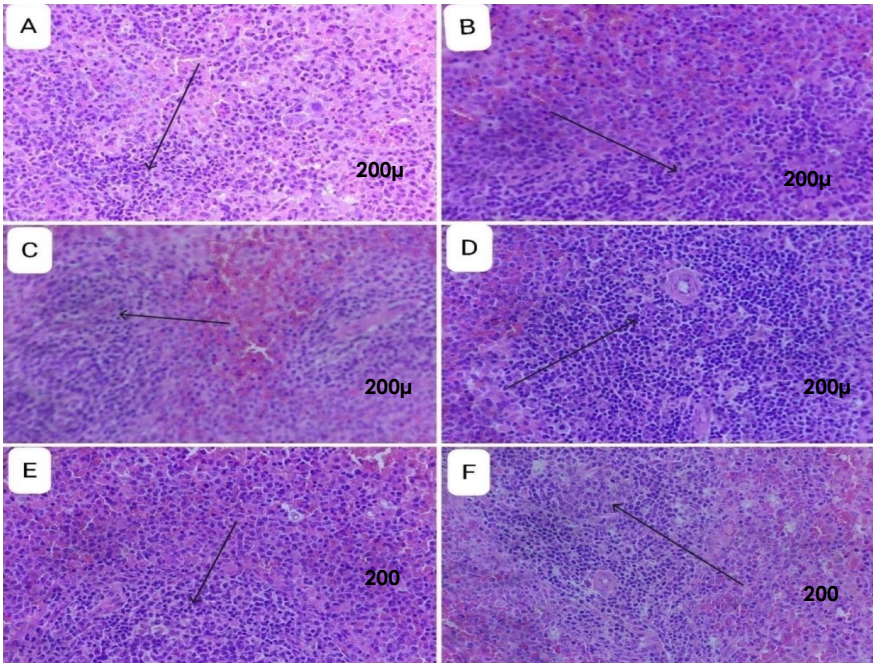

Figure 4. Histopathology of Spleen

The spleen section of histology was stained with hematoxylin and eosin (Scale bar 10X magnification).

(a) Normal control (Vehicle),

(b) Standard (Ferrous sulphate 100 mg/kg (p.o)),

(c) Inducer (Phenylhydrazine 40 mg/kg (i.p)),

(d) Low dose (200 mg/kg (p.o)),

(e) Middle dose (400 mg/kg (p.o)),

(f) High dose (800 mg/kg (p.o)).

Where A & B showed normal white and red pulps with a few numbers of megakaryocytes and deposition of hemosiderin pigments and C showed congestion of sinusoids and blood vessels and D, E & F showed improvement by reduction in the number of megakaryocytes and deposition of hemosiderin pigments.

The phenylhydrazine injections by an intraperitoneal route at the dose of 40 mg/kg for 2 consecutive days induce anemia in rats. Treatment with *Moringa oleifera* flower extract at a dose of 200 mg/kg, 400 mg/kg, and 800 mg/kg respectively, improved RBCs, Hb, HCT, MCV, MCHC, PCV, and MCH levels in phenylhydrazine induced anemic rats dose-dependently. Furthermore, it also reversed pathological changes in the spleen and kidney. The antianemic activity of *Moringa oleifera* flower extract might be due to presence of iron and vitamin C content in them. Further study is required to exactly understand how the phytoconstituents of *Moringa oleifera* flower interact with biochemical pathways in the blood to the presence of its antianemic activity.

STATEMENT OF ETHICS

The animal experimentations were approved by Institutional Animal Ethics Committee (IAEC) of Sri Adichunchanagiri College of Pharmacy, B.G Nagara. (IAEC Approval number: SACCP-IAEC/2022-02/68). Experiments were performed in accordance with the guidelines provided by the Committee for the Control and Supervision of Experiments on Animals (CCSEA), India.

CONFLICT OF INTEREST STATEMENT

The authors declare that they have no competing interests.

AUTHOR CONTRIBUTIONS

NM: Design, acquisition of data, analysis of data, drafting of manuscript, statistical analysis. MRK: Design, acquisition of data. SSA: Design, critical review

of manuscript, supervision. AB, KS: Design, plant collection and authentication, BDR, BR: Design, critical review of manuscript, supervision.

ACKNOWLEDGMENTS

The authors would like to extend a heartfelt thanks to the principal and management of Sri Adichunchanagiri College of Pharmacy for facilitating this research.

REFERENCES

1. Hoffbrand AV, Moss PA, Pettit JE. Erythropoiesis and general aspects of anaemia. Essential Haematology. 5th ed. UK: Blackwell Publishing, 2006;18:20.

2. Allen LH, Benoist DB, Dary O, Hurrell R. Guidelines on food fortification with micronutrients. Geneva: World Health Organization, 2006:13-25.

3. Manish M, Sankar S, Yadav A. A novel approach for iron deficiency anaemia with liposomal iron: concept to clinic. J Biosci Med, 2020;9:27. Doi: 10.4236/jbm.2020.89003

4. Karine T, Friedman JF. An update on anemia in less developed countries. Am J Trop Med Hyg, 2007;77:44-51. Doi: 10.4269/ajtmh.2007.77.44

5. Ogunka-Nnoka C, Amadi B, Agomuo E, Amadi P. Ameliorative effects of some natural blood boosters on cyclophosphamide-induced anemia in rats. J Appl Life Sci In, 2017;10:1-11. Doi: 10.9734/JALSI/2017/31294

6. Akah PA, Okolo CE, Ezike AC. The haematinic activity of the methanol leaf extract of *Brillantasia nitens* Lindau in rats. Afr J Biotechnol, 2009; 8: 2389-2393.

7. Koffuor GA, Sam GH, Dadzeasah PE, Owiafe EO, Gyapong AA. Erythropoietic effect of the ethanolic root bark extract of *Carissa edulis* in phenylhydrazine-induced anemic Sprague-Dawley rats. Pharmacol Res, 2012;6:20-24. Doi: 10.3923/rjpharm.2012.20.24

8. Mahin MD. The heme oxygenase system: a regulator of second messenger gases. Annu Rev Pharmacol Toxicol, 1997;37: 517-554. Doi: 10.1146/annurev.pharmtox.37.1.517

9. Li K, Menon MP, Karur VG, Hegde S, Wojchowski DM. Attenuated signaling by a phosphotyrosine-null Epo receptor form in primary erythroid progenitor cells. Blood, 2003;102:3147-3153. Doi: 10.1182/blood-2003-01-0078

10. Rathnayake AR, Navaratne SB, Uthpala TG. *Moringa oleifera* plant and the nutritional and medicinal properties of *Moringa oleifera* leaves Trends & Prospects in Processing of Horticultural Crops, 2019:251-268.

11. Tahir MK, Mugal T, Haq IU. *Moringa oleifera*: a natural gift – a review. J Pharm Sci, 2010;2:775.

12. Kalappurayil TM, Joseph BP. A review of pharmacognostical studies on *Moringa oleifera* lam. flowers. Pharmacogn J, 2019;1:81-84. Doi: 10.5530/pj.2017.1.1

13. Sánchez-Machado DI, Núñez-Gastélum JA, Reyes-Moreno C, Ramírez-Wong B, López-Cervantes J. Nutritional quality of edible parts of *Moringa oleifera*. Food Anal Methods, 2010;3:175-180. Doi: 10.1007/s12161-009-9106-z

14. Vyas S, Kachhwaha S, Kothari SL. Comparative analysis of phenolic contents and total antioxidant capacity of *Moringa oleifera* Lam. Pharmacogn J, 2015;7:44-51. Doi: 10.5530/pj.2015.7.5

15. Abdullrazis AF, Ibrahim MD, Kntayya SB. Health benefits of *Moringa oleifera*. Asian Pac J Cancer Prev, 2014;15:8571-8576. Doi: 10.7314/apjcp.2014.15.20.8571

16. Ahmed K, Banik R, Hossain M, Jahan I. Vitamin C (L-ascorbic acid) content in different parts of *Moringa oleifera* grown in Bangladesh. Am Chem Sci J, 2016;11:1-6. Doi: 10.9734/ACSJ/2016/21119

17. Mahmood KT, Mugal T, Haq IU. *Moringa oleifera*: a natural gift-A review. J Pharm Sci, 2010;2:775.

18. Gyawali R, Paudel PN, Basyal D, Setzer WN, Lamichhane S, Paudel MK, et al. A review on ayurvedic medicinal herbs as remedial perspective for COVID-19. J Kar Aca Health Sci, 2020;26:1-21. Doi: 10.3126/jkahs.v3i0.29116

19. Singh D, Choudhury S, Singh TU, Garg SK. Pharmacodynamics of uterotonic effect of *Moringa oleifera* flowers extract. J Vet Pharmacol Ther, 2008;7:12-15.

20. Sheth PA, Pawar AT, Mote CS, More C. Antianemic activity of polyherbal formulation, Raktavardhak Kadha, against phenylhydrazine-induced anemia in rats. J Ayurveda Integr Med, 2021;12:340-345. Doi: 10.1016/j.jaim.2021.02.009

21. Ochei J, Kolhatkar A. Medical Laboratory Science: Theory and Practice. McGraw Hill Education, 2000.

22. Diallo A, Gbeassor M, Vovor A, Eklu-Gadegbeku K, Aklikokou K, Agbonon A, et al. Effect of *Tectona grandis* on phenylhydrazine-induced anaemia in rats. Fitoterapia, 2008;79:332-336. Doi: 10.1016/j.fitote.2008.02.005

23. Criswell KA, Sulkanen AP, Hochbaum AF, Bleavins MR. Effects of phenylhydrazine or phlebotomy on peripheral blood, bone marrow and erythropoietin in Wistar rats. J Appl Toxicol, 2000;20:25-34. Doi: 10.1002/(sici)1099-1263(200001/02)20:1<25::aid-jat624>3.0.co;2-7

Acta Pharm. Sci. Vol 62:(2), 2024
Research article
DOI: 10.23893/1307-2080.APS6229

Sprayable microemulsion of diphenhydramine hydrochloride for dermal delivery

Muhammet Davut ARPA[1*], Tuğba ARSLAN[1], Huriye ERASLAN[1], Neslihan ÜSTÜNDAĞ OKUR[2]

1 Istanbul Medipol University, School of Pharmacy, Department of Pharmaceutical Technology, Istanbul, Türkiye
2 University of Health Sciences, Faculty of Pharmacy, Department of Pharmaceutical Technology, Istanbul, Türkiye

ABSTRACT

In this work, a sprayable microemulsion of diphenhydramine hydrochloride (DPH HCl) was developed for use in conditions that cause itching, such as insect bites, mild sunburns, and skin irritations. Microemulsions were prepared using oleic acid and isopropyl myristate as the oil phase (1:2), Tween 20 and Transcutol HP as surfactants, isopropyl alcohol as co-surfactant, and water. The microemulsions (M1, M2, and M3) that presented greater area were selected as lead microemulsions and loaded with 2% DPH HCl (w/w). The physical stabilities of drug-loaded formulations with a droplet size of 15.998-19.030 nm, polydispersity index of 0.404-0.516, and turbidity of 2.41-2.50 Ntu were evaluated as appropriate. The microemulsions showed a great spread area in sprayability studies. Moreover, DPH HCl release from microemulsions reached 80-100% within one hour. The sprayable microemulsions were highly suitable for topical application of DPH HCl and can be evaluated for clinical applications with further studies.

Keywords: diphenhydramine hydrochloride, microemulsion, dermal delivery, topical application, topical spray

*Corresponding author: Muhammet Davut ARPA
E-mail: mdarpa@medipol.edu.tr
ORCIDs:
Muhammet Davut ARPA: 0000-0001-9290-2404
Tuğba ARSLAN: 0000-0002-7131-0570
Huriye ERASLAN: 0009-0002-7466-9842
Neslihan ÜSTÜNDAĞ OKUR: 0000-0002-3210-3747
(Received 5 Jan 2024, Accepted 6 Feb 2024)

INTRODUCTION

Microemulsions, characterized by small droplet sizes up to 200 nm, emerge as interesting and promising submicron carriers for dermal drug delivery owing to their thermodynamic stability, transparency, optically isotropic, and spontaneous formation[1,2]. Microemulsions are usually formed by the dropwise addition of a water phase to a mixture of oil, surfactant, and cosurfactant[3]. They exhibit low interfacial tension attributed to the presence of surfactants and these properties contribute to the maintenance of stability[4]. Microemulsions offer significant advantages including providing higher drug loading capacity by enhancing the solubility of the active ingredient, increasing the thermodynamic activity of the drug, and improving the permeability of the drug thanks to its components[5]. Additionally, it enables the combination of water-soluble and oil-soluble substances[6]. These formulations with low viscosity can be used in this form, as well as they can be designed as microemulsion-based gel with the addition of a gel-forming agent[7]. The solution-like low viscosity of microemulsions allows them to be designed as sprayable formulations[8] that provide high patient compliance in terms of application.

Diphenhydramine (DPH) was initially synthesized in 1943 by Dr. George Rieveschl from the University of Cincinnati and it was FDA's first approval for an antihistamine drug. DPH attempts as an antagonist of the H-1 receptor, counteracting the impact of histamine and relieving allergic reaction symptoms[9]. Its oral tablet and liquid preparations are commercially available on the market[10]. However, the short half-life (2-9 h) of DPH along with the first-pass effect resulting in low oral bioavailability (40-60%), necessitates frequent administration (from 25 mg to 50 mg, 3 to 4 times a day) to maintain the aimed plasma levels[11]. Since the high systemic side effects resulting from oral delivery will decrease patient compliance, dermal delivery, which has fewer systemic side effects, can be preferable[12]. DPH, this first-generation antihistamine, has perfect anesthetic and antipruritic effects when used topically[13]. Therefore, they effectively reduce itching caused by local allergic reactions to insect bites, mild sunburns, mild skin irritations, etc., and ensure good patient compliance with relief of pain and suffering[9,12].

Studies have been conducted on the topical application of diphenhydramine hydrochloride (DPH HCl), including microemulsion[12,14-17]. However, no sprayable microemulsion formulations of DPH HCl were found. This study aimed to develop a novel sprayable microemulsion formulation loaded with DPH HCl, which is the soluble salt of DPH, and propose an optimized formulation for treating seasonal allergies, insect bites, stings, and rashes. The physicochemical characterization and *in vitro* drug release profiling of the formulated microemulsions were investigated for this aim.

METHODOLOGY

Materials

DPH HCl, oleic acid, acetonitrile, and phosphate buffer tablet (PBS, pH 7.4) were purchased from Sigma-Aldrich, USA. Transcutol HP (diethylene glycol monoethyl ether, HLB 4.2) and Isopropyl myristate (IPM) were purchased from Alfa Aesar, USA. Tween 20 (polyoxyethylene sorbitan laurate, HLB 16.7) was purchased from Merck, Germany. Isopropyl alcohol (IPA) was purchased from Carlo Erba, Italy.

Solubility of DPH HCl

The solubility of DPH HCl was investigated at ambient temperature in various solvents, including distilled water, IPM, oleic acid, IPA, Transcutol HP, and Tween 20. The studies were performed with minor revisions to the previous study[18]. An excess amount of DPH HCl was dispersed in a microcentrifuge tube with one mL of the solvent. Each tube was shaken for 24 h in a horizontal shaker (SSL2, Stuart, UK), and then the mixture was centrifuged (3-18KS, Sigma, Germany) at 14,000 rpm for 30 min. The supernatant was subjected to dilution with the mobile phase (acetonitrile: water, 35:65, v/v) at different ratios and subsequently analyzed by an HPLC method. The same procedure was separately carried out for each solvent.

An HPLC method was developed and validated for the quantification of DPH HCl. Analysis conditions were recorded on the HPLC device (1100 series, Agilent, USA) having a UV detector as in Table 1. A C18 column (InertSustain C18, 150x4.6mm, 5µm, GL Sciences, Japan) was used during the analysis.

Table 1. Conditions of the HPLC method for the quantification of DPH HCl

HPLC condition	
Mobile phase	Acetonitrile: pH 3 phosphate buffer (35:65, v/v)
Flow rate	1.2 mL/min
Wavelength	225 nm
Column temperature	30 °C
Injection volume	20 µL

Preparation of microemulsion formulations

Pseudo-ternary phase diagrams were meticulously created to determine an optimal concentration of the components within a microemulsion design. In this diagram, typically one corner represented a mixture of surfactants, while the other corners were the oil and water components. All the formulation components were mixed in proportions ranging from 0 to 100%. Then, each system was visually observed, and the resulting phase boundaries were drawn[19]. During the studies, various substances were used in different concentrations. As an oil mixture, jojoba oil, IPM, and oleic acid were studied in different ratios and pairs. It was observed that formulations containing jojoba oil did not result in a stable microemulsion. Consequently, in the preparation of microemulsion systems, IPM and oleic acid were selected as the oil phase, Transcutol HP and Tween 20 as the surfactants, and IPA as a co-surfactant.

For preliminary studies, the surfactant and co-surfactant were mixed in different ratios (w/w), namely 3:1, 2:1, 1:1, 1:2, and 1:3. The oil phase and the mixture of surfactant were stirred within a beaker on a magnetic stirrer (Mr-Hei Standard, Heidolph, Germany) at 300 rpm until the mixture homogenized. These mixtures were titrated, drop-by-drop, with first IPA and then distilled water. Addition of distilled water was maintained until the mixture became blurred. While all processes were carried out at ambient temperature, the appearance of the formulation was followed visually. After marking the values that ensure the formation of a clear microemulsion in the phase diagram, the center of the formed microemulsion region was accepted as the lead microemulsion. Drug-loaded formulations were prepared as before. DPH HCl (2%, w/w) was added to the lead microemulsion at the last stage and dissolved by stirring at 300 rpm for 15 min.

Characterization of microemulsion formulations

Characterization studies carried out to assess the suitability of the drug-loaded and blank microemulsions were carried out at least three times.

Viscosity

The viscosities of formulations were measured by a vibrational viscometer (SV-10, AND Vibro Viscometer, Japan)[20]. A sample of 10 mL microemulsion was filled into a plastic container, and measurements were taken at room temperature until the value was constant. The viscosity studies of each batch were repeated three times, and each measurement was conducted twice.

Droplet size, polydispersity index (PDI), and conductivity

Average droplet size, PDI, and conductivity of the drug-loaded and blank microemulsions were determined using the dynamic light scattering method by a zetasizer (Zetasizer Ultra, Malvern Instruments, Worcestershire, UK) at ambient temperature[21,22]. Disposable cuvettes were used for the measurement of the droplet size and PDI of the formulations. Folded capillary cells were used for the determination of the conductivity of the microemulsions.

Turbidity, refractive index, and physical stability

The turbidity of the formulations was assessed using a digital turbidity meter (TB 210 IR, Lovibond, UK) The instrument was calibrated using solutions of varying turbidity levels specific to the instrument. Subsequently, the microemulsion was filled into a glass bottle up to the marked line and the measurement was performed upon insertion into the device. The refractive index was determined using a digital refractometer (DR 301-95, Kruss, Germany)[23]. Physical stability tests were performed under temperature and centrifuge conditions to determine whether there were changes in the physical stability of the microemulsions such as phase separation or sedimentation. Six cycles of cooling (5±1°C)-heating (45±2°C) conditions were applied to the microemulsions. Additionally, the microemulsions were centrifuged (3-18KS, Sigma, Germany) at 25 °C and 5,000 rpm for 30 min. At the end of the procedures, the microemulsions were assessed visually[7].

Sprayability

A sample of 10 g from each formulation was separately weighed into a spray bottle. Subsequently, a certain amount of a dye (E133) was added to the bottles, and the formulation was stirred using a magnetic stirrer at 500 rpm for 45 min. Following our previous studies[24], a texture analyzer (TA.XT.*Plus*C, Stable Micro Systems, Haslemere, Surrey, UK) was employed for sprayability studies. As shown in Figure 1, a white plate was horizontally positioned 15 cm away from the bottle, and the spray process was conducted five times for each sample. After the process, the diameter of the spray area on the plate was measured.

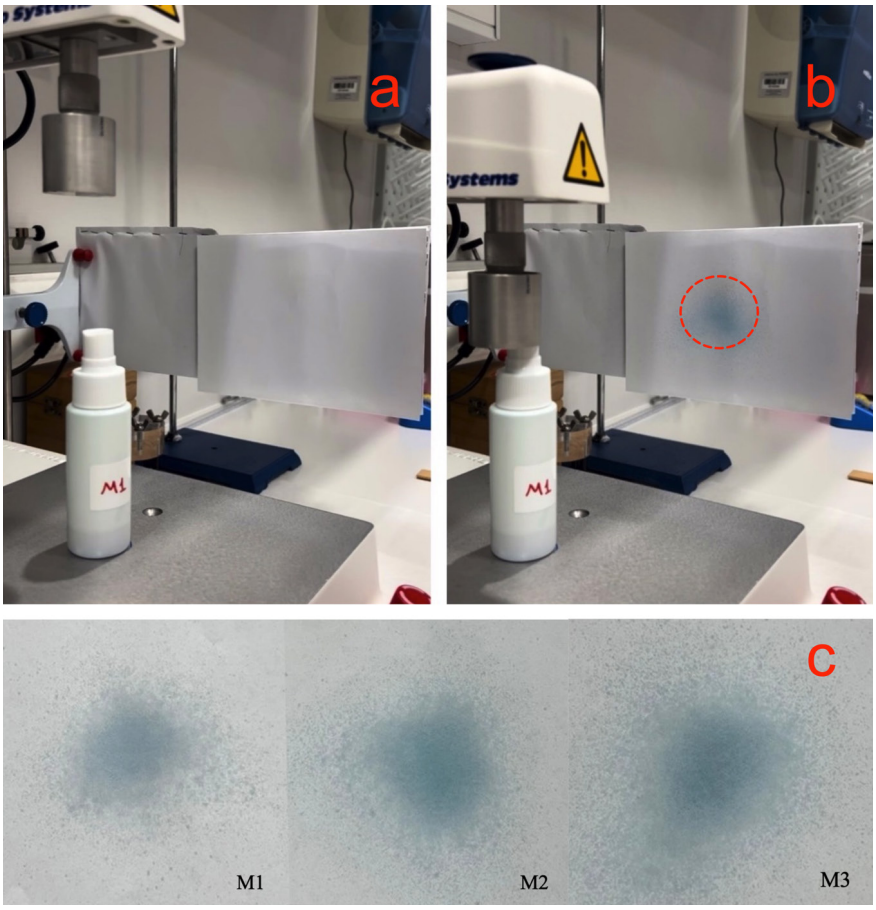

Figure 1. Images of sprayability studies. (a) Before the spray process. (b) After the spray process. (c) The spreading area of M1, M2, and M3 formulations after the spray application

In vitro drug release

In order to evaluate the release profile of the formulations, the DPH HCl-loaded microemulsions were studied through the dialysis bag method, following the procedures from previous studies[22,24]. A sample of 0.5 g formulation was transferred to a dialysis bag. After the bag was tightly closed, it was placed in a beaker containing 200 mL of pH 7.4 phosphate buffer (PBS). The studies were conducted on a magnetic stirrer at 50 rpm and 32±2°C. At seven distinct time points (5, 10, 15, 20, 30, 45, and 60 min), one mL was withdrawn from the release medium using an injector. Following each sampling, one mL of fresh PBS was added to maintain a constant volume. The samples were analyzed by HPLC at 225 nm. The experiments were performed four times for each batch.

On the one hand, the release of DPH HCl from the formulations was evaluated utilizing model-independent approaches, which were the difference factor (f1) and similarity factors (f2)[25,26]. On the other hand, the release profiles were assessed using model-dependent kinetics such as zero order, first order, Higuchi, and Hixson-Crowell[22].

Statistical analyses

The data were presented as mean±SD. Statistical analysis was performed using a student's t-test.

RESULTS and DISCUSSION

Solubility of DPH HCl

The solubility of DPH HCl in various solvents was analyzed using HPLC. It was observed that all formulation components, except IPM, dissolved the active substance (Table 2). DPH HCl was found to be freely soluble in distilled water and Transcutol HP, while the solubility of DPH HCl was lowest in IPM (0.011 mg/mL) compared to other solvents.

Table 2. Solubility of DPH HCl in different solvents

Solvent	Concentration (mg/mL±SD)
Distilled water	622.358±2.515
IPA	23.541±1.018
Tween 20	59.131±2.111
Transcutol HP	129.706±3.001
Oleic acid	10.850±0.300
IPM	0.011±0.001

Preparation of microemulsion formulations

Microemulsions consist of four main components: water, oil, surfactant, and co-surfactant phases. In this project, IPM, chosen as the oil phase for the formulation of microemulsion systems, demonstrates a robust effect in enhancing permeation and biocompatibility[7,27]. Oleic acid, a monounsaturated fatty acid, is frequently used as the oily phase in the formation of microemulsions and is well-compatible with IPM[28,29]. The ratio of oleic acid to IPM was 1:2 (w/w) for all formulations. Transcutol HP, monoethyl ether of diethylene glycol, has been comprehensively studied as a penetration enhancer in various

transdermal therapeutic systems, with the potential to enhance drug solubility and improve drug delivery[30]. Additionally, Hernandez et al. found that a high concentration of Transcutol HP reduces the surface tension and leads to the formation of small droplets[31]. Polysorbate 20 or Tween 20, the most hydrophilic surfactant among polysorbates, is nonionic and biocompatible. This surfactant, a sorbitan monolaurate derivative ethoxylated with approximately 20 ethylene oxide units, has the effect of increasing the solubility capacity. Thanks to these properties, it is frequently used in microemulsion formulations[32,33].

The most crucial stage for the preparation of the microemulsions to acquire the desirable composition of the used compounds is to construct a pseudo-ternary phase diagram. These diagrams serve to determine the range of microemulsion existence and explore the influence of varying component weight ratios on the size of a stable microemulsion area[26]. The corners of the phase diagram represent the components of the microemulsion (water, oil, and surfactant: cosurfactant). Any point in the diagram reveals the proportions of these components that make up the formulation so that there is a total of 100%. The center of the area, where the microemulsion is formed, is considered to be the ideal microemulsion. The pseudo-ternary phase diagrams of the formulations were created using the Microsoft Excel program. Then, three formulations that provide the greatest microemulsion area were selected. Figure 2 shows the pseudo-ternary phase diagrams of the selected microemulsion formulations. The surfactant: cosurfactant ratios of M1, M2, and M3 formulations were 1:1, 1:2, and 1:3, respectively. Accordingly, the ideal formulations were determined and drug-loaded microemulsions were prepared by adding DPH HCl (2%, w/w) following the composition ratios (Table 3).

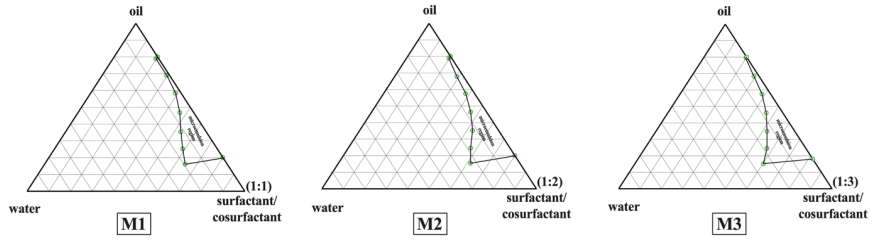

Figure 2. Pseudo-ternary phase diagram of selected microemulsions, which provide greater microemulsion region

Table 3. Composition of the drug-loaded ideal microemulsion formulations (w/w)

Component (%)	M1	M2	M3
DPH HCl	2	2	2
Oleic acid	10.78	10.94	10.46
IPM	21.56	21.89	20.90
Transcutol HP	21.15	13.64	10.14
Tween 20	9.23	5.96	4.43
IPA	30.38	39.20	43.74
Distilled water	4.90	6.37	8.33

Characterization of microemulsion formulations

Viscosity

The viscosity of topical formulations represents a significant physical attribute affecting the rate of drug release. In general, increasing the viscosity of the formulation results in a hard structure and reduced drug release rate[34]. Contrarily, low viscosity plays a positive impact on the sprayability of formulations[35]. The viscosity results are presented in Table 4. For the blank formulations, viscosity values ranged between 5.74 and 7.92 mPa·s. Similarly, formulations incorporating DPH HCl demonstrated viscosities spanning from 5.96 to 8.30 mPa·s, offering a beneficial aspect for improved sprayability. Monton et al.[36] stated that the oral spray microemulsions they prepared using clove oil, tween 80, and PEG were suitable for administration with viscosity values between 12.8 and 65.8 mPa·s. However, the results indicated that the addition of the active ingredient to the formulations increased viscosity ($p<0.05$). In addition, consistent with the literature, it was detected that viscosity decreased as alcohol or water amounts increased in the microemulsion formulations[7,37,38] because of the low viscosities of these solvents.

Table 4. Characterization of the developed blank and DPH HCl-loaded microemulsion formulations

Formulation	Viscosity (mPa·s±SD)	Droplet size (nm±SD)	Turbidity (Ntu±SD)	PDI (±SD)	Refractive index (nD±SD)	Conductivity (µS/cm±SD)
M1	7.92±0.13	4.362±0.345	2.28±0.08	0.327±0.031	1.415±0.001	0.016±0.000
$M1_{DPH\ HCl}$	8.30±0.02	17.451±1.807	2.42±0.04	0.462±0.017	1.418±0.001	0.094±0.000
M2	6.43±0.08	5.501±0.658	2.08±0.03	0.326±0.028	1.410±0.001	0.011±0.000
$M2_{DPH\ HCl}$	6.82±0.17	19.030±0.707	2.50±0.04	0.516±0.029	1.414±0.001	0.127±0.001
M3	5.74±0.04	5.809±0.315	2.29±0.05	0.249±0.024	1.406±0.001	0.005±0.000
$M3_{DPH\ HCl}$	5.96±0.08	15.998±1.294	2.41±0.14	0.404±0.040	1.408±0.001	0.169±0.001

Droplet size, PDI, and conductivity

The droplet size of blank microemulsions was between 4.362 and 5.809 nm, while that of drug-loaded microemulsions was between 15.998 nm and 19.030 nm (Table 4). While microemulsions are generally characterized by droplet sizes of average 10-200 nm[39], smaller droplet sizes such as 1-10 nm can also be obtained[22,33,40,41]. These rather small droplet sizes can be attributed to the fact that the co-surfactant penetrates the interfacial film of the oil droplets and affects the fluidity and viscosity[20]. Additionally, the increase in droplet size may be associated with the addition of the active ingredient. Sarheed et al.[42] found an increase in droplet size in half of the formulations by adding lidocaine to blank nanoemulsions. The PDI of the microemulsions was found between 0.249 and 0.516 (Table 4). A PDI of less than 0.5 indicates that the formulations have narrow and homogeneous droplet size distribution[43].

Conductivity level is one of the key indicators for detecting the internal and external phases of the microemulsion. The presence of non-ionic surfactants and cosurfactants and low water content causes this value to be close to zero[22]. Additionally, since the oil phase mostly does not contain electrolytes, it causes low electrical conductivity values, and this may indicate that the external phase is oil[4,20]. The conductivity of both the drug-loaded and the blank microemulsions was found to be approximately zero (Table 4). Considering the obtained findings, it was determined that the formulations are W/O type microemulsions.

Turbidity, refractive index, and physical stability

Turbidity in a liquid formulation refers to blur in the formulation caused by suspended particles and particle size, which can affect both the formulation's

visual clarity and its physical stability[44,45]. An optimal microemulsion usually has minimal turbidity or high transparency, signifying a well-structured and stable formulation with finely dispersed and homogeneously mixed oil, water, and surfactant phases. The turbidity of the formulations was determined to range from 2.08 to 2.50 Ntu, as given in Table 4. The low turbidity values obtained indicated that the formulations were good in terms of physical appearance and stability. The results were consistent with the literature[46,47]. The refractive index is useful for characterizing and differentiating chemicals, evaluating their purity and clarity, and offering insight into the interactions and composition of pharmaceutical systems. The refractive index of all prepared microemulsions ranged between 1.408 and 1.418 (Table 4), and there was no significant difference in the presence and absence of DPH HCl although there was a very small increase with drug loading ($p>0.05$). This slight change indicated that drug loading was ensured without any phase change in the microemulsion, which was a complex system[4]. The physical stability of the formulations was demonstrated by the fact that no physical change was observed in drug-loaded and blank microemulsions subjected to challenging conditions such as temperature and centrifugation.

Sprayability

Sprayability is crucial for topical drug delivery as offers advantages such as the ability to deliver the formulation to difficult-to-apply areas and large areas for dermal application, short application time, and homogeneous distribution for colloidal preparations[48]. In addition, with all these advantages and ease of use, patient compliance is enhanced[49]. Therefore, the characterization of sprayability is necessary to evaluate the suitability of the formulation. The features and composition of the formulation, the size and shape of the nozzle, the pump's design, the reservoir's capacity, and the amount left in the spray bottle can impact the formulation's spray characteristics[50]. As shown in Figures 1a and 1b, to investigate the sprayability of the DPH HCl microemulsion, the formulations were sprayed to the horizontal plate using the texture analyzer. The spreading diameter of the formulations after one spray process was found to be between 5.150 and 6.240 mm (Table 5, Figure 1c). Due to the absence of leakage from the spray nozzle of the bottle and the large spray area, the sprayability of all tested formulations was evaluated as good. It was noted that the results were consistent with the viscosity, indicating that as viscosity decreased, the diameter of the spreading area increased[51].

Table 5. Diameter of spreading area of the drug-loaded formulations after one spray process (n=5)

Formulation	Diameter (cm±SD)
M1	5.150±0.137
M2	6.100±0.386
M3	6.240±0.185

In vitro drug release

The *in vitro* release study of the formulations was performed by the dialysis bag method. This method is a frequently preferred method for evaluating the release profiles of microemulsions[20,22]. DPH HCl release from the microemulsion formulations reached between 80% and 100% within 60 min (Figure 3). In a study, Aziz et al.[12] investigated the release profiles of DPH HCl-loaded chitosan nanoparticles by the dialysis bag method. It was observed that the drug reached 50-80% release levels within 60 min and 60-90% within 120 min. In our previous study[52], it was determined that the DPH HCl release from diatomite-chitosan composites was 60-90% within 60 min. The fact that the cumulative drug release reached 80-100% in a short time was consistent with the literature and this may be associated with the high water solubility of DPH HCl[52].

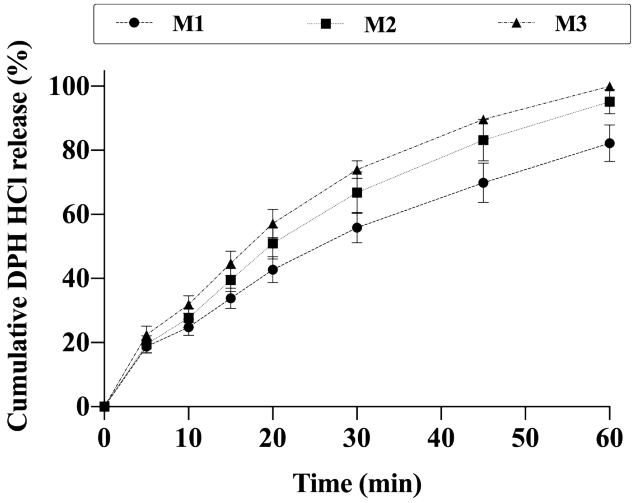

Figure 3. DPH HCl release profiles of the microemulsions (n=4)

The M3 formulation with the highest water content and the lowest viscosity provided higher drug release compared to others. Differences in the viscosities and the water content may have affected the drug release from the microemulsions. It is shown that there is generally a negative relationship between viscosity and drug release rate[41,53,54]. In a study, Kumari et al. developed the microemulsion formulations of valsartan and investigated the solubility of valsartan in microemulsion components. They also indicated the solubility of valsartan in the developed microemulsions. Among the microemulsions with no significant difference between their viscosities, M5 had the highest valsartan solubility and provided a higher cumulative release of valsartan compared to the other microemulsions[55]. The release profiles of the formulations were evaluated with model-dependent kinetics and it was found that the profiles were compatible with Higuchi kinetics, in which the highest r^2 value was determined (Table 6). This model suggests that drug release from microemulsions occurs through diffusion[22,56,57]. The similarity between the drug release profiles of the formulations was investigated by model-independent kinetics. The fact that the difference factor (f1) is less than 15 and the similarity factor (f2) is greater than 50 indicates the similarity of the drug release profiles of the formulations[25]. The release profiles of the M2 and M3 microemulsion pair were found to be similar (f1=10, f2=63) (Table 7).

Table 6. Release kinetics data of DPH HCl-loaded microemulsions

Formulation	Zero order (r^2)	First order (r^2)	Higuchi (r^2)	Hixson-Crowell (r^2)
M1	0.9711	0.8919	0.9909	0.9289
M2	0.9642	0.8578	0.9939	0.9021
M3	0.9486	0.8412	0.9898	0.8840

Table 7. Similarity and dissimilarity factors of the prepared formulations

Formulation pairs	Difference factor (f1)	Similarity factor (f2)
M1 – M2	17	52
M1 – M3	28	42
M2 – M3	10	63

Microemulsions are very convenient carriers for the penetration of active ingredients into the skin due to the penetration enhancers they contain, small droplet sizes, and the combination of oil and water. In addition to these advantages, their low viscosity allows them to be sprayed, providing ease of application and high patient compliance. In this study, a novel sprayable microemulsion formulation was designed for the dermal application of diphenhydramine hydrochloride, a first-generation antihistamine. The formulation with a surfactant/cosurfactant ratio of 1:3 showed the widest microemulsion region. The characterization studies of the obtained water/oil-type microemulsions have revealed their physical stability. The drug-loaded microemulsions (2%) with viscosity values of between 5.96 and 8.30 mPa·s were evaluated as having good sprayability with a great spreading area. *In vitro* drug release studies revealed that DPH HCl release from the microemulsions reached approx. 100% within 60 min and the best fit kinetic model for the DPH HCl release profiles was Higuchi, which suggests that the drug release occurs by diffusion. The findings indicated that these novel sprayable DPH HCl formulations are promising with high patient compliance for the topical treatment of itching-causing ailments such as insect bites, mild burns, and irritation.

STATEMENT OF ETHICS

Ethical approval was not required to perform this study.

CONFLICT OF INTEREST STATEMENT

The authors declare that there is no conflict of interest.

AUTHOR CONTRIBUTIONS

Muhammet Davut Arpa: Supervision, Investigation, Project administration, Methodology, Writing – original draft, Writing - review and editing; Tuğba Arslan: Investigation, Methodology, Writing – original draft; Huriye Eraslan: Investigation, Methodology, Writing – original draft; Neslihan Üstündağ Okur: Supervision, Investigation, Writing - review and editing.

REFERENCES

1. Kaur L, Kumar R, Rahi DK, Sinha VR. Formulation and evaluation of microemulsion based gel of oriconazole for topical delivery. Anti-Infective Agents, 2017;15(2):95-104. Doi: 10.2174/2211352515666170619074437

2. Alkrad JA, Assaf SM, Hussein-Al-Ali SH, Alrousan R. Microemulsions as nanocarriers for oral and transdermal administration of enoxaparin. J Drug Deliv Sci Technol, 2022;70(103248):1-9. Doi: 10.1016/j.jddst.2022.103248

3. Szumała P, Macierzanka A. Topical delivery of pharmaceutical and cosmetic macromolecules using microemulsion systems. Int J Pharm, 2022;615(121488):1-12. Doi: 10.1016/j.ijpharm.2022.121488

4. Lamoudi L, Akretche S, Hadjsadok A, Daoud K. Fusidic acid microemulsion based on a pseudoternary phase diagram: development, characterization, and evaluation. J Pharm Innov, 2022. Doi: 10.1007/s12247-022-09668-4

5. Hajjar B, Zier KI, Khalid N, Azarmi S, Löbenberg R. Evaluation of a microemulsion-based gel formulation for topical drug delivery of diclofenac sodium. J Pharm Investig, 2018;48(3):351-362. Doi: 10.1007/s40005-017-0327-7

6. Muzaffar F, Singh UK, Chauhan L. Review on microemulsion as futuristic drug delivery. Int J Pharm Pharm Sci, 2013;5(3):39-53.

7. Üstündağ Okur N, Çağlar EŞ, Arpa MD, Karasulu HY. Preparation and evaluation of novel microemulsion-based hydrogels for dermal delivery of benzocaine. Pharm Dev Technol, 2017;22(4):500-510. Doi: 10.3109/10837450.2015.1131716

8. Zhang Q, Jiang X, Jiang W, Lu W, Su L, Shi Z. Preparation of nimodipine-loaded microemulsion for intranasal delivery and evaluation on the targeting efficiency to the brain. Int J Pharm, 2004:275:85-96. Doi: 10.1016/j.ijpharm.2004.01.039

9. Miller SM, Cumpston KL. Diphenhydramine. Philip Wexler (Ed.) In Encycl Toxicol (Third Ed), 2014;2:195-197. Doi: 10.1016/B978-0-12-386454-3.00724-7

10. Gumieniczek A, Lejwoda K, Data N. Chemical stability study of H(1) antihistaminic drugs from the first and the second generations, diphenhydramine, azelastine and bepotastine, in pure APIs and in the presence of two excipients, citric acid and polyvinyl alcohol. Molecules, 2022;27(23):8322. Doi: 10.3390/molecules27238322

11. Baby A, Shivakumar HN, Alayadan P. Formulation and evaluation of film forming solution of diphenhydramine hydrochloride for transdermal delivery. Indian J Pharm Educ Res, 2022;56(1):43-49. Doi: 10.5530/ijper.56.1.6

12. Aziz SN, Badawy AA, Nessem DI, Abd El Malak NS. Promising nanoparticulate system for topical delivery of diphenhydramine hydrochloride: in-vitro and in-vivo evaluation. J Drug Deliv Sci Technol, 2020;55:101454. Doi: 10.1016/j.jddst.2019.101454

13. Pavlidakey PG, Brodell EE, Helms SE. Diphenhydramine as an alternative local anesthetic agent. J Clin Aesthet Dermatol, 2009;2(10):37-40.

14. Neubert RHH, Schmalfuß U, Wolf R, Wohlrab WA. Microemulsions as Colloidal Vehicle Systems for Dermal Drug Delivery. Part V: Microemulsions without and with Glycolipid as Penetration Enhancer. J Pharm Sci, 2005;94(4):821-827. Doi: 10.1002/jps.20233

15. Sanna V, Peana AT, Moretti MDL. Development of new topical formulations of diphenhydramine hydrochloride: In vitro diffusion and in vivo preliminary studies. Int J PharmTech Res, 2010;2(1):863-869.

16. Kotwal V, Bhise K, Thube R. Enhancement of iontophoretic transport of diphenhydramine hydrochloride thermosensitive gel by optimization of pH, polymer concentration, electrode design, and pulse rate. AAPS PharmSciTech, 2007;8(4):E1-E6. Doi: 10.1208/pt0804120

17. Schmalfuß U, Neubert R, Wohlrab W. Modification of drug penetration into human skin using microemulsions. J Control Release, 1997;46(3):279-285. Doi: 10.1016/S0168-3659(96)01609-4

18. Arpa MD, Ünükür MZ, Erim ÜC. Formulation, characterization and in vitro release studies of terbinafine hydrochloride loaded buccal films. J Res Pharm, 2021;25(5):667-680. Doi: 10.29228/jrp.58

19. Berkman M, Güleç K. Pseudo Ternary Phase Diagrams: a practical approach for the area and centroid calculation of stable microemulsion regions. Istanbul J Pharm, 2021;51(1):42-49. Doi: 10.26650/istanbuljpharm.2020.0090

20. Yozgatlı V, Üstündağ Okur N, Okur ME, Sipahi H, Charehsaz M, Aydın A, et al. Managing allergic conjunctivitis via ophthalmic microemulsions: Formulation, characterization, in vitro irritation studies based on EpiOcular™ eye irritation assay and in vivo studies in rabbit eye. J Surfactants Deterg, 2023;26(6):853-866. Doi: 10.1002/jsde.12691

21. Okur ME, Kolbaşı B, Şahin M, Karadağ AE, Reis R, Çağlar EŞ, et al. A novel approach in the treatment of osteoarthritis: in vitro and in vivo evaluation of *Allium sativum* microemulsion. J Surfactants Deterg, 2022;25(5):621-633. Doi: 10.1002/jsde.12605

22. Çağlar EŞ, Okur ME, Aksu B, Üstündağ Okur N. Transdermal delivery of acemetacin loaded microemulsions: Preparation, characterization, in vitro-ex vivo evaluation and in vivo analgesic and anti-inflammatory efficacy. J Dispers Sci Technol, 2023:1-11. Doi: 10.1080/01932691.2023.2175691

23. Karasulu HY, Oruç N, Üstündağ Okur N, Ilem Özdemir D, Ay Şenyiğit Z, Barbet Yilmaz F, et al. Aprotinin revisited: formulation, characterization, biodistribution and therapeutic potential of new aprotinin microemulsion in acute pancreatitis. J Drug Target, 2015;23(6):525-537. Doi: 10.3109/1061186X.2015.1015537

24. Arpa MD, Kesmen EE, Biltekin SN. Novel sprayable thermosensitive benzydamine hydrogels for topical application: development, characterization, and in vitro biological activities. AAPS PharmSciTech, 2023;24(8):1-16. Doi: 10.1208/s12249-023-02674-w

25. Arpa MD, Üstündağ Okur N, Gök MK, Özgümüş S, Cevher E. Chitosan-based buccal mucoadhesive patches to enhance the systemic bioavailability of tizanidine. Int J Pharm, 2023;642(123168):1-13. Doi: 10.1016/j.ijpharm.2023.123168

26. Sahoo S, Pani NR, Sahoo SK. Microemulsion based topical hydrogel of sertaconazole: formulation, characterization and evaluation. Colloids Surfaces B Biointerfaces, 2014;120:193-199. Doi: 10.1016/j.colsurfb.2014.05.022

27. Yang, J, Xu H, Wu S, Ju B, Zhu D, Yan Y, et al. Preparation and evaluation of microemulsion-based transdermal delivery of *Cistanche tubulosa* Phenylethanoid Glycosides. Mol Med Rep, 2017;15(3):1109-1116. Doi: 10.3892/mmr.2017.6147

28. Moghimipour E, Farsimadan N, Salimi A. Ocular delivery of quercetin using microemulsion system: design, characterization, and ex-vivo transcorneal permeation. Iran J Pharm Res, 2022;21(1):e127486. Doi: 10.5812/ijpr-127486

29. Malakar J, Sen SO, Nayak AK, Sen KK. Development and evaluation of microemulsions for transdermal delivery of insulin. ISRN Pharm, 2011;780150:1-7. Doi: 10.5402/2011/780150

30. Ita K. Chemical Permeation Enhancers. Ita K (Ed.). In Transdermal Drug Delivery, Academic Press,2020:p. 63-96. Doi: 10.1016/b978-0-12-822550-9.00005-3

31. Hernandez C, Jain P, Sharma H, Lam S, Sonti S. Investigating the effect of transcutol on the physical properties of an O/W cream. J Dispers Sci Technol, 2020;41(4):600-606. Doi: 10.1080/01932691.2019.1609362

32. Schmidt RF, Prause A, Prévost S, Doutch J, Gradzielski M. Phase behavior and structure of a biocompatible microemulsion based on Tween 20, 2-ethylhexylglycerine and isopropyl palmitate in water. Colloid Polym Sci, 2023;301(7):753-762. Doi: 10.1007/s00396-023-05119-9

33. Bergonzi MC, Hamdouch R, Mazzacuva F, Isacchi B, Bilia AR. Optimization, characterization and in vitro evaluation of curcumin microemulsions. LWT-Food Sci Technol, 2014;59(1):148-155. Doi: 10.1016/j.lwt.2014.06.009

34. Binder L, Mazál J, Petz R, Klang V, Valenta C. The role of viscosity on skin penetration from cellulose ether-based hydrogels. Ski Res Technol, 2019;25(5):725-734. Doi: 10.1111/srt.12709

35. Mahdi MH, Conway BR, Smith AM. Development of mucoadhesive sprayable gellan gum fluid gels. Int J Pharm, 2015;488(1-2):12-19. Doi: 10.1016/j.ijpharm.2015.04.011

36. Monton C, Settharaksa S, Suksaeree J, Chusut T. The preparation, characterization, and stability evaluation of a microemulsion-based oral spray containing clove oil for the treatment of oral candidiasis. J Drug Deliv Sci Technol, 2020;57:101735. Doi: 10.1016/j.jddst.2020.101735

37. Manyala DL, Varade D. Formation and characterization of microemulsion with novel anionic sodium n-lauroylsarcosinate for personal care. J Mol Liq, 2021;343:117657. Doi: 10.1016/j.molliq.2021.117657

38. Sharma H, Kumar Sahu G, Kaur CD. Development of ionic liquid microemulsion for transdermal delivery of a chemotherapeutic agent. SN Appl Sci, 2021;3(2). Doi: 10.1007/s42452-021-04235-x

39. Bhalke RD, Kulkarni SS, Kendre PN, Pande VV, Giri MA. A facile approach to fabrication and characterization of novel herbal microemulsion-based UV shielding cream. Futur J Pharm Sci, 2020;6(1):1-10. Doi: 10.1186/s43094-020-00075-5

40. Moghimipour E, Salimi A, Eftekhari S. Design and characterization of microemulsion systems for naproxen. Adv Pharm Bull, 2013;3(1):63-71. Doi: 10.5681/apb.2013.011

41. Salimi A, Noorafrooz R, Fouladi M, Soleymani, SM. Design and assessment of a microemulsion-based transdermal drug delivery system for meloxicam; examination of formulation ingredients. Fabad J Pharm Sci, 2023;48(3):359-372. Doi: 10.55262/fabadeczacilik.1187620

42. Sarheed O, Dibi M, Ramesh KVRNS. Studies on the effect of oil and surfactant on the formation of alginate-based O/W lidocaine nanocarriers using nanoemulsion template. Pharmaceutics, 2020;12(12):1-21. Doi: 10.3390/pharmaceutics12121223

43. Alnusaire TS. Olive leaves (*Olea europaea* L.) extract loaded lipid nanoparticles: optimization of processing parameters by box-behnken statistical design, *in-vitro* characterization, and evaluation of anti-oxadant and anti-microbial activity. J Oleo Sci, 2021;70(10):1403-1416. Doi: 10.5650/jos.ess21149

44. Ningrum YP, Budhiyanti SA. Formulation and stability of *Ulva lactuca* fatty acid oil in water (O/W) microemulsion. Food Research, 2022;6(4):120-127. Doi: 10.26656/fr.2017.6(4).575

45. Cho YH, Kim S, Bae EK, Mok CK, Park J. Formulation of a cosurfactant-free O/W microemulsion using nonionic surfactant mixtures. J Food Sci, 2008;73(3):115-121. Doi: 10.1111/j.1750-3841.2008.00688.x

46. Çilek A, Çelebi N, Tirnaksiz F. Lecithin-based microemulsion of a peptide for oral administration: preparation, characterization, and physical stability of the formulation. Drug Deliv, 2006;13(1):19-24. Doi: 10.1080/10717540500313109

47. Xiao L, Hou J, Wang W, Raj I. Development of a novel high-temperature microemulsion for enhanced oil recovery in tight oil reservoirs. Materials, 2023;16(19):6613. Doi: 10.3390/ma16196613

48. Pleguezuelos-Beltrán P, Gálvez-Martín P, Nieto-García D, Marchal JA, López-Ruiz E. Advances in spray products for skin regeneration. Bioact Mater, 2022;16:187-203. Doi: 10.1016/j.bioactmat.2022.02.023

49. Umar AK, Butarbutar M, Sriwidodo S, Wathoni N. Film-forming sprays for topical drug delivery. Drug Des Devel Ther, 2020;14:2909-2925. Doi: 10.2147/DDDT.S256666

50. Gholizadeh H, Messerotti E, Pozzoli M, Cheng S, Traini D, Young P, et al. Application of a thermosensitive in situ gel of chitosan-based nasal spray loaded with tranexamic acid for localised treatment of nasal wounds. AAPS PharmSciTech, 2019;20(7):1-12. Doi: 10.1208/s12249-019-1517-6

51. Prüfert F, Hering U, Zaichik S, Le NMN, Bernkop-Schnürch A. Synthesis and in vitro characterization of a preactivated thiolated acrylic acid/acrylamide-methylpropane sulfonic acid copolymer as a mucoadhesive sprayable polymer. Int J Pharm, 2020,583:119371. Doi: 10.1016/j.ijpharm.2020.119371

52. Özkan Z, Arpa MD, Özçatal M, Çiftçi H. Preparation of Diatomite-Chitosan Composites for Loading and Release of Diphenhydramine HCl. JournalMM, 2023;4(2):542-560. Doi: 10.55546/jmm.1326482

53. Mali KK, Dhawale SC, Dias RJ. Microemulsion based bioadhesive gel of itraconazole using tamarind gum: in-vitro and ex-vivo evaluation. Marmara Pharm J, 2017;21(3):688-688. Doi: 10.12991/marupj.323593

54. Kamila MM, Mondal N, Gupta BK, Ghosh LK. Preparation, characterization and in-vitro evaluation of sunflower oil-Tween 80-glycerol-based microemulsion formulation of a BCS class-II drug. Lat Am J Pharm, 2009;28(4):622-627.

55. Kumari P, Kumar K, Joshi A, Chauhan V, Rajput V. Development and evaluation of microemulsion Formualatons of Valsartan for Solubility Enhancement. J Drug Deliv Ther, 2023;13(10):117-120. Doi: 10.22270/jddt.v13i10.5990

56. Shewaiter MA, Hammady TM, El-Gindy A, Hammadi SH, Gad S. Formulation and characterization of leflunomide/diclofenac sodium microemulsion base-gel for the transdermal treatment of inflammatory joint diseases. J Drug Deliv Sci Technol, 2021;61:102110. Doi: 10.1016/j.jddst.2020.102110

57. De Stefani C, Vasarri M, Salvatici MC, Grifoni L, Quintela JC, Bilia AR, et al. Microemulsions enhance the in vitro antioxidant activity of oleanolic acid in RAW 264.7 Cells, Pharmaceutics, 2022;14(10):2232. Doi: 10.3390/pharmaceutics14102232

Acta Pharm. Sci. Vol 62:(2), 2024
Research article
DOI: 10.23893/1307-2080.APS6230

Study of different factors affecting spreadability and release of Ibuprofen from carbopol gels using screening design methodology

Lama AL HAUSHEY*

Department of Pharmaceutics and Pharmaceutical Technology, Faculty of Pharmacy, Tishreen University, Lattakia, Syria

ABSTRACT

The objective of this study was to prepare carbopol gels and to evaluate the effect of various solvents on gel spreadability and release properties of Ibuprofen (a hydrophobic compound) using screening design methodology. Five solvents of different polarities were chosen)alcohol, glycerin, PEG_{400}, acetone, PG(. The statistical analysis of the results allowed determining the most influent solvents. Considering the whole results, it appeared that carbopol reduced spreadability while alcohol, glycerin, PEG_{400} and PG increased spreadability. The total released amounts of Ibuprofen were altered by both gel viscosity and Ibuprofen solubility, hence, when Ibuprofen, alcohol and acetone quantities were increased, the quantity of released Ibuprofen per cm^2 inhanced. On the other hand, Carbopol, glycerin, PEG_{400} and PG decreased Ibuprofen release. An optimized experiment was carried out to verify the mathematical model and in order to maximize Ibuprofen release. Gel spreadability was good and enhanced Ibuprofen release was observed for the objective of relieving pain effectively.

Keywords: carbopol, Ibuprofen, spreadability, *in vitro* release, screening design methodology

*Corresponding author: Lama AL HAUSHEY
E-mail: lamaalhaushey239@gmail.com
ORCID: 0009-0003-8751-5049
(Received 14 Sep 2023, Accepted 24 Oct 2023)

INTRODUCTION

Nowadays, there is a great interest in the field of transdermal drug delivery and vast drugs are evaluated for percutaneous absorption. The skin has been used to deliver drugs to the epidermis, dermis, deeper tissues and to systemic circulation[1].

Among the dermal delivery systems, gels have many advantages; they are easy for administration, nongreasy and can increase patient compliance. They have high residence time on the skin and good drug release parameters[2,3]. Gels are semi-solid systems in which the movements of the dispersion medium are restricted by an interlacing network of macromolecules of the dispersed phase[4]. Various studies of drug release have revealed that drugs in gel vehicle are better absorbed than creams or ointments[5].

Many researchers reported that drug release depends on the vehicle and on the drug physicochemical properties[6-9]. The solubility of the drug is among the critical factors that affect drug release in the vehicle and in receptor medium[1]. In addition, it is necessary not only to develop an effective topical dosage form with good stability but it is important to define the diffusion parameters in the gel base[10].

Among the vast number of gelling agents, carbomers are still interesting molecules for the research[11,12]. Carbomers or carbopols are polymers of acrylic acid that form a gel structure in alkaline solutions due to repulsion of the carboxyl groups charged negatively[13]. Carbopols are ideal for both hydro- and hydroalcolic gels[14,15]. Ibuprofen was the most popular and commonly used NSAID for its relief of pain and inflammatory action[16] associated with injure, rheumatoid arthritis and musculoskeletal problems[17,18]. Topical administration of NSAIDs (including Ibuprofen) has been designed as an alternative to the oral route[19]. Ibuprofen has poor aqueous solubility (log P=3.68)[20] resulting in difficulties in designing dosage forms. Dermal administration of Ibuprofen is useful for minimizing gastrointestinal side-effects[21,22] and hepatic metabolism[23]. Topical delivery systems of Ibuprofen are believed to improve patient compliance[9,24] and bioavailability[25,26]. Cosolvents are added to different formulations to help dissolution of drugs and to prevent their precipitation upon storage[27]. Also, they are added as release and permeation enhancers[28]. Several studies have been attempted to prepare transdermal preparations however a few numbers have focused on the effects of different parameters mathematically and statistically.

The main goal of this study was to develop carbopol gels containing Ibuprofen (a hydrophobic drug) by means of factorial design methodology. Carbopol gels must release Ibuprofen in sufficient amount for rapid pain relief. The screening design methodology was used to investigate the effect of different factors

[carbopol, Ibuprofen, alcohol, glycerin, polyethylene glycol 400 (PEG_{400}), acetone and propylene glycol (PG) concentrations] on gel properties (spreadability and Ibuprofen release). The experiments for the screening study were structured by Plackett and Burman Algorithm[29].

METHODOLOGY

Materials

Ibuprofen was supplied from IOL (India). PEG_{400} was purchased from SRL (India). NaH_2PO_4 and Na_2HPO_4 were obtained from Merck (Germany(. Carbopol 940 and all other solvents and chemicals employed [Glycerin, alcohol, acetone, propylene glycol and triethanolamine) TEA [(were of analytical grade.

Determination of Ibuprofen solubility

An excess amount of Ibuprofen was added to phosphate buffer (pH 7.4), the suspension was stirred at 37° C for 24 hours (Monotherm, variomog, Germany). The mixture was filtered and the difference in weight of filter paper before and after filtration referred to the insoluble fraction of Ibuprofen and the soluble Ibuprofen was calculated and expressed in mg/mL.

Preparation of gel systems

A defined quantity of carbopol (X_1) was dispersed in 15 g of water and left overnight for complete hydration. Ibuprofen at different concentration)X_2(was solubilized in a mixture of various solvents at different concentrations (alcohol X_3, glycerin X_4, PEG_{400} X_5, acetone X_6 and PG X_7). Ibuprofen solution was poured into carbopol dispersion. A determined quantity of triethanolamine (1.5 % of carbopol quantity) in the remaining water quantity was added to the mixture to give rise the viscosity.

Construction of the screening design

A preliminary study showed that the formulation parameters (carbopol, Ibuprofen and cosolvents quantities) had an influence on gel properties (spreadability, amount released). Considering the great number of parameters, a screening design was constructed to determinate the effect and the weight of formulation variables on gels properties in a simple and low cost methodology. According to the preliminary results, the two levels of the studies factors were defined. The experimental domain for each factor is summarized in Table 1.

Table 1. Experimental factors and levels

Factor	Factor signification	Level (-1)	Level (+1)
X_1	Carbopol concentration (%)	0.5	2
X_2	Ibuprofen concentration (%)	0.5	2.5
X_3	Alcohol concentration (%)	4	25
X_4	Glycerin concentration (%)	4	15
X_5	PEG400 concentration (%)	4	15
X_6	Acetone concentration (%)	2	10
X_7	PG concentration (%)	4	8

Eight experiments, structured according to the Plackett and Burman Algorithm were carried out. The calculated model was:

$Y(\text{response}) = b_0 + b_1X_1 + b_2X_2 + \cdots + b_nX_n$.

*b*0: average of the responses for the 8 experiments. $b_1, b_2, \ldots, b_n$: coefficients of the factors $X_1, X_2, \ldots, X_n$ (representing the effect of each factor ordered within $-1, +1)^{30}$.

Table 2 shows the following design obtained of 8 experiments.

Table 2. Experimental design

Experiment	X_1 Carbopol (%)	X_2 Ibuprofen (%)	X_3 Alcohol (%)	X_4 Glycerin (%)	X_5 PEG_{400} (%)	X_6 Acetone (%)	X_7 PG (%)
1	2	2.5	25	4	15	2	4
2	0.5	2.5	25	15	4	10	4
3	0.5	0.5	25	15	15	2	8
4	2	0.5	4	15	15	10	4
5	0.5	2.5	4	4	15	10	8
6	2	0.5	25	4	4	10	8
7	2	2.5	4	15	4	2	8
8	0.5	0.5	4	4	4	2	4

The coefficients (*bi*) were calculated by multiple linear regression and the results were analyzed. The statistical analysis provided several information:

- the regression quality was evaluated by the statistical indicator: the determination coefficient R^2
- the coefficients values *bi* and their S.D. The coefficients were evaluated by using a student test. In this study, the coefficients with significativity lower than 5 %, were assumed to be statistically different from 0. Thus, they have a significant effect on the response.

Gel systems characterization

The prepared gels were evaluated for: visual inspection, pH determination, spreadability and *in vitro* release.

Visual inspection

The bases were inspected for color, appearance, presence of any aggregation or phase separation[23]. A number from 0 to 4 was used to quantify gel consistence visually (Table 1), 0 was attributed to the more fluid preparation and 4 to the more rigid one.

pH determination

One g of each gel was weighed and diluted 40 times with water. The mixture was shaken for 2 hours under magnetic agitation at 100rpm (Monotherm, variomog, Germany). The pH was then determined by pH meter)Sension 3, Model 51910, HACH, USA) in triplicate. The pH of the prepared gel must be suitable for both gel viscosity[31] and dermal application[32].

Spreadability test

Spreadability is a measure of lubricity[33] and reflects the ease of dermal application[27,34]. It depends on viscosity of the formulation and on physical properties of the gelling polymers[34]. Higher spreadability values increase surface area available for drug permeation[35]. Hence, therapeutic efficacy may be enhanced[24].

This test was run according to previous study[36] with little modifications. Briefly, 1 g of each gel (after 24 hours of preparation) was placed between two horizontal plates (20 cm × 20 cm) and the weight of the upper plate was standardized at 1 kg. The experiments were performed at room temperature. The mean spreading diameter «d» (in vertical and horizontal axes) was determined after one minute and the areas of circles «S» ($S=d^2\pi/4$) were noted as spreadability values.

In vitro release study

According to previous study[28], a cylindrical glass tube (with effective diffusional surface area of 3.8 cm^2) opened at the two ends was used in this study. A determined amount of each formulae (0.5 g) was spread uniformly on the surface of cellulose nitrate membrane (Sartorious Stedim Biotech Gmbh, 0.22 μ, Germany). The filter paper was secured in place with a rubber and the filter acted as a membrane for drug release. The system was fixed in such way that the lower end of the tube containing samples just touched (1 mm depth) the surface of receptor medium i.e. 50 mL of phosphate buffer (pH 7.4) at 32±1° C. The receptor medium was stirred with a magnet bar at 100 rpm (Monotherm, variomog, Germany) during 4 hours. Sink conditions were maintained in the experiments (e.g. the concentration of Ibuprofen at the end of the experiments was less than 10 % of its solubility)[37]. Samples of 3 mL were pipetted from the receptor medium after 10, 20, 35, 50, 60, 90, 120, 150, 180, 210 and 240 minutes and replaced with an equal volume of freshly prepared phosphate buffer. The samples were then analyzed spectrophotometrically at 272 nm (Jasco V-530 UV/Vis Spectrophotometer, Japan(. The concentration of Ibuprofen was estimated from the regression equation of the calibration curve (Y= 1.359X+0.004, R^2=0.999) against a suitable blanch.

Determination of diffusion coefficients of Ibuprofen in the gel formulations

Diffusion coefficients were calculated using data obtained from drug diffusion study and Higuchi equation[38]:

$$Q= 2C_0(Dt/\pi)^{0.5}$$

Q is the amount of drug released into the receptor phase per unit area (mg/cm^2), C_0 is the initial drug concentration in the vehicle (mg/ml), D is the diffusion coefficient of the drug (cm^2/min), t is the time after application (min).

Release data were plotted against and the slopes of obtained straight lines were used to calculate $D_{(s)}$. D was used to give an idea about Ibuprofen mobility in gel bases.

RESULTS and DISCUSSION

Gels containing Ibuprofen were prepared using five different cosolvents. The calculated solubility of Ibuprofen was 1.47 mg/mL.

The prepared gels were very different in consistence (Table 1). Carbopol at level -1 (e.g. 0.5%) couldn't form gel structure sufficiently when the quantity of solvents increased, and the score of visual consistence decreased significantly.

All pH values were in suitable range for dermal application without irritation[23,39,40]. The results of the eight experiments carried out are summarized in Table 3.

Table 3. Experiment results

Experiment	Appearance	pH measurements	Spreadability (mm^2) Y_1	Amount released (mg/cm^2) Y_2
1	4	6.12	379.94	1.278129
2	1	6.08	1287.596	1.88839
3	0	6.8	1589.625	0.425455
4	3	6.99	358.6591	0.467837
5	1	6.07	1263.862	1.573604
6	3	7.1	333.9316	0.498763
7	4	6.22	362.8663	1.061023
8	2	6.86	900.7998	0.557522

Influence of the investigated parameters on spreadability (response Y_1)

Increasing gel viscosity decreased their spreadability[33,34]. Therefore, the changes in spreadability in this study will be related to viscosity.

The surface of spreading circles ranged from 334 to 1590 mm^2 depending on variation of different factors (Table 3 and Figure 1). The statistical analysis (Table 4) showed the significant effects of the whole studied parameters.

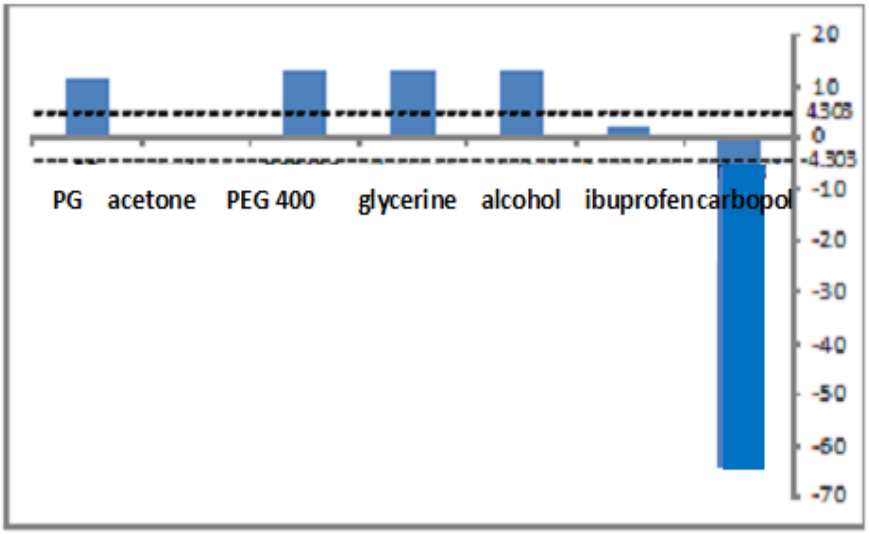

Figure 1: Effects of different factors on the response Y1 (spreadability), the dash line represents the maximal limit over which the factor is statically significant

Table 4. Statistical analysis of Y1 results (spreadability)

Name	Coefficient value	S.D	t exp. Student	Significativity (%)
b_0	809.66	6.98	115.9971	*
b_1	-450.811	6.98	-64.5861	*
b_2	13.90615	6.98	1.992285	-
b_3	88.11318	6.98	12.62367	*
b_4	90.02662	6.98	12.8978	*
b_5	88.36156	6.98	12.65925	*
b_6	1.352285	6.98	0.193737	-
b_7	77.91125	6.98	11.16207	*
R^2	1	FD = 2		

R^2: determination coefficient; FD: freedom degrees which are estimated after repeating experiment 4 three times; the asterisk in the significativity column shows the most influent factors.

The gels spread easily when carbopol quantity was decreased because the gelling agent increased the viscosity of different formulations[41,42]. Increasing polymer concentration increases cohesiveness within the system and the spreading of a delivery vehicle is inversely proportional to its cohesiveness because strong cohesive forces reduce the spreadability[33].

Alcohol decreased viscosity of carbomer gels and a larger carbomer amount might be required to overcome the loss of viscosity[43]. The various other solvents containing OH in their structure (glycerin, PEG_{400} and PG) were known to increase viscosity of carbomer systems[44] however in this investigation, viscosity decreased with these solvents. This might be attributed to the fact that increasing any of these solvents resulted in a new hydrophilic cosolvent system that attracted water from carbomer chains hence the viscosity decreased. The small quantity of carbomer couldn't enter in competition against cosolvent mixture that attracted water. Therefore, the presence of carbopol in small amounts (experiments 2, 3 and 5) couldn't restrict the solvent quantity. In order to reform this gel structure, the quantity of solvents must be decreased (experiment 8) or an increase in carbopol concentration might be required to overcome the loss of viscosity. For example, the formula 5 containing 41 mL of different solvents was fluid while formula 6 containing 51 mL of solvents was gelled considering carbopol concentration (e.g. 2 %). The new additional amount of carbomer (for formula 6) would be hydrated by water and other cosolvents, hence the viscosity would increase in the system in which there was no more free cosolvent.

Ibuprofen and acetone appeared to have no effect on spreadability at studied levels.

Influence of the investigated parameters on the Cumulated released amount of Ibuprofen (response Y_2)

Figure 2 and Table 5 showed the significant factors on the cumulated released amount of Ibuprofen (response Y_2). Differences in released amounts per cm^2 (Figure 3) are mainly due to the differences in both solubility of the active ingredient in the vehicle and viscosity of gel matrix[45,46,47]. The viscosity of the gel base may play an important role in modifying drug release into the receptor medium[10,48,49]. Therefore, the released amounts of Ibuprofen will be discussed in terms of viscosity and solubility.

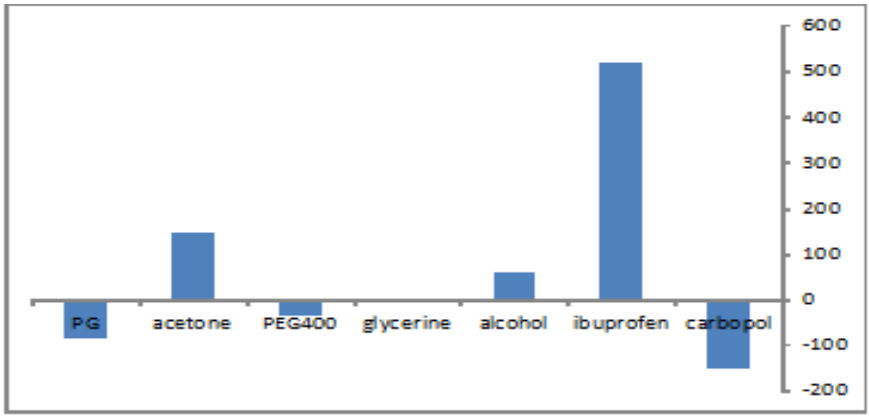

Figure 2: Effects of different factors on the response Y_2 (amount released)

Figure 2. Effects of different factors on the response Y_2 (released amount)

Table 5. Statistical analysis of Y2 results (cumulated released amount /cm^2)

Name	Coefficient value	S.D	t exp. Student	Significativity (%)
b_0	0.96884	0.00093	1041.764	*
b_1	-0.1424	0.00093	-153.121	*
b_2	0.481446	0.00093	517.684	*
b_3	0.053844	0.00093	57.8968	*
b_4	-0.00816	0.00093	-8.77862	*
b_5	-0.03258	0.00093	-35.0367	*
b_6	0.138308	0.00093	148.7183	*
b_7	-0.07913	0.00093	-85.0852	*
R^2	1	FD = 2		

R^2: determination coefficient; FD: freedom degrees which are estimated after repeating experiment 4 three times; the asterisk in the significativity column shows the most influent factors

The factors enhancing the release of Ibuprofen were concentrations of Ibuprofen, alcohol and acetone while the factors decreasing the released amount were: concentrations of carbopol, glycerin, PEG_{400} and PG.

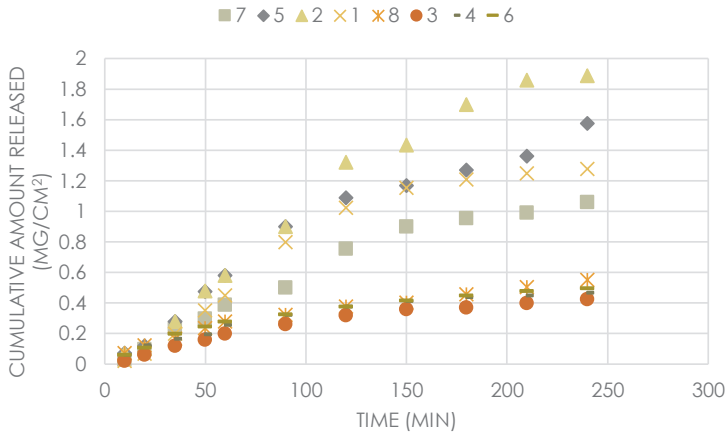

Figure 3. Cumulated released amount of Ibuprofen from different gels

When carbopol concentration was increased in the system, the spreadability was decreased leading to a decrease in released amount[50]. At molecular level, increasing carbopol concentration results in higher viscosity and more tortuous path of migration as a consequence of reduced solvent content[51].

An increase in Ibuprofen concentration led to an increase in released amount per cm² and this was in accordance with other previous studies[28,52]. Increasing drug concentration in the vehicle increases drug release according to Higuchi equation[38].

It was observed that an increase in concentrations of alcohol and acetone was followed by an increase in the total amount of released Ibuprofen. This might be explained partially by the decrease in associated viscosity (expressed by lower diameters of the spreading areas). This agreed with the results of Hasçicek C (2009) who explained the increased released amounts with decrease in viscosity[19]. Additionally, acetone being a solvent of choice for Ibuprofen[53], it increased the amount liberated of Ibuprofen and this might be due to the increase of the solubilized form of Ibuprofen without increasing its affinity to the system. It was reported that the solubility was enhanced in presence of certain solvent and consequently the release rate increased[28,54].

For glycerin, PEG_{400} and PG, it was noted that there was a lack of correlation between spreadability (related to viscosity) and the released amount and this indicated that the viscosity was not the main factor for release[55,56]. This lack of correlation might be explained by the enhanced Ibuprofen solubility and higher affinity for the vehicles (less thermodynamic activity) thus, it was difficult for Ibuprofen to migrate. These data revealed the important action of glycerin,

PEG_{400} and PG as cosolvents, because flux declined as the affinity of the drug to the vehicle raised[54,57,58].

In this paper, it was observed that neither viscosity nor solubility played alone the main role of release but these two physiochemical properties complete each other in determining the release parameters.

The rank order of the gel formulations based upon their maximum Ibuprofen release is indicated in Table 6. This table illustrates the relationship between released Ibuprofen (per cm^2) and concentrations of both Ibuprofen and carbopol.

Table 6. Effect of Ibuprofen and carbopol concentrations on Ibuprofen release

Experiment	Ibuprofen %	Carbopol %	Cosolvents %	Amount released (mg/cm^2)
2	+	-	58	1.88839
5	+	-	41	1.573604
1	+	+	50	1.278129
7	+	+	33	1.061023
8	-	-	18	0.557522
6	-	+	51	0.498763
4	-	+	48	0.467837
3	-	-	65	0.425455

Data from Table 4 reveal that the concentration of Ibuprofen had the greatest effect on release from carbopol gels (experiments in the order: 2 > 5 > 1 > 7) followed by the carbopol concentration (the experiments 5 and 2 had the greatest released amount wherein the level of carbopol was at -1, the same matter for experiments 8). The calculated diffusion coefficients of Ibuprofen for experiments 2 and 5 ($8.82*10^{-6}$ cm^2/min and $5*10^{-6}cm^2$/min respectively) were greater than those for experiments 1 and 7 ($4.39*10^{-6}$ cm^2/min and $2.58*10^{-6}$ cm^2/min respectively). The nature and concentration of cosolvent played a significative role in Ibuprofen release and might overcome carbopol concentration at level -1 (experiment 3).

In order to test the factorial design used in this study, an additional experiment was prepared in order to increase the released amount of Ibuprofen for accelerating pain relief and inflammation[16]. The coded factor level for this experiment had to be in Table 7:

- +1 for Ibuprofen for increasing released amount, also, level +1 for acetone for its role in solubilizing Ibuprofen.
- Intermediate values {≈} for carbopol, alcohol, Glycerin, PEG_{400}, PG concentrations (for good consistency and good release parameters).

Table 7. Conditions for experiment 9

Factor	Factor signification and value
X_1	Carbopol concentration (%): 1
X_2	Ibuprofen concentration (%): 2.5
X_3	Alcohol concentration (%): 14.5
X_4	Glycerin concentration (%): 9.5
X_5	PEG_{400} concentration (%): 9.5
X_6	Acetone concentration (%): 10
X_7	PG concentration (%): 6

The prepared gel was homogenous and of good consistence. The percentage of released Ibuprofen from this optimal gel reached at ~53 % of initial amount at 4 hours of the study and theoretically it may preserve releasing Ibuprofen for further time and in suitable amounts for improving therapeutic efficacy. The released amount from this new gel (1.742 mg/cm², $D=3.23*10^{-6}$ cm²/min) was important in comparison with formulas 1 and 7 containing the maximal initial carbopol concentration, thus, good therapeutic efficacy can be expected. The formulas 2 and 5 were neglected in the comparison because they were very fluid.

STATEMENT OF ETHICS

Not applicable for this study.

CONFLICT OF INTEREST STATEMENT

The author has no conflict of interest to declare.

AUTHOR CONTRIBUTIONS

The author confirms sole responsibility.

FUNDING SOURCES

This research did not receive any funding.

REFERENCES

1. Reddy KR, Sandeep K, Reddy PS. In vitro release of ibuprofen from different topical vehicles. Asian J Pharm Sci Res, 2011;1(2):141-197.

2. Kumar S, Himmelsten K. Modification of in situ gelling behavior of Carbopol solution by Hydroxypropyl methylcellulose. J Pharm Sci, 1995;84(3):344-348. Doi: 10.1002/jps.2600840315

3. Rao RP, Diwan PV. Formulation and in vivo evaluation of polymeric film diltiazem Hydrochloride and Indomethacin for transdermal administration. Drug Dev Ind Pharm. 1998;24(4):327-336, Doi: 10.3109/03639049809085627

4. Parrott EL. Pharmaceutical Technology, Fundamental pharmaceutics. 1st ed. India: Surjeet Publications; 1985. p. 320.

5. Gopi C, Vijaya Kumar TM, Dhanaraju MD. Design and evaluation of novel ibuprofen gel and its permeability studies. Inter J Biophar, 2010;1(2): 82-84.

6. Shima K, Matsuska C, Hirose M, Noguchi T, Yamahira Y. Biopharmaceutical characteristics of indometacin gel ointment. Chem Pharm Bull, 1981;29(8):2338-2343. Doi: 10.1248/cpb.29.2338

7. Uekama K, Hirayama F, Irie T. Cyclodextrin drug carrier systems. Chem Rev, 1998;98(5):2045-2076. Doi: 10.1021/cr970025p

8. Rasool BKA, Abu-Gharbieh EF, Fahmy SA, Saad HS, Khan SA. Development and evaluation of ibuprofen transdermal gel formulations. Trop J Pharm Res, 2010;9(4):355-363. Doi: 10.4314/tjpr.v9i4.58928

9. Lakshmi PK, Kumar MK, Sridharan A, Bhaskaran SH. Formulation and evaluation of ibuprofen topical gel: a novel approach for penetration enhancement. Inter J App Pharm, 2011;3(3):25-30.

10. Bregni C, Chiappetta D, Faiden N, Carlucci A, García R, Pasquali R. Release study of diclofenac from new carbomer gels. Pak J Pharm Sci, 2008;21(1):12-16.

11. Taş Ç, Ozkan Y, Savaşer A, Baykara T. In vitro and ex vivo permeation studies of chlorpheniramine maleate gels prepared by carbomer derivatives. Drug Dev Ind Pharm, 2004;30:637-647. Doi: 10.1081/ddc-120037665

12. Barreiro-Iglesias R, Alvarez-Lorenzo C, Concheiro A. Incorporation of small quantities of surfactants as a way to improve the rheological and diffusional behavior of carbopol gels. J Control Rel, 2001;77:59-75. Doi: 10.1016/S0168-3659(01)00458-8

13. Bremecker VKD, Strempel H, Klein G. Nitrosamine–free polyacrylate gels: use of new type of bases for neutralization. J Pharm Sci, 1984;73:548-553.

14. Jain NK. Controlled and novel drug delivery. New Delhi, India: CBS Publishers & Distributors; 2019.

15. Singh J, Tripathi KP and Sakia TR. Effect of penetration enhancers on the in vitro transport of ephedrine through rat skin and human epidermis from matrix based transdermal formulations. Drug Dev Ind Pharm, 1993;19(13):1623-1628. Doi: 10.3109/03639049309069331

16. Stahl J, Wohlert M, Kietzmann M. The effect of formulation vehicles on the in vitro percutaneous permeation of ibuprofen. BMC Pharmacol, 2011;11(12):1-5. Doi: 10.1186/1471-2210-11-12

17. Djekic L, Martinovic M, Stepanovi´c-Petrovi´c R, Micov A, Tomi´c M, Primorac M. Formulation of hydrogel-thickened nonionic microemulsions with enhanced percutaneous delivery of ibuprofen assessed in vivo in rats. Eur J Pharm Sci, 2016;92:255-265. Doi: 10.1016/j.ejps.2016.05.005

18. Celebi D, Guy RH, Edler KJ, Scott JL. Ibuprofen delivery into and through the skin from novel oxidized cellulose-based gels and conventional topical formulations. Int J Pharm, 2016;514:238-243. Doi: 10.1016/j.ijpharm.2016.09.028

19. Hasçicek C, Bediz-Ölçer A, Gönül N. Preparation and evaluation of different gel formulations for transdermal delivery of meloxicam. Turk J Pharm Sci, 2009;6(3):177-186.

20. Bolla PK, Clark BA, Juluri A, Cheruvu HS, Renukuntla J. Evaluation of formulation parameters on permeation of Ibuprofen from topical formulations using Strat-M® Membrane. Pharmaceutics, 2020;12:151. Doi: 10.3390/pharmaceutics12020151

21. Baigent C, Bhala N, Emberson J, Merhi A, Abramson S, Arber N, et al. Vascular and upper gastrointestinal effects of non-steroidal anti-inflammatory drugs. Lancet, 2013;382(9894):769-779. Doi: 10.1016/s0140-6736(13)60900-9

22. Wisudyaningsih B, Ameliana L. Effect of gelling agent and penetration enhancer on the release rate of ibuprofen-PEG6000 solid dispersion from gel preparations. Pharm Educ, 2022;22(2):55-59. Doi: 10.46542/pe.2022.222.5559

23. Parhi R, Sai Goutam SV, Mondal S. Formulation and evaluation of transdermal gel of Ibuprofen: use of penetration enhancer and microneedle. IJPS, 2020:16(3):11-32.

24. Kashyap A, Das A, Ahmed AB. Formulation and evaluation of transdermal topical gel of Ibuprofen. JDDT, 2020;10(2):20-25. Doi: 10.22270/jddt.v10i2.3902

25. Prausnitz MR, Mitragotri S, Langer R. Current status and future potential of transdermal drug delivery. Nat Rev Drug Discov, 2004;3(2):115-124. Doi: 10.1038/nrd1304

26. Prausnitz MR, Langer R. Transdermal drug delivery. Nat Biotech, 2008;26(11):1261-1268. Doi: 10.1038/nbt.1504

27. Abdel-Mottaleb MMA, Mortada ND, Elshamy AA, Awad GAS. Preparation and evaluation of fluconazole gels. Egypt J Biomed Sci, 2007;23. Doi: 10.4314/ejbs2.v23i1.40309

28. Mehsen MB. Effect of propylene glycol, poly ethylene glycol 400 and pH on the release and diffusion of Ibuprofen from different topical bases. Al-Mustan J Pharma Sci, 2011;9(1):80-93. Doi: 10.32947/ajps.v9i1.274

29. Plackett RL, Burman JP. The design of optimum multifactorial experiments. Biometrika, 1946;33:305-325. Doi: 10.1093/biomet/33.4.305

30. Box GEP, Hunter WG, Hunter JS. An introduction to design, data analysis, and model building. Statistics for Experiments, 1978;374-434.

31. Quiñones D, Ghaly ES. Formulation and characterization of nystatin gel. Puerto Rico Heal Sci J, 2008; 27(1):61-67.

32. Salunkhe SS, Bhatia NM, Bhatia MS. Rheological investigation of nystatin loaded liposomal gel for topical application: factorial design approach. Int J Pharm Bio Sci, 2013;4(4):497-512.

33. Garg A, Aggarwal D, Garg S, Singla AK. Spreading of semisolid formulations: an update. Pharm Technol N Am, 2002;26(9):84-105.

34. Rao M, Sukre G, Aghav Sh, Kumar M. Optimization of metronidazole emulgel. J Pharm, 2013:1-9. Doi: 10.1155/2013/501082

35. Bachhav YG, Patravale VB. Formulation of meloxicam gel for topical application: in vitro and in vivo evaluation. Acta Pharm, 2010;60(2):153–163. Doi: 10.2478/v10007-010-0020-0

36. Lardy F, Vennat B, Pouget P, Pourrat A. Functionalisation of hydrocolloids: principal component analysis applied to the study of correlations between parameters describing the consistency of hydrogels. Drug Dev Ind Pharm, 2000;26(7),715-721. Doi: 10. 1081/ddc-100101289

37. Riccia EJ, Lunardib LO, Nanclaresb DMA, Marchettia JM. Sustained release of lidocaine from Poloxamer 407 gels. Inter J Pharm, 2005;288:235-244. Doi: 10.1016/j.ijpharm.2004.09.028

38. Higuchi WI. The analysis of data on the medicament release from ointments. J Pharm Sci, 1962;51:802-804. Doi: 10.1002/jps.2600510825

39. Malay KD, Abdul BA. Formulation and ex vivo evaluation of rofecoxib gel for topical application**.** Acta Pol Pharm, 2007;64(5):461-467.

40. Sougata J, Sreejan M, Amit KN, Kalyan KS, Sanat KB. Carbopol gel containing chitosan-egg albumin nanoparticles for transdermal aceclofenac delivery. Colloids Surf B, 2014;114:36-44. Doi: 10.1016/j.colsurfb.2013.09.045

41. Jelvehgaria M, Rashidib MR, Samadi H. Mucoadhesive and drug release properties of benzocaine gel. Iran J Pharma Sci, 2006;2(4):185-194.

42. Sandeep DS, Kiran A, Kumar P. Ibuprofen emulgels as promising topical drug delivery system - A study of formulation design and In vitro evaluation. Asian J Pharm, 2021;15(4):435.

43. Allen LV, Popovich NG, Hc A. Disperse systems. In Ansel's Pharmaceutical Dosage Forms and Drug Delivery Systems. 8th ed. Lippincott Williams & Wilkins; 2005. p. 420.

44. Walters KA, Brain KR. Pharmaceutical Preformulation and Formulation. A practical guide for candidate drug selection to commercial dosage form. In: Gibson M, editor. Informa Healthcare. 2009. p. 501-502.

45. Martinez MAR, Gallardo JLV, Munoz de Benavides M, Lopez-Duran JG, Lara VG. Rheological behavior of gels and meloxicam release. Int J Pharm, 2007;333:17-23. Doi: 10.1016/j.ijpharm.2006.09.045

46. Csoka I, Csanyi E, Zapantis G, Nagy E, Feher-Kiss A, Horvath G, Blazso G, Eros I. In vitro and in vivo percutaneous absorption of topical dosage forms: case studies. Int J Pharm, 2005;291:11-19. Doi: 10.1016/j.ijpharm.2004.07.038

47. Güngör S, Bergişadi N. In vitro release studies on topical gel formulations of nimesulide. Pharmazie, 2003;58(2):155-156.

48. Tas Ç, Özkan Y, Savaşer A, Baykara T. In vitro release studies of chlorpheniramine maleate from gels prepared by different cellulose derivatives. II Farmaco, 2003;58:605-611. Doi: 10.1016/S0014-827X(03)00080-6

49. Akhtar N, Yazan Y. Formulation and characterization of a cosmetic multiple emulsion system containing macadamia nut oil and two antiaging agents. Turkish J Pharm Sci, 2005;2(3):173-185.

50. Patel J, Patel B, Banwait H, Parmar K, Patel M. Formulation and evaluation of topical aceclofenac gel using different gelling agent. Inter J Drug Dev Res, 2011;3(1):156-164.

51. Gallagher SJ, Trottet L, Heard ChM. Ketoprofen: release from, permeation across and rheology of simple gel formulations that simulate increasing dryness. Inter J Pharm, 2003;268(1-2):37-45. Doi: 10.1016/j.ijpharm.2003.08.012

52. Fergany AM. Topical permeation characteristics of diclofenac sodium from Na CMC gels in comparison with conventional gel formulation. Drug Dev Ind Pharm, 2001;27(10):1083-1097. Doi: 10.1081/ddc-100108371

53. British Pharmacopoeia. London. Volumes I and II: Medicinal Substances; 2009.

54. Setty CM, Babubhai SR, Pathan IB. Development of valdecoxib topical gels: effect of formulation variables on the release of valdecoxib. Inter J Pharm Pharma Sci, 2010; 2(1):70-73.

55. Gendy AME, Jun HW, Kassem AA. In vitro release studies of flurbiprofen from different

topical formulations. Drug Dev Ind Pharm, 2002;28:823-831. Doi: 10.1081/ddc-120005628

56. Guangwei L, Jun HW. Diffusion studies of methotrexate in carbopol and poloxamer gels. Int J Pharm, 1998;160:1-9. Doi: 10.1016/S0378-5173(97)00187-7

57. Arellano A, Santoyo S, Martin C, Ygartua P. Influence of propylene glycol and isopropyl myristate on the in vitro percutaneous penetration of Diclofenac sodium from carbopol gels. Eur J Pharm Sci, 1998;7:129-135. Doi: 10.1016/S0928-0987(98)00010-4

58. Goundaliya DP, Pundarikakshudu K. Studies on penetration, characterization and transdermal permeation of Nimesulide from aqueous and emulgel. Ind Drugs, 2002;39(9):465-473.